COMB-BRANCH LIQUID CRYSTALLINE POLYMERS: THE SYNTHESIS AND CHARACTERISATION OF BOTH CHIRAL AND NON-CHIRAL STRUCTURES

A Thesis submitted to the
University of Stirling
for the degree of
Doctor of Philosophy

HUGH WILLIAM HUNTER

Hugh W Hunter

Department of Chemistry
March 1989

PREFACE

This thesis is submitted for the degree of Doctor of Philosophy at the University of Stirling, having been submitted for no other degree. It is a record of research undertaken in the Department of Chemistry. This work is wholly original except where due reference is made.

DEDICATION

To my parents, Ella and Hugh.

ACKNOWLEDGEMENTS

I wish to thank my supervisor, Professor J M G Cowie, for his guidance, advice and enthusiasm throughout this period of study.

I must also thank Dr I J McEwen for many helpful discussions and for his expert instruction in instrumental and analytical techniques.

Special thanks are due to Dr H H Wu, not only for his advice on all things practical, but for his encouragement and his unique sense of humour.

This thesis would not be complete without some form of acknowledgement to the members (and past members) of the Chemistry Department at Stirling, both academic and services, for their assistance during my time at Stirling. In particular, I would like to thank Mrs P Brown for typing this manuscript, Mr D F Dance for performing some of the nmr work, and Mr G Castle for the provision of various chemicals from his store.

I must sincerely thank my family for their encouragement and support, and all of the friends I have made at Stirling for all of the good times.

Finally, I must acknowledge Dutch State Mines for their generous financial support and Drs Vriesema and Roerdink from this organisation for their advice and assistance.

ABSTRACT

Various comb-branch, thermotropic liquid crystalline copolymers having both chiral and non-chiral structures have been prepared and studied by differential scanning calorimetry and polarising microscopy. These copolymers were found to display either smectic, nematic or chiral nematic phases, or a combination of them.

The novel smectogenic monomer di[6-(4-methoxy-4'-oxybiphenyl)hexyl]-2-methylene butane-1,4-dioate (DMBI-6) and the nematogenic monomer 4-cyanophenyl-4-(6-acryloyloxyhexyloxy)-benzoate (CPBA-6) were prepared and characterised. DMBI-6 was copolymerised with both achiral and chiral non-mesogenic monomers; the resultant copolymers were observed to form both smectic A and B phases. CPBA-6 was copolymerised with a chiral, non-mesogenic monomer and phases which appeared to be nematic in nature were detected. These copolymers showed a tendency to form crosslinked gels at high conversions. One of these materials was partially characterised and its elastomeric-liquid crystalline behaviour studied.

Two novel cholesteric monomers, namely 1-[1-(cholesteryloxy)carbonyl]-10-decanyl]-2-methylene-4-methyl butane-1,4-dioate (ChMI-10) and di[1-[(cholesteryloxy)carbonyl]-10-decanyl]-2-methylene butane-1,4-dioate (DChI-10) were synthesised. Copolymers of one of these, ChMI-10, with CPBA-6 was found to form the cholesteric phase predominantly. The attempted polymerisation of DChI-10 was studied.

Three novel, chiral mesogenic monomers bearing the chiral

centre in the flexible spacer were synthesised. Two of these monomers, namely (S)-1-(4-methoxy-4'-oxybiphenyl)-2-methacryloyloxypropane (MBM*) and (S)-1-(4-cyano-4'-oxybiphenyl)-2-methacryloyloxy propane (CBM*) were copolymerised with DMBI-6 and both smectic and chiral nematic phases were seen to result. Copolymers of CBM* and CPBA-6 yielded only chiral nematic phases. Copolymers prepared from CPBA-6 and (S)-1-(4-methoxy-4'-oxybiphenyl)-2-(2-methacryloyloxy-1-ethoxy)propane (XMBM*) formed either chiral nematic or crystalline phases.

An attempt has been made to rationalise the temperature and composition dependent optical properties of the chiral nematic phases formed in terms of the hindered rotation of the chiral mesogens around their long molecular axis. The results were found to compare favourably with previously reported results and theories.

CONTENTS

ABBREVIATIONS

The following abbreviations are used throughout this thesis:

g glass

k : crystalline

Other abbreviations are noted elsewhere in the text.

CHAPTER ONE

INTRODUCTION

1. PREFACE TO INTRODUCTION

The field of liquid crystals has experienced phenomenal growth in the past twenty years. This has arisen primarily because of their increasingly successful application in areas of high technology, particularly in the area of electro-optical displays. Consequently, the demand for specialist materials and devices has acted as a stimulus and focus for materials research by scientists from such diverse fields as organic chemistry, physics and electrical and electronic engineering. From a combination of this intensive, multi-disciplinary activity and ongoing research into the synthesis of uniaxial, high-modulus fibres, the field of liquid crystal polymers emerged.

Polymer liquid crystals are now the subject of intense interest in their own right, both from the points of view of liquid crystal behaviour and of macromolecular science. However, in comparison with conventional liquid crystals, polymer liquid crystal research is still in its infancy and much work needs to be carried out before a true understanding of the nature of these materials can be gained.

The properties of the liquid crystalline phases of these polymers have been shown to be somewhat similar to those of their low molecular weight counterparts and, as a consequence, the same definitions, terminologies and methods of analysis are employed in both fields. Since this thesis presents a study of liquid crystalline polymers, it is therefore pertinent to start with an introduction to the study of conventional liquid crystals followed by their applications. Polymer liquid crystals are then introduced followed by the main topic of the thesis, namely chiral comb-branch liquid crystalline

polymers, which is accompanied by a literature survey of the area. Finally, the aims of the work embodied in the thesis are presented.

1.1 Historical Background

It is now 100 years since the Austrian botanist Reinitzer first discovered and recognised the existence of the liquid crystalline phase by the observation of irridescent colour phenomena which arise when melts of cholesteryl acetate and in a more pronounced form, cholesteryl benzoate are cooled.[1] He noted that a carefully purified sample of cholesteryl benzoate "melted" at 145.5°C to give a turbid fluid which, on further heating, suddenly became transparent at 178.5°C. Subsequent cooling produced colour effects which are now known to be characteristic of cholesteric "mesophases". Reinitzer observed that on cooling the transparent melt of cholesteryl benzoate, "there appeared at a certain point a deep blue colour which spread out rapidly through the whole mass and almost as quickly disappeared again, leaving in its place a uniform turbidity". He also noted that the melt remained turbid but fluid and that on further cooling a similar colour effect occurred for a second time, to be followed by a crystallisation of the mass and the simultaneous disappearance of the colour effect.

Using a polarising microscope, Lehmann[2,3] confirmed the Austrian botanist's observations and recorded other similarities, thus prompting him to lend the term: "Liquid Crystalline" to this new intermediate state of matter. This terminology is still in use today and is used synonymously with the terms "mesomorphic" and "mesophase" to describe these highly anisotropic fluids which have a state of order between that of the crystalline solid and the amorphous isotropic liquid.

Following Lehmann's studies, synthetic work was initiated by

organic chemists in Germany in an attempt to elucidate the relationship between molecular structure and liquid crystallinity, and these workers found that molecules possessing a rigid anisometric shape, i.e. cylindrical lath-like, disk-like or lamellar structures, formed mesophases. Since this early pioneering work, several tens of thousands of organic substances which exist in the liquid crystalline phase have been synthesised and are generally termed as mesogens. From structure-property relationship studies it can be seen that in addition to a molecular shape which is longer than it is wide, mesophasic thermal stability is favoured by molecular rigidity, permanent dipoles (within the molecules) and a high level of molecular polarisability.

These features give rise to the anisotropic properties (e.g. mechanical, optical, electrical and magnetic) usually associated with crystalline materials in addition to the rheological properties normally associated with liquids. This unique combination of properties has led to the use of liquid crystals in many diverse technological applications, such as digital displays, flat screen televisions and thermal mapping, etc. (see section 1.4).

1.2 Liquid Crystal Mesophases and their Classification

Liquid crystalline materials can be firstly classified as being either lyotropic or thermotropic in nature.

Lyotropic liquid crystals[4,5,6] are generally formed from rod-like compounds with an amphiphilic character, dissolved in a suitable solvent (commonly water), where the structured anisotropic phases consist mainly of ordered arrangements of micelles, occurring when the solute concentration is sufficiently high. Although the rod-like

materials giving rise to these phases are generally much larger than those which give rise to thermotropic phases, their axial ratios seldom exceed ~15. Many synthetic polypeptides as well as DNA and certain viruses (e.g. Tobacco mosaic virus) all form lyotropic phases and are thus important biologically. It should also be noted here that even polypeptides without amphiphilic character (e.g. poly-γ-benzyl-L-glutamate) also form lyotropic mesophases.[7]

Thermotropic liquid crystals on the other hand, are usually non-amphiphilic organic structures and the phases are formed by either heating the crystalline solid or by cooling the isotropic liquid, i.e. by thermal effects.

Since the study in this thesis is focussed on thermotropic liquid crystalline systems no further attention will be paid to lyotropic liquid crystals.

A widely adopted scheme for the classification of the molecular structure of non-amphiphilic mesophases was first proposed by Friedel in 1922.[8] From detailed optical studies of these states and from support by citations in other areas (e.g. X-ray diffraction, electric and magnetic field behaviour), Friedel was able to distinguish clearly three different types of mesophase which he termed nematic, cholesteric and smectic.

An extensive classification of liquid crystals is shown in figure 1.1.

1.2.1 Nematic order.

Nematic phases are characterised by an unordered, statistical distribution of the centres of gravity of the molecules and by the quasi-long-range orientational order of the molecular long axes

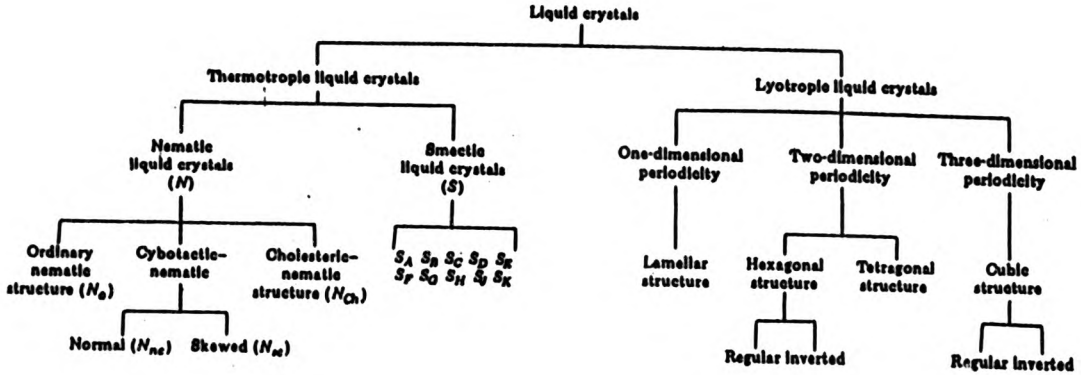

FIGURE 1.1 **Classification of liquid crystalline structures. In addition to the normal smectic C phase, the chiral smectic C or S_C* has been identified.**

which tend to be parallel to a common director n. This is shown schematically in figure 1.2.

The thermal fluctuations of the individual molecular long axes can be described by the order parameter S (average value) as introduced by Maier and Saupe,[9] where

$$S = 1/2 < 3\cos^2\theta - 1> \qquad (1.1)$$

The angle θ denotes the mean deviation of the molecular axis with respect to the director. These characteristic features account for the macroscopic properties usually displayed by nematic phases, such as their fluidity and their optically positive uniaxial behaviour. The latter property is caused by the extraordinary refractive index of the phase (n_e) being larger than its ordinary refractive index (n_o) and since $\Delta n = n_e - n_o$, the birefringence (Δn) has a positive value.

In some nematic phases there also exists short-range layer-like or "smectic-like" order, usually in the form of clusters. These groups are called cybotactic groups,[10] and the molecular centres of each group are arranged in layers either tilted (skewed) at an angle to the main director or parallel to the director. These modifications have the abbreviations Nsc and Nnc respectively, with the ordinary nematic phase being termed No or N (see figure 1.1).

1.2.2 Cholesteric order.

The cholesteric mesophase (shown schematically in figure 1.3) can be described as a helically disturbed nematic phase, with the cholesteric phase having similar ordering to the nematic phase on a

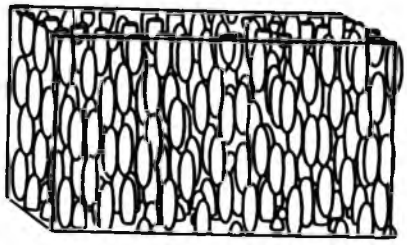

FIGURE 1.2 Schematic representation of the nematic phase.

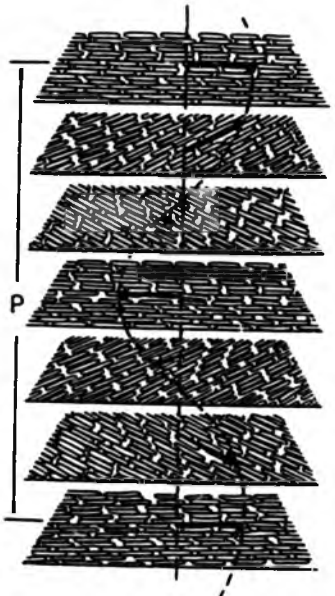

FIGURE 1.3 Schematic representation of the cholesteric or chiral nematic phase where p = pitch length.

local scale but on a layered scale having the director continuously twisted about an axis perpendicular to the director, resulting in a macroscopic helical structure. The distance where the director is twisted by $\theta = 2\pi$, is called the pitch p of the cholesteric helix and has a positive sign for a right handed helix and a negative sign for a left handed helix. This twisting phenomenon arises from a chiral perturbation, usually the presence of an optically active centre in the molecules that comprise the mesophase. This chiral perturbation minimises the energy content of the stacked array (relative to other arrangements) in which each molecule is skewed at an average angle θ with respect to its neighbours above and below.

From the theories of Goosens and Vertogen[11,12] the cholesteric phase can be described by the following order parameters (average values),

$$S = F_1 = 1/2 \langle 3 \cos^2\theta - 1 \rangle \qquad (1.2)$$

$$D = F_2 = \langle \cos 2\varphi \sin^2\theta \rangle \qquad (1.3)$$

where S characterises the orientational long range order (as in the case of the nematic phase) and D accounts for biaxiality and hindered rotation about the long molecular axis (φ denotes the angle of rotation).

This phase was termed cholesteric since the first molecules to show this effect were the cholesteryl esters first reported by Reinitzer.[1] However, cholesteric mesophase formation is by no means restricted to cholesteryl derivatives, since nematogenic molecules which contain a chiral centre also exhibit this unique

phenomenon and are termed "chiral nematic" liquid crystals. In fact, it has been demonstrated that the chiral nematic mesophase can also be realised by merely doping a host nematic phase with either mesogenic or non-mesogenic chiral molecules.[13]

Owing to the helical structure, and more precisely, the fact that the dimensions of the constituent helical aggregates of the mesophase are of the order of the wavelength of light, spectacular optical properties can be observed on the irradiation of light parallel to the optical (helical) axis.

Firstly, the mesophase has an extremely high optical activity, being able to rotate plane-polarised visible light by as much as 10^3-10^5 degrees/mm.[14,15] This is enormous in comparison to the optical rotations of optically active isotropic liquids which are normally in the region of 10^{-2}-10^2 degrees/mm.[16]

Secondly, the cholesteric mesophase, when homogeneously orientated exhibits a remarkable circular dichroism effect, being able to reflect selectively, circularly polarised light of wavelength λ_R on the irradiation of white light. This is shown schematically in figure 1.4.

The reflected light (50% of the initial intensity) is right handed circularly polarised (rcp) if the cholesteric phase forms a right handed helix (dextro form, $p>0$) and the transmitted light is left handed circularly polarised (lcp). The reverse holds true for a phase forming a left handed helix (levo form, $p<0$).

The wavelength of reflected light is related to the pitch by

$$\lambda_R = np \qquad (1.4)$$

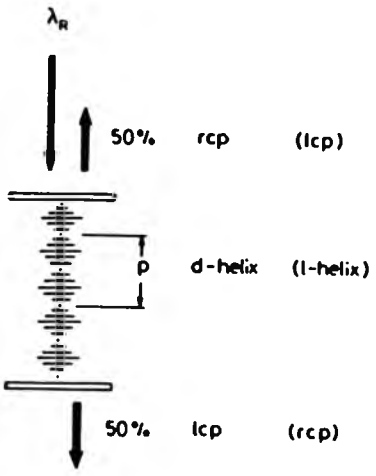

FIGURE 1.4 Circular dichroism of a cholesteric (chiral nematic) phase having a d-helix (l-helix) owing to the selective reflection of circularly polarised light of the wavelength λ_R. For a cholesteric phase having a d-helix, 50% of the initial light is reflected, being right handed circularly polarised (rcp). 50% passes the sample, being left handed circularly polarised (lcp). For a cholesteric phase having a l-helix, lcp light is reflected and rcp light passes the sample.

where n is the average refractive index of the cholesteric phase.[17] The pitch is also known to be temperature dependent in some systems and the colour of reflected light will normally change from blue to red upon cooling.

Lastly, the cholesteric phase is optically uniaxial negative, with the ordinary refractive index n_o being larger than the extraordinary refractive index, in contrast to nematic phases.

The cholesteric or chiral nematic phases are usually abbreviated as N*.

1.2.3 Smectic order.

Smectic phases are characterised by long range positional order in addition to the long range orientational order typical of mesomorphic phases. This causes the molecules to be arranged in layers with respect to their centres of gravity, the inter-layer attractions being weak in comparison to the lateral forces existing between the molecules, thus making layer slippage possible. This gives rise to the fluid characteristics of the smectic phases, however, their viscosity is markedly higher than that of the corresponding nematic and cholesteric phases.

Of the eleven different smectic modifications identified to date (alphabetically termed smectic A to K and abbreviated S_A, etc.)[18] those with lower ordering have the molecules within the layers randomly distributed, and those with higher ordering have the molecules arranged in a lattice-like two dimensional structure. In the latter case the arrangement can be almost crystal-like and there has been some contention in the past as to whether the said phases were in fact liquid crystalline.[19] Some modifications of both lower

and higher order also have a tilted structure, with the molecules being tilted at an angle to the layer normal. This is usually attributed to strong dipole effects between the molecules.

Only the four more well-defined smectic phases will be discussed in the following section since they are the most commonly observed phases, especially in the case of liquid crystalline polymers. The other modifications, although no less important, are structurally similar and are therefore not considered here for reasons of brevity.

1.2.3.1 The smectic A phase.

The smectic A mesophase is the smectic polymorphic modification which possesses least order. If the smectic A mesophase is present in addition to other smectic phases, then it usually precedes the others on cooling either the isotropic liquid or the nematic phase.

Although studied by Friedel as early as 1922[8] and termed as smectic in nature, Friedel only studied smectogens of the A type, therefore smectic polymorphism lay undetected for many years. It was not until much later that it was assigned the code letter A by Sackmann and Demus.[20]

Early structural studies (e.g. X-ray diffraction) carried out on this mesophase have shown that the molecules are arranged with their long molecular axes perpendicular to the plane of the layers, the lateral distribution of the molecules within the layers being random. This is shown schematically in figure 1.5, with the smectogens being represented as cylinders due to their ability to undergo rotation about their long axes.

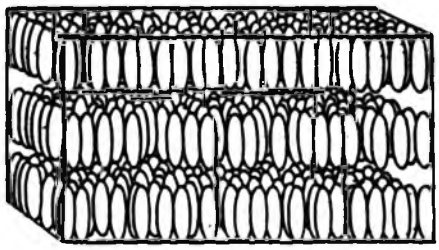

FIGURE 1.5 Schematic representation of the smectic A phase showing the random distribution of mesogens within the layers.

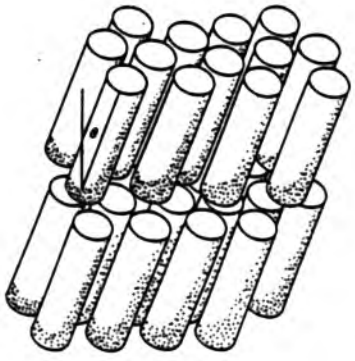

FIGURE 1.6 Schematic representation of the smectic C phase with tilt angle θ. There is no regular arrangement of the mesogens in the planes of the unstructured layers.

Although this simple model is acceptable for most purposes, more detailed investigations carried out in recent years have revealed a number of deficiencies.

Firstly, numerous X-ray and neutron diffraction studies have shown the lamellar spacing to be much shorter than the corresponding calculated "all-trans" molecular length. This has been attributed to the molecules being randomly tilted within the layers, with each molecule having the ability to oscillate a small distance up or down within the layers. This can be accompanied by either a rotation about the long axis or a precession about the molecular centre of mass (depending on the angle of tilt)[21,22] and therefore suggests a very diffuse layer situation, in contrast to the simple layer model.

Secondly, in some cases, notably those where the molecules contain a terminal cyano group, the lamellar spacing has been shown to be greater than the molecular length (by approximately 1.4:1). Evidence from X-ray diffraction and neutron scattering has shown this to be due to an inter-digitated anti-parallel bilayer structure caused by the highly polar end groups.[23]

The orientational ordering in the smectic A mesophase can be described by the order parameter S as used in section 1.2.1 to describe the nematic phase. The smectic A phase is also said to be optically positive uniaxial,with the optical axis being parallel to the long molecular axes.

1.2.3.2 The smectic C phase.

The smectic C mesophase can be considered as the directionally

tilted analogue of the smectic A phase, with the molecules being tilted from the layer normal by an angle θ and the direction of tilt being constant over a considerable number of volume elements. (In the smectic A phase the molecules are only locally tilted and the angle on the whole averages out to zero.) A simple structural diagram is shown in figure 1.6.

Various models and theories have been proposed and these have been adequately discussed by Gray and Goodby.[18] Generally, it should be noted that molecules containing two alkoxy end groups with opposing dipole moments (originating from the ether oxygen atoms) favour the formation of the smectic C phase and that the tilt is probably caused by a dipole-induced dipole interaction between the molecules.

1.2.3.3 The chiral smectic C phase.

The smectic C mesophase exhibited by compounds that are chiral in nature is itself optically active and is termed chiral smectic C (denoted S_C^*). Its structure is essentially similar to that of the achiral smectic C phase except for the distribution of the molecular tilt directions. By considering a particular layer in a chiral smectic C phase, one can assume that the tilt directions of the molecules in the layers directly above and below are turned through small angles in opposite senses with respect to the tilt director of the reference layer - see figure 1.7.

The tilt directors therefore form a helical distribution on moving from layer to layer with the helix having a temperature sensitive pitch length and tilt angle. As in the case of cholesteric liquid

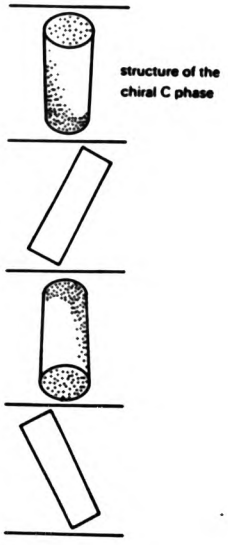

FIGURE 1.7 Schematic representation of the helical structure of the chiral smectic C phase.

crystals, when the pitch length is of a suitable size the reflection of irridescent colours can be observed, the wavelength and colour of the light being temperature dependent. In all of the chiral smectic C phases studied so far the temperature dependence of the wavelength of reflected light has been shown to be the opposite of that observed in most cholesteric phases, i.e. the colour of the chiral smectic C phase changes from red to blue on cooling. This is consistent with an increasing tilt angle and decreasing pitch.

Chiral smectic C phases also display a spontaneous net polarisation parallel to the layers due to the presence of the chiral centre, causing the molecules to have ferro-electric properties. Thus, by applying an external electric field it has been shown that it is possible to switch the molecules from one orientation to another in very fast (μs) times. Current nematic switching displays operate at much slower rates (ms).[24]

1.2.3.4 The smectic B phase.

In contrast to the smectic A and C mesophases, the smectic B is of a more ordered nature, possessing order within the layers. Early X-ray diffraction and microscopic studies of the smectic B phase showed that the molecules were arranged in layers with the molecular centres positioned in a hexagonally close-packed array. The long molecular axes have been shown to be orthogonal to the layer planes and this gives rise to the positive uniaxial optical characteristics of the material. Rapid cooperative rotation of the molecules about their long molecular axis has also been shown to occur. Figure 1.8 shows a simplified model of the B phase.

As with the smectic A phase the smectic B phase was not

assigned a code letter until 1966. However, since then there has been much contention in the literature as to the true nature of the mesophase, i.e. as to whether it is a highly ordered mesophase or in fact a crystalline solid phase. More recent work has shown that some materials can form both a crystal smectic B and a liquid crystalline (hexatic) smectic B phase, with the enthalpy associated with the crystal B-hexatic B transition being very small indeed (0.02-0.05 cal/g). A detailed discussion of published works in this area is provided in "Smectic Liquid Crystals" by Gray and Goodby (reference 18).

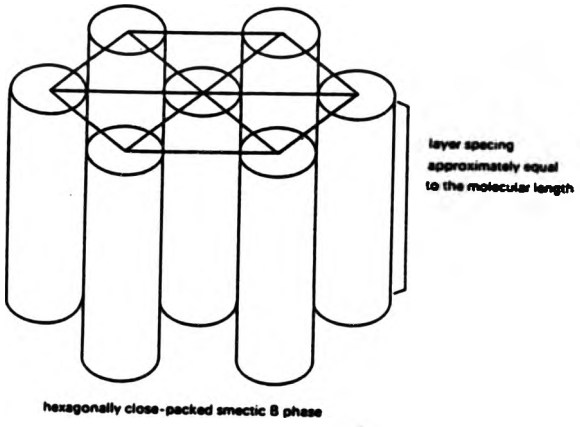

FIGURE 1.8 Schematic representation of the hexagonally close-packed smectic B phase (simplified model). The rotating molecules are orthogonal to the layers and are depicted as smooth cylinders.

1.2.4 Liquid crystalline polymorphism.

Many thermotropic materials have been observed to pass through more than one mesophase on either heating or cooling. The order of stability of these mesophases can be predicted by making use of the fact that raising the temperature of a material results in the progressive destruction of molecular order. Thus, the more ordered the mesophase, the closer in temperature it lies to the solid phase. From the descriptions of the various types of order discussed earlier, the following conclusions can be drawn:

1. If a material exists in the nematic phase as well as the smectic A, B and C phases, then the order of mesophase stability with respect to temperature will be

   solid ⟶ smectic B ⟶ smectic C ⟶ smectic A ⟶ nematic ⟶ isotropic

   This order of stability agrees with experimental observation.[18]
2. It has also been confirmed experimentally that, for a material having nematic and/or smectic phases, but not all of those listed in 1, the order of stability can be deduced from 1 by simply deleting those phases not present.[18]
3. For materials exhibiting both cholesteric and smectic phases the order is identical to that shown in 1 except 'nematic' is replaced by 'cholesteric', e.g.

   solid ⟶ smectic A ⟶ cholesteric ⟶ isotropic.

It should also be noted that there are no known examples of polymorphism involving both nematic and cholesteric phases unless in the presence of an external field where the cholesteric helix can be 'untwisted' to form the nematic phase.[25,26]

Materials which show the same mesophases on heating as on cooling are termed 'enantiotropic' liquid crystals. Those which show

meta-stable mesophases only on cooling are termed 'monotropic'.

Liquid crystal polymers also show the same polymorphism. However, most of the polymers synthesised have only exhibited the smectic A, B, C and S_C^* phases. It is only recently that a polymer exhibiting the smectic F and smectic G phases has been reported.[27]

1.3 Chemical Constitution of Liquid Crystals

As mentioned in section 1.1, molecules which give rise to thermotropic mesophases are normally lath-like or rod-like in shape, fairly rigid, contain permanent dipoles, and exhibit a high level of polarisability.

Most of the liquid crystalline materials synthesised until now can be typified by the following general structure;

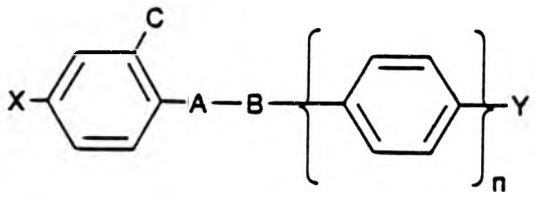

(I)

where X and Y represent a range of terminal substituents such as alkyl, alkoxy, alkylcarboxy and cyano groups; A-B represents a

linking unit which maintains molecular rigidity, planarity and linearity; C can be a laterally attached small group such as bromo, chloro or nitro; and n normally has a small integer value. Various examples of terminal groups, central linking units and laterally attached substituents are shown in figure 1.9.

Terminal groups which extend the molecules along the molecular axis without increasing the breadth too much usually increase the thermal stability (isotropisation temperature or clearing temperature, T_{Cl}) of a mesophase. Such substituents increase the anisotropy of molecular polarisability ($\Delta\alpha$), particularly if they conjugate with the aromatic ring(s). Likewise, central groups which preserve conjugation throughout the core structure increase $\Delta\alpha$ and conversely, large or extremely polar lateral substituents decrease $\Delta\alpha$. Smectic mesophase formation is favoured at the expense of nematic or cholesteric phases when long alkyl terminal groups are present and nematic phase formation is favoured by the presence of short, polar terminal groups e.g. methoxy and cyano moieties.

By substituting either or both of the aromatic rings for a cycloalkyl moiety one would expect the mesophase stability to decrease due to the resulting decrease in $\Delta\alpha$. However, it has been found that molecules containing cyclohexyl moieties enhance the mesophase stability and in fact the presence of [2.2.2] bicyclooctane rings in some molecules can enhance the stability even further.[28] Gray has proposed that molecules may display an unexpectedly high mesophase stability when they have regions of high and low polarisability.[29] It is worth remembering at this point that the first liquid crystals studied were derivatives of cholesterol,[1] which are of

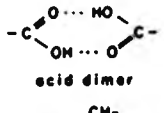

acid dimer

-CH=CH-

olefin

-C≡C-

acetylene

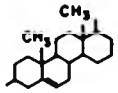

Δ^5 - steroid

-CH=N-

azomethine
(Schiff's base)

nitrone

-N=N-

azo

azoxy

ester

$CH_3(CH_2)$-	ALKYL - MAY BE BRANCHED
RO-	ALKYLOXY; ALSO INTERNAL ETHERS
	CARBOALKOXY
	ALKYLCARBOXY
	ALKYLCARBONATO
F, Cl, Br, I	HALOGEN
- CN	CYANO
$-NO_2$	NITRO
R_2N-	AMINO R MAY BE H

FIGURE 1.9 **Examples of central linking units and terminal groups. The latter four examples can also be laterally attached substituents.**

course largely composed of cyclohexyl ring units and that these derivatives owe their ability to form mesophases to their long rod-like shape:

(II)

1.4 Applications of Liquid Crystals

Low molecular weight liquid crystals have the unique ability to change their macroscopic properties (colour, light transmittance, etc.) instantaneously when subjected to small external perturbations. These may include slight changes in electric, magnetic or thermal fields, stress, or even changes in the chemical composition of their environment. This has led to their application in many diverse areas of technology such as electronics, electro-optic displays, holography, thermal mapping and remote pressure, chemical or radiation sensoring.[30] Uses have also been found in chemistry as media for chemical reactions[31,32] and they are actively used in medicine as disposable thermometers. More recently they have been used to produce temperature sensitive coloured textiles, works of art and mood-indicating jewellery.[14]

It is obvious that in some of the cases mentioned above the liquid crystalline material itself cannot meet the necessary structural

requirements. Usually, these materials are hermetically sealed in membranes by polymer dispersion techniques or micro encapsulation so that they can be shaped or coated and also remain protected from any harmful external effects. The logical step forward from this approach was therefore to incorporate the liquid crystalline units into a polymer chain, either as part of the main back-bone or as a pendant comb-branch. This has resulted in the concept of polymer liquid crystals (PLCs) and has led to the synthesis of materials which successfully combine the unique properties of low molecular weight liquid crystals (LCs) with the properties normally associated with the polymer matrix (fibre and film forming properties, ease of processing, etc.).

1.5 Polymeric Liquid Crystals and their Thermal Properties.

One of the main differences between PLCs and LCs which originates from the macromolecular nature of the former, is the ability of some PLCs to undergo a glass transition (Tg) at lower temperatures. The Tg of a polymer can be simply defined as the temperature below which an amorphous polymer is in the glassy state and above which the polymer is rubber-like. On a molecular level, the Tg can be defined as the temperature above which long-range cooperative motion of the backbone can occur (macro-Brownian motion) and below which the motion is frozen.

In the case of PLCs, the polymer is normally transformed into a rubbery liquid crystalline state above the Tg, unless crystalline structure is present, in which case the crystalline phase precedes the

LC phase. Figure 1.10 shows the relationship between Tg, the melting temperature (Tm) and the clearing (isotropisation) temperature (T_{Cl}) for both crystallisable and non-crystallisable PLCs.

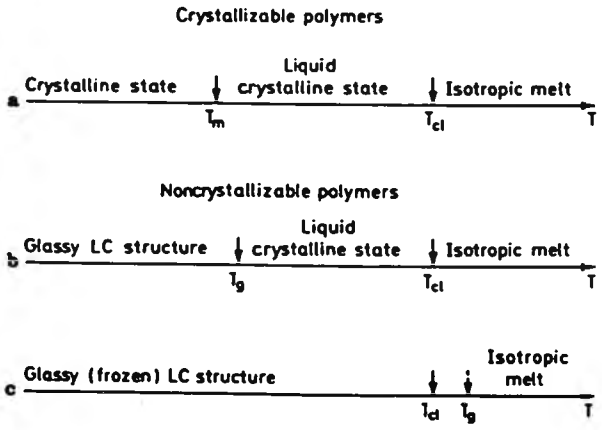

FIGURE 1.10 Relationship between the glass transition temperature (Tg), melting temperature (Tm) and the clearing point (T_{Cl}) for LC polymers.

In figure 1.10a the typical thermal behaviour of a crystallisable polymer is outlined, which is analogous to that of small molecule LCs. It is mainly polymers of the main chain type or linear polymers which show this behaviour.

In figure 1.10b and c on the other hand, the step-wise thermal

behaviour of non-crystallisable polymers is shown. The situation when the Tg is well below T_{Cl} is illustrated in figure 1.10b. This type of thermal behaviour is characteristic of the majority of side chain (comb-branch) polymers where the mesogen is separated from the backbone by a flexible spacer (e.g. small polymethylene chain), as depicted in figure 1.11. In contrast to small molecule LCs which usually crystallise on cooling, polymers such as these undergo a glass transition before crystallisation of the mesogenic segments can occur. This is because the cooperative motions of the polymer backbone, on cooling below Tg become progressively restricted, and consequently the motions of the anisotropic side chains are also slowed down, thereby impeding crystallisation. Below Tg, only localised segmental motion can occur, along with the possible rotation of the mesogenic units in the side chains.

Since the flexible spacer portion of the polymer has the effect of 'decoupling' the cooperative motions of the backbone from the anisotropic interactions of the side chains, the chemical constitution of the backbone, although having a strong influence upon the Tg, has little or no effect on the nature of the mesophase.[33] Only the chemical constitution of the mesogenic side chains influence the nature of the mesophase. This means that simply by choosing an appropriate backbone, it is possible to control the Tg of the system without affecting the type of mesophase. In other words, the LC structure, which is in the form of ordered domains 'dispersed' in a statistically disordered polymer matrix, can be 'frozen' into the glass at a temperature determined mainly by the nature of the polymer backbone, with no appreciable effect on the structure (as long as the cooling rate is fast enough).[34] The 'spacer' concept is discussed

further in section 1.6.3.

The possibility of fixing the LC phase of these comb-branch polymers in the glass has led to their application in information storage systems, e.g. as laser addressed data storage media,[35] passive display media[36] and holographic image storage media.[37,38] It also leads to the possibility of fixing the cholesteric structure in the glass.[34]

If no flexible spacer is present between the mesogen and the backbone, then the situation depicted in figure 1.10c arises, where the Tg is higher than the hypothetical T_{Cl}. This results in LC order being 'frozen-in' on polymerisation of the LC monomer. However, if the temperature is raised past Tg then all the LC order is irreversibly lost and cannot be reformed on cooling. This is also discussed further in section 1.6.3.

1.6 Polymer Liquid Crystals and their Classification.

At present, at least four main types of thermotropic polymer liquid crystals have been identified - these are:

1. The melts of some linear crystallisable polymers;
2. Polymers with mesogenic groups incorporated within the backbone;
3. Polymers bearing pendant mesogenic groups (comb branch PLCs); and
4. Polymers that are a combination of 2 and 3.

Figure 1.11 outlines types 2, 3 and 4.

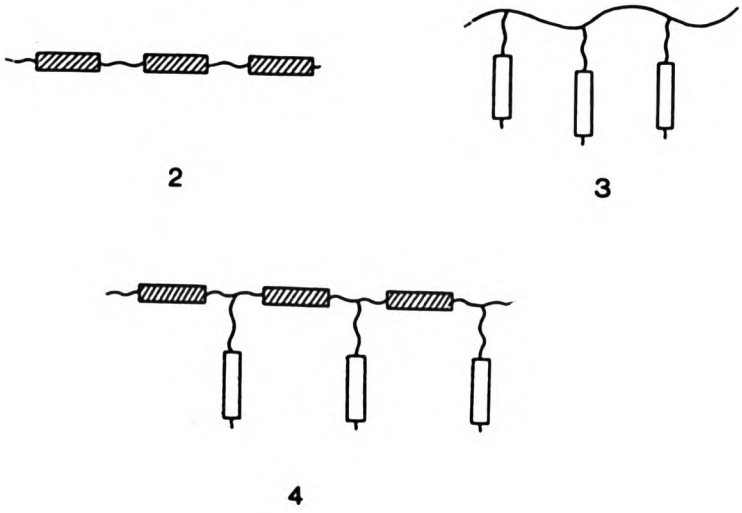

FIGURE 1.11 Schematic representations of some different types of liquid crystalline polymers.

1.6.1 The liquid crystalline state in the melts of linear crystallisable polymers.

For the overwhelming majority of flexible-chain polymers which do not contain distinct mesogenic structures the sizes of the regions of spontaneously ordered segments formed is too small for the manifestation of the anisotropic LC state (in the absence of external orienting fields). Nevertheless, a number of investigators have reported LC formation in the melts of some linear polymers;[39] their results are based on the electron diffraction studies of a series of crystalline polymers (e.g. poly(ethylene), poly(trifluorochloro ethylene) and poly(ethylenesebacate)). These workers showed that some of the ordered regions (up to 25Å) exhibit a nematic-like ordering of the chains. Quenched isotactic poly(propylene) which has a helical conformation has also been reported to possess a metastable LC state.[40] In this case the helical chains are said to be arranged parallel to each other in an almost smectic-like fashion.

Both poly (diethylsiloxane)[41] and a variety of alkoxy- and aryloxy-poly(phosphazenes)[42,43] have also been shown to produce stable liquid crystalline melts. However, the causes of the formation and the exact nature of the mesophase in these cases still remains unclear. It should be noted that most of the investigators of these polymers (and others) tend to conclude that LC structural order, but not a thermodynamically stable LC phase is present.

1.6.2 Main chain liquid crystalline polymers.

As early as 1956 Flory postulated the criteria for the formation of a single anisotropic phase in solutions of rigid and semi-flexible

polymers.[44,45] It was shown later[46] that some lyotropic systems, namely poly(γ-benzyl-L-glutamate), compared favourably with Flory's predictions, with the anisotropic (nematic) solutions exhibiting very low shear-rates and viscosities,[47] lower even than those of the isotropic fluid phase. This led to intensive research in both industry and academia, with the realisation of the possibility of producing high tensile strength fibres by spinning these anisotropic solutions. Consequently, Du Pont commercialised their exceptional Kevlar^{R} polyamide,[48] whose structure is based upon poly(p-phenylene terephthalamide), by spinning the fibre from anisotropic solutions of the polymer in sulphuric acid.

The criteria postulated by Flory[44,45] can also be interpreted as applying to polymers where the solvent concentration is zero, and therefore to thermotropic as well as lyotropic systems, with the first examples of deliberately synthesised main chain thermotropic PLCs being reported in 1975. Among these was a paper by Roviello and Sirigu[49] which reported a series of polyesters consisting of regularly alternating rigid and flexible segments, where the rigid segment was derived from a nematic compound of low molecular weight. This is the type of polymer depicted in figure 1.11.

A vast amount of work on this type of polymer has since been published, with the main impetus being to produce novel high modulus fibres. Some of this work has described polymers containing chiral centres in the flexible portion, with the realisation of cholesteric phases and the possibility of the production of high-strength coloured mouldings.[50,51] The use of cyclo-alkyl rings as substitutes for either the rigid or flexible segments for such structures has also been reported.[51]

1.6.3 Comb-branch liquid crystalline polymers.

Early studies on the synthesis of side chain (comb-branch) PLCs afforded mainly polymers with the mesogenic unit attached directly to the backbone.[52] In most cases, LC monomers which consisted of a mesogen coupled directly to a vinyl moiety were polymerised to produce only non-mesomorphic polymers. The order was either apparently lost on polymerisation, or else locked-in to the glassy state of the polymer and subsequently lost irreversibly, after heating above Tg. This is presumably due to both the excessively high Tg being above the hypothetical clearing point (as shown in figure 1.10c) and the anisotropic packing of the side chains becoming sterically hindered. There are, however, exceptions to this effect, as shown by poly(p-biphenyl acrylate)[53] and in polymers where the original LC phase of the monomer has been retained by crosslinking.[54]

In an attempt to produce enantiotropic liquid crystalline polymers which would exist in a stable LC phase above Tg and have a thermal behaviour as described in figure 1.10b, Finkelmann[55,56] and Shibaev and Plate[57] introduced the 'spacer' concept. These workers independently showed that LC polymers exhibiting distinct LC phases could be prepared by introducing a flexible spacer between the polymer backbone as the mesogen. As mentioned earlier in section 1.5, the effect of this flexible spacer is to decouple the cooperative motions of the polymer main chain from the anisotropic interactions of the mesogenic side chains, thereby allowing the mesogenic character of the monomer to be preserved in the polymer.

These comb-branch PLCs bear strong similarities to

conventional small molecule LC compounds. Both smectic and nematic materials may be obtained, and as is commonly observed in small molecule systems, the tendency towards an increased smectic character grows as either the spacer length is increased or the terminal tail is lengthened, i.e. as m and n in the following structure are increased:

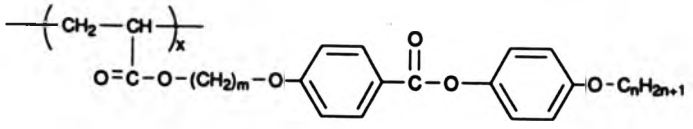

(III)

Also, by substituting the alkyl tail with the more polar nitrile group, nematic polymers are possible and by making the backbone more flexible, the mesophase temperature range can be increased (lower Tg) with little effect on T_{Cl}.[33]

Observations such as these led Finkelmann[58] to conclude that, providing the polymer main chain does not influence the mesogenic side groups too strongly, i.e. when the spacer is sufficiently long, then formation of the polymer LC phase will essentially follow the principles for conventional LCs.

Finkelmann[58] also suggested that an increase in LC order would occur on going from the monomer to the polymer, since his results[55,56,58] and others[57] showed that nematic polymers were usually produced from non-mesomorphic or monotropic nematic monomers, and similarly, nematic monomers gave rise to smectic

polymers. Vast numbers of publications in following years have since borne this out.[39]

There are two possible routes to the synthesis of such comb-branch polymers - these are:

1. Synthesis of monomers containing mesogenic units and their subsequent polymerisation (or copolymerisation).
2. Reaction of low molecular weight LCs with suitably reactive polymer sites (polymer analogous reaction).

Figure 1.12 shows these pathways in schematic form.

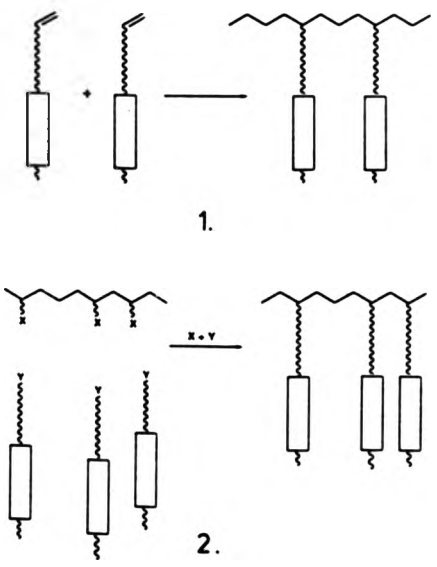

FIGURE 1.12 Schematic diagram of the synthetic routes to comb-branch liquid crystalline polymers. Route 1 is the mesogenic monomer polymerisation method and route 2 is the polymer analogous method.

Route 1 is the most commonly followed route, since control of the functionality of the final product is possible, i.e. the structure of each monomeric moiety within the polymer is exactly the same. The only disadvantage of this approach is the unknown polymerisability of the newly made monomers and the possibility of obtaining only oligomeric material when very large monomers are used.

Route 2 on the other hand requires 100% reaction of all the polymer sites, which of course is not always possible. This leads to some ambiguity about the sequence of mesogenic segments bound to the polymer and the possible detrimental effect of having unreacted groups present which may adversely affect mesophase formation.

The most widely employed polymer analogous reactions are those where poly(hydrogen methyl siloxane) is combined with the appropriate olefin-terminated mesogenic species in the presence of a platinum catalyst.[59,60] It appears that the reproducibility of the results of this hydrosilylation reaction are very dependent on both the source of the polymer and on the age of the catalyst when Spier's catalyst (hexachloroplatinic acid in 2-propanol) is employed.[61] Percec, however, has recently found dicyclopentadienyl-platinum(II) chloride in toluene to be superior.[62]

Other methods reported include condensing poly(acyl-chlorides) with suitable hydroxy-terminated species[63] and condensing the sodium or potassium salt of a poly-acid (e.g. poly(acrylic acid)) with a suitable bromo-terminated mesogenic species as first reported by Keller.[64] The latter method has recently been called into dispute in the open literature however, after Chen and Maa re-examined Keller's procedure and found the products to be low molecular

weight compounds rather than the expected polymer.[65]

1.7 Comb-branch Liquid Crystalline Polymers with Chiral Side Chains.

The primary aim of the work embodied in this thesis was to synthesise and characterise novel chiral nematic and cholesteric PLCs which would exhibit selective light reflection in the visible region of the spectrum. Because of the polymeric nature of these materials it is possible to freeze the textures that give rise to their unique optical properties (see section 1.2.2) in the glass by quenching the material from the chiral nematic phase. This can only be achieved if there are no smectic or crystalline phases present at lower temperatures (i.e. existing between the glass and chiral nematic phases). This quenching process can lead to the possibility of obtaining monochromatic films which could be utilised as selective light reflectors, dichroic filters or as coloured coating materials. It should be noted here that the colour reflected (as in the case of coatings) is due only to the helical nature of the mesophase and is not imparted by any dye or chromophore in the polymer matrix.

As a large number of publications have already appeared in the literature concerning this aspect of PLC research, it was thought appropriate to review these works in order to identify new approaches to the synthesis of these materials. Publications appearing before 1984 have already been adequately reviewed by Chiellini and Galli;[66] Finkelmann and Rehage;[33] and Shibaev and Plate.[34] These will only be discussed briefly here.

Early attempts to prepare cholesteric PLCs by the

homopolymerisation of cholesteryl containing monomers (e.g. cholesteryl acrylate and cholesteryl methacrylate) resulted in only smectic structures.[67,68,69] This is due to the effect observed and interpreted by Finkelmann[58] (noted in section 1.6.3), where the mesophase of the monomer becomes more ordered on polymerisation. Finkelmann later managed to circumvent this problem by reacting isotropic, optically active, olefin-terminated 'monomers' with poly(hydrogen methyl siloxane) by the hydrosilylation method mentioned in the previous section.[70,71] The following polymers were prepared and the reflection of infra-red and visible light from homogeneously oriented samples reported.

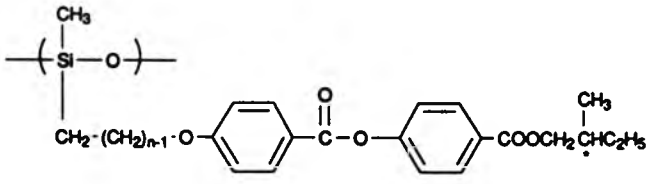

(IV)

The most convenient and controllable route to chiral nematic polymers later stemmed from the principles employed by Finkelmann and a large number of cholesteric structures having the desired properties have since been prepared. These are generally prepared by the copolymerisation of either:

1. Two optically active mesogenic monomers.
2. Non-mesogenic, optically active monomers with achiral mesogenic monomers, or

3. Optically active, mesogenic monomers with achiral mesogenic or non-mesogenic monomers.

Table 1 shows examples of some of the structures studied, where the chiral monomer is a cholesteryl derivative in all but one case.

The advantage of this route to cholesteric polymers is in the ability with which the wavelength of reflected light (λ_R) can be controlled. λ_R, which is directly proportional to the pitch of the helix (section 1.2.2) has been found to vary in an inverse manner to the mole fraction of chiral moieties in the copolymer (F_{CH}), i.e.

$$\lambda_R \propto 1/F_{CH} \qquad (1.5)$$

In other words, by increasing the mole fraction of chiral monomer in the polymer, λ_R can be shifted to the blue end of the spectrum. It has also been observed by these workers that λ_R does not depend on temperature, except in the case of copolymers 5.1, 5.2 and 5.3, where the pitch (and λR) decreases when the temperature is raised. This effect is common in small molecule cholesteryl LCs[78] and in some PLCs,[79] when smectic phases are present at temperatures below the cholesteric phase and can be attributed to an un-twisting of the helical structure.

Since 1984 cholesteryl containing polymers have continued to be of interest, particularly to Soviet workers.[80,81] However, there has also been increased interest in homopolymers where the chiral monomer is not a cholesteryl derivative, but instead contains the (S)-2-methylbutyl residue.[82-87] This chiral moiety is attached to the tail-end of the mesogen by either an ester or an ether linkage, as in

TABLE 1 Cholesteric LC Copolymers Containing Chiral Units

No.	General formula of the copolymer		Concentration of chiral units in the copolymer,* mole %	T_g, °C	T_{cl}, °C	λ max of selective reflection of light, nm (20°C)	Reference
1.1	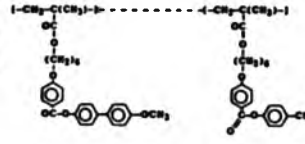		90.6	70	247	1260	72
1.2			83.6	73	229	712	
1.3			79.8	77	216	562	
1.4			75.3	80	203	467	
2.1	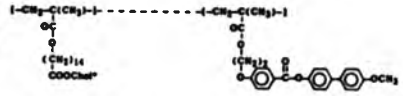		12	132	260	1500	73
2.2			16	125	245	1200	
2.3			24	117	238	1100	
3.1	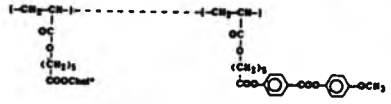		35	48	103	495	74
4.1	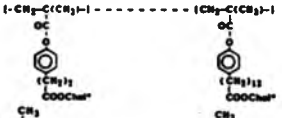		51†	–	209	–	75
5.1	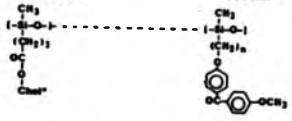	n = 3	3-15	–	–		76
5.2		n = 4	5-15†	–	–		
5.3		n = 5	5-15†	–	–		
6.1	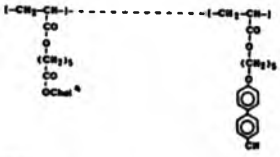		19	50	98		77
6.2			28	50	102		
6.3			36	55	105		
6.4			52	55	115		

*The chiral group in the copolymer is indicated by an asterisk.
†Concentration of the chiral monomer in the initial monomeric mixture.

the following example:[83]

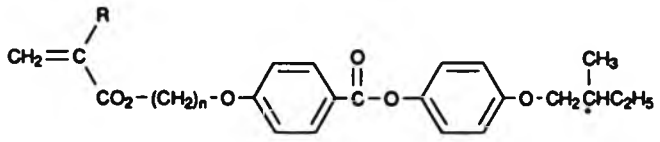

R = H, Cl or CH_3; n = 2, 6 or 11.

(v)

The main reason behind the synthesis of these types of polymer is that, in addition to chiral nematic phases, they also exhibit chiral smectic C phases (S_C^*) at lower temperatures. Utilising these types of polymers as ferro-electric molecular switches is of evident interest (see section 1.2.3.3).

Another area of interest where these types of polymer are applicable is in their utilisation as stationary phases for high resolution gas chromatography.[88] The reported polymers had, in addition to the terminal (S)-2-methylbutyl groupings, short flexible spacers (one or three carbons) and flexible siloxane backbones. These polymers exhibited smectic phases in addition to chiral nematic phases and the presence of the smectic phases were said to enhance the separation properties of the chromatographic medium substantially.

A new series of polymers, some of which are reported to exhibit

chiral nematic phases were recently reported by Finkelmann's group in Freiburg.[89] The polymers reported are a new variety of biaxially nematic and chiral nematic side chain polymers, where the mesogenic groups are attached laterally to a polymethacrylate backbone:

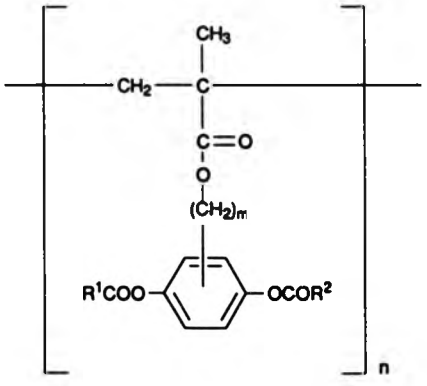

(VI)

The copolymer exhibiting a chiral nematic phase consisted of 87.5 mol% of a monomer where m=11, R^1=R^2=4-n-butoxy phenyl and 12.5 mol% of a monomer where m=11 and R^1=R^2=4-(S)-2-methyl butoxy phenyl. However, no planar microscopic textures exhibiting selective light reflection were reported.

1.8 Aims and Scope of Present Work.

The main aim of this work was to synthesise and characterise

novel chiral nematic polymer liquid crystals of the comb-branch type, with the intention that they may be of use as new coloured coatings materials, or possibly as optical filters etc.

Of the polymers reported in the literature so far, the majority contain the cholesteryl grouping. This almost precludes the possibility of their use as coatings materials, especially in external environments, due to their susceptibility to oxidative degradation. A worthwhile study was therefore the examination of stable, non cholesteryl-containing polymer systems.

Two main objectives can be identified from this. Firstly, from the literature it was apparent that no-one had yet prepared optically active, mesogenic comonomers where the chiral centre is incorporated in the flexible spacer part of the molecule. A novel synthetic route to this type of monomer was therefore established and three monomers were prepared. These monomers were then copolymerised with non-optically active mesogenic monomers, some of which were also novel, and the resultant copolymers were found to exhibit chiral nematic phases at certain compositions.

An alternative route to the formation of chiral nematic phases was also investigated. This stemmed from the observation that when host nematic phases of conventional liquid crystals are doped with small amounts of optically active, non-mesogenic materials, the phase is transformed into a chiral nematic phase.[13]

By transferring this concept to PLCs, an attempt was made to arrive at induced chiral nematic phase formation by the copolymerisation of mesogenic monomers with non-mesogenic, optically active monomers.

In addition to the approaches outlined above, two previously unreported cholesteryl-containing monomers based on itaconic acid were prepared. One of these was copolymerised with a known, previously reported monomer and the resultant copolymers were found to exhibit chiral nematic phases.

CHAPTER TWO

MESOPHASE IDENTIFICATION

2. MESOPHASE IDENTIFICATION

Four of the most definitive techniques used for the identification of the mesophases of low molecular weight liquid crystals are the following:

1. Thermal characterisation by differential scanning calorimetry (dsc).
2. Textural observations by polarising microscopy.
3. Miscibility studies of the newly synthesised compounds with known compounds having well characterised phases.
4. X-ray diffraction studies on either powder or oriented samples.

In the case of comb-branch PLCs however, a combination of these methods is generally required, owing to the high viscosity, the broad molecular weight distribution, and the existence or co-existence of poly crystalline and amorphous phases in these materials. Nevertheless, in many cases mesophase identification can be achieved by using only the first two methods.

2.1 Differential Scanning Calorimetry

The essential features of the phase behaviour of comb-branch liquid crystalline polymers is now relatively well established[90,91] and the dsc technique is widely used as a reliable method for the detection of thermotropic mesophase transitions in conjunction with hot-stage polarising microscopy (hsm).

Conventional liquid crystals typically show two (or sometimes more) first order endothermic events on the dsc heating trace which are usually associated with the crystal-mesophase and mesophase-isotropic transitions. Additional endotherms indicate either mesophase-mesophase or crystalline-crystalline transitions. Figure

2.1(a) shows an example of this.

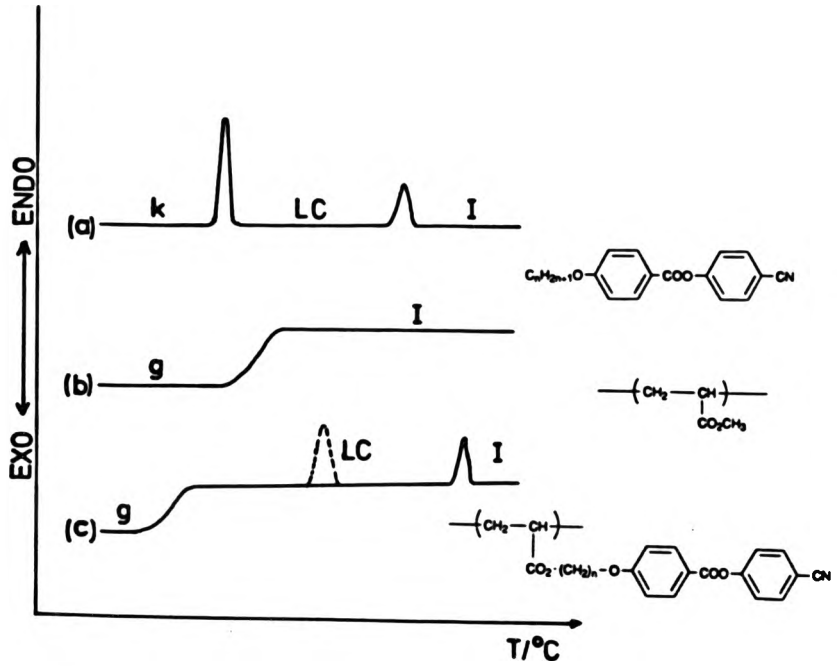

FIGURE 2.1 Dsc curves of (a) a typical low molecular weight LC, (b) a conventional polymer, and (c) a liquid crystalline comb-branch polymer. The dotted peak represents either a crystalline-crystalline, crystalline-mesophase or a mesophase-mesophase transition.

The dsc heating trace of a comb-branch liquid crystalline polymer may have as its features a glass transition which is characteristic of the polymer backbone and a first order endothermic peak which is indicative of the transformation from the mesophase

to the isotropic melt. The latter transition is due (in most cases) only to the anisotropic, mesogenic side chains. Figures 2.1(b) and (c) show typical dsc heating traces for an ordinary polymer and a comb-branch liquid crystalline polymer respectively. It should be noted that the mesophase thermal stability (T_{LC-I}) of the conventional liquid crystal is substantially increased when it is attached to the polymer backbone. This is because the polymer backbone restricts translational and rotational motions and forces the mesogens together, thus increasing their anisotropic interactions.[33,56]

The glass transition of a comb-branch PLC is also normally lower than that of the corresponding polymer backbone on its own (e.g. compare figures 2.1(b) and (c)). This is merely due to internal plasticisation of the backbone by the mesogenic side chains,[34,92] when these are more flexible than the main chain.

There are, however, some complicating features which may arise from time to time whilst analysing some materials (whether they are low molecular weight or polymeric in nature) by dsc. For example, it is very difficult to assign transitions associated with the smectic C phase. Transitions such as those between the smectic A phase (which normally occurs at higher temperatures) and the smectic C phase, are usually only accompanied by a slight shift in the dsc baseline[18,93] and are said to be second order in nature.[18] In this case, microscopy and/or X-ray diffraction investigations are essential techniques for the unambiguous identification of the smectic C mesophase and its transitions.

Other difficulties also arise when analysing highly ordered or crystalline comb-branch polymers by the dsc technique. The glass transition temperature is sometimes very difficult to observe, due to the small change in heat capacity associated with this transition.[94]

In this case a technique such as dilatometry[95] must be employed for identification of the glass transition.

2.2 Textural Identification by Polarising Microscopy

Polarising microscopy is one of the most powerful and economically practical techniques currently used for the identification of liquid crystalline mesophases. Analysis of the optical textures of these materials between "crossed polarisers" mainly reveals information on the phase type present (i.e. whether it is nematic, cholesteric or smectic), and, especially in the case of low molecular weight liquid crystals, distinction can be made between the various smectic modifications. Reference works such as "Smectic Liquid Crystals" by Gray and Goodby[18] and "Textures of Liquid Crystals" by Demus and Richter[96] are therefore indispensable for comparison purposes in these investigations.

The textures of polymer liquid crystals on the other hand are sometimes a little harder to identify. This is because of their macromolecular nature, i.e. their high viscosity, the presence of molecular entanglements and structural defects etc. These materials therefore require longer annealing times in order to allow the mesogens to untangle themselves and align in such a fashion as to produce textures which are similar to those of their low molecular weight counterparts. Generally, PLCs form the same textures as conventional LCs (with the exception that they may not always be as perfect and that more defects due to chain entanglements are present), therefore the descriptions of the various textural features below can apply to both.

2.2.1 Textures of the nematic phase

Three of the most commonly observed textures of the nematic phase are the schlieren, threaded and marbled nematic textures.[91,96] The formation of these textures is the same for each when the isotropic melt is cooled: As the melt cools, nematic droplets separate from the isotropic liquid and, as cooling continues, they grow and coalesce to form large domains. These droplets characterise the nematic texture since they are not associated with any other mesophase.[96] The size and perfection of the domains formed from these droplets then determines the nature of the texture formed, along with any surface effects emanating from the glass-slides.

Homogeneous, planar textures where the molecules lie parallel to the glass-slides can only be obtained by specially treating the glass surfaces of the slides. This treatment can take the form of either the oblique evaporation of solid materials onto the surface or rubbing the surface in one direction with a material such as cotton.[97] Textures produced like this are normally of uniform birefringence and exhibit no interference colours. When untreated slides are used to produce nematic textures, the schlieren texture commonly arises. This texture can be described as a planar texture with regions of inhomogeneity which give rise to schlieren, or "dark brushes".[97] The photomicrograph in figure 2.2 shows a typical schlieren texture. These dark brushes, which meet at certain points, correspond to areas of extinction in the nematic liquid where the mesogens are aligned perpendicularly to the glass surface. Points can be seen where either two or four brushes meet. These points indicate structural defects[96] and from the observation of the former, the

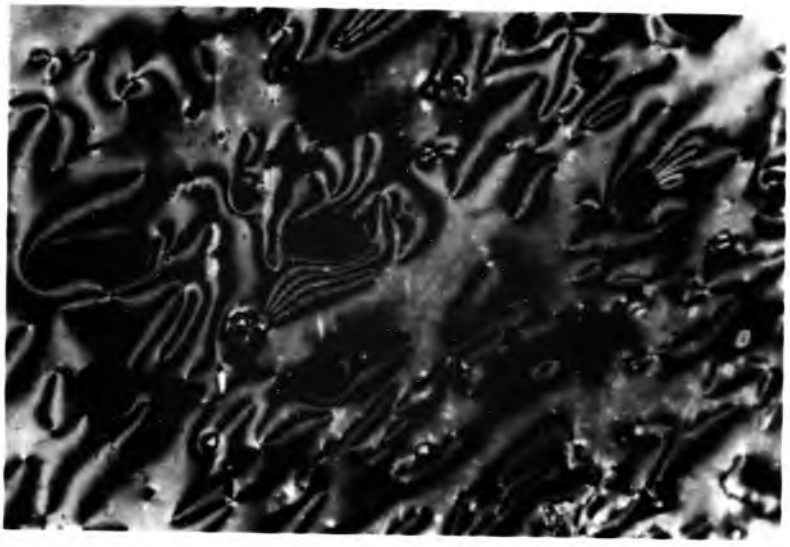

FIGURE 2.2 Photomicrograph showing a typical schlieren nematic texture (magnification x100).

FIGURE 2.3 Photomicrograph showing the marbled texture (all areas) and the threaded nematic texture (upper areas and left hand side areas) (magnification x200).

phase can be unambiguously identified as the nematic phase. Phases such as the smectic C or chiral smectic C give rise to schlieren textures with only four brushes.[18] Another point to note from the photomicrograph in figure 2.2 is its blurred appearance. This is especially typical in photomicrographs of low molecular weight nematic phases and is caused by the Brownian motion of the mesogens. This motion is much faster than the camera shutter speed and therefore causes the photomicrographs to appear blurred.

The photomicrograph displayed in figure 2.3 displays both of the other typical nematic textures, namely the marbled texture and the threaded texture (which can be seen in the upper and left hand sides of the photomicrograph). The marbled texture consists of several areas of different molecular orientation, with the orientation being nearly homogeneous in each of the areas. These areas of different molecular orientation are characterised by different interference colours. The threaded texture which is also seen to be present in the photomicrograph in figure 2.3 is caused by surface defects.[96] These defects give rise to the appearance of thin, thread-like lines, which are seen to adhere to the surface of the glass-slides.

In addition to the above textures, the nematic phase can also form the homeotropic texture if the glass-slides are suitably treated.[91] In this texture the mesogens (and therefore their optical axes) lie perpendicular to the glass-slides, therefore no birefringence is apparent. In contrast to the isotropic phase however, merely touching the coverslip of a slide on which there is a sample with a homeotropic texture, causes the field of view to brighten instantly. This is due to the applied mechanical force tilting the mesogens out of homeotropic alignment. Homeotropic textures can be prepared by

soaking the glass-slides in concentrated nitric acid for an hour, washing with distilled water the then finally rinsing them with acetone or propan-2-ol.[18]

2.2.2 Textures of the smectic A phase

Only two important microscopic textures are exhibited by the smectic A phase - the homeotropic texture and the fanned focal-conic texture.[18]

As in the case of the previously discussed nematic homeotropic texture, the smectic A homeotropic (or pseudo isotropic texture as it is sometimes known) is formed when the mesogens lie perpendicular to the glass-slides. Preparation of this texture is by the same technique as described for nematic homeotropic textures.

The focal-conic fanned texture is probably the most commonly observed texture of the smectic A phase. A typical example of this texture is shown in figure 2.4. This phase usually separates from either the isotropic liquid or nematic phase on cooling, in the form of bâtonnets[18,98] which are essentially needle-like, birefringent entities. This feature is caused by the rate of mesophase growth from the nucleation site being greater in one direction than another. After further cooling these bâtonnets grow, coalesce and reorganise their shape until finally, a focal-conic fanned texture is formed. Figure 2.5 shows an example of bâtonnets of the smectic A phase of a comb-branch polymer in the process of growing. The formation of these bâtonnets corresponds to the formation of droplets of the nematic phase.

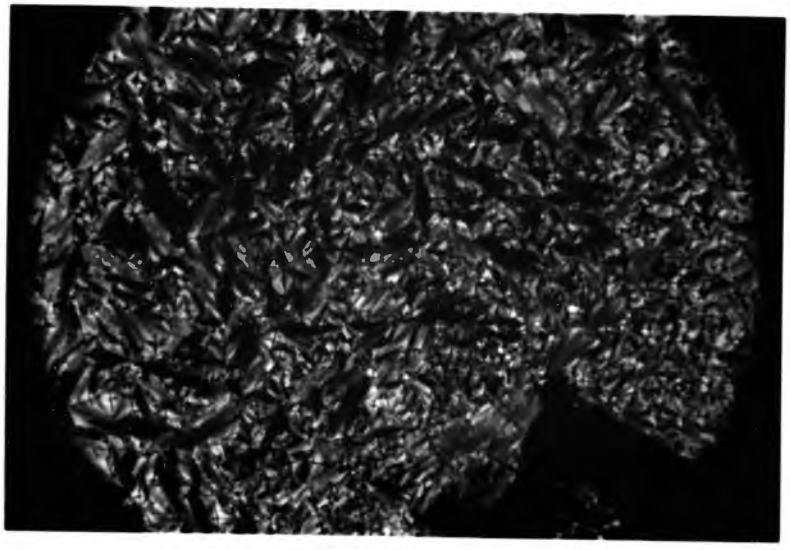

FIGURE 2.4 Photomicrograph of a typical smectic A fanned focal-conic texture (magnification x100).

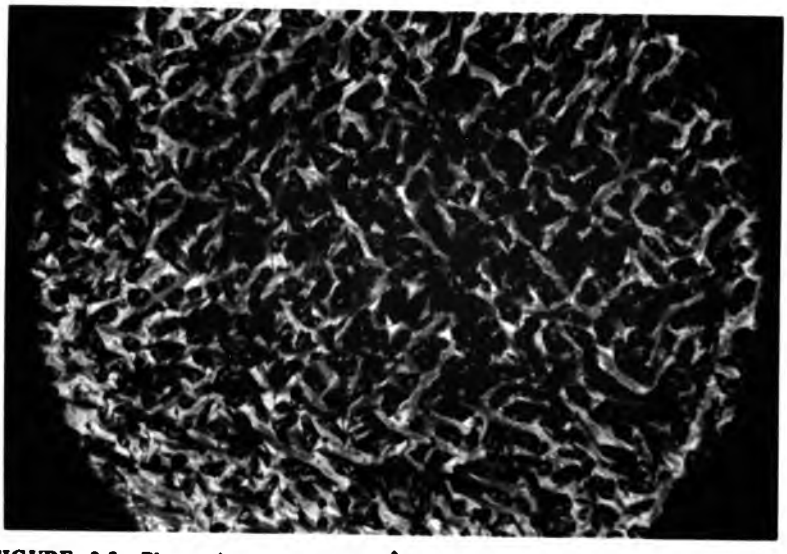

FIGURE 2.5 Photomicrograph of bâtonnets of the smectic A phase growing and beginning to coalesce (magnification x100).

2.2.3 Textures of the smectic B phase

There are two naturally occurring textures of the smectic B phase, namely the homeotropic texture and the mosaic texture.[18,96] These textures are termed natural, since they are only formed on cooling either the nematic phase or the isotropic liquid. As with the smectic A phase, the homeotropic texture is characterised by the layer planes of the molecules lying parallel to the glass supports (i.e. the mesogens themselves are perpendicular to the supports). The natural mosaic texture on the other hand is characterised by having several areas of different molecular orientation. These areas appear as platelets[18] in the microscopic texture, as displayed by the photomicrograph in figure 2.6.

The smectic B phase also exhibits a paramorphotic focal-conic fanned texture. This is not a natural texture and is only formed when the preceding phase, on cooling, is the smectic A phase, with the texture of the smectic A phase being the fanned focal-conic texture. In other words, the smectic B phase "inherits" the focal-conic fanned texture from the smectic A phase. In practice, it is very difficult to distinguish between these textures, as there is normally very little change at the transition between them. Sometimes, however, as the transition is neared on either heating or cooling, the appearance of bars or lines across the backs of the fans become apparent. These disappear soon after the transition and are known as "transition bars".[18]

The photomicrograph in figure 2.7 shows the focal-conic fanned texture at the transition between the smectic A and smectic B phase. The transitory phenomenon of "transition bars" can be seen in some areas as black lines.

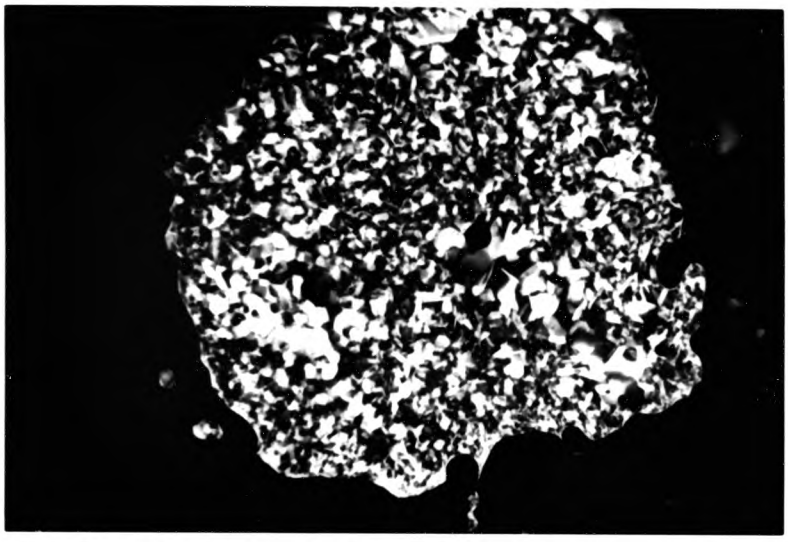

FIGURE 2.6 Photomicrograph of a typical mosaic texture of the smectic B phase (magnification x100).

FIGURE 2.7 Photomicrograph of the focal-conic fanned texture at the transition between the smectic A and B phases. Transition bars can be seen across the backs of the fans (magnification x100).

2.2.4 Textures of the smectic C phase

The smectic C phase exhibits two microscopic textures, namely the schlieren texture and the broken focal-conic fanned texture.[18]

The schlieren texture of the smectic C phase is slightly different from that exhibited by the nematic phase, since only point defects with four radiating brushes (or schlieren) are present. The nematic texture has both two and four brushes radiating from point defects.

The broken focal-conic fanned texture of the smectic C phase is predominantly formed by cooling the smectic A phase. This texture is characterised by an almost total disruption of the smooth fan texture of the smectic A phase and therefore, the fans have a grained or sanded appearance.[18,34] This disruption of the texture is caused by the irregular packing of the tilted smectic C phase into the focal-conic domains formed during smectic A phase formation.

The chiral smectic C phase also shows similar highly coloured textures which are coloured because of their optical activity, the colour changing from red to blue on cooling (see section 1.2.3.3). A more detailed discussion of the peculiarities of the textures of the chiral smectic C phase is presented in reference 18.

2.2.5 Textures of the smectic phases of some polymeric materials

Some polymeric materials do not form well-defined smectic textures on cooling, especially if there is no preceding nematic phase. These textures normally have a sanded or grained appearance with little or no distinguishable features.[34,92,95] An example of this

type of texture is displayed in figure 2.8. Shibaev and co-workers[92] described this type of texture as consisting of a group of birefringent regions, each of which having dimensions in the order of 2-10μm. These workers showed that prolonged annealing of such textures near to T_{CI} for several hours eventually produced fanned textures characteristic of the smectic phase, with the domain size being much increased (~100μm). Behaviour such as this is consistent with the formation of a smectic phase in which the molecules experience difficulty in achieving rapid, uniform alignment because of the sample's high viscosity. This results in the formation of small smectic domains which, during the annealing process, may coalesce to form much larger domains and ultimately more typical textures.

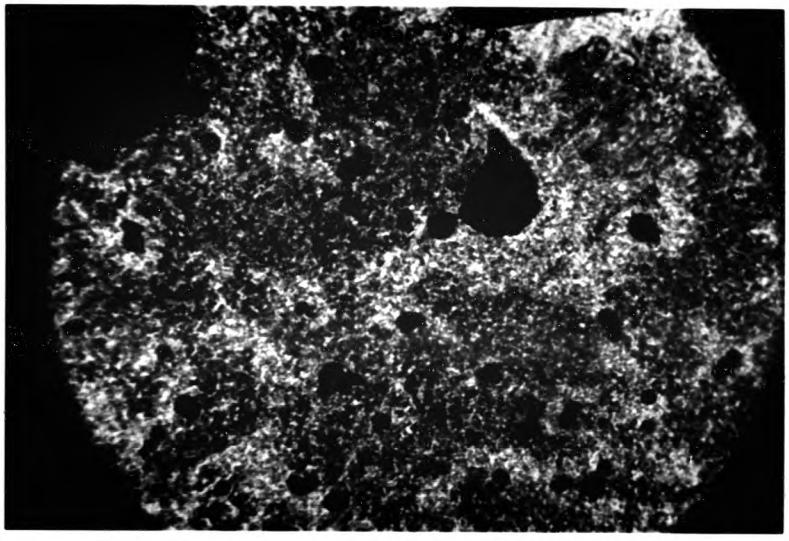

FIGURE 2.8 **Photomicrograph showing the sanded texture of a polymeric smectic phase (Magnification x 200).**

2.2.6 Textures of the cholesteric or chiral nematic phases.

Cholesteric or chiral nematic phases usually exhibit either planar or non-planar textures and, in addition, these textures may either closely resemble nematic textures or smectic textures, depending on the helical pitch.[96] Textures closely resembling those of the smectic phases arise when the helix is highly twisted and those resembling nematic textures arise when the helical twisting is very weak.

Cholesteric or chiral nematic planar textures are characterised by the molecules and their layers being parallel and the helix axis being perpendicular, to the glass-slides. This gives rise to textures which are homogeneous, with some areas having "oily streaks" which are caused by defects.[96] Additionally, due to the helical nature of the phase, bright reflection colours are sometimes observed. This is discussed in section 1.2.2 and in the results and discussion sections of this thesis. Figure 2.9 shows a typical planar or Grandjean texture which exhibits both white oily streaks and the selective reflection of blue light.

Non-planar textures exhibited by the cholesteric or chiral nematic phase include focal-conic type textures similar to those of the smectic A phase and a polygonal texture, where the quasi-nematic layers are in oblique positions relative to the glass-slides.

Finally, the last distinguishing feature of the cholesteric or chiral nematic phases (of reasonably short pitch lengths) is that no homeotropic textures are formed due to the helical arrangement of the molecules.

FIGURE 2.9 **Photomicrograph of the planar or Grandjean texture of the cholesteric phase, showing oily streaks and a bright-blue reflection colour (magnification x100).**

2.3 Miscibility Studies

Definitive identification of a mesophase type can be achieved from miscibility studies, using materials which exhibit known phases, textures and phase transition temperatures. This is an extremely useful tool for assessing the type of mesophase present when, for example, the same texture is observed for two LC phases separated by a phase transition. According to Sackmann and Demus,[99] isomorphous LC materials are considered equivalent and are therefore characterised by the same symbol. However, it is important to note that whilst uninterrupted miscibility establishes isomorphism, the converse is not necessarily true. Techniques such as dsc or polarising microscopy are normally used to assess the miscibility of LC compounds.

In this study, model compounds of similar structure or having similar phase transition temperatures to those synthesised were not available, therefore this technique could not be used as a means of phase identification.

2.4 X-ray Diffraction Studies

X-ray diffraction studies provide information concerning the arrangement and mode of packing of molecules and the types of order present in a mesophase. This technique is therefore used for definitive identification of a mesophase type. Although the smectic and nematic phases of some materials can be distinguished using X-ray diffraction of their unoriented powder samples, distinction of the actual type of smectic phase present is often difficult. The X-ray diffraction of oriented samples on the other hand provides much more structural information and smectic phase identification is

therefore possible.

Since this technique has not been used in this study it will not be discussed further here. For the reader's interest, more detailed discussions on the use of this technique can be found in the reviews by Noel,[91] Lipatov et al.[100] and De Vries.[101]

CHAPTER THREE

EXPERIMENTAL

(SYNTHESIS AND CHARACTERISATION)

3.1 Monomer Synthesis

The reagents employed in this work were used as received, unless otherwise noted.

All solvents used were distilled prior to use. Tetrahydrofuran (THF) and diethyl ether (Et_2O) were refluxed over calcium hydride, distilled, stirred over lithium aluminium hydride and then distilled again prior to use. Benzene and toluene were refluxed over calcium hydride, distilled, then stored over sodium. Pyridine was stored over potassium hydroxide pellets then distilled prior to use. Dimethyl formamide (DMF) was stored over potassium hydroxide pellets then distilled under vacuum from barium oxide using a nitrogen bleed, immediately before use. Ethanol and methanol were dried by the conventional technique for obtaining 'super-dry' ethanol and methanol,[102] then stored over 4A molecular seives. Other solvents were purified by normal procedures.

Chromatographic purifications were carried out by using either flash chromatography[103] with Fluka Kieselgel-60 (230-400 mesh ASTM) or by conventional means using Fisons silica gel (60-120 mesh). Analytical thin-layer chromatography (tlc) was carried out using plastic-backed Kieselgel 60 F_{254} (Merck).

The following spectrometers were used in this work, within their standard modes: Perkin-Elmer R32 (90 MHz ^1H nmr spectrometer), Bruker WP80 (80 MHz ^1H nmr Fourier transform spectrometer), both with tetramethyl silane (TMS) as the internal standard; Jeol D-100 mass spectrometer, Shimadzu IR-435 (infra-red spectrometer) and Perkin-Elmer Lambda 3 (UV-vis spectrometer). Elemental analyses were carried out using a Carlo

Erba elemental analyser (C, H and N), model 1106. Specific rotations were carried out using a Perkin-Elmer 141 polarimeter.

3.1.1 Di[6-(4-methoxy-4'-oxybiphenyl)hexyl]-2-methylene butane-1,4-dioate(5)(DMBI-6)

DMBI-6 was synthesised in a manner similar to that described by Finkelmann et. al.[94] for an analogous methacrylate monomer. Firstly, biphenol (1) was converted into the mono-methoxybiphenyl compound (2) using dimethyl sulphate and sodium hydroxide, as first reported by Van Alphen.[104] The spacer group was then introduced by a Williamson etherification procedure to give the alcohol (3) which was subsequently esterified with itaconic acid (4) to give DMBI-6 (5) (Scheme 1).

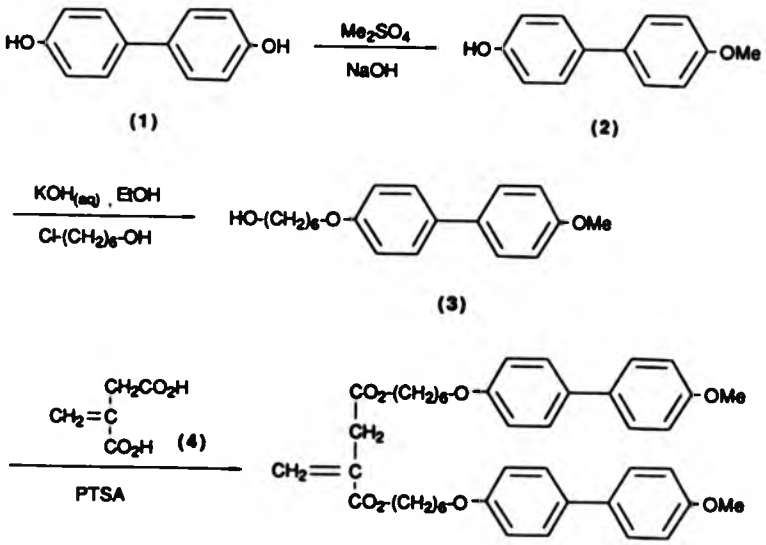

SCHEME 1

4-Methoxy-4'-hydroxybiphenyl (2)[104]

Biphenol (1) (75g. 0.402 mol) was dissolved in 10% sodium hydroxide solution (0.804 mol equiv.) and a little extra water added to keep the salt in solution. Dimethyl sulphate (50.7g, 38ml, 0.402 mol) was then added and the mixture stirred mechanically for 30 minutes, after which time the resultant precipitate was filtered and washed with 10% sodium hydroxide solution, followed by water. The precipitate was dissolved in boiling water and filtered to remove any residual dimethoxybiphenyl. 2M H_2SO_4 was added carefully to the hot filtrate and the resultant product collected by filtration. The dried product was recrystallised from ethanol to furnish white crystals. Yield: 31.3g, 39%; mp 183-185°C (lit[104]: 183-5°C).

4-Methoxy-4'-(6-hydroxyhexyloxy)biphenyl (3)[94]

4-Methoxy-4'-hydroxybiphenyl (2) (30g, 0.15 mol) was dissolved in hot ethanol (200ml) and potassium hydroxide (9.26g, 0.165 mol) in water (45ml) added under stirring. 1-Chloro-6-hydroxyhexane (22.5g, 0.165 mol) was introduced and the mixture refluxed for 24 hours. The solution was then diluted with an equal volume of water and the ethanol distilled off. The resultant precipitate was filtered and washed repeatedly with hot 10% potassium hydroxide solution until tlc analysis of the material showed it to be free of the starting biphenyl. After washing with water the filtrate was dried and recrystallised from ethanol. Yield: 30.6g, 68%; mp 130°C.

^1H nmr: δ ppm (Acetone-d6; 90 MHz) 1.2-2.0 (m, 8H) R-$(CH_2)_4$-R; 3.69 (t, 2H) R-CH_2-OH; 3.85 (s, 3H) $ArOCH_3$; 4.0 (t, 2H) RCH_2OAr;

6.90 (d, J=9 Hz, 4H) Ar-H; 7.44 (d, J=9 Hz, 4H) Ar-H; ROH unresolved.

$C_{19}H_{24}O_3$ (300 $gmol^{-1}$) Calc.: C 76.00% H 8.00%

Found: C 76.09% H 8.31%

Di[6-(4-methoxy-4'-oxybiphenyl)hexyl]-2-methylene butane-1,4-dioate (5)

The alcohol (3) (15.36g, 51 mmol), itaconic acid (4) (2.21g, 17 mmol) and p-toluene sulphonic acid (0.4g, 2 mmol) were refluxed together in toluene (200ml) for 48 hours, using Dean and Stark apparatus. After this time toluene (200ml) was added and the toluene solution washed with 10% sodium hydroxide soution (3x100ml) followed by water (100ml). The dried ($MgSO_4$) organic layer was evaporated in vacuo and the crude product purified by column chromatography using silica gel (Fisons) and 5% ethyl acetate in chloroform as the eluant. Unreacted starting material was eluted with 15% ethyl acetate in chloroform. Yield: 10g, 85%; mp k 68°C S_B 108°C I, as taken from the dsc experiment.

^1H Nmr: δ ppm ($CDCl_3$; 90 MHz) 1.2-2.0 (m, 16H) R-$(CH_2)_4$-R; 3.32 (s, 2H) vinyl-CH_2-CO_2R; 3.8 (s, 6H) $ArOCH_3$; 3.85 (t, 4H) R CH_2OAr; 4.1 (t, 4H) RCH_2OCO-; 5.68 (s, 1H) vinylic H trans to carbonyl; 6.32 (s, 1H) vinylic H cis to carbonyl; 6.90 (d, J=9 Hz, 8H) Ar-H; 7.44 (d, J=9 Hz, 8H) Ar-H.

$C_{43}H_{50}O_8$ (694 $gmol^{-1}$) Calc.: C 74.35% H 7.20%

Found: C 74.92% H 7.30%

See appendix A for ^1H nmr spectrum.

3.1. 2 4-Cyanophenyl-4-(6-acryloyloxyhexyloxy) benzoate[105] (9) (CPBA-6)

The title monomer CPBA-6 was prepared by the route reported by Portugall et. al.[105], which is shown in the following scheme:

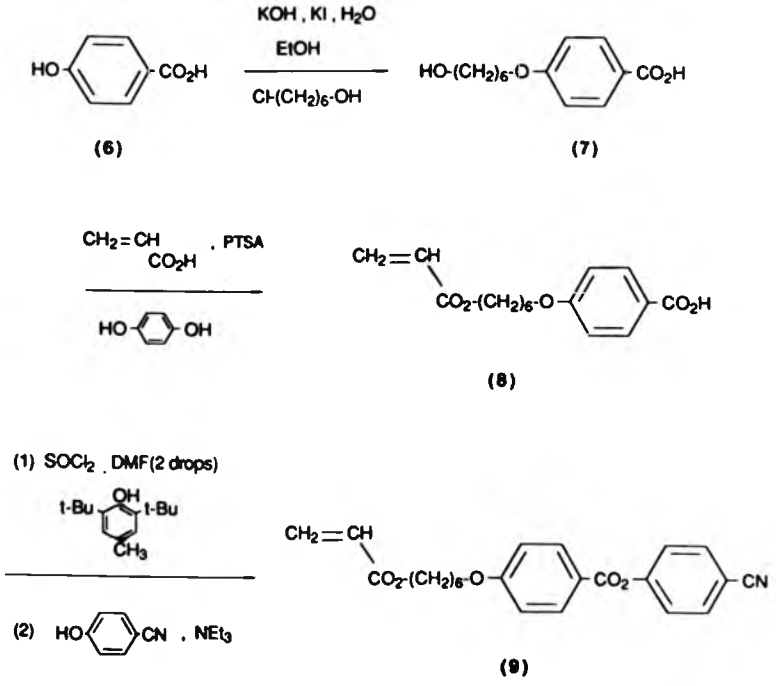

SCHEME 2

4-(6-Hydroxyhexyloxy)benzoic acid (7)

4-Hydroxybenzoic acid (6) (25.5g, 0.185 mol) was dissolved in a mixture of ethanol (65 ml), water (28 ml), potassium hydroxide (27.75g, 0.49 mol) and a pinch of potassium iodide. 1-Chloro-6-hydroxyhexane (23g, 0.168 mol) was then added slowly, dropwise and the mixture refluxed for 20 hours. After cooling the mixture, the ethanol was evaporated in vacuo and the residue dissolved in water (200 ml). This aqueous solution was washed with diethyl ether (3x50 ml) then adjusted to pH2 with 2N HCl and the resultant precipitate collected by filtration. After washing with water and drying, the product was recrystallised from ethanol.
Yield: 21.6g, 54%; mp 139-142°C (Lit:[105] 139°C).

4-(6-Acryloyloxyhexyloxy)benzoic acid (8)

A modified procedure of that used by Portugall et. al.[105] was used to prepare the acrylate compound (8):-
The alcohol (7) (21.6g, 0.09 mol) was esterified azeotropically with freshly distilled acrylic acid (26g, 0.36 mol) in benzene (300 ml) using p-toluene sulphonic acid (6g, 0.03 mol) as the catalyst and hydroquinone (2g, 0.018 mol) as the polymerisation inhibitor. Reflux was continued for a further 20 hours. On cooling, the reaction mixture was diluted with diethyl ether (1000 ml) and washed carefully with warm water until no more acrylic acid was detected. The organic layer was dried ($MgSO_4$), evaporated and the crude product recrystallised from isopropanol to afford the liquid crystalline benzoic acid derivative.
Yield: 17.6g, 67%; mp k 86°C N 90°C I (Lit: k 88°C N 92°C I).

$C_{16}H_{20}O_5$ (292 $gmol^{-1}$) Calc.: C 65.75% H 6.84%
Found: C 66.22% H 6.99%

4-Cyanophenyl-4'-(6-aryloyloxyhexyloxy)benzoate (9)

The monomer (9) was prepared by firstly converting the acid (8) into the corresponding acid chloride then condensing this with p-cyanophenol. The acid (8) (17.32g, 0.059 mol) was stirred with thionyl chloride (35.7g, 0.3 mol) in the presence of DMF (2 drops) and 2,6-di-t-butyl-4-methyl phenol (4.4g, 0.02 mol). After ca. 25 minutes, by which time solution was achieved, the excess thionyl chloride was removed by rotary evaporation and high vacuum (1-2 hours). The acid chloride residue was dissolved in anhydrous chloroform (30 ml) then added slowly dropwise into a stirred solution of p-cyanophenol (7.03g, 0.059 mol) and triethylamine (6.07g, 0.06 mol) in chloroform (20 ml) at O^oC. After the addition the mixture was stirred at room temperature for 24 hours then chloroform (200 ml) added. This solution was washed with water (50 ml) followed by 2N sodium hydroxide solution (3x50 ml) and water (2x50 ml). The organic layer was dried ($MgSO_4$), evaporated then subjected to flash chromatography, using dichloromethane as both the solvent and the eluant. The monomer was finally recrystallised from isopropanol and shown to be pure by tlc.
Yield: 16g, 69%; mp 72-75°C (Lit:[105] 72°C).
^1H Nmr: δ ppm ($CDCl_3$; 90 MHz) 1.2-2.1 (m, 8H) $R(CH_2)_4R$; 4.01-4.13 (overlapping t's) 2x2H) $ArOCH_2R$ and RCH_2OCO; 5.63-6.5 (m, 3H) vinylic H; 6.78-8.2 (4xd, 8H) Ar-H.

$C_{23}H_{23}NO_5$ (393 $gmol^{-1}$) Calc.: C 70.23% H 5.85% N 3.56%
Found: C 71.15% H 5.97% N 3.61%

3.1.3 Synthesis of Cholesteryl-containing itaconate derivatives (DChI-10 and ChMI-10)

Two cholesteryl-containing monomers based on itaconic acid, namely Di[1-[(cholesteryloxy)carbonyl]-10-decanyl]-2-methylene butane-1,4-dioate (DChI-10) and 1-[1-[(cholesteryloxy)carbonyl]-10-decanyl]-2-methylene-4-methyl butane-1,4-dioate (ChMI-10) were prepared from the common precursor cholesteryl-11-bromo undecanoate (12). Cholesterol (10) was esterified with 11-bromo undecanoyl chloride (11) by the procedure reported by Friedzon and co-workers.[106] This bromo-cholesteryl compound was then condensed with either the di-cesium salt of itaconic acid (13) to give the monomer DChI-10 (14) or the cesium salt of mono-methyl itaconate (15) to give the monomer ChMI-10 (16). This is outlined schematically in scheme 3. By using this method of condensation in the synthesis of ChMI-10 rather than the usual acid catalysed method, the possibility of trans-esterification is eliminated. By following the aforementioned acid salt route, only one product is possible.[107]

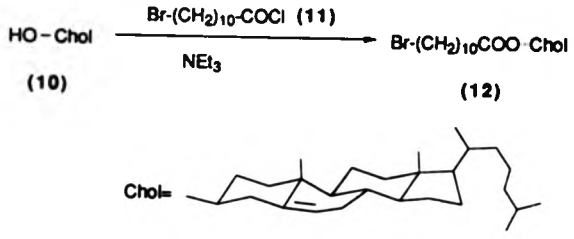

SCHEME 3 /

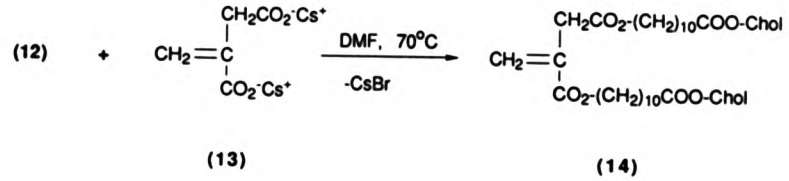

(13) (14)

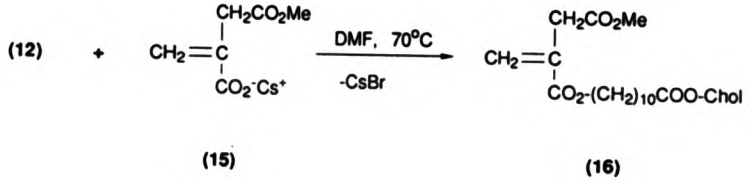

(15) (16)

SCHEME 3

Cholesteryl-11-bromo undecanoate (12)

Redistilled and dried triethylamine (4.05g, 0.04 mol) was added to a solution of cholesterol (10) (11.6g, 0.03 mol) in anhydrous benzene (150 ml) and the mixture vigorously stirred whilst 10-bromo undecanoyl chloride (11) (11.35g, 0.04 mol) was added slowly dropwise, at room temperature. The resultant pink coloured solution was stirred for a further two hours and then the benzene removed in vacuo. Diethyl-ether (200 ml) was added to the mixture along with water (100 ml), the layers were separated and the organic phase washed with two further portions of water (2x50 ml). The dried ($MgSO_4$) organic phase was reduced to about one quarter of its original volume and poured into a large excess of methanol to precipitate the product which was then collected by filtration. After washing with methanol the product was dried and analysed for purity by tlc. No further purification was needed.
Yield: 14.6g, 77%; mp 104-106°C (Lit:[106] 105°C).

Di[1-[(cholesteryloxy)carbonyl]-10-decanyl]-2-methylene butane 1,4-dioate (14) (DChI-10)

Anhydrous dicesium itaconate (13) (2.6g, 6.6 mmol) was prepared by dissolving the relative amounts of itaconic acid (4) and cesium hydroxide in methanol and evaporating to dryness. (Care must be taken at this point to ensure that the hygroscopic salt remains dry, as this affects the final yield.) The salt was added to a solution of cholesteryl-11-bromo undecanoate (12) (9.5g, 15 mmol) in dry DMF (100 ml) and the heterogeneous mixture stirred at ca. 70°C for 24 hours under a blanket of nitrogen. It is important to

keep the reaction temperature at 70°C or below to avoid isomerisation of the itaconate ester into the citraconate ester. On cooling the reaction mixture, DMF was co-evaporated in vacuo with xylene. Chloroform (250 ml) and water (50 ml) were added and the mixture shaken. The organic layer was washed with a further portion of water (50 ml) followed by saturated sodium bicarbonate solution (2x50 ml) and finally water (50 ml). The dried ($MgSO_4$) organic layer was evaporated in vacuo and the crude product purified by column chromatography using silica gel (Fisons). Unreacted bromide was eluted with toluene (R_f = 0.88, toluene) and the desired diester (14) eluted with a 10% chloroform in toluene mixture (R_f = 0.46, toluene).

Yield: 5.1g, 63%; mp k $\underset{}{39^oC}$ S_A $\underset{}{65^oC}$ N $\underset{}{72^oC}$ I.

^1H Nmr: δ ppm ($CDCl_3$; 80 MHz) 0.5-3.25 (m, 124H) cholesteryl R-H, undecyl $R(CH_2)_8COO$-, vinyl-CH_2CO_2-; 4.15 (t, 4H) RCH_2OCO; 4.6 (m, 2H) 3α-H; 5.34 (m, 2H) cholesteryl 6-H (olefinic); 5.8 (s, 1H) vinylic H trans to carbonyl; 6.32 (s, 1H) vinylic H cis to carbonyl.

Ir: $\bar{\nu}$ (thin film) 2850, 1720, 1660, 1470, 1395, 1180 cm^{-1}.

$C_{81}H_{134}O_8$ (1234 $gmol^{-1}$) Calc.: C 78.78% H 10.86%

Found: C 79.98% H 10.96%.

1-[1-[(Cholesteryloxy)carbonyl]-10-decanyl]-2-methylene-4-methyl butane-1,4-dioate (16) (ChMI-10)

Monomethyl itaconate (6.34g, 4.4 mmol) from the esterification of methanol with itaconic acid in the presence of acetyl chloride[108] was dissolved in anhydrous methanol (15 ml) and cesium hydroxide (6.74g, 4.4 mmol) added. After complete dissolution the methanol was evaporated to reveal the cesium salt of monomethyl itaconate

(15). Anhydrous DMF (120 ml) was added and the mixture stirred at 50°C for two hours in the presence of hydroquinone (ca 0.5g). Cholesteryl-11-bromo undecanoate (12) (7g, 1.1 mmol) was then added and the mixture stirred for a further 24 hours under nitrogen at 50°C. After cooling, DMF was co-evaporated with xylene in vacuo and the residue dissolved in chloroform (200 ml). After washing with water (50 ml) the organic layer was washed with saturated sodium bicarbonate (2x50 ml) and then water (50 ml). The chloroform layer was dried ($MgSO_4$), evaporated and subjected to column chromatography using silica gel (Fisons). The bromide starting material was eluted with toluene (R_f = 0.88, toluene) and the desired mixed ester (16) was eluted with a 20% chloroform in toluene mixture (R_f = 0.22, toluene).

Yield: 2.27g, 74%; mp k $\xrightarrow{16^oC}$ S_A $\xrightarrow{42^oC}$ N* $\xrightarrow{54^oC}$ I.

^1H Nmr: δ ppm ($CDCl_3$; 90 MHz) 0.5-3.25 (m, 63H) cholesteryl R-H, undecyl $R(CH_2)_8$-COO-, vinyl $-CH_2CO_2-$; 3.7 (s, 3H) RCO_2CH_3; 4.13 (t, 2H) $R-CH_2OCO-$; 4.6 (m, 1H); 3α-H; 5.34 (m, 1H) cholesteryl 6-H (olefinic); 5.8 (s, 1H) vinylic H, trans to carbonyl; 6.3 (s, 1H) vinylic H, cis to carbonyl.

$C_{44}H_{72}O_6$ (696 $gmol^{-1}$) Calc.: C 75.79% H 10.33%

Found: C 76.19% H 10.81%

3.1.4 Di-but-2-yl-2-methylene butane-1,4-dioate (17) (DBI) (Di-but-2-yl itaconate)

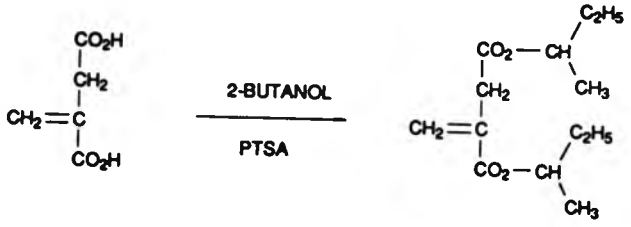

(4) (17)

SCHEME 4

Itaconic acid (4) (13g, 0.1 mol) was refluxed together with 2-butanol (44.4g, 0.6 mol) and p-toluene sulphonic acid (ca. 2g) in toluene (200 ml) for 12 hours, using Dean and Stark apparatus. On cooling the reaction, the organic phase was washed with water (3x50 ml), dried ($MgSO_4$) and evaporated in vacuo to reveal an oil, which after distillation gave a clear liquid (17). The diester was characterised by ir spectroscopy.

Yield: 22g, 90%; bp 127-131°C/10-12mm Hg (Lit:[109] 127°C/10mm Hg) .Ir: $\bar{\nu}$ (thin film) 1725, 1710, 1650, 1270, 1200 cm^{-1}.

3.1.5 2-[1-[(S)-2-(Ethoxycarbonyl)propyl]carbamyl] ethylmethacrylate (20) (MCP*)

The chiral carbamate monomer (20) was prepared by reacting

isocyanato ethylmethacrylate (18) with (S)-ethyl lactate (19) in the presence of stannous octoate and a polymerisation inhibitor:-

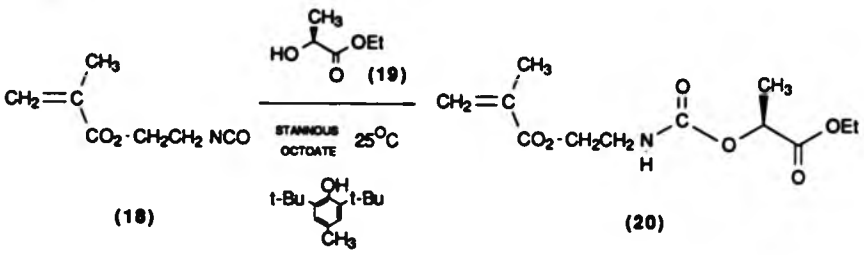

(18) (20)

SCHEME 5

A solution of IEM (18) (isocyanato ethylmethacrylate, supplied by Dow Chemical Co., Michigan, USA) (4.66g, 4.24 ml, 30 mmol) in anhydrous benzene (15 ml) was added slowly dropwise to a stirred solution of (S)-(-)-ethyl lactate (19) (3.54g, 30 mmol), stannous octoate (0.06g, 0.15 mmol) and 2,6-di-t-butyl-4-methylphenol (ca. 0.1g) in anhydrous benzene (15 ml) at room temperature. The reaction was left to stir overnight then methanol (30 ml) added to neutralise any remaining IEM. After evaporation of the solvent in vacuo the title compound (20) was purified by vacuum distillation.
Yield: 4.1g, 50%; bp 150°C/12mm Hg; $[\alpha]_D^{26}$ = -5.71°($CHCl_3$).
^1H Nmr: δ ppm ($CDCl_3$, 90 MHz) 1.25 (t, 3H) ethyl CH_3; 1.45 (d, 3H) H-C-CH_3; 1.92 (s, 3H) vinyl-CH_3; 3.45 (t, 2H) R-CH_2-NH; 4.5-4.35 (overlapping t and q, 2H, 3H) vinyl-CO_2 CH_2R and ethyl CH_2; 4.98 (q, 1H) CH_3-C-H; 5.55 (S, 1H) vinylic-H trans to carbonyl; (6.1, 1H) vinylic H cis to carbonyl; 6.35 (bs, 1H) N-H.
Ir: $\bar{\nu}$ (thin film) 3400, 1800, 1700(s), 1640, 1520, 1160(s) cm^{-1}.

3.1.6(S)-Methyl(2-methyl-3-methacryloyloxy) propionate (22) (MMMP*)

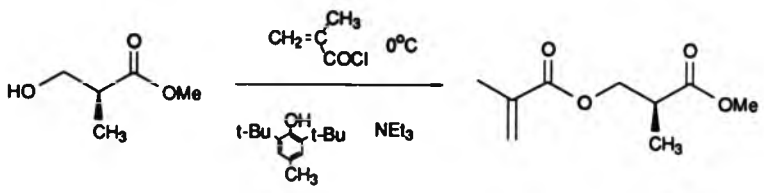

(21) (22)

SCHEME 6

Methacryloyl chloride (4.6g, 4.3 ml, 44 mmol) in anhydrous benzene (10 ml) was added slowly, dropwise to a stirred solution of the readily available (S)-(+)-methyl-3-hydroxy-2-methylpropionate (21) (5g, 42 mmol), triethylamine (4.45g, 44 mmol) and 2,6-di-t-butyl-4-methyl phenol (ca 0.2g) in benzene (30 ml) at $0^{o}C$. The reaction was allowed to warm up to room temperature after the addition, and stirring was continued overnight. Diethylether (100 ml) and water (50 ml) were then added and the mixture shaken. The organic layer was separated and washed several times with water (3x50 ml) then dried ($MgSO_4$). Tlc analysis indicated that three products were present (other than the starting materials) and that these had R_f values of 0.17, 0.23 and 0.30 (10% ethyl acetate in 40-60 petroleum ether). After careful separation by flash chromatography using 5% ethyl acetate in 40-60 petroleum ether as the eluant, the products were analysed by nmr and ir spectroscopy. The product having R_f = 0.23 was found to be the desired

methacrylate ester (22).

Yield: 4.75g, 58%; isolated as an oil. $[\alpha]_D^{26}$ = + 21.97° (CH_2Cl_2).

^1H Nmr: δ ppm ($CDCl_3$, 90 MHz) 1.22 (d, 3H) H-C-CH_3; 1.93 (s, 3H) vinyl-CH_3; 2.85 (m, 1H) tertiary C-H; 3.67 (s, 3H) RCO_2CH_3; 4.27 (d, 2H)-HC-CH_2-OCO; 5.51 (s, 1H) vinylic H, trans to carbonyl; 6.06 (s, 1H) vinylic H, cis to carbonyl.

Ir: $\bar{\nu}$ (thin film) 1730, 1720, 1640, 1200, 1160 (s) cm^{-1}.

$C_9H_{14}O_4$ (186 $gmol^{-1}$) Calc.: C 58.06% H 7.53%

Found: C 58.29% H 7.59%

3.1.7 1-(4-Toluenesulphonoxy)-2-(tetrahydro-2-pyranoxy)propane (25) (TTP)

The title compound TTP (25) was prepared by the procedures reported by Ghirardell[110] and Otterholm et.al.,[111] starting from (s)-ethyl lactate (19) which is readily available in high enantiomeric purity. Firstly, the alcohol functionality of the starting material was protected by converting it into its tetrahydropyranyl ether (23). Reduction of the ester function in (23) with lithium aluminium hydride in diethylether resulted in the alcohol (24). Tosylation of the alcohol group in (24) afforded the chiral intermediate TTP (25) (Scheme 7).

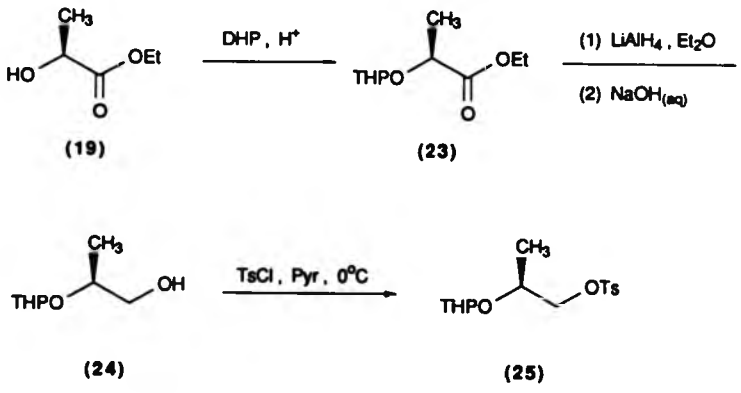

SCHEME 7

Ethyl-2-(tetrahydro-2-pyranoxy)propanoate (23)

Dihydro-2H-pyran (63g, 0.75 mol) followed by 12N HCl (5

drops) were added to (S)-ethyl lactate (19) (53.1g, 0.45 mol) under stirring. Heat evolution was controlled by means of a water/ice bath. Stirring was continued for 20 hours, after which time sodium bicarbonate (ca. 5g) was added. After a further 2 hours stirring the solution was filtered and concentrated by rotary evaporation at 50°C. The pure diastereomeric products (since the THP ring introduces a second chiral centre) were isolated by distillation through a short Vigreaux column.

Yield: 76.3g, 84%; bp: 64-68°C/0.03 mm Hg (Lit.:[110] 66-68°C/0.25 mm Hg).

^{1}H Nmr: δ ppm ($CDCl_3$, 90 MHz) 1.2-1.8 (m, 12H) CH_3-R and R-CH_2-R; 3.3-4.1 (m, 2H) pyranyl H-6; 4.21 (overiapping q's, 3H) methine-H and $RCO_2CH_2CH_3$; 4.7 (bs 1H) pyranyl H-2.

Ir: $\bar{\nu}$ (thin film) 2900, 1740, 1190, 1130, 1020, 980 cm^{-1}.

2-(Tetrahydro-2-pyranoxy)-1-propanol (24)

Lithium aluminium hydride (8.0g, 0.214 mol) was slurried in cold (0°C) anhydrous diethylether (270 ml) under nitrogen and a solution of the ester (23) (67g, 0.335 mol) in anhydrous diethylether (100 ml) added slowly, dropwise over two hours. After the addition the ice-bath was removed and the mixture refluxed gently for 48 hours. On cooling, water (8 ml), 20% sodium hydroxide solution (6 ml) and water (13 ml) were added successively in a dropwise manner. After standing overnight the ether was evaporated and the remaining mixture subjected to extraction with diethylether in a Sohxlet apparatus for four hours. Distillation of the alcohol (24) from the evaporated ether solution gave the major fraction as a liquid.

Yield: 53.5g, 65%; bp 42-44°C/0.1 mm Hg (Lit.:[111] 101-105°C/8 mm Hg).

^{1}H Nmr: δ ppm ($CDCl_3$, 90 MHz) 1.11 and 1.22 (two d, 3H) methine-C-CH_3; 1.35-2.20 (m, 7H) R-CH_2-R and ROH; 3.30-3.70 (m, 3H) pyranyl H-6 and methine H; 3.70-4.10 (m, 2H) RCH_2OH; 4.60 and 4.67 (two unresolved m, 1H) pyranyl H-2.

Ir: $\tilde{\nu}$ (thin film) 3400, 2900, 2850, 1120, 1075, 1020 cm^{-1}.

$C_8H_{15}O_3$: Mol.wt.obs. 159.1035 (M-1), calc. 160.1022. Ms [m/e (% rel.int.)] 159 (M^+ ion-1, 6.6), 101 (10.5), 85 (100), 84 (28.6).

1-(4-Toluenesulphonoxy)-2-(tetrahydro-2-pyranoxy)propane (25)

p-Toluenesulphonyl chloride (19.06g, 100 mmol) was added in small portions, over a period of 15 minutes to a cold (O°C) solution of the alcohol (24) (13.5g, 84 mmol) in anhydrous pyridine (50 ml). The solution was stirred during the addition and overnight whilst the reaction was kept at O°C. The precipitated pyridine hydrochloride salt was filtered off, washed with diethylether (2x10 ml) and the combined filtrate and washings concentrated. Pyridine (15 ml) was added, followed by water (20 ml) and the mixture stirred for two hours in an ice-bath, after which time tlc showed no tosyl chloride to be present. Diethylether (200 ml) and water (100 ml) were then added and the mixtures separated. The organic layer was washed several times with aqueous copper sulphate solution followed by water (100 ml), saturated sodium bicarbonate solution (2x100 ml) and finally water (100 ml). The organic layer was dried ($MgSO_4$) and evaporated to reveal a slightly pink coloured oil which was shown to be pure by tlc analysis.

Yield: 24.8g, 94%.

^{1}H Nmr: δ ppm ($CDCl_3$, 90 MHz) 0.96-1.29 (m, 3H) methine-C-CH_3; 1.29-2.0 (m, 6H) R-CH_2-R; 2.41 (s, 3H) Ar-CH_3; 3.15-4.2 (m, 5H) RCH_2OSO_2-, pyranyl H-6 and methine-H; 4.6 (bs, 1H) pyranyl H-2; 7.26 (d, 8.5 Hz, 2H) Ar-H; 7.71 (d, 8.5 Hz, 2H) Ar-H.

Ir: $\bar{\nu}$ (thin film) 2950, 1600, 1460, 1360, 1200, 860, 840, 660 cm^{-1}.

$C_{15}H_{22}O_5S$ (314g mol^{-1}) Calc.: C 57.32% H 7.00% S 10.19%

Found: C 57.39% H 7.24% S 10.21

3.1.8 (S)-1-(4-Methoxy-4'-oxybiphenyl)-2-methacryloyloxypropane (28) (MBM*)

The chiral monomer MBM* (28) was prepared in three steps from the tosylate (25). The first step involved displacement of the tosyl group in (25) by the sodium salt of 4-methoxy-4'-hydroxy biphenyl (2) in DMF, to give (26). Deprotection of the alcohol functionality in acidic ethanol gave the chiral alcohol (27) which was finally converted into the monomer (28) by esterification with methacrylic acid (scheme 8).

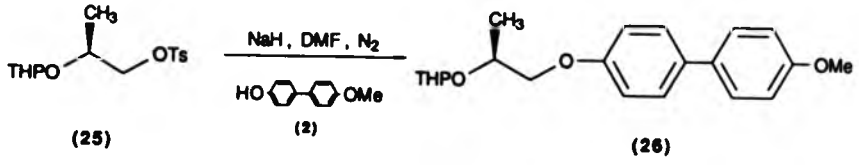

(25) (2) (26)

/scheme 8

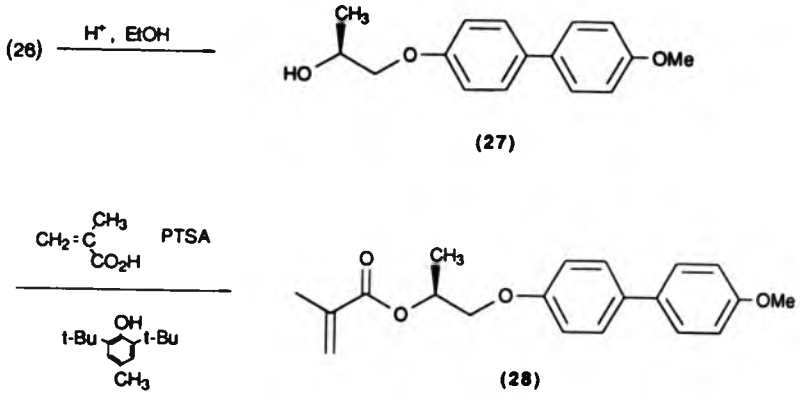

SCHEME 8

1-(4-Methoxy-4'-oxybiphenyl)-2-(tetrahydro-2-pyranoxy) propane (26)

Sodium hydride(0.69g, 29 mmol) was slurried in anhydrous DMF (15 ml) under a flow of nitrogen and a solution of 4-methoxy-4'-hydroxybiphenyl (2) (5.6g, 28 mmol) in anhydrous DMF (50 ml) added slowly, dropwise. The mixture was stirred mechanically and heated to 50°C for ca one hour after the addition, during which time the phenoxide precipitated out of solution. A solution of the tosylate (25) (8g, 25 mmol) in DMF (20 ml) was then added slowly, dropwise into the heterogeneous mixture whilst it was stirred vigorously. Stirring was continued for a further 12 hours at 50°C, by which time the mixture had become homogeneous. After cooling, DMF was

removed from the reaction mixture by co-evaporation with xylene in vacuo, the last traces being removed by rotary vacuum pump. The crude mixture of product and starting material were separated by washing the solids with hot, 20% sodium hydroxide solution using a Buchner funnel etc (water-pump). Washing was continued until tlc analysis confirmed that only the desired product remained on the filter. After washing with water (120 ml) the product was dissolved in chloroform (100 ml) and the solution dried ($MgSO_4$). Filtration and evaporation afforded the title compound as a white solid, pure by tlc.

Yield: 6.67g, 78%; mp 102-106°C; $[\alpha]_D^{20}$ = -18.02° ($CHCl_3$).

$C_{21}H_{26}O_4$ (342 $gmol^{-1}$) Calc.: C 73.68% H 7.60%

Found: C 73.72% H 7.66%

(S)-1-(4-Methoxy-4'-oxybiphenyl)-2-hydroxypropane (27)

A suspension of the biphenyl (26) (5.1g, 14.9 mmol) in acidified ethanol (100 ml) (prepared from a 1% solution of 0.1M HCl in ethanol) was heated at reflux with stirring until complete solution had occurred. Reflux was continued for 15-20 minutes, by which time tlc analysis indicated the reaction had gone to completion. Water (25 ml) was added to the cooled mixture, the product collected by filtration and dried under vacuum. Careful recrystallisation from ethanol afforded the chiral alcohol (27) as a white crystalline solid;

Yield: 3.42g, 89%; mp 152-154°C; $[\alpha]_D^{30}$ = +13.86° (Acetone).

^1H Nmr: δ ppm (Acetone d-6, 90 MHz) 1.30 (d, 3H) methine C-CH_3; 2.37 (bs, 1H) ROH; 3.81 (s, 3H) ArOCH_3; 3.89 (t, 2H) -CH_2OAr; 4.18 (m, 1H) methine H; 6.90 (d, J=9 Hz, 4H) Ar-H; 7.44 (d, J=9Hz, 4H) Ar-H.

Ir: $\tilde{\nu}$ (KBr) 3400, 1610, 1500, 1275, 1250, 1010, 820, 800 cm^{-1}.

$C_{16}H_{18}O_3$ (258 $gmol^{-1}$) Calc.: C 74.42% H 6.98%

Found: C 75.07% H 7.04%

(S)-1-(4-Methoxy-4'-oxybiphenyl)-2-methacryloyloxypropane (28).

Methacrylic acid (8,6g, 100 mmol), the chiral alcohol (27) (2g, 7.75 mmol), p-toluene sulphonic acid (ca 0.1g) and 2,6-di-t-butyl-4-methyl phenol (ca. 0.5g) were refluxed together in toluene (100 ml) for 12 hours using Dean and Stark apparatus. After cooling, the toluene was evaporated in vacuo and chloroform (160 ml) and water (80 ml) added. After separating the layers, the organic layer was washed with 10% sodium hydroxide solution (3x30 ml) followed by water (30 ml), then dried ($MgSO_4$). After filtration the solution was concentrated and the crude product purified by column chromatography, using silica gel (Fisons) and chloroform as both the solvent and eluant.

Yield: 1.72g, 68%; mp 78-80°C; $[\alpha]_D^{18}$ = -18.1° ($CHCl_3$).

^1H Nmr: δ ppm ($CDCl_3$, 90 MHz) 1.41 (d, 3H) methine-C-CH_3; 1.95 (s, 3H) vinyl-CH_3; 3.77 (s, 3H) $ArOCH_3$; 4.02 (dd, 2H) -CH_2OAr; 5.30 (sex., 1H) methine-H; 5.5 (s (with fine structure), 1H) vinylic H trans to carbonyl; 6.09 (s, 1H) vinylic H cis to carbonyl; 6.90 (d, J=9Hz, 4H) Ar-H; 7.40 (d, J=9Hz, 4H) Ar-H.

$C_{20}H_{22}O_4$ (326 $gmol^{-1}$) Calc.: C 73.62% H 6.75%

Found: C 74.07% H 6.97%

See appendix A for ^1H nmr spectrum.

3.1.9 (S)-1-(4-Cyano-4'-oxybiphenyl)-2-methacryloyloxypropane (31) (CBM*)

The title monomer CBM* (31) was synthesised in three steps from the tosylate (25), in an almost analogous manner to the procedure used for the synthesis of MBM*. In this case, esterification was achieved by using methacryloyl chloride rather than methacrylic acid and the yields were consequently much improved (scheme 9).

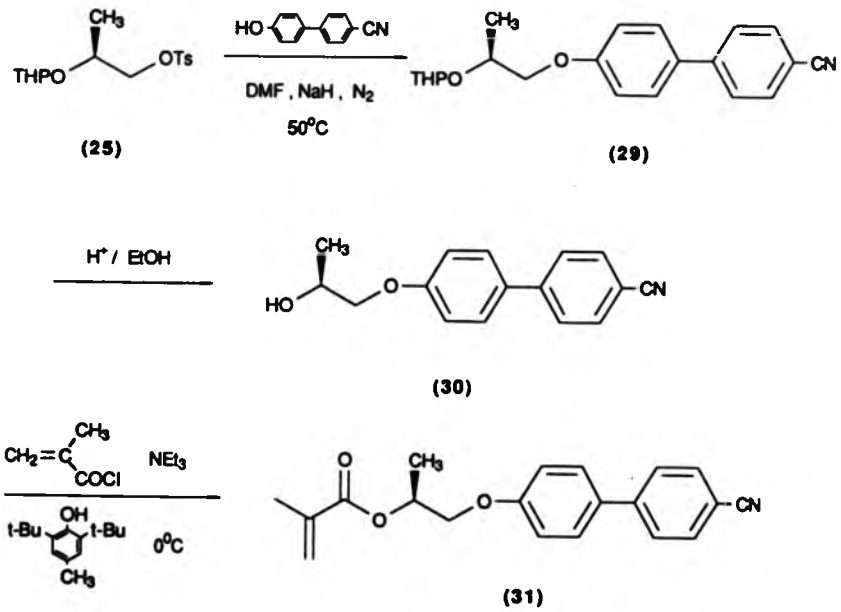

SCHEME 9

1-(4-Cyano-4'-oxybiphenyl)-2-(tetrahydro-2-pyranoxy) propane (29)

This compound was prepared by similar methods to those used for the methoxybiphenyl (26): Sodium hydride (0.69g, 29 mmol) was slurried in anhydrous DMF (15 ml) under a flow of nitrogen and a solution of 4-cyano-4'-hydroxybiphenyl (BDH Chemicals) (5.46g, 28 mmol) in anhydrous DMF (15 ml) added slowly, dropwise to the stirred slurry. Stirring was continued for 45 minutes, by which time the solution was a lime-yellow colour, then a solution of the tosylate (25) (8g, 25 mmol) in anhydrous DMF (10 ml) was aded dropwise. After the addition the temperature was raised to 50°C and stirring continued for 12 hours. DMF was removed from the reaction mixture by co-evaporation with xylene in vacuo then chloroform (150 ml) and water (150 ml) added. The separated organic layer was washed with 20% potassium hydroxide solution (3x100 ml) followed by water (100 ml), dried ($MgSO_4$), concentrated and subjected to flash chromatography using chloroform as the eluant. The product was isolated as an oil, pure by tlc.

Yield: 7.58g, 90%; $[\alpha]_D^{20} = -17.5^o$ ($CHCl_3$);

$C_{21}H_{23}NO_3$ (337 $gmol^{-1}$) Calc.: C 74.78% H 6.82% N 4.15%

Found: C 74.24% H 6.83% N 3.71%

(S)-1-(4-Cyano-4'-oxybiphenyl)-2-hydroxypropane (30)

Deprotection of the THP protected compound (29) (7g, 20.7 mmol) was effected by dissolving it in acidified ethanol (100 ml) (1% solution of 0.1M HCl in ethanol) and refluxing for 15 minutes, by which time tlc analysis indicated that only product was present.

Ethanol was evaporated in vacuo and chloroform (100 ml) and water (100 ml) were added. The organic layer was separated and washed with two further portions of water (2x100 ml), then dried ($MgSO_4$) and evaporated to reveal an oil, which eventually crystallised into transparent needles.

Yield: 4.97g, 95%, mp 103-104°; $[\alpha]_D^{20}$ = +12.42° ($CHCl_3$);

^1H Nmr: δ ppm ($CDCl_3$, 90 MHz) 1.32 (d, 3H) methine-C-CH_3; 2.39 (s, 1H) ROH; 3.95 (d, 2H) RCH_2OAr; 4.20 (sex., 1H) methine-H; 6.97 (d, J=9 Hz, 2H) Ar-H; 7.48 (d, J=9 Hz, 2H) Ar-H; 7.61 (s, 4H) Ar-H.

$C_{16}H_{15}NO_2$ (253 $gmol^{-1}$) Calc.: C 75.89% H 5.93% N 5.53%

Found: C 75.80% H 5.49% N 5.50%

(S)-1-(4-Cyano-4'-oxybiphenyl)-2-methacryloyloxypropane (31)

Methacryloyl chloride (1.16g, 11 mmol) was added dropwise to an ice-cooled, stirred solution of the chiral alcohol (30) (2.78g, 11 mmol), triethylamine (1.3g, 13 mmol) and 2,6-di-t-butyl-4-methyl phenol (ca. 0.2g) in anhydrous benzene (75 ml). After the addition the ice-bath was removed and the solution stirred vigorously for four hours. Benzene (100 ml) was then added, the mixture washed with water (100 ml), 10% sodium hydroxide solution (2x100 ml) and finally water (100 ml), dried ($MgSO_4$), then evaporated in vacuo at low temperature (ca 30°C). The crude product was purified by flash chromatography using silica gel (Fluka Kieselgel 60, 230-400 mesh ASTM) and petroleum ether (40-60)/ethyl acetate (6:1) mixture to yield white, needle-like crystals.

Yield: 3.3g, 94%; mp 58-60°C; $[\alpha]_D^{20}$ = -19.2° ($CHCl_3$);

^1H Nmr: δ ppm ($CDCl_3$, 90 MHz) 1.43 (d, 3H) methine C-CH_3; 1.95 (s,

3H) vinyl-CH_3; 4.09 (dd, 2H) RCH_2OAr; 5.32 (sex., 1H) methine-H; 5.53 (s (with fine structure) 1H) vinylic H trans to carbonyl; 6.10 (s, 1H) vinylic H cis to carbonyl; 6.96 (d, J=9 Hz, 2H) Ar-H; 7.45 (d, J=9 Hz, 2H) Ar-H; 7.53 (s, 4H) Ar-H.

$C_{20}H_{19}NO_3$ (321 $gmol^{-1}$) Calc.: C 74.77% H 5.91% N 4.36%

Found: C 75.32% H 6.22% N 4.23%

See appendix A for ^1H nmr spectrum.

3.1.10 (S)-1-(4-Methoxy-4'-oxybiphenyl)-2-(2-methacryloyloxy-1-ethoxy)propane (36) (XMBM*)

The chiral monomer XMBM* (36), having an extended "spacer" was synthesised by reacting the chiral alcohol (27) with the THP-protected alcohol, 2-bromoethanol (33) to form the ether (34). After deprotection of the alcohol functionality of (34), the resultant alcohol (35) was esterified with methacryloyl chloride to give the required extended spacer monomer (36) (scheme 10).

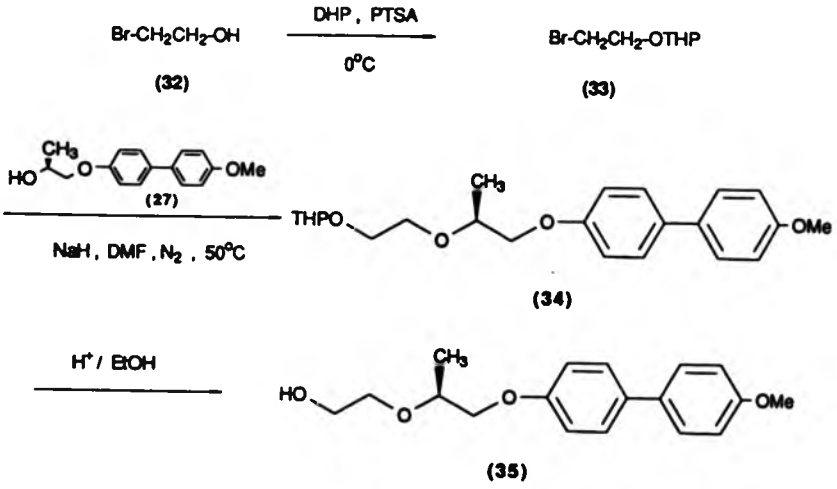

SCHEME 10 /

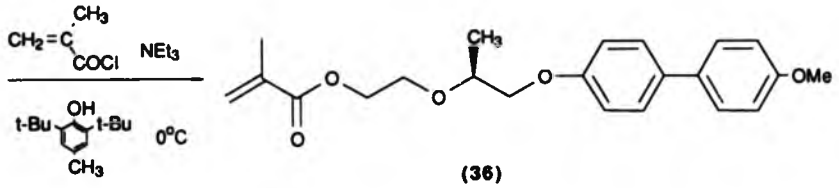

(36)

SCHEME 10

1-Bromo-2-(tetrahydro-2-pyranoxy)ethane (33).

Bromoethanol (32) was protected by a method somewhat similar to that described by Newkome et. al.:[112] Dihydropyran (21g, 23`ml, 0.25 mol) was added slowly, dropwise into a stirred mixture of redistilled bromoethanol (12.5g, 7.2 ml, 0.1 mol) and p-toluene sulphonic acid (5 grains) at O°C. The ice-bath was then removed and the mixture stirred for a further four hours, after which time sodium bicarbonate (ca. 5g) was added and the mixture stirred for a further hour. After filtration and washing with diethylether the filtrate was evaporated and distilled to reveal an oil. 14.8g, 71%; bp 94°C/14 mm Hg (Lit.:[112] 75°C/1 mm Hg).

^{1}H Nmr: δ ppm ($CDCl_3$, 90 MHz) 1.3-2.3 (m, 6H) -CH_2-; 3.3-4.1 (m, 6H) ROCH_2CH_2Br, -CH_2OR ; 4.6 (t, unresolved, 1H) -CH.

1-(4-Methoxy-4'-oxybiphenyl)-2-[2-(tetrahydro-2-pyranoxy)-1-ethoxyl]propane (34).

The chiral alcohol (37) (3.0g, 10 mmol) in anhydrous DMF (15 ml) was added slowly, dropwise to a stirred slurry of sodium hydride (0.26g, 11 mmol) in DMF (10 ml) under a flow of nitrogen. The mixture was stirred for one hour then a solution of the protected bromoethanol (33) (3.13g, 15 mmol) in DMF (10 ml) was added

dropwise into the mixture. After the addition, the temperature was raised to ca. 50°C and stirring was continued for eight hours. On cooling, the DMF was removed as usual and chloroform (100 ml) and water (100 ml) were added. The organic layer was subsequently washed with a further portion of water (100 ml), dried ($MgSO_4$) then evaporated to dryness, revealing the crude product which was freed of starting materials by flash chromatography using a petroleum ether (40-60)/ethyl acetate mixture (9:1) as the eluant.
Yield: 1.35g, 35%; mp 56°C; $[\alpha]_D^{20}$ = -10.00° ($CHCl_3$).
$C_{23}H_{30}O_5$ (386 $gmol^{-1}$). Calc.: C 71.50% H 7.77%
Found: C 72.02% H 8.29%

<u>(S)-1-(4-Methoxy-4'-oxybiphenyl)-2-(2-hydroxy-1-ethoxy)-propane (35)</u>

The previously synthesised THP protected alcohol (34) (2.14g, 5.54 mmol) was deprotected using acidified ethanol as in a procedure mentioned earlier, to yield a white crystalline solid, pure by tlc;
Yield 1.5g, 94%; mp 101-103°C; $[\alpha]_D^{25}$ = -5.72° (Acetone).
^1H Nmr: δ ppm (Acetone d-6, 90 MHz) 1.25 (d, 3H) methine C-CH_3; 2.79 (s, 1H) ROH; 3.3-4.21 (m, 9H) ArOCH_3, RCH_2OAr and ROCH_2CH_2OH; 4.55 (sex., 1H) methine H; 6.93 (d, J=9Hz, 4H) Ar-H; 7.47 (d, J=9Hz, 4H) Ar-H.
$C_{18}H_{22}O_4$ (302 $gmol^{-1}$) Calc.: C 71.52% H 7.28%
Found: C 72.06% H 7.44%

(S)-1-(4-Methoxy-4'-oxybiphenyl)-2-(2-methacryloyloxy-1-ethoxy) propane (36)

A solution of methacryloyl chloride (0.94g, 0.87 ml, 9 mmol) in anhydrous benzene (10 ml) was added slowly dropwise into a stirred solution of the aforementioned chiral alcohol (35) (1.16g, 3.84 mmol), triethylamine (0.91g, 9 mmol) and 2,5 di-t-butyl-4-methylphenol (ca. 0.1g) in anhydrous benzene (10 ml) at O°C. The solution was then allowed to warm to room temperature and stirred for a further eight hours. Benzene was removed from the reaction mixture by rotary evaporator, dichloromethane (200 ml) added and the mixture washed with water (2x50 ml), sodium bicarbonate (4x50 ml) and finally water (100 ml). After drying ($MgSO_4$), the dichloromethane was evaporated and the crude compound purified by flash chromatography using chloroform as the eluant to reveal a fine, white crystalline solid.

Yield: 1.49g, 82%; mp 59-61°C; $[\alpha]_D^{20}$ = -6.36°($CHCl_3$).

^1H Nmr: δ ppm ($CDCl_3$, 90 MHz) 1.25 (d, 3H) methine C-CH_3; 1.93 (s, 3H) vinyl CH_3; 3.60-4.10 (m, 7H) ArOCH_3, RCH_2OAr and -CH_2CH_2O-C; 4.27 (t, 2H) COO-CH_2-; 4.55 (sex., 1H) methine H; 5.49 (s, 1H) vinylic H trans to carbonyl; 6.10 (s, 1H) vinylic H cis to carbonyl; 6.89 (d, J=9Hz, 4H) Ar-H; 7.40 (d, J=9 Hz, 4H) Ar-H.

$C_{22}H_{26}O_5$ (370 $gmol^{-1}$) Calc.: C 71.35% H 7.02%

Found: C 71.85% H 7.22%

See appendix A for ^1H nmr spectrum.

3.2 Polymer Synthesis and Characterisation

3.2.1 Polymer characterisation

3.2.1.1 Thermal analysis using Differential Scanning Calorimetry (dsc)

The dsc technique was used extensively in this study to enable a complete characterisation of the various thermal parameters of both polymers and mesomorphic monomers. The measurement of parameters such as the glass transition temperature (Tg), the melting temperature (Tm) and various mesophase transition temperatures was therefore possible. In this work the Tg was taken as the onset temperature of the glass transition.

The instruments employed in this study were the Du Pont Thermal Analyser 900 fitted with a dsc cell and a Perkin Elmer DSC-2 model equipped with a low temperature mode accessory. Measurements using the latter were therefore possible in the range –173 to +727^{o}C.

3.2.1.2 Optical microscopy

An indispensable tool for the analysis and identification of different anisotropic liquid crystalline mesophase "textures" is the polarising microscope. [113] The polarising microscope is essentially a compound microscope fitted with a polariser and analyser, below and above the sample stage respectively.

In this study a Reichert Thermovar polarising microscope fitted with a hot-stage accessory was employed. The magnification used was either 100 or 200 times, and photomicrographs were taken

through the eye-piece lens, using a Pentax 'ME super' 35mm single lens reflex camera fitted with the appropriate adaptor.

Generally, the liquid crystalline samples under investigation were placed between a glass microscope slide and a thin glass cover-slip, then loaded onto the hot-stage. The temperature of the stage was increased gradually through the glass, melting, mesomorphic and isotropic transitions, then cooled gradually through the same transitions unless quenching or annealing processes were attempted. The use of polarising microscopy for mesophase identification is discussed in chapter 2.

3.2.1.3 Molecular weight determination[114]

Some of the polymeric materials made in this study were characterised by determining their number average molecular weight (Mn) using techniques based on the colligative properties of their dilute solutions. In this study both membrane osmometry and vapour phase osmometry were used to determine Mn.

The membrane osmometer used was a Knauer model and the membranes used were Sartorius 11539 50N regenerated cellulose membranes. These were conditioned to the operating solvent (chloroform) in the normal stepwise manner, firstly to ethanol then to chloroform. The instrument was calibrated using a known external pressure and the polymer solutions of 4 to 10 gdm^{-3} were introduced in increasing concentrations at an operating temperature of 33°C. Measurements under these conditions were shown to be reasonably accurate down to a lower limit of Mn $\simeq$10,000 $gmol^{-1}$.

The vapour-phase osmometer used was a Hewlett-Packard 302b instrument and the solvent used was 1,1,2 trichloroethane at a

temperature of 41°C. The instrument was calibrated using benzil (Mn = 210 $gmol^{-1}$) in a range of solutions of concentration 10-50 gdm^{-3} to give the calibration constant K = $4.98x10^3$ $\mu V dm^3 mol^{-1}$. Polymer solutions of concentration 10-50 gdm^{-3} were then analysed successively and the molecular weight calculated from the relation

$$M_n = K/(V/C)_{C=O} \qquad (2.1)$$

where V is a measure of the Wheatstone bridge imbalance with a solution of concentration C.

3.2.1.4 Copolymer composition analysis by Nuclear Magnetic Resonance (nmr) Spectroscopy

The composition of the copolymers synthesised in this study were analysed by ^1H nmr using either a Perkin-Elmer R-32 90 MHz instrument or a Bruker WP80 80 MHz instrument. Each were operated within their standard modes using tetramethylsilane as the internal standard.

The copolymer analysis consisted of a comparison of the integration values of two separate (in terms of chemical shift), distinguishable resonances or sets of resonances, each of which correspond to a distinct environment in one of the comonomer species. The relative proportions of each comonomer in the copolymer can then be calculated from these integration values by sytems of equations.

3.2.2 Copolymer synthesis

General procedure for copolymer synthesis

A standard 25 ml round-bottomed seal-off ampoule was charged with the required amount of each monomer to give a combined total weight of between 0.5 and 0.7 gms. The initiator, 0.5 mol % recrystallised 2,2'-azo-bis-isobutyronitrile (AIBN) and anhydrous solvent (2-3 ml) were then added and the ampoule sealed-off under vacuum, using the freeze-thaw technique to remove dissolved oxygen. The ampoule was placed in a thermostatted oil bath at the appropriate temperature, which was 70°C for polymerisations where DMBI-6 (5) was one of the monomers, or 60°C for all others (except where noted).

Work-up and polymer isolation was achieved by removing the ampoules from the bath at a time corresponding to 10-15% conversion or less, breaking open the ampoules and pouring the contents into methanol (150 ml). The resultant precipitate was collected by either filtration or centrifugation, dissolved in a small amount of a suitable solvent (e.g. chloroform or dichloromethane) and the polymer isolated by pouring this solution into a large amount (ca. 100-150 ml) of the appropriate non-solvent (see tables 3.1 to 3.8). Collection of the resultant precipitate was usually by centrifuge. The latter precipitation technique was repeated until tlc analysis indicated that no more monomer was present (usually about 3-6 times). All samples were then dried in a vacuum oven at 60°C for several days.

Copolymerisation conditions and results.

Copolymerisation conditions and results are reported in tabular form in the following. The copolymer compositions are recorded as the mole fraction (F) of one of the monomeric units in the copolymer. The feed ratio of this monomer in the polymerisation is also recorded as a mole fraction (f). Percentage conversion (% Conv.) is recorded in weight-percent, and molecular weights (where measured) are recorded in grams per mole. The average degree of polymerisation DPn is also recorded.

TABLE 3.1 Details of the copolymerisation of DBI with DMBI-6 in toluene at 70°C [a]

Copolymer Number	f_{DBI}	F_{DBI}	Time/hours	% Conv.	Precipitant[b]	10^{-3}Mn/gmol^{-1}	DPn
1a	0.00	0.00	48	40	Acetone	8.0	12
1b	0.05	0.10	30	10	$CHCl_3$/MeOH (1:1)		
1c	0.12	0.23	32	15	$CHCl_3$/MeOH (2:3)	7.2	15
1d	0.58	0.45	30	10	$CHCl_3$/MeOH (2:3)		
1e	0.80	0.55	32	7	$CHCl_3$/MeOH (2:3)		
1f	0.90	0.59	30	5	$CHCl_3$/MeOH (2:3)		
1g	1.00	1.00	48	45	MeOH	25.7	106

a - DMBI-6 was homopolymerised in bulk, in vacuo, using 0.5 mole % lauroyl peroxide as the free radical initiator at a temperature of 138°C.

b - The solvent used for precipitation purposes was chloroform.

TABLE 3.2 Details of the copolymerisation of MCP* with DMBI-6 in benzene at 70°C[a]

Copolymer Number	f_{MCP*}	F_{MCP*}	Time/hours	% Conv.	Precipitant[b]	10^{-3}Mn/gmol^{-1}	DP_n
1a	0.00	0.00	48	40	Acetone	8.0	12
2a	0.20	0.29	15	10	Acetone		
2b	0.40	0.51	15	5	Acetone	12.5	32
2c	0.60	0.62	13.5	9	$Et_2O/CHCl_3$ (85:15)		
2d	0.80	0.78	11	9	$Et_2O/CHCl_3$ (85:15)		
2e	1.00	1.00	48	65	Et_2O	25.8	94

a - DMBI-6 was homopolymerised in bulk, in vacuo, using 0.5 mole% lauroyl peroxide as the free radical initiator at a temperature of 138°C.

b - The solvent used for precipitation purposes was chloroform for polymers 1a and 2a-2d and acetone for polymer 2e.

TABLE 3.3 Details of the copolymersiation of MMMP* with CPBA-6 in benzene at 60°C.

Copolymer Number	f_{MMMP*}	F_{MMMP*}	Time/hours	% Conv.	Precipitant[a]	$10^{-3}Mn/gmol^{-1}$	DP_n
3a	0.00	0.00	24	60	Cold Et_2O	65.0	165
3b	0.05	0.24	4	9	"		
3c	0.20	0.51	4.5	20	"		
3d	0.30	0.61	6	15	"	126.0	540
3e	0.50	0.79	4	7	"		
3f	0.75	0.92	4	12	"		
3g	1.00	-[b]	2	5	-[b]	-	-

a - The solvent used for precipitation purposes was dichloromethane.

b - Only crosslinked homopolymer was obtained. Excess monomer was removed by washing with Et_2O.

TABLE 3.4 Details of the copolymerisation of ChMI-10 with CPBA-6 in benzene at 60°C[a]

Copolymer Number	$f_{ChMI-10}$	Time/hours	% Conv.	Precipitant[b]	$10^{-3}Mn/gmol^{-1}$	DP_n
3a	0.00	24	60	Cold Et_2O	65.0	165
4a	0.10	6	11	EtOH		
4b	0.25	8.5	5	EtOH	30.0	
4c	0.50	9	5	EtOH		
4d	0.75	12	4	EtOH		
4e	1.00	48	45	MeOH	9.7	14

a - ChMI-10 was polymerised in bulk, in vacuo, using 0.5 mole % AIBN as the free-radical initiator at 70°C.

b - The solvent used for precipitation purposes was dichloromethane.

TABLE 3.5 Details of the copolymerisation of MBM* with DMBI-6 in benzene at 70°C[a]

Copolymer Number	f_{MBM*}	F_{MBM*}	Time/hours	% Conv.	Precipitant[b]	10^{-3}Mn/gmol^{-1}	DP_n
1a	0.00	0.00	48	40	Acetone	8.0	12
5a	0.15	0.32	23	6	Acetone		
5b	0.26	0.63	10	10	Acetone	41.0	101
5c	0.34	0.70	14	11	Acetone/MeOH (9:1)		
5d	0.50	0.83	4	8	Acetone/MeOH (9:1)		
5e	0.75	0.95	8	8	Acetone		
5f	1.00	1.00	32	69	Acetone	425.0	1304

a - DMBI-6 was homopolymerised in bulk, in vacuo, using 0.5 mole % lauroyl peroxide as the free radical initiator at 138°C.

b - The solvent used for precipitation purposes was chloroform.

TABLE 3.6 Details of the copolymerisation of CBM* with DMBI-6 in tetrahydrofuran at 55°C[a]

Copolymer Number	f_{CBM*}	F_{CBM*}	Time/hours	% Conv.	Precipitant[b]	10^{-3}Mn/gmol^{-1}	DP_n
1a	0.00	0.00	48	40	Acetone	8.0	12
6a	0.10	0.26	23	10	Acetone	7.4	14
6b	0.25	0.47	10	12	Acetone	12.0	27
6c	0.40	0.62	5.5	11	Acetone/MeOH (9:1)	230.0	570
6d	0.60	0.76	5.5	8	Acetone/MeOH (9:1)	89.0	241
6e	0.75	0.85	8	7	Acetone/MeOH (9:1)	67.0	191
6f	1.00	1.00	48	62	MeOH	200.0	623

a - DMBI-6 was homopolymerised in bulk, in vacuo, using 0.5 mole% lauroyl peroxide as the free radical initiator at 138°C.

b - The solvent used for precipitation purposes was chloroform.

TABLE 3.7 Details of the copolymerisation of CBM* with CPBA-6 in benzene at 60°C.

Copolymer Number	f_{CBM*}	Time/hours	% Conv.	Precipitant[a,b]	10^{-3}Mn/gmol^{-1}	DP_n
3a	0.00	24	60	Cold Et_2O	65.0	165
7a	0.10	4	8	"		
7b	0.15	4	8	"		
7c	0.25	4.5	4	"		
7d	0.50	2	13	"	72.0	-
7e	0.75	0.5	5	"		
6f	1.00	48	62	MeOH	200.0	623

a - The solvents used for precipitation purposes were dichloromethane for polymers 3a, 7a-7e and chloroform for polymer 6f.

b - An additional precipitation was carried out in methanol for polymers 7a-7e.

TABLE 3.8 Details of the copolymerisation of XMBM* with CPBA-6 in benzene at 60°C.

Copolymer Number	f_{XMBM*}	F_{XMBM*}	Time/hours	% Conv.	Precipitant[a,b]	10^{-3}Mn/gmol^{-1}	DP_n
3a	0.00	0.00	24	60	Cold Et_2O	65.0	165
8a	0.10	0.39	5	8	"		
8b	0.20	0.45	5.5	10	"		
8c	0.30	0.53	6	8	"		
8d	0.50	0.73	5.5	15	"	153.5	409
8e	0.75	0.85	2.5	10	Acetone		
8f	1.00	1.00	7	38	Acetone	60.4	163

a - The solvent used for precipitation purposes was dichloromethane.

b - An additional precipitation was carried out in methanol for copolymers 8a-8d.

3.2.3 Attempted synthesis of PDChI-10

The monomer DChI-10 proved to be very difficult to polymerise. Three different methods of polymerisation were examined, in addition to a "polymer analogous" type synthesis of the polymer.

Attempted solution and bulk polymerisation proved fruitless, with the exception that the contents of the bulk polymerisation flask appeared to have solidified. No material was isolated by precipitation and it was therefore assumed that the solid material was probably dimeric or trimeric in nature.

In order to avoid the precipitation of dimer from the melt of DChI-10 the polymerisation was repeated in a two-necked, seal-off ampoule using a concentrated benzene solution of DChI-10 and 0.5 mole% AIBN. The contents of the flask were observed closely for an increase in viscosity, which occurred after about five hours. At this point a further amount of AIBN (0.5 mole%) in benzene (0.5 ml) was syringed into the flask via the side-neck. After 48 hours the viscosity was again noticeably more viscous. Precipitation of the material several times from dichloromethane into a chloroform/ methanol mixture (1:4) produced a globular-like product which was found to be oligomeric material of very low molecular weight (microscopy analysis showed that the transition temperatures of this material were barely higher than those of the starting material).

The attempted synthesis of PDChI-10 (39) by polymer analogous reaction of the di-cesium salt of polyitaconic acid with cholesteryl-11-bromoundecanoate (12) was carried out as follows: Poly(dicesium itaconate) (38) was prepared by refluxing

poly(monomethylitaconate) (37) (0.68g, 4.72 mmol) with cesium hydroxide (2.7g, 18 mmol) in water (60 ml) for one hour. The reaction was then cooled slowly to room temperature and the solution added to a large excess of ethanol. After decanting off the yellow coloured super-natant liquid, the polymeric precipitate was washed repeatedly with ethanol until the yellow colour had disappeared, then dried under vacuum. Yield: 0.7g, 37%; ir: $\bar{\nu}$ (KBr disc) 1580, 1380 cm^{-1}.

The attempted synthesis of PDChI-10 by the phase-transfer catalysed reaction of poly(dicesium itaconate) (38) with cholesteryl-11-bromo undecanoate (12) was carried out by the procedure described by Keller[64] for a similar system (scheme 11):

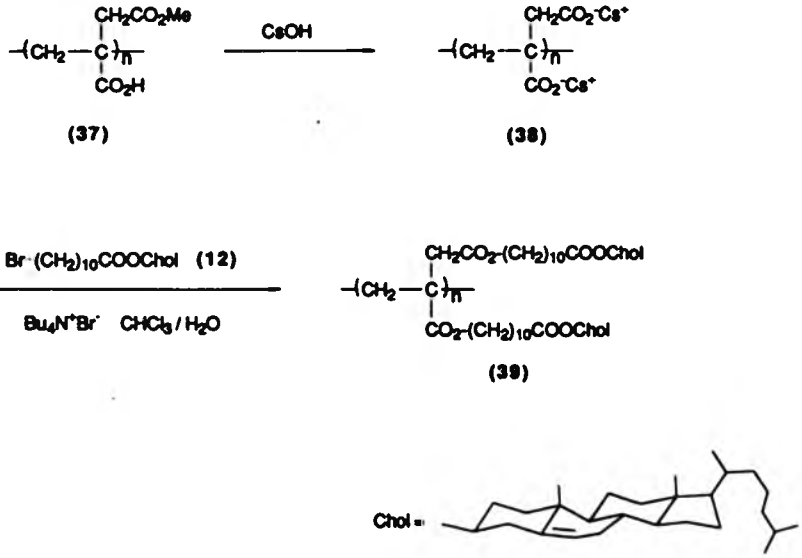

SCHEME 11

Poly(dicesium itaconate) (38) (0.68g, 1.72 mmol) was dissolved in water (10 ml) and added to a solution of the bromo-cholesteryl compound (12) (2.45g, 3.87 mmol) and tetra butyl ammonium bromide (0.21g, 0.64 mmol) in chloroform (35 ml). The mixture was stirred vigorously and heated under reflux for a period of 96 hours, during which time the amount of cholesteryl derivative in the chloroform layer was monitored by tlc. However, even after this time tlc showed little or no reduction in the amount of bromide present and only a very small, weak spot at R_f = 0.00 that might have corresponded to polymeric material. Analysis of the dried and evaporated chloroform layer by hot-stage microscopy revealed only the crystalline starting material which melted at 103°C (Lit.:[106] 105°C).

This experiment was repeated using poly(di-sodium itaconate). Again, the anticipated cholesteryl substituted polyitaconate DChI-10 was not found.

CHAPTER FOUR

MESOGENIC/NON-MESOGENIC

CHIRAL COPOLYMER SYSTEMS

4. MESOGENIC/NON- MESOGENIC CHIRAL COPOLYMER SYSTEMS

It is now well established that when host nematic phases, whether they are low molecular weight or polymeric in nature, are doped with small amounts of optically active species, induced chiral nematic phases result.[13,33] This phenomenon has been shown to occur whether the optically active dopant molecule is mesogenic or non-mesogenic in nature and even molecules such as carvone or verbenone which do not have the pre-requisite long, rigid, lath-like shape have been found to induce chiral nematic phases on addition to small molecule nematics.[13] In this work Finkelmann and Stegemeyer found that chiral molecules with more than one chiral centre or large optical rotations and long planar shapes produced the greatest helical twisting power. From their results it is obvious why the cholesteryl derivatives are very successful as dopant molecules.

According to Goosens,[11] Vertogen[12] and Finkelmann,[13] the spontaneous helical twist arises from both hindered rotation about the molecular long axis of the chiral molecules and dipole-quadrupole interactions between the mesogens and the chiral species. However, the treatment of these theories in any depth is outwith the scope of this thesis.

It is of interest to discover whether the same induced helical twisting phenomenon would occur in the case of comb-branch polymers, where the non-mesogenic chiral centre is chemically linked to the polymer backbone rather than merely dispersed in the polymer matrix.[33] Polymers of this type were arrived at by the copolymerisation of mesogenic, non-chiral monomers with chiral, non-mesogenic monomers.

Three systems were investigated in this study and the copolymerisation behaviour as well as the mesomorphic behaviour of these systems are reported and discussed, after a short introduction to copolymerisation and the "terminal model".

4.1 Copolymerisation and the Terminal Model

When two monomers are copolymerised, the relative rates at which the two monomers add to the growing chain governs the composition of the copolymer, and ultimately its properties. The order, as well as the ratios, in which the monomers add are determined by their relative reactivities in the propagation step of the polymerisation reaction. These reactivities are dependent on such factors as the resonance stability of each monomer and their radicals, the polarity of the side groups attached to the vinyl double bond and on steric effects.

The copolymerisation model used in this work is the Mayo-Lewis model or "terminal" model of copolymerisation.[115] This model is a mathematical treatment of Dostals' hypothesis[116] which states that the rate of addition of a monomer to a radical is independent of the size and nature of the radical chain and is influenced only by the nature of the radical end group. Based on these assumptions, four different modes of propagation become apparent, 4.1-4.4:

$$-M_1. + M_1 \xrightarrow{k_{11}} M_1M_1. \qquad (4.1)$$

$$-M_1. + M_2 \xrightarrow{k_{12}} M_1M_2. \qquad (4.2)$$

$$-M_2\cdot + M_1 \xrightarrow{k_{21}} M_2M_1\cdot \qquad (4.3)$$

$$-M_2\cdot + M_2 \xrightarrow{k_{22}} M_2M_2\cdot \qquad (4.4)$$

where k_{11} and k_{22} are the rate constants for self-propagation and k_{12} and k_{21} are the corresponding rate constants for cross-propagation. $-M_1$ indicates that the terminal repeat unit in the growing radical is monomer 1 etc. By separately assuming steady state conditions for each radical one can derive a copolymer equation which relates the instantaneous copolymer composition, $d[M_1]/d[M_2]$, to the monomer feed concentrations:

$$\frac{d[M_1]}{d[M_2]} = \frac{[M_1]}{[M_2]} \cdot \frac{r_1[M_1]+[M_2]}{r_2[M_2]+[M_1]} = \frac{1+r_1[M_1]/[M_2]}{1+r_2[M_2]/[M_1]} \qquad (4.5)$$

where $r_1 = k_{11}/k_{12}$ and $r_2 = k_{22}/k_{21}$.

The ratios r_1 and r_2 are the monomer reactivity ratios. These correspond to the ratios of the rate constants for a given radical adding to its own monomer to that for it adding to the other monomer. For example, a value of $r > 1$ means that the radical prefers to add to its own monomer rather than the comonomer. Large values of r (both r_1 and $r_2 > 1$) indicate a tendency for the monomers to form long homopolymer-like sequences whereas small values of r (both r_1 and $r_2 \simeq 0$) indicate the occurrence of rapid cross-propagation reactions and reflect a tendency for the monomers

to alternate in the polymer chain. Whilst the latter mode of addition is frequently encountered in copolymerisation[117] the former is much rarer.[118] Ideal copolymers are formed when the two radicals show the same preference for both self- and cross-propagation: $k_{11}/k_{12} = k_{21}/k_{22}$, or $r_1 = 1/r_2$. In this case the nature of the end group has no influence on the rate of addition and "statistical" polymers result.

Generally most cases lie between alternating and ideal systems; $0 < r_1 r_2 < 1$.

Since the reactivity ratios are the factors which control the copolymer composition, it is important to obtain reliable values of r_1 and r_2 if copolymerisation systems are to be fully characterised. The reactivity ratios can be determined by analysing the composition of various copolymers prepared from a number of monomer feed ratios at low conversions and employing this data in one of the forms of equation (4.5). Low conversions (<10%) are used so as to avoid composition drift.[119]

In this work the reactivity ratios were calculated from a best fit of the experimental composition versus feed data, computed by employing the Levenberg-Marquardt iterative non-linear least squares curve fitting procedure to equation (4.5). A plot of composition versus feed such as this, presents a convenient visual representation of the mode of addition involved in the copolymerisation. However, additional information is often required for conclusive proof of the mode involved, such as sequence distribution analysis.[120]

4.2 Copolymers of DMBI-6 and DBI

The monomer chosen as the mesogenic monomer in this study is the previously unreported itaconate-based methoxybiphenyl monomer DMBI-6. This monomer is also mesomorphic in nature and its properties are discussed briefly in section 4.2.2. The structure of the monomer is shown below.

In this section, the aim of the study was to prepare copolymers from DMBI-6 and the non-mesogenic, non-chiral itaconate monomer DBI. This was carried out with the expectation that information would be gained on the ability of the bulky DBI monomer to disrupt the resultant copolymer mesophase. It was then perceived that should this monomer disorder the mesophase sufficiently and transform the ordered smectic homopolymer into a nematic copolymer, then by substituting a similar chiral monomer for DBI it would be possible to induce a helical structure.

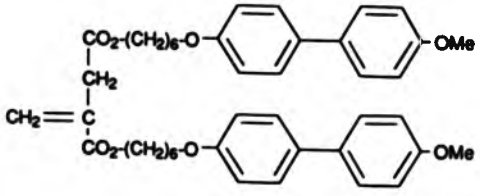

DMBI-6

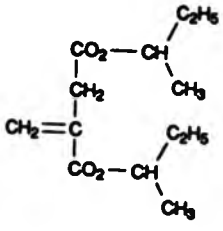

DBI

4.2.1 Copolymerisation characteristics of DMBI-6 and DBI

The copolymer composition curve, plotted as the mole fraction of DBI in the copolymer (F_{DBI}) versus the mole fraction of DBI in the monomer feed (f_{DBI}) is displayed in figure 4.1 along with the calculated reactivity ratios for each monomer. Composition, feed and molecular weight data are recorded in table 3.1, chapter 3.

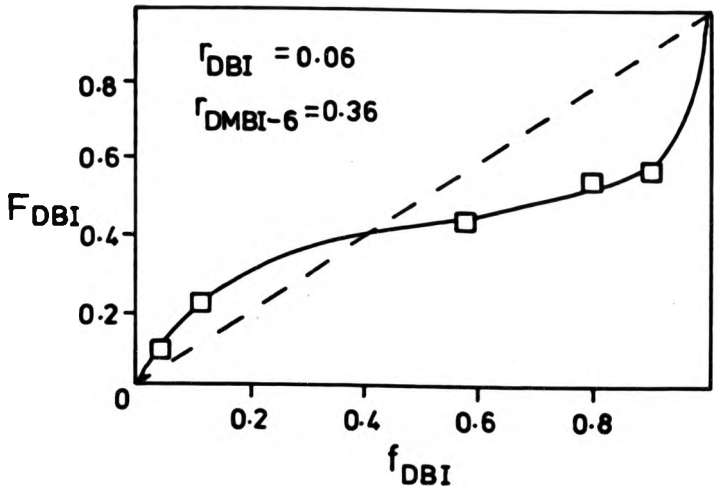

FIGURE 4.1 **A plot of mole fraction of DBI in the copolymer (F_{DBI}) versus the mole fraction of DBI in the monomer feed (f_{DBI}) and the corresponding reactivity ratios for each monomer.**

(□) : Experimental point

(—) : Calculated best fit to experimental data.

The copolymer curve shows that the system tends to produce a copolymer of constant composition over a wide feed range, with the azeotropic composition point occurring at $F_{DBI}=f_{DBI}=0.40$. Shapes such as these are characteristic of alternating polymerisation, as is the product of the reactivity ratios which is tending towards zero.[117] Rationalisation of this copolymerisation behaviour is difficult, since both monomers have the same itaconate vinyl moiety with essentially similar side groups having similar polarities (see structures at the beginning of this section). This would normally tend to suggest the polymerisation to be random in nature, since in most cases alternating copolymers are usually only formed when comonomers with widely differing polarities are reacted together. However, by consideration of the steric effects involved, i.e. the bulky side chains in DBI impeding the accessibility of the vinyl bond, it may be possible that it is too difficult for an incoming DBI monomer to successfully approach a DBI terminated radical chain. Access of a DMBI-6 monomer to the radical chain end may therefore be more favourable. In other words, the activation energies associated with the cross-propagation steps are much lower than the activation energy associated with the DBI self propagation step. This is exemplified by the reactivity ratios calculated for the system, $r_{DMBI\text{-}6} > r_{DBI}$.

Another clue to this unusual behaviour could be the low conversion (45%) after 48 hours reaction time of the homopolymerisation of DBI. The molecular weight of the resultant polymer is also fairly low (25700 $gmol^{-1}$, $DP_n=106$). This may also be an indication of the inability of this bulky monomer to undergo facile homopolymerisation, although the possibility of chain transfer to both the toluene solvent and other itaconate monomers due to

hydrogen abstraction cannot be ruled out. Steric considerations have also been cited as a factor in the unusual alternating tendency of the copolymerisation of ethylene with cyclopentene in the presence of a Zeigler catalyst.[121]

On the basis of the composition data and the steric arguments given above, it can only be tentatively assumed that the system is tending towards alternation. Other evidence such as sequence analysis by ^{1}H nmr[122] would be needed to confirm this hypothesis however. Additionally, it must be recognised that the composition of the copolymer chains may not be homogeneous, i.e. there may be a distribution of chain compositions, especially at low molecular weight values such as those reported for this system.

The measured degrees of polymerisation of the three selected polymers from this system were 12, 15 and 106 for DMBI-6, DMBI-6/DBI (F_{DBI} = 0.23) and PDBI respectively. It would be reasonable to assume that the DP_n of the other copolymers were of a similar order. As mentioned previously in the case of PDBI, the low DP_n values could be attributed to a combination of degradative chain transfer of the radical site to another monomer (this is also known as "auto inhibition"), chain transfer to toluene solvent, steric effects and possibly the mode of termination. These effects are all known to produce lower molecular weights in itaconate polymerisations.[123] In the case of PDMBI-6 an additional factor may contribute to the low value of DP_n observed, namely the use of a rather high bulk polymerisation temperature (138°C). The use of a higher temperature usually increases the rate of polymerisation, but decreases the average chain length, especially if the temperature is near the ceiling temperature of the system where the

depolymerisation reaction becomes energetically favourable.[124] Unfortunately, no data on the ceiling temperature of itaconate monomers such as those described is available in the literature.

Polymerisation of DMBI-6 was achieved only in the bulk state, since attempted solution polymerisation resulted in only very low conversions (<3%). Bulk polymerisations such as these are problematical however, since a sufficiently high temperature must be used so as to allow the liquid monomer phase to act as a solvent for the new phase of the polymer being formed. In the case of PDMBI-6, the temperature was kept above 130°C since at temperatures below this the polymer or oligomers in their crystalline state tended to phase separate from the monomer liquid. Observations such as these have previously been reported in the literature.[55,125]

4.2.2 Mesomorphic properties of DMBI-6/DBI copolymers

All of the copolymers prepared from DBI and DMBI-6 exhibit enantiotropic liquid crystalline properties, including the homopolymer PDMBI-6. The monomer DMBI-6 also exhibits mesomorphic properties and from dsc and microscopy investigations it was found to form the smectic B phase. Microscopy revealed the presence of the typical smectic B mosaic texture, similar to that shown in figure 2.6, chapter two. The phase transition temperatures of DMBI-6 as measured by dsc were found to be:

$$k \xrightarrow{68^{\circ}C} S_B \xrightarrow{108^{\circ}C} I$$

Table 4.1 summarises the various phase transition temperatures of the copolymers as determined by both dsc and hot stage microscopy. These results are also shown in graphical form in figure 4.9 which will be discussed shortly. Importantly, it should be remembered that the mesophase transition temperatures, as well as the Tg of a polymer, are strongly molecular weight dependent, especially in regions of low molecular weight.[39] Stevens and co-workers[126] found a critical limit for molecular weight dependence of $Dp_n \simeq 10$ when they examined a comb-branch siloxane polymer bearing methoxyphenylbenzoate side chains. Although this value is possibly less than that for any of the polymers described here, it is conceivable that the critical DP_n value of these copolymers may be higher than $DP_n \simeq 10$. Unfortunately, copolymers of higher molecular weight could not be prepared in order to ascertain the molecular weight dependence of the thermal transitions in this system.

The identification of the phase transition temperatures and the mesophase type of the copolymers was determined by a combination of both dsc and hot-stage polarising microscopy, and the dsc traces and microscopy results are discussed in the following three sub-sections.

4.2.2.1 Thermal and textural behaviour of homopolymer 1a (PDMBI-6)

The transitions shown on the dsc heating and cooling traces of polymer 1a in figure 4.2 are well separated and therefore fairly easy to identify. The corresponding optically located transitions are noted on each trace.

On increasing the temperature of the polymer sample during

TABLE 4.1 The phase transition temperatures of DBI/DMBI-6 copolymers[a]

Copolymer Number	F_{DBI}	Tg/°C	Tm/°C [c]	$T_{S_B-S_A}$/°C	$T_{S_A-S_A/I}$/°C [d]	$T_{S_A/I-I}$/°C [d]	$\Delta T_{BIPHASIC}$
1a	0.00	64	125	-	150	157	7
1b	0.10	62	117	125	143	151	8
1c	0.23	48	103	119	125	135	10
1d	0.45	50	94	123	130	135	5
1e	0.55	53[b]	-	-	125	127	2
1f	0.59	56[b]	-	-	126	129	3
1g	1.00	66	-	-	-	-	-

a - All temperatures are recorded during the second dsc heating cycle at a rate of 20°C/minute.

b - At the Tg value indicated polymers 1e and 1f are transformed into a smectic liquid crystalline phase. No crystallinity was detected in these samples by either dsc or microscopic observations.

c - Tm is the melting temperature and indicates a transition from the crystalline phase to either the smectic A phase or smectic B phase as determined by either dsc or microscopic observations.

d - $T_{S_A-S_A/I}$ indicates the transition from a smectic A phase to a biphasic smectic A/isotropic region. This temperature is taken as the maximum of the smectic A-isotropic endotherm on the dsc trace. $T_{S_A/I-I}$ indicates the final disappearance of mesomorphic order and is correlated with microscopic observations.

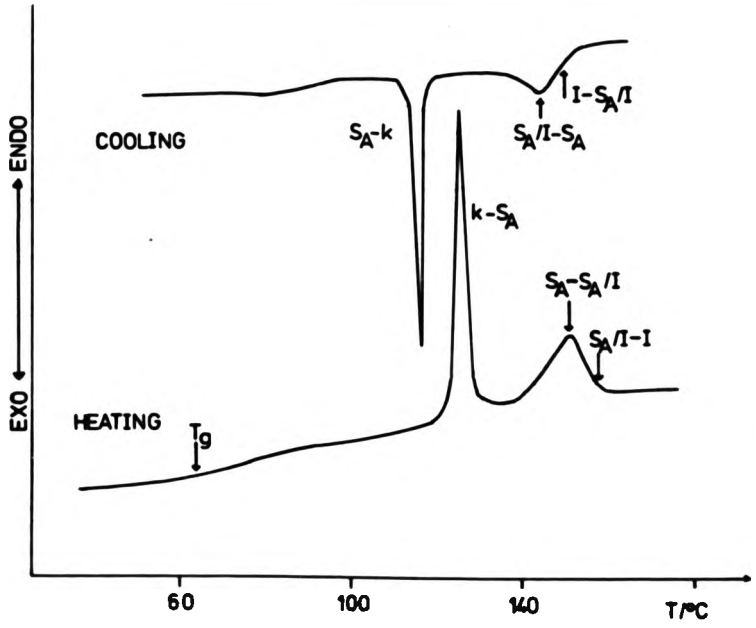

FIGURE 4.2 **Dsc heating and cooling traces of polymer 1a recorded at 20°C/minute. The heating trace was recorded during the second heating scan and the cooling trace was recorded immediately after.**

the heating scan, the first transition encountered is the glass transition at 64°C. On further heating one arrives at a large, sharp first-order endotherm centred at 125°C followed by smaller, broader first-order endotherm centred at 150°C. From microscopic investigations these have been assigned as crystalline to smectic A and smectic A to isotropic transitions respectively. On cooling, the

same phase transformations are encountered, with the exception that these both occur at slightly lower temperatures, i.e. the transitions have been supercooled. The super cooling phenomenon associated with the crystalline-mesophase transition has been well documented in the past[127,128] and the value obtained for PDMBI-6 of 10°C is comparable for the heating rate used. Supercooling of the isotropic liquid, however, is less common.[91,127,128] It is therefore worthy of note that PDMBI-6 shows an isotropic liquid supercooling of 5°C at 20°C/minute cooling rate.

Microscopy observations showed that on cooling the isotropic melt of PDMBI-6, the smectic A phase separated from the melt in the form of bâtonnets[96,98] which, after further growth and coalescence, gave rise to a focal-conic fanned texture typical of the smectic A phase. This texture, shown in figure 4.3, closely resembles the textures of the smectic A phases reported for other side chain polymers[84,92] and low molecular weight compounds.[18] Annealing of this phase in the region near the clearing temperature resulted in a more perfect texture.

An additional feature of the mesomorphic nature of this homopolymer is the existence of a stable, biphasic smectic A-isotropic liquid region. This type of behaviour has previously been reported for both side chain[129] and main chain[130,131] PLCs and is a consequence of the polydispersity of the sample.[132] This effect is most clearly observed by microscopy on heating, where, on reaching the temperature corresponding to the maximum of the smectic A to isotropic endotherm in the dsc experiment, some of the focal-conic domains are transformed into the isotropic liquid. This transition is designated the S_A-S_A/I transition. As the temperature is increased

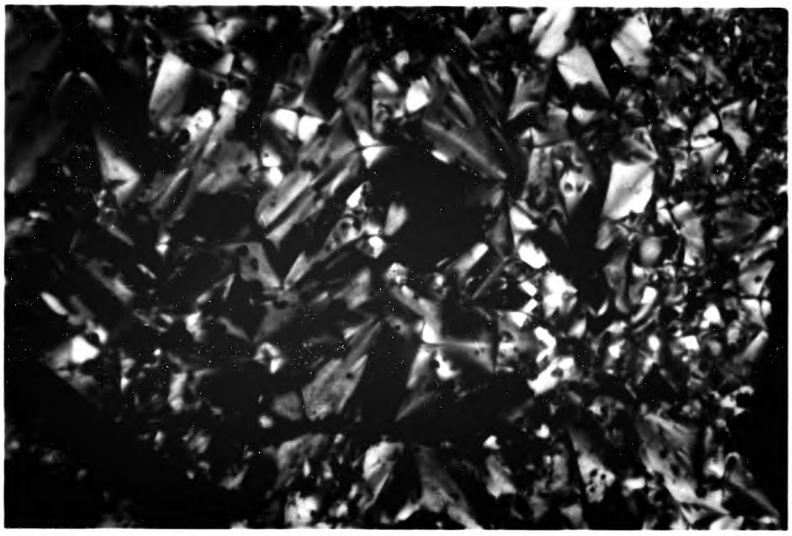

FIGURE 4.3 **Photomicrograph showing the fanned focal-conic texture of the smectic A phase of polymer 1a (PDMBI-6) (Magnification x200).**

further, the size of the isotropic phase increases at the expense of the focal-conic domains until a certain point is reached where the remainder of the LC phase is transformed into the isotropic fluid. This is designated the S_A/I-I transition and is detected only by polarising microscopy or by other optical techniques such as thermal optical analysis.[129,133] This effect is typified by broad dsc endotherms and the reverse effect can also be seen on cooling.

4.2.2.2 Thermal and textural behaviour of copolymers 1b-1d.

The representative dsc heating traces of copolymers 1c and 1d displayed in figure 4.4 show less-well defined transitions than those shown by polymer 1a. Nevertheless, with the use of hot-stage polarising microscopy the phases and transitions were identifiable without too much difficulty.

Copolymer 1c exhibits, as well as the glass transition at 48°C, a small endotherm at 103°C which appears almost as a shoulder to a much larger endotherm at 119°C. Another larger shoulder is also apparent on the high temperature side of the large endotherm (125°C). The cooling trace (not shown) shows quite similar events, with all of the transitions being subject to super cooling. This is 5°C for the isotropic transition and 10°C for each of the lower transitions.

Similarly, the same endothermic transitions occur on heating copolymer 1d with the exception that the lowest temperature endotherm appears at a much lower temperature of 94°C. Supercooling effects of similar magnitudes also occur.

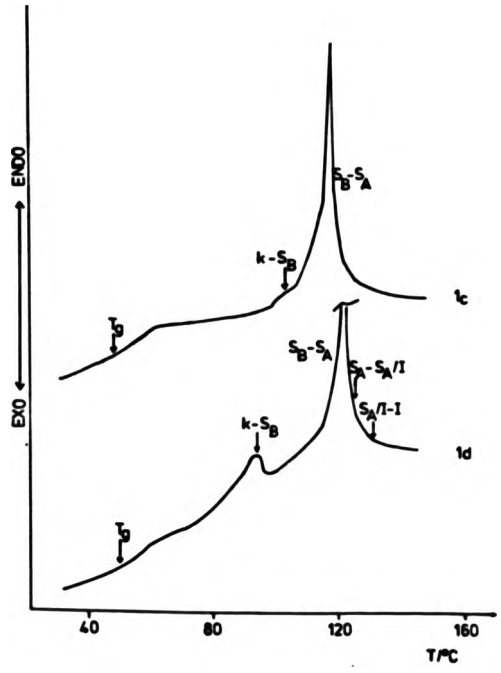

FIGURE 4.4 **Dsc heating traces of copolymers 1c and 1d recorded during the second heating scan at 20°C/minute.**

The thermal events associated with copolymers 1c, 1d and 1b (for which no dsc trace is shown) have been identified by correlation with microscopy observations, and all polymers have been found to exhibit the same sequential phase behaviour. For example, on cooling the isotropic melt of polymer 1c, the formation of bâtonnets followed by the focal-conic fanned texture via the previously discussed biphasic phenomenon suggests that the highest temperature event on the dsc trace corresponds to a smectic A-isotropic phase transition. Figures 4.5(a) and (b) show the fanned

focal-conic texture and the biphasic smectic A-isotropic liquid textures respectively, of polymer 1c.

On further cooling of the focal-conic fanned texture no immediately obvious changes were observed, even after cooling below the transition temperature associated with the large dsc endotherm. Initially, this was confusing. However, after close inspection of the focal-conic fans on repeated heating and cooling cycles through the transition, transition bars were detected. These transitory effects are of course usually only observable at the transition between the smectic A and B phases (see section 2.2), thus the lower temperature phase is designated as the smectic B phase.[18] Very little change in the focal-conic texture with the transition to the smectic B phase is expected, since the smectic B phase is also known to exhibit a "paramorphotic" focal-conic fanned texture, i.e. it inherits the texture from the smectic A phase.[18,96] This is because the rearrangement of the mesogens to form the smectic B phase does not disrupt the focal-conic fanned texture. Although no examples of these transition bars are shown for copolymer 1c, figure 4.6(a) shows the focal-conic texture of copolymer 1b exhibiting this transitory phenomenon.

Further evidence that the phase type was smectic B was found by quickly cooling the homeotropic texture of the smectic A phase of copolymer 1b (homeotropic texture preparation is discussed in chapter 2) and shearing the sample. This process resulted in a mosaic-like texture which is characteristic of the smectic B phase (figure 4.6(b)).[18] It was also possible to obtain these textures for copolymers 1c and 1d. Of course, one cannot determine or specify the exact structure of the smectic B phase, i.e. whether it is crystal-like or hexatic, unless additional information from X-ray scattering

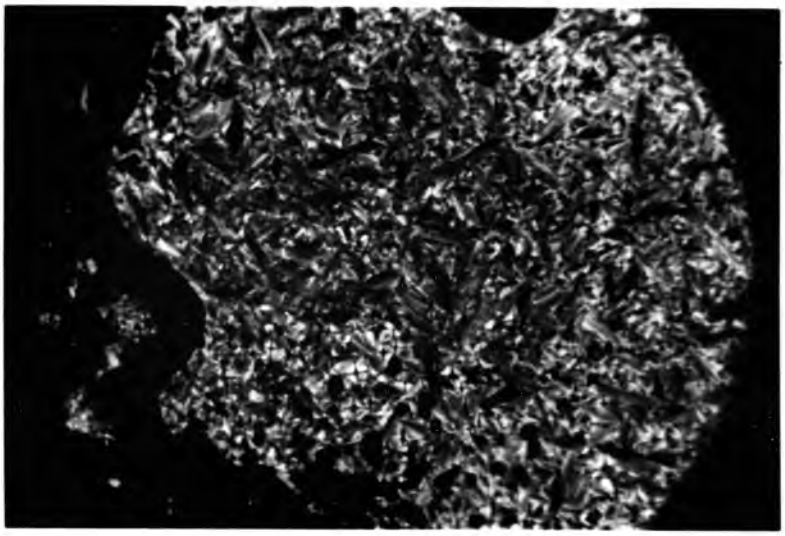

FIGURE 4.5 (a) Photomicrograph showing the fanned focal-conic texture of the smectic A phase of copolymer 1c (Magnification x 100).

FIGURE 4.5 (b) Photomicrograph showing the biphasic smectic A/isotropic liquid region of copolymer 1c (Magnification x 200).

FIGURE 4.6 (a) Photomicrograph showing the fanned focal-conic texture with transition bars at the smectic A to smectic B transition of copolymer1b (Magnification x 100).

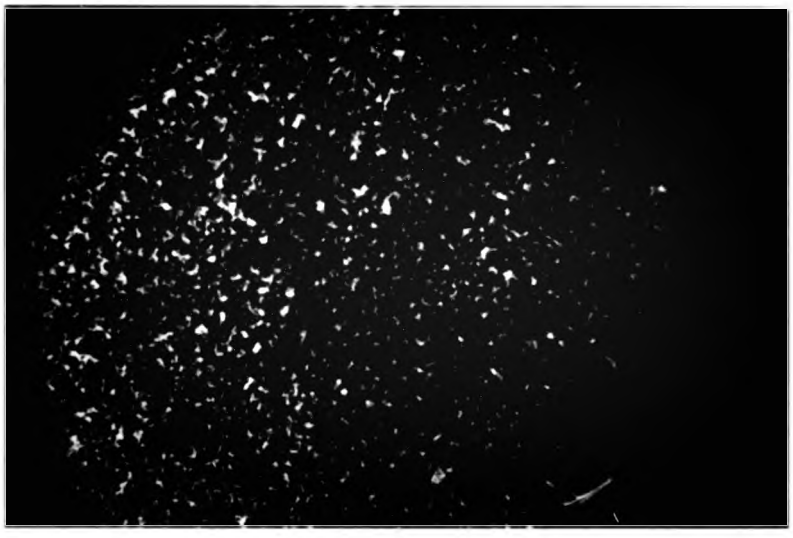

FIGURE 4.6 (b) Photomicrograph showing the mosaic texture of the smectic B phase of copolymer 1b (Magnification x 100).

experiments or other techniques is available.

The lowest temperature endotherms shown on the dsc heating traces for copolymers 1c and 1d could not be correlated with microscopic investigations. However, by varying the cooling rate in the dsc experiment before carrying out the heating scan, it was seen that the magnitude of this endotherm increased when slow cooling rates were employed. Additionally, the glass transition became less distinct and, when fast cooling rates were employed, considerable supercooling was observed. These observations tend to suggest that this transition is associated with the crystalline phase.

From all of the above observations on the thermal and optical properties of copolymers 1b to 1d it can be assumed that the enantiotropic transitions associated with these polymers are

crystal $\longleftrightarrow$ smectic B $\longleftrightarrow$ smectic A $\longleftrightarrow$ isotropic liquid.

4.2.2.3 Thermal and textural behaviour of copolymers 1e and 1f.

In contrast to the previously described copolymers, copolymers 1e and 1f do not exhibit any crystallinity. Only one endotherm and the glass transition are apparent on their dsc traces. Figure 4.7 shows the representative dsc heating trace of copolymer 1e.

The lack of crystallinity in these copolymers can be understood from the fact that they both have a fairly high DBI content (55 and 59% for copolymers 1e and 1f respectively), which would tend to separate the mesogenic DMBI-6 monomer units and consequently reduce their anisotropic interactions and hence their ability to crystallise on cooling. There must be, however, enough interaction to allow the formation of the liquid crystalline state.

This weakening in anisotropic interaction is also manifest in the optical behaviour of the copolymers.

Both copolymers exhibit a much weaker birefringence in comparison to the previously described copolymers. This again infers that the non-mesogenic side chains, which are present in sufficient quantities, prevent efficient mesogenic side chain interaction because of both the increased distance between the mesogens and the thermal motions of the non-mesogenic side chains, which tend to screen the mesogenic side chains to some extent.

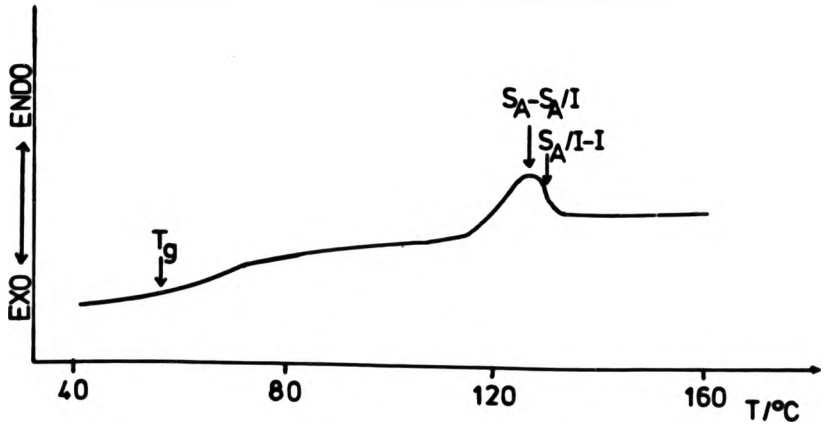

FIGURE 4.7 **Dsc heating trace of copolymer 1e recorded during the second heating scan at 20°C/minute.**

These effects also reduce the clearing temperatures of the copolymers compared to the mesogenic homopolymer.

Definite identification of the phase type of these similar copolymers is difficult due to both their apparent low birefringence and their inability to form well-defined textures. For example, on cooling the isotropic melt of copolymer 1e to below the isotropic-mesophase transition, bâtonnets are formed. On further cooling however, they do not grow and coalesce as is normal; instead a stable biphasic region exists which does not undergo change, even after annealing the sample for two hours. These features are shown in the photomicrograph in figure 4.8(a). On further cooling of the sample to just below ~120°C an unidentifiable, sand-like, grainy texture was seen to form (figure 4.8(b)). This type of texture has previously been reported by other workers[92,95] and is a common feature of some freshly-prepared polymeric smectic textures (see section 2.2.5). Each of the grains or birefringent regions correspond to particular smectic domains, each with their own orientation. Normally, annealing a texture such as this will produce a typical smectic texture. However, the samples under investigation here have produced no well-defined textures, even after prolonged annealing times or further cooling. It can therefore only be tentatively concluded that the phase is smectic in nature, with the implication that it may be smectic A arising from the occurrence of the bâtonnets.

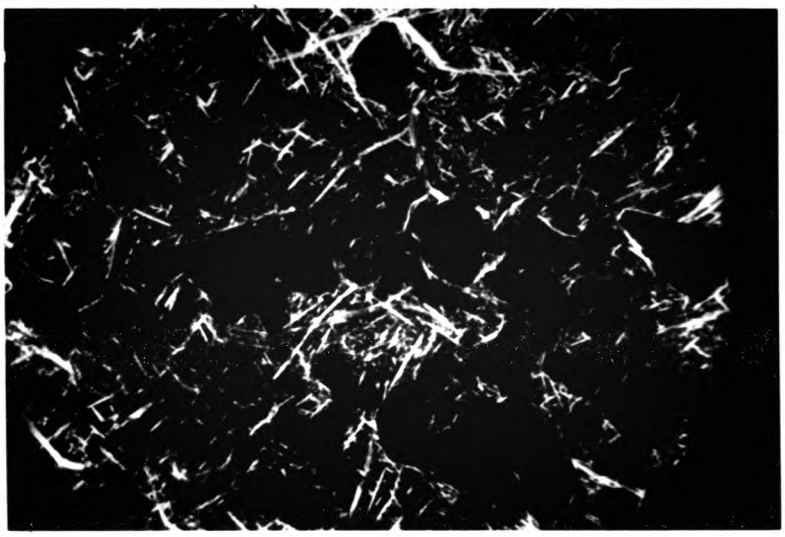

FIGURE 4.8 (a) Photomicrograph of copolymer 1e showing the stable biphasic region with bâtonnets (Magnification x 100).

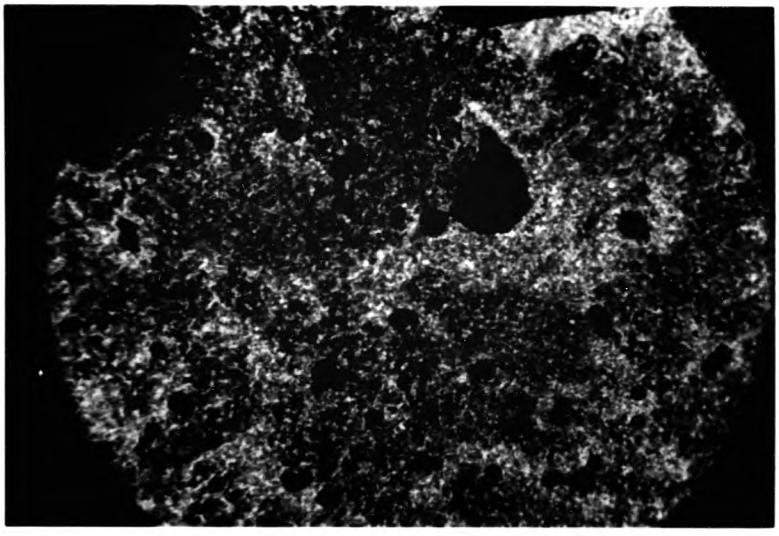

FIGURE 4.8 (b) Photomicrograph showing the grainy sand-like texture of the smectic phase of copolymer 1e (Magnification x 100).

4.2.3 General properties and trends associated with the DMBI-6/DBI system.

The general features and trends of the mesomorphic properties of the above copolymers are shown graphically in figure 4.9 and are summarised in the following.

The Tg of the copolymers can be seen to deviate in a negative sense from linear Tg versus composition behaviour. Deviations such as these are common and have been explained, in the case of amorphous polymers, by either taking into account changes in the free volume contribution associated with the different amounts of comonomers in the polymer,[134,135] or the sequence distribution of the monomers and the fractions of rotatable bonds per unit.[136] These deviations are normally caused by each comonomer having widely differing properties and the monomer diads AA, AB and BB in the polymer having different rotational barriers. In the present system however, the presence of crystallinity and liquid crystallinity may also affect the Tg-composition behaviour to some extent. The "drop" in Tg over the DMBI-6 rich end of the diagram may therefore, in part, be due to reducing crystallinity in the sample.

The melting temperature of the copolymers is seen to decrease at the same rate as the initial decrease in Tg. This is due to the incorporation of non-crystallisable monomeric units into the homopolymer and has the effect of depressing Tm in an analogous manner to the melting temperature depression usually observed on the addition of impurities into a low molecular weight diluent.

As greater amounts of DBI are incorporated into the copolymer, $T_{S_A\text{-}S_A/I}$ and $T_{S_A/I\text{-}I}$ are seen to decrease and then level off in an analogous manner to the trend shown by the Tg

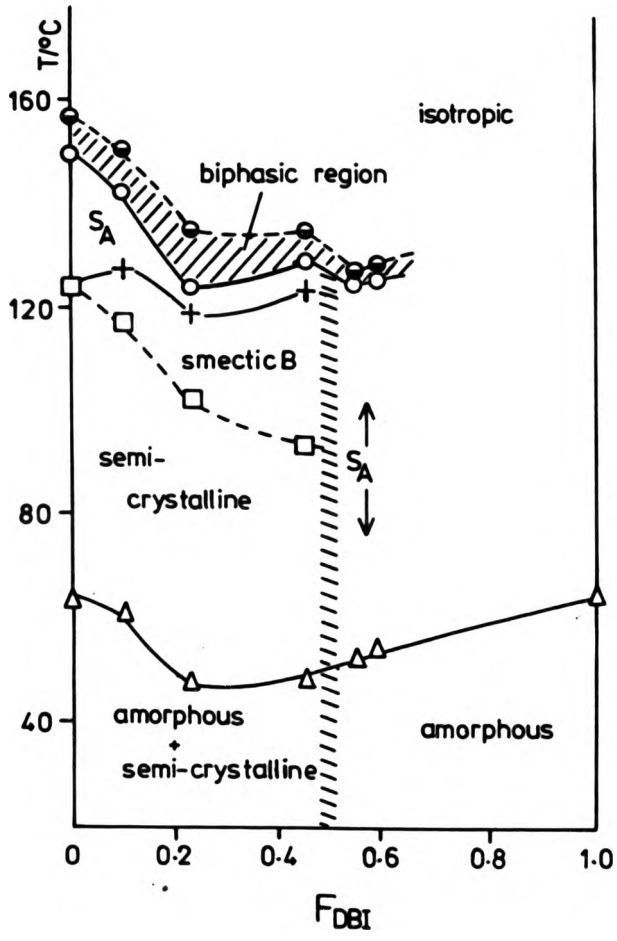

FIGURE 4.9 **Plot of phase transition temperatures (°C) of DMBI-6/DBI copolymers versus the copolymer composition (F_{DBI}).**
(Δ) = Tg; (□) = Tm; (+) = $T_{S_B-S_A}$;
(O) = $T_{SA-S_A/I}$; (Θ) = $T_{SA/I-I}$.

values, i.e. the aforementioned transition temperatures decrease by almost the same amount as the Tg, as more DBI is incorporated. As mentioned before, this is due to the mesogenic groups being 'diluted' with the DBI monomers and the non-mesogenic side chains of DBI screening, and therefore reducing the anisotropic interactions of the DMBI-6 mesogens.[34] Similar trends have previously been reported for other mesogenic/non-mesogenic systems.[137,138,139]

Another feature of this system is that incorporation of the non-mesogenic DBI units into the PDMBI-6 homopolymer has not changed the mesophase type. The smectic A phase persists throughout the whole of the compositional range studied. This type of behaviour has been reported before[139] and is fairly typical of non-mesogenic/mesogenic copolymer systems.[34] Exceptions to this behaviour are known also, where increased backbone flexibility in the copolymer has caused a mesophase change from smectic to nematic[140,141] and, conversely, a smectic copolymer has resulted on the incorporation of non-mesogenic units into a nematic homopolymer.[142]

Similar to the latter example, incorporation of the non-mesogenic DBI monomer into the smectic A homopolymer enhances the order in the system and the smectic B phase becomes apparent. This can be explained in the following way. It is well known that the polymerisation of an LC monomer usually results in a more ordered LC polymer, since the polymeric backbone aids ordering and packing.[58] In the case of DMBI-6 however, which exhibits the smectic B phase, polymerisation results in the less-ordered smectic A phase. This is because the higher density and hence increased steric crowding of the side chains due to the di-functionality of the

itaconate monomer units hinders the efficient packing of these side groups into the smectic B phase. Thus, only the less ordered smectic A phase is formed. Copolymerisation of DMBI-6 with DBI will therefore separate the itaconate monomer units and allow the side chains to pack more easily into the smectic B phase. This would be especially favoured if the monomers were placed in the chains in an alternating fashion, which they may be in this case. Although seemingly contradictory, the more favoured ordering of the side chains is accompanied by a decrease in the clearing temperature on copolymerisation with DBI. This is due to the increased number of DBI unit's side chains having more available volume and consequently requiring less energy to become thermally mobile. These side chains therefore become more disruptive to the anisotropic interactions of the mesogens at progressively lower temperatures. In other words, incorporation of DBI favours the more ordered packing of the mesogenic units, but, as a consequence of its own more thermally-labile side chains, also causes the clearing temperature to be reduced. Eventually, a point is reached where the content of DBI is so great that the backbone, which will be tending to take on a statistical conformation, will prevent the mesogens from forming the hexagonally close-packed smectic B phase. Only the less ordered smectic phase (which is probably smectic A) will then be formed, which is itself, eventually destroyed.

In conclusion then, copolymerisation of a bulky monomer such as DBI with the mesogenic monomer DMBI-6 has not disrupted the ordering of the resultant mesophase to any great extent. In fact, the order has been seen to increase.

4.3 Copolymers of DMBI-6 and MCP*

From the previous section, it was demonstrated that copolymerisation of DMBI-6 with the disubstituted itaconate monomer DBI resulted unexpectedly in copolymers having increased order relative to the homopolymer (smectic B phase), even although the non-mesogenic comonomer was of a very bulky nature. No phases of a lesser order than that of the homopolymer, such as the nematic phase were observed.

The work in this section reports an attempt to destroy the ordering to some extent by the use of a non-mesogenic comonomer with a single, much longer side chain. Additionally, this comonomer contained an optically active chiral centre situated near the end of the side chain. With a structure such as this it was hoped that the chiral centre would "mix" with, and perturb the mesogens in the appropriate manner. Of course, the copolymer would need to be of a sufficiently disordered nature before this could occur.

The structure of the chiral, non-mesogenic monomer MCP* is as follows:

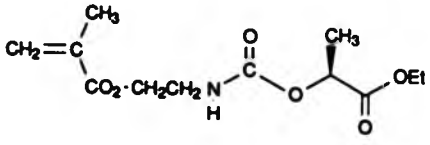

MCP*

4.3.1 Copolymerisation characteristics of DMBI-6 and MCP*

In contrast to the DMBI-6/DBI system, the copolymerisation of DMBI-6 and MCP* tends to occur in an almost statistical manner, as is shown by the copolymerisation curve displayed in figure 4.10. The composition and feed data from which the curve was drawn and molecular weight data are recorded in table 3.2, chapter 3.

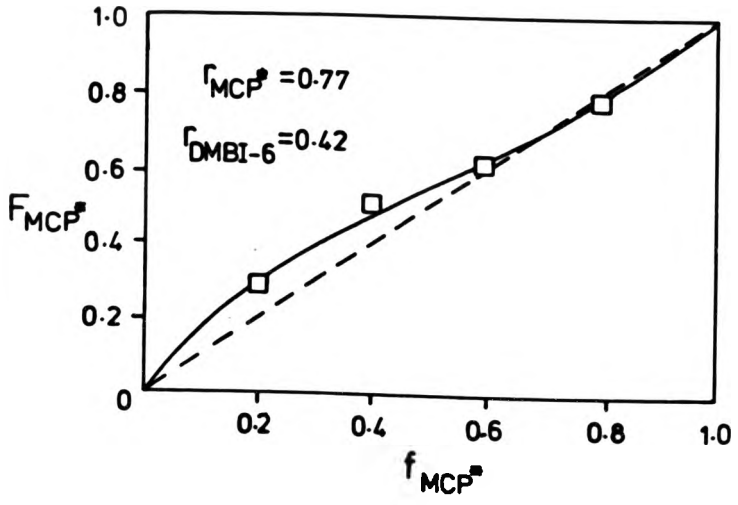

FIGURE 4.10 **A plot of the mole fraction of MCP* in the copolymer (F_{MCP*}) versus the mole fraction of MCP* in the monomer feed (f_{MCP*}) and the corresponding reactivity ratios for each monomer.**

(□): Experimental point.

(—): Calculated best fit to experimental data.

From the curve and the reactivity ratios (r_{MCP*} = 0.77 and r_{DMBI-6} = 0.42) it is evident that the methacrylate monomer is more reactive than the itaconate monomer, as one would expect. This is because of the reduced steric bulk around the methacrylate double bond and the inductive effect of the vinyl methyl group. This latter effect destabilises the methacrylate radical relative to the itaconate radical, therefore causing it to be more reactive.

The measured values of DP_n for the polymers 2b (F_{MCP*} = 0.51) and PMCP* are 32 and 94 respectively. It is assumed that the values of DP_n for the other copolymers will be of the same order as that of copolymer 2b (51%MCP*). Several reasons for the increase in DP_n of the polymers relative to the previous DMBI-6/DBI system can be identified. Firstly, the use of benzene as the polymerisation solvent rather than toluene will have the effect of reducing chain transfer to solvent.[143]

The next two reasons for the increase in DP_n are due to the fact that only one of the comonomers is an itaconate monomer, therefore the total number of monomers in the system having activated allylic hydrogens is reduced. This means that the effects of degradative chain transfer and termination by disproportionation are reduced, since the methacrylate comonomer has no allylic hydrogens.[123] Whether degradative chain transfer can occur via other sites on the methacrylate monomer is not known.

Lastly, the reduced steric bulk around the vinyl bond of the methacrylate monomer relative to DBI should facilitate the propagation reaction and therefore increase the kinetic chain length.[123]

4.3.2 Mesomorphic properties of DMBI-6/MCP*

As with the previously discussed system the copolymers reported here have been found to exhibit enantiotropic liquid crystalline phases. These have been characterised by both dsc and hot-stage microscopy, and the various phase transition temperatures are reported in table 4.2. Again, it must be stressed that the transition temperatures of these copolymers are both molecular weight and molecular weight distribution dependent. Since the DP_n values are significantly higher than in the DMBI-6/DBI system however, the effect may not be too great.

All of the copolymers prepared from DMBI-6 were found to exhibit the same phases and phase transition behaviour. This is evident from the dsc heating traces of the copolymers which are displayed in figure 4.11. These all show the following transitions which were correlated with microscopy investigations:

amorphous/crystalline ⟷ crystalline ⟷ smectic B ⟷ smectic A ⟷ isotropic liquid

In this section the textural behaviour of the copolymers will be discussed, followed by their thermal properties and the general trends associated with the system.

4.3.2.1 Texture observations.

The optical microscopy investigations of the MCP*/DMBI-6 copolymers revealed similar textural behaviour in all cases. The textures obtained were again reminiscent of those of conventional small molecule liquid crystals.[18]

The textural behaviour of one of these copolymers, 2a, is chosen as a typical example for discussion.

TABLE 4.2 The phase transition temperatures of MCP*/DMBI-6 copolymers.[a]

Copolymer Number	F_{MCP*}	Tg/°C [b]	Tm/°C [c]	$T_{S_B-S_A}$/°C	$T_{S_A-S_A/I}$/°C [d]	$T_{S_A/I-I}$/°C	$\Delta T_{BIPHASIC}$
1a	0.00	64	125	-	150	157	7
2a	0.29	50	105	125	145	155	10
2b	0.51	44	104	122	138	148	10
2c	0.62	45	97	123	128[e]	131	3
2d	0.78	45	95	125	131	136[f]	5
2e	1.00	43	-	-	-	-	-

a - All temperatures are recorded during the second dsc heating scan at a rate of 20°C/minute.

b - The Tg for polymers 2a-e were recorded using the DuPont thermal analyser (dsc). The Tg for polymer 1a and all other transitions were recorded using the Perkin-Elmer dsc 2.

c - Tm indicates the melting temperature and indicates a transition to either the smectic B or smectic A phase, as determined by dsc and/or microscopy.

d - $T_{S_A-S_A/I}$ indicates the transition from a smectic A phase to a biphasic smectic A/isotropic region. This temperature is recorded as the maximum of the smectic A-isotropic endotherm in the dsc trace.

e - The actual $T_{S_A-S_A/I}$ value may be lower than the result quoted since the endotherm occurs very close to the $T_{S_B-S_A}$ endotherm and is seen as a shoulder.

f - Determined by microscopy only.

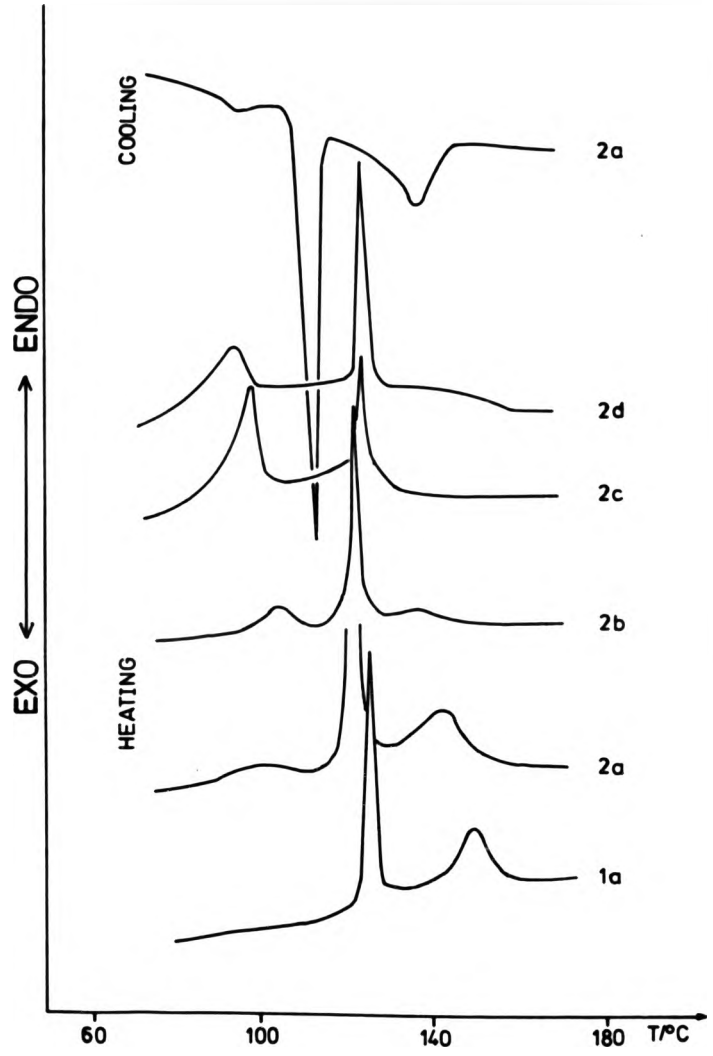

FIGURE 4.11 DSC heating traces for polymers 1a and 2a-d and the dsc cooling trace for polymer 2a. All traces were recorded at 20°C/minute and the heating traces were recorded on the second heating scan. The traces for polymers 2a-d do not show the glass transition and Tg. These were recorded using a different instrument.

On cooling the isotropic melt of polymer 2a the smectic A phase was seen to separate from the isotropic melt at about 140°C in the form of bâtonnets. On further cooling these began to grow and coalesce in the normal fashion. This behaviour is shown by the photomicrograph in figure 4.12(a). The top right hand side of the micrograph shows clearly the presence of coalescing bâtonnets in a biphasic region. The lower left hand side shows a monophasic area having smaller, less-well defined domains. Further cooling allowed greater coalescence of the bâtonnets into the usual focal-conic fans, as shown by the photomicrograph in figure 4.12(b). The smaller domains in the lower left hand side of the picture can now also be seen to have reorganised in some areas and started to form fans. This reorganisation can be seen to become more extensive by annealing the sample as close to the smectic A - biphasic smectic A/ isotropic transition as possible. Immediately preceeding the next transition on cooling, transition bars across the fan backs become apparent which disappeared quickly after passing through the transition at 120°C. This effect was again found to be reversible for at least the first few heating/cooling cycles and is only associated with a transition to the smectic B phase.[18] Unfortunately, a reasonably steady temperature could not be maintained at the transition point therefore there are no photomicrographs displaying this effect for this copolymer system. Different treatment of the smectic A phase on cooling produced the mosaic texture of the smectic B phase. This procedure consisted of cooling from the isotropic liquid to the smectic B phase very quickly, so as to prevent

the formation of focal-conic type regions. The texture produced was very similar to that displayed in figure 4.6(b) in the previous section. Finally, on further cooling crystallisation was seen to occur at about 100°C, as shown by the photomicrograph in figure 4.12(c).

Peculiar textural effects were also displayed by some of these copolymers when the cooling rate through the biphasic region was varied or when the sample was annealed at a temperature just above the biphasic - smectic A transition. The most striking of these effects is shown by polymer 2b.

At a normal cooling rate of approximately 10°C/minute, the coalescence of bâtonnets from the isotropic melt of polymer 2b was seen to proceed normally followed by the usual, focal-conic domain formation as shown in figures 4.13(a) and (b) respectively. However, when a much slower cooling rate was employed and the sample annealed at about 142°C for three hours, an unusual "worm-like" texture evolved. Further cooling of this texture, which is shown in figure 4.13(c) failed to produce the normal focal-conic texture or any other typical textures or textural changes. Meurisse and co-workers[98] described somewhat similar textures which were exhibited by polyesters prepared from both a terphenyl-dicarboxylic acid and ethanediol and biphenyl-dicarboxylic acid and hexanediol. These textures eventually gave rise to normal smectic textures however. The texture depicted in figure 4.13(c) is obviously caused by extensive growth of the bâtonnets in one direction only, followed by coalescence, generally in the same direction. Ordinarily, growth is only slightly greater in one direction than the other and coalescence usually occurs in all directions. Explanation of this peculiar texture is difficult, even on the basis of the information available on the smectic A phase in the literature. It may be

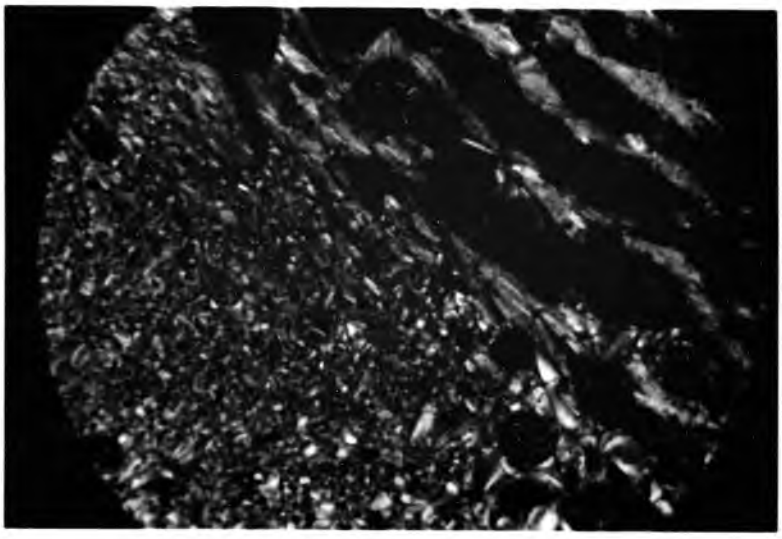

FIGURE 4.12 (a) Photomicrograph of the smectic A phase of polymer 2a, showing bâtonnets coalescing in a biphasic region (top right hand side) and a monophasic region with smaller domains (lower left hand side) (Magnification x 200).

FIGURE 4.12 (b) Photomicrograph of the smectic A phase of polymer 2a, showing focal-conic fanned domains (top right hand side) and less well formed fanned domains (lower left hand side) (Magnification x 200).

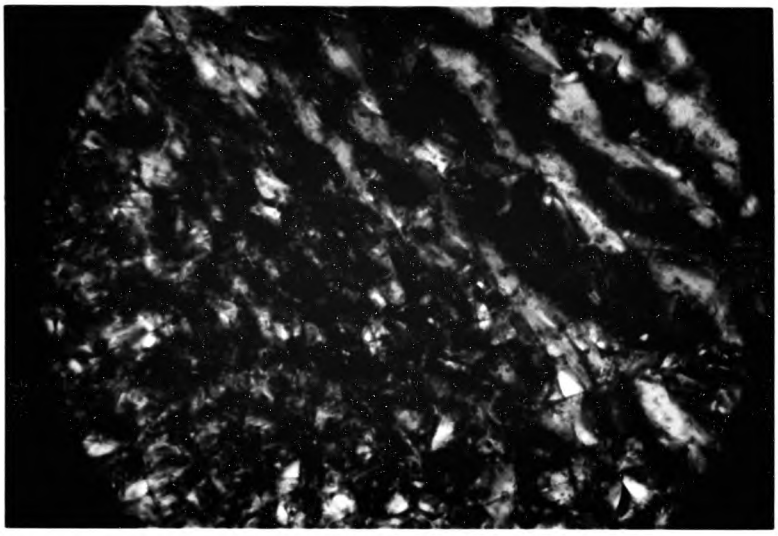

FIGURE 4.12 (c) Photomicrograph of polymer 2a, showing crystallisation of the mesophase (Magnification x 200).

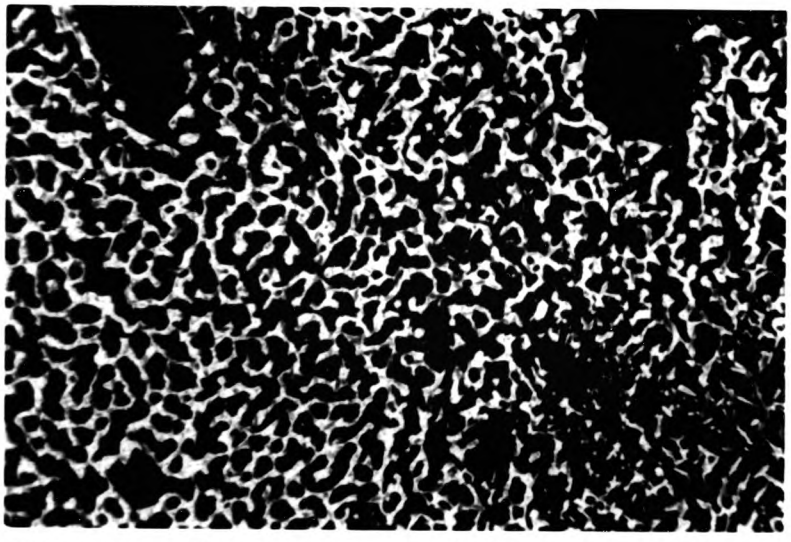

FIGURE 4.13 (a) Photomicrograph of polymer 2b, showing the biphasic smectic A/isotropic region (Magnification x 100).

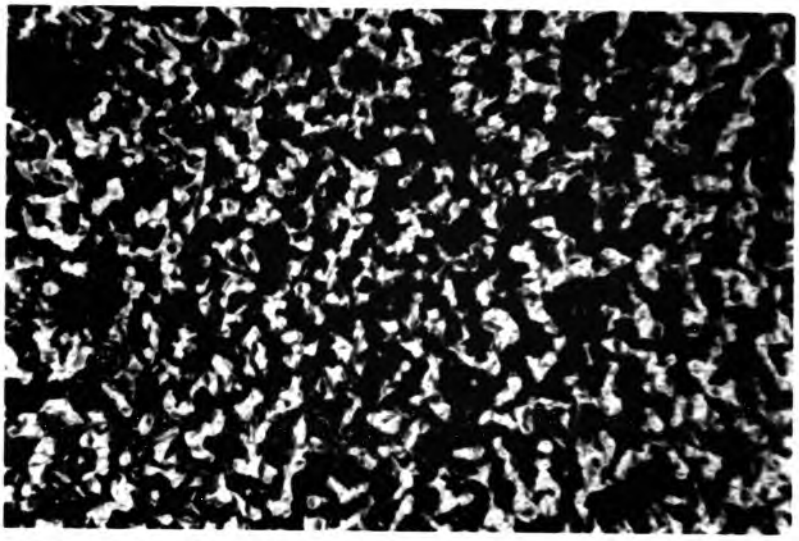

FIGURE 4.13 (b) Photomicrograph of the smectic A phase of polymer 2b, showing the bâtonnets coalescing and forming focal conic domains (Magnification x 100).

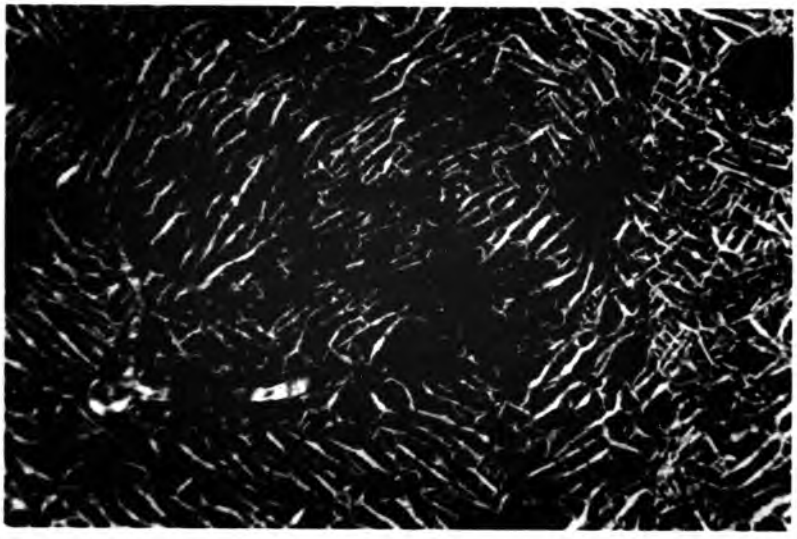

FIGURE 4.13 (c) Photomicrograph showing the unusual "worm-like" texture of polymer 2b obtained after very slow cooling and annealing at 142°C for 3 hours (Magnification x 100).

possible that during this thermal treatment the presence of hydrogen bonding emanating from the carbamate linkage (if it is still present at such temperatures) affects the manner in which the layers build up after nucleation. Clearly, more work using a technique such as electron microscopy,[144] in combination with polarising microscopy using greater magnification, needs to be carried out. This unfortunately is outwith the scope of this present work.

4.3.3 General properties and trends associated with the DMBI-6/MCP* system.

From the dsc heating traces of polymers 2a-d in figure 4.11 the broadened smectic A to isotropic phase transitions can again be associated with biphasic phenomena, as shown by microscopy studies. These transitions are very broad in the case of polymers 2a and 2b and this can be attributed to broad molecular weight distributions or perhaps a wide distribution of copolymer sequences. The biphasic regions of polymers 2c and 2d on the other hand exist over a much narrower temperature interval (3°C and 5°C respectively). This may be due to these polymers having narrower molecular weight or copolymer sequence distributions, or it may be associated with the narrower temperature interval of the smectic A phase of polymers 2c and 2d. Without number average or weight average molecular weight measurements no final conclusions can be drawn about this effect.

Supercooling of the isotropic phase is again observed with these copolymers as typically shown by the dsc heating and cooling traces of polymer 2a in figure 4.11. Supercooling of the isotropic phase by 7°C was again observed whilst the smectic A to B and smectic B to crystalline transitions were found to be supercooled by

11°C and 8°C respectively. These effects are of a similar magnitude to those shown by the DBI/DMBI-6 copolymers.

The general trends of the thermal and mesomorphic behaviour of these copolymers as a function of composition are displayed graphically in figure 4.14. Several conclusions may be drawn from these results.

With this copolymer system and in contrast to the previous system, the Tg values of the copolymers do not deviate to any great extent from a linear composition versus temperature relationship. This is surprising when one considers how different the side chains are and how different the rotational barriers between the copolymer monomer pairs will be from the rotational barriers between monomer pairs in each respective homopolymer.[136] Normally one would expect these differences to cause fairly large deviations from linear behaviour.

The melting temperature can also be seen to follow the same decreasing trend as that of the Tg values and this is again due to the incorporation of the non-crystallisable MCP* monomer into the homopolymer. It is of note here that the crystalline phase extends to at least 78% MCP* (polymer 2d) in this system. This can be explained by the presence of hydrogen bonding due to the carbamate linkage which can hydrogen bond with either itself, ether or ester oxygen atoms. This may then stabilise the anisotropic interactions in the highly ordered mesophase and the crystalline phase, even at low biphenyl content. By comparison with the DMBI-6/DBI system, crystallinity and the smectic B phase were seen to be destroyed when the percentage of mesogenic side chains dropped below 55%. Here both phases still exist with as little as 36%

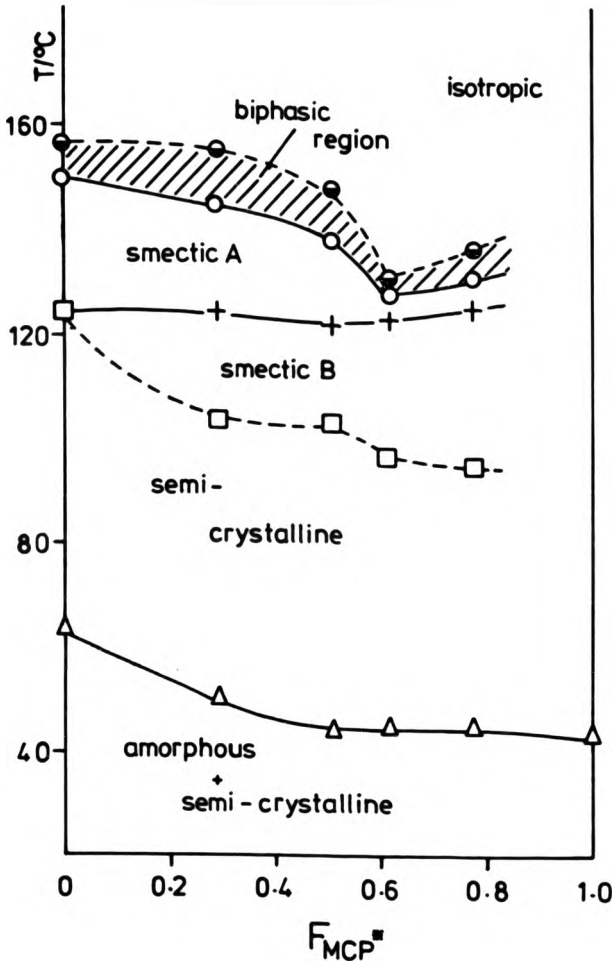

FIGURE 4.14 **Plot of phase transition temperatures (°C) versus the composition of DMBI-6/MCP* copolymers (F_{MCP^*}).**
(Δ): Tg; (□): Tm; (+): T_{S_B}-S_A; (O): T_{S_A}-S_A/I; (⊖): T_{S_A}/I-I.

mesogenic side chains in the polymer.

As expected, the $T_{S_A\text{-}S_A/I}$ temperature, or in other words the smectic A mesophase thermal stability, decreases as increasing amounts of MCP* are incorporated into the homopolymer. As was previously discussed in secton 4.2.3, this is due to the increasingly disruptive thermal motions of the non-mesogenic side chains affecting the anisotropic interactions of the main chains.[34] The decrease in $T_{S_A\text{-}S_A/I}$ is not as steep as one would expect when copolymerising with a non-mesogenic monomer having a long side chain such as MCP*. Intuitively the long side chain would suggest a much steeper decrease. By studying the phase transitions of copolymers of cholesteryl-11-methacryloyloxyalkanoate with various alkyl methacrylates, Yamaguchi and co-workers[137] found that the decrease became steeper as the carbon chain increased in length up to $\simeq$12 carbons. The less-steep decrease in the case of the DMBI-6/MCP* copolymers (where the chain length is 10 atoms), must again be due to hydrogen bonding which stabilises the anisotropic interactions of the mesogens.

The sharp "drop" in thermal stability of the smectic A phase on going from polymer 2b to 2c on the other hand is difficult to rationalise, especially since the thermal stability of the smectic B phase remains relatively unchanged. Perhaps this deviation from the apparent trend may be due to polymers 2c and 2d having a different distribution of monomer sequences in the copolymer. This could cause smectic B phase formation to be favoured over smectic A phase formation. One possibility that can be ruled out, however, is the effect of molecular weight. If polymers 2c and 2d had lower molecular weights than the previous copolymers, then the thermal

stability of the smectic B mesophase would also have "dropped" by a similar amount.

The observation that the smectic B to smectic A transition does not decrease with increasing content of MCP* must also be ascribed to hydrogen bonding which must help stabilise the hexagonal packing of the mesogens in the smectic B phase.

In conclusion then, copolymerisation of DMBI-6 with the chiral derivative MCP* bearing a long side chain did not reduce the ability of the biphenyl mesogens to assemble themselves in a highly ordered manner. In fact, this process appears to be aided by the presence of hydrogen bonding to such an extent that even the copolymer with only 36% mesogenic side chains exhibited the highly ordered smectic B phase.

From the microscopic textures observed it was difficult to assess whether the chiral centre had in fact perturbed the highly ordered phases to such an extent that a chiral modification of the phase had been formed. Without further evidence such as X-ray analysis, assessment of this possibility or even the effect of hydrogen bonding on these modifications is impossible. If any modification of the smectic A and B phases has occurred however, it must only be slight since the optical microscopic textures show little change from the normal reported textures.[18]

Clearly a different approach to induced chiral nematic phases must be sought. This is detailed in the following section.

4.4 Copolymers of CPBA-6 and MMMP*

From the results obtained in the previous two sections, it is clear that the copolymers still have an ability to form ordered structures, even when comonomers with bulky or long, chiral side chains were used. Evidently, the presence of the itaconate mesogenic monomer DMBI-6 in the system tends to encourage ordering. In order to arrive at copolymer systems that might be susceptible to chiral perturbation and therefore give rise to chiral nematic phases, a different approach was taken using a different mesogenic species. Perceptibly, if a monomer that normally gives rise to a nematic homopolymer on polymerisation is used, i.e. a monomer with latent mesogenic tendencies,[58] then copolymerisation with a chiral, non-mesogenic monomer should produce the required structures. These copolymers may then give rise to induced chiral nematic phases.

The monomers chosen for this purpose were the following:

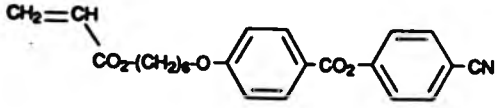

CPBA-6

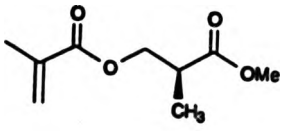

MMMP*

Monomer CPBA-6 is known to form the nematic mesophase on polymerisation,[105] whilst monomer MMMP* has a specific rotation of about 22° and was prepared by a route which should have preserved the enantiomeric purity of the starting material.

4.4.1 Copolymerisation characteristics of CPBA-6 and MMMP*

The copolymerisation of MMMP* with CPBA-6 can be seen to deviate substantially from ideality, as shown by the copolymerisation curve displayed in figure 4.15. The composition and feed data from which the curve was drawn and the molecular weight data are recorded in table 3.3, chapter 3.

The deviation from ideality is of course due to the greater reactivity of the methacrylate monomer MMMP* ($r_{MMMP*} = 3.00$) relative to the acrylate monomer CPBA-6 ($r_{CPBA-6} = 0.15$) which causes it to enter the growing copolymer chain much more frequently. Thus, one would expect the copolymer chains to contain fairly long sequences of MMMP*. The increased reactivity of MMMP* relative to CPBA-6 is due mainly to the radical reactivity of the methacrylate terminated chain being enhanced by the destabilising, inductive effect of the vinyl methyl group.[145] In addition, the reactivity of CPBA-6 may be reduced because of the size of its side chain.

During the preparation of these copolymers crosslinking was found to be a problem, especially when the percentage of MMMP* in the feed was high or when the polymerisation was allowed to run to high conversions. This problem was highlighted in the attempted homopolymerisation of MMMP*, which resulted in crosslinked

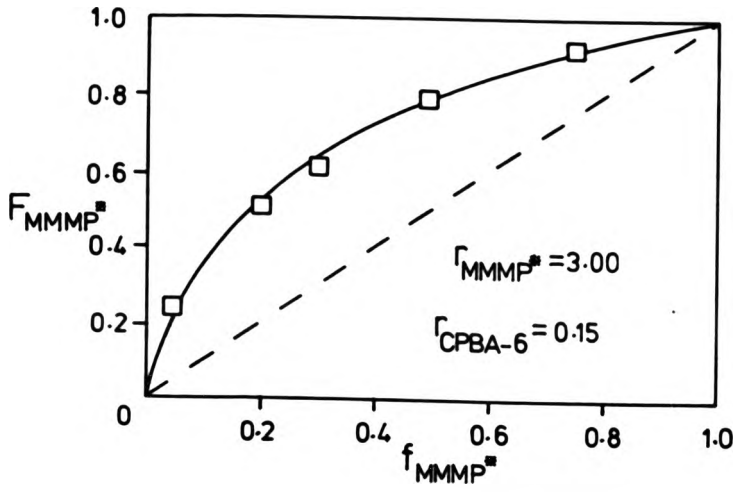

FIGURE 4.15 **A plot of the mole fraction of MMMP* in the copolymer (F_{MMMP*}) versus the mole fraction of MMMP* in the monomer feed (f_{MMMP*}) and the corresponding reactivity ratios for each monomer.**
(□): Experimental point.
(——): Calculated best fit to experimental data.

polymer whether it was attempted in bulk or dilute solution, or even at very low conversions (5%). Careful observation of this polymerisation in solution showed that it appeared to proceed normally up to a point, after which extensive crosslinking occurred and the polymer network became insoluble in the polymerisation solvent. This point is known as the Gel point[146] and is known to occur at a well defined stage in the polymerisation of poly-functional

monomers, or monomers which are capable of undergoing crosslinking reactions. According to the Gelation theory described by Flory,[146] the degree of crosslinking and the instant at which the gel point occurs are both dependent on the molecular weight distribution of the propagating species. Conceivably, the mechanism for this crosslinking process could be via the abstraction of the tertiary hydrogen atom from the chiral carbon atom in the side chain of MMMP*. This new radical site could then initiate further polymerisation and further branching, followed eventually by crosslinking and the occurrence of the gel point. It is probable that the newly formed radical will be at least as reactive as the methacrylate-terminated polymer radical, due to their similar structures. It should be remembered here that branching will occur early in such polymerisations (i.e at very low conversions), therefore each of the copolymers prepared in this study may have a significant amount of branching which will obviously affect their macromolecular and liquid crystalline properties, especially in copolymers rich in MMMP*. The effect of branching on the liquid crystalline properties is discussed in section 4.4.4.

The measured average degrees of polymerisation of PCPBA-6 and copolymer 3d (F_{MMMP*} = 0.61) were found to be 165 and 540 respectively. From these representative values it can be assumed that the DPn values of the other copolymers will be of a similar order, i.e. the values will be in a region where their liquid crystalline properties are not too molecular weight dependent.

4.4.2 Mesomorphic properties of CPBA-6/MMMP* copolymers

The dsc and microscopy results for this system revealed that the only liquid crystalline phase exhibited by these copolymers was the nematic phase or an induced chiral nematic phase having a very long pitch length. From the results in table 4.3, only polymers 3a to 3c exhibited enantiotropic phases of the nematic (or chiral nematic) type which gave rise to birefringent microscopic textures and typical thermal behaviour. In addition, polymer 3d exhibited weak birefringence, especially after shearing the sample. These results are discussed below.

4.4.2.1 Thermal and textural behaviour of homopolymer 3a (PCPBA-6)

Polymer 3a has previously been prepared by Portugall and co-workers[105] therefore it will only be discussed here briefly.

Polarising microscope studies on polymer 3a revealed the presence of a marbled texture[96] which is characteristic of the nematic phase and quite similar to the textures exhibited by some conventional liquid crystals. As is normal with PLCs, this texture was most easily formed by cooling the isotropic melt, where on reaching T_{I-N}, the nematic phase typically separated from the isotropic phase in the form of droplets. These droplets were then seen to grow and coalesce to form the larger domains of the marbled nematic texture. Such observations are typical only for the nematic phase[91,96] and occur for no other mesophase types. The dsc traces of polymer 3a (not shown here) are also consistent with the formation of the nematic phase. These show the Tg at 37°C and a

TABLE 4.3 **The phase transition temperatures of MMMP*/CPBA-6 copolymers[a,b]**

Copolymer Number	F_{MMMP*}	Tg/°C	T_{N-I}(dsc)/°C	T_{N-I}(hsm)[c]/°C	Remarks
3a	0.00	37	126	130	marbled nematic texture
3b	0.24	23	102	105	marbled nematic texture
3c	0.51	8	81	90	
3d	0.61	11		(80)[d]	Very weak birefringence which increases on shearing
3e	0.79	22			
3f	0.92	22			

a - All temperatures are recorded during the second dsc heating scan at a rate of 20°C/minute.

b - The Tgs were recorded using the Du Pont thermal analyser (dsc) and the other transition temperatures were recorded using the Perkin-Elmer dsc2.

c - T_{N-I}(hsm) refers to the temperature at which birefringence disappears totally, during the microscopy experiment.

d - The value of T_{N-I} recorded is placed in brackets since the birefringence is very weak and therefore there may be little or no mesomorphism present.

first order nematic to isotropic transition at 126°C. These results are slightly different to those reported by Portugall and co-workers[105] however:

$$g \xrightarrow{33^{\circ}C} N \xrightarrow{133^{\circ}C} I$$

These differences can of course be due to the use of different thermal analysis instrumentation, different methods of polymerisation and differences in molecular weight.

4.4.2.2 Thermal and textural behaviour of polymers 3b-3f

On the incorporation of the chiral monomer MMMP* into the nematic homopolymer no "induced" chiral nematic phases were observed using the microscopy and dsc techniques. The textures formed appeared to be nematic textures, not the anticipated homogeneous, planar chiral nematic (cholesteric) textures that usually exhibit characteristic "oily streaks"[96] or the selective reflection of visible light.

Copolymer 3b which contained 24% of the chiral monomer MMMP* was found to exhibit a marbled nematic texture similar to that shown by polymer 3a. The texture was found to develop further on annealing just below the clearing temperature, at about 95°C and is displayed by the photomicrograph in figure 4.16. The blurred areas are due to "scintillations", or Brownian motion[91,96] of the polymer chains or parts of the chains. These motions are reduced on cooling the sample and it is possible to retain the marbled texture in spite of thermal shock, by cooling or quenching

FIGURE 4.16 Photomicrograph of copolymer 3b, showing the marbled nematic texture with "scintillations" (Magnification x 100).

the sample to below Tg. This feature is well known for nematic comb-branch polymers.[91] Similar to polymer 3a, the biphasic region exhibited by polymer 3b was narrow (3°C). Observation of a distinct biphasic region on heating (or cooling) of the sample in the microscope experiment is difficult and its range can only be determined by recording the clearing temperature (T_{N-I}) by both dsc and microscopy.

Polymer 3c shows a different texture to that of polymers 3a or 3b. The sample slowly forms a planar type of texture after annealing for about 24 hours near the clearing temperature. The texture, shown in figure 4.17(a) has been reported before for both comb-branch nematic polymers[91] and main chain nematic polymers.[51] Figure 4.17(b) shows the texture after shearing of the microscope slides. The textures illustrated in both of these figures also show homeotropic regions and some regions of limited birefringence. The latter eventually become more birefringent (i.e. the phase becomes more ordered) after long (>24 hours) annealing times are employed.

The last copolymer to exhibit a structure of some order is polymer 3d. The birefringence in this case was very weak indeed, although shearing of this highly viscous texture produced an increase in the intensity of the birefringence, which disappeared completely at 80°C. Unfortunately, no photomicrographs were obtained of this texture. Dsc studies did not reveal any transitions other than the glass transition, therefore it is difficult to assess whether the birefringence is actually due to mesomorphism or whether the shearing effect only forcibly aligned the mesogens temporarily, causing birefringence. X-ray diffraction studies would need to be carried out to determine the presence of any ordering.

FIGURE 4.17 (a) Photomicrograph of polymer 3c showing the planar homogeneous texture and homeotropic regions (Magnification x 200).

FIGURE 4.17 (b) Photomicrograph of polymer 3c showing the planar, homogeneous texture and homeotropic regions after shearing (Magnification x 200).

4.4.3 Mesomorphic behaviour of an elastomeric LC copolymer

Comb-branch liquid crystalline elastomers have been studied for the past few years, mainly by Finkelmann and co-workers[33,147,148] and recently by Zentel et al.[149] These workers have examined mainly the thermoelastic and photoelastic properties and the stress-induced orientational behaviour of such materials. With the MMMP*/CPBA-6 copolymer system crosslinked elastomers can be prepared relatively easily, therefore one such copolymeric elastomer (3x) was prepared, analysed and its mesomorphic properties compared with the properties of similar, already reported elastomers.

Crosslinking was achieved by allowing the copolymerisation of a monomer pair with $f_{MMMP*} = 0.1$ to run to high conversion (~30%). Unreacted monomer and sol material were removed from the gel by washing with chloroform, then the gel carefully de-swollen with methanol. The gel was dried in vacuo at 40°C for 48 hours.

As with the previous copolymers, the Tg of elastomer 3x was recorded using the Du Pont thermal analyser (dsc) and was found to occur at 18°C. The mesophase transition of 3x was recorded using the Perkin-Elmer dsc2. However, compared to the previous copolymers, the transition was seen to occur over a range of 25°C or so, with the maximum occurring at 98°C. The dsc trace of the crosslinked polymer is shown in figure 4.18 below. Microscopy studies revealed that the mesophase was the nematic phase.

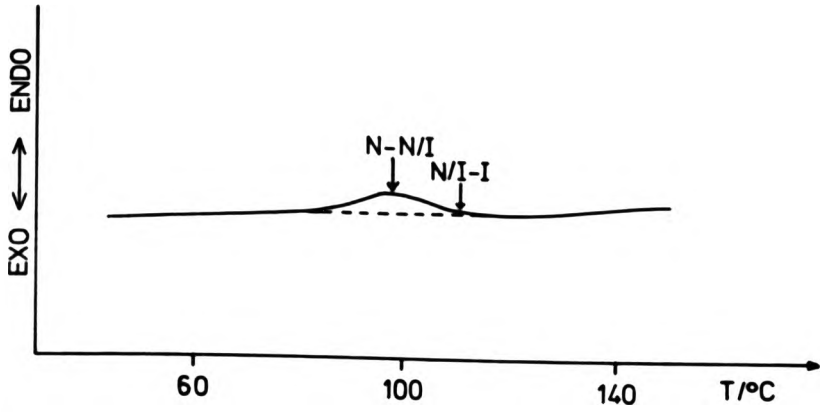

FIGURE 4.18 Dsc heating trace of crosslinked elastomer recorded at 20°C/minute (2nd heating scan).

The width of the nematic to isotropic phase transformation is much wider than that recorded for the similar, uncrosslinked polymer 3b which is only ~3°C or so. The increase in width is most likely due to there being nematic domains of different sizes, each with their own inherent thermal stability. Conceivably, this may be due to there being a distribution of molecular weights between crosslinks. It may also be possible that the crosslinked structure is not homogeneous and that some areas may be more densely crosslinked than others. This would cause nematic phase formation in the densely crosslinked regions to be impeded, therefore giving rise to a decreased thermal stability in those regions relative to less

crosslinked regions. By comparing the temperature of the endotherm maximum of elastomer 3x (98°C) with that of the polymer with similar feed ratios, polymer 3b (102°C), it can be seen that crosslinking of the copolymer does not have a gross, overall effect on the thermal properties of the mesophase, or alter the mesophase type. The latter observation has also been reported by Finkelmann[147,148] and Zentel.[149] Similarly, the Tg recorded here (18°C) is also comparable to that of polymer 3b (23°C). On the other hand, Finkelmann,[147] in his study of the crosslinking of siloxane polymers bearing pendant, methoxyphenylbenzoate mesogens, found that the transition temperatures decreased on crosslinking. In the case of Finkelmann's work this decrease is caused by his use of a difunctional, non-mesogenic siloxane crosslinking agent which plasticises and dilutes the system. In the CPBA-6/MMMP* crosslinked copolymer, no additional crosslinking units are used, therefore there are no large changes due to dilution or plasticisation.

Microscopy invetigations carried out on elastomer 3x revealed a brightly coloured nematic texture. This texture was seen to develop on slow cooling of the isotropic state and also when the sample was annealed at about 85°C for several hours. A typical texture is displayed in figure 4.19, the photomicrograph being taken after annealing the sample for four hours at 85°C. This texture appears to be a rather indistinct marbled nematic texture. The lack of a distinct texture is due to the constraints imposed on the mesogens by the network. On heating, birefringence was seen to increase at about 90°C, decrease after about 100°C and then eventually vanish (except when a shearing force was applied) at about 110°C. This is consistent with the dsc trace in figure 4.18. Lastly, no textures typical of the chiral nematic phase were observed.

FIGURE 4.19 Photomicrograph of crosslinked copolymer 3x taken in the nematic region at 85°C after annealing for 4 hours (Magnification x 200).

One of the features peculiar to liquid crystalline comb-branch elastomers is the ability of their side chains to undergo macroscopic orientation on the application of a uniaxial mechanical stress, both in the liquid crystalline and isotropic states.[33] This can be considered analogous to the orientational effects caused by the application of electrical or magnetic fields.

The crosslinked polymer 3x also exhibits such effects. For example, the unstretched elastomer in the LC state is turbid. This is because it behaves like a monomeric LC melt, where, because of thermal fluctuations, the optical axis constantly changes its direction causing strong light scattering. When the network is unaxially deformed by stretching the sample, the mesogenic groups also become macroscopically ordered and the sample becomes uniformly transparent. This type of behaviour has also been reported by Finkelmann and Rehage[33] and the potential application of these materials as optical strain guages is obvious. Other photo-elastic properties are also common to these materials, however time did not allow for a fuller investigation of these properties.

4.4.4 General properties and trends associated with the CPBA-6/MMMP* system.

The general mesomorphic features and trends associated with the aforementioned copolymers are displayed graphically in figure 4.20 and summarised in the following.

As with the DBI/DMBI-6 copolymer system, the Tg values of the copolymers were seen to show the expected, negative deviation from linear Tg versus composition behaviour, with polymer 3c having the lowest Tg value of 8^{o}C. The causes of this deviation have

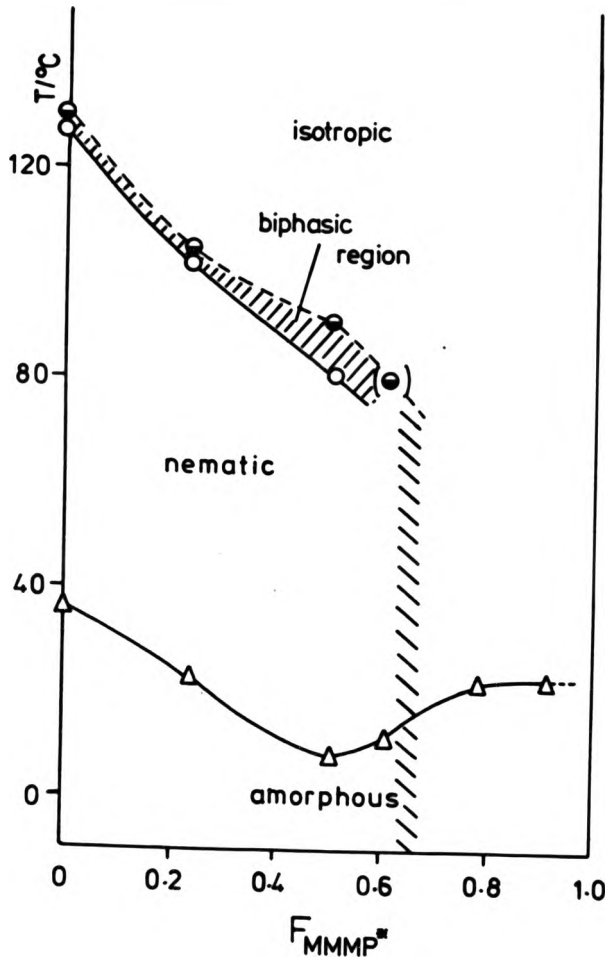

FIGURE 4.20 Plot of phase transition temperature (^{o}C) versus the composition of CPBA-6/MMMP* copolymers (F_{MMMP*}).
(Δ): Tg; (O): T_{N-I} from dsc;
(⊖): T_{N-I} from microscopy.

already been discussed, therefore they will not be repeated here.

As expected, the clearing temperature (T_{N-I}) (or the mesophase thermal stability) is seen to fall quite sharply, at much the same rate as the decrease in Tg on incorporation of MMMP* into the nematic homopolymer. There are several reasons for this. Firstly, this sharp decrease may be due to the dilution effect and increasing thermal disruption of the mesophase by the MMMP* side chains.[34] Secondly, the steep drop and poor mesophase persistence to only 50-60% incorporation of MMMP* may be due to the tendency of MMMP* to form long sequences in the copolymer because of its increased reactivity relative to CPBA-6. This would have the effect of spreading the CPBA-6 mesogens out in the polymer chain, thereby decreasing their ability to interact effectively. Lastly, the sharp reduction in mesophase stability may also be due to the increase in chain branching with increasing incorporation of MMMP*. The branches, which would contain fairly long sequences of MMMP*, must also screen the mesogens and therefore reduce the mesophase thermal stability.

The biphasic region associated with T_{N-I} is also seen to follow much the same trend, although it is much narrower in this copolymer system. This could be due to the copolymers having a much narrower molecular weight distribution in this system.[132]

It is clear from the texture observations that the only liquid crystalline phase present in the copolymers is the nematic phase, i.e. incorporation of MMMP* into the nematic homopolymer has not changed the phase type. Again, this is typical of mesogenic/non-mesogenic copolymer systems.[139] Retention of this phase type was also observed on crosslinking one of the mesomorphic copolymers and this is likewise a common feature of such materials.[147]

Although chiral nematic textures were not observed for any of the mesomorphic copolymers, it cannot be said that the presence of the chiral centre did not affect and perturb the mesogens. It may be possible that this perturbation is very small indeed and that only chiral nematic structures with very large pitch lengths resulted. This can be rationalised on the basis of the theories proposed by Goosens,[11] Vertogen[12] and Finkelmann and Stegemeyer.[13] These theories argue that the chiral "dopant" molecules induce the most significant helical twist in the mesophase when it is highly asymmetric and has a planar shape. These features cause an increase in the dipole-quadrupole interactions between the chiral species and the mesogens, and hinder the rotation of the chiral material around its long molecular axis. This subsequently induces the helical twist. However, MMMP* does not possess a planar shape or an asymmetry anything like that of the successful cholesteryl dopant molecules,[13] for example, therefore any perturbation which is present may be limited. If this was the case and large pitch lengths did result, then any reflected light would be observed well into the infra red region of the electromagnetic spectrum. It is worth remembering at this point that the nematic type of structure is merely a special case of a chiral nematic structure where the helix pitch is infinitely long. Any further work in this area would have to include a much more sensitive method for examining chiral nematic structures with long pitch lengths. One such method could be the Cano-method,[150] where the samples are analysed between a rubbed quartz plate and a rubbed convex lens by microscopic means, at a variety of temperatures. On the other hand, chiral nematic phases may not exist in this type of system, since it is possible that the

chiral centres would not mix with, or be dispersed throughout, the nematic domains but would instead associate themselves with regions of the backbone only. Without further work it is impossible to draw any firm conclusions as to the nature of the interaction (if any) between these species.

4.5 Conclusions

The approaches employed in this chapter for the attempted preparation of induced chiral nematic phases via the copolymerisation of "dopant" chiral, non-mesogenic monomers with "host" achiral, mesogenic monomers have unfortunately met with little success. The copolymers prepared either exhibited highly ordered smectic and crystalline phases in the case of the DMBI-6-containing copolymers, or nematic phases in the case of the MMMP*-containing copolymers. In the latter case this observation was explained by the lack of planarity associated with the chiral dopant monomer (MMMP*) and its reduced level of asymmetry. On the basis of the theories advanced by Goosens,[11] Vertogen[12] and Finkelmann and Stegemeyer[13] these features may cause the pitch length of the induced chiral nematic helix to be very long, possibly to the extent of the phase being nematic in nature. Nevertheless, several important results were obtained from this study and these are outlined in the following.

Contrary to expectations, the copolymer composition data from the copolymerisation of DMBI-6 and DBI were seen to suggest that the copolymers prepared tended towards a constant composition. Although this is usually indicative of alternating polymerisation, no other conclusive evidence was presented in support of this. The possibility that this mode of polymerisation could in fact be alternating in nature was rationalised on the basis of steric rather than polarity or electronic effects. The copolymers produced were found to form smectic phases of the A and B types as well as crystalline phases and this was attributed to the "smectogenic" nature of DMBI-6 and its tendency to form layered

structures. In contrast to most other mesogenic/non-mesogenic copolymer systems, the copolymers of this system were found to be of a more ordered nature than the original mesogenic homopolymer, PDMBI-6. This was ascribed to the bulky DBI monomers separating the mesogens and therefore allowing them to pack more effectively into ordered structures. Lastly, the clearing temperature was found to decrease as the copolymers became richer in the non-mesogenic component, however, this is a typical feature of such mesogenic/non-mesogenic copolymer systems.

Similar to the above system, the DMBI-6/MCP* copolymers were also found to form smectic A and smectic B phases as well as crystalline phases, even to compositions very rich in MCP*. This observation was again attributed to the MCP* monomers separating the DMBI-6 monomers and the possible presence of hydrogen bonding which may occur via the carbamate linkage of MCP*. The latter effect is also thought to account for the less-steep decrease in $T_{S_A\text{-}I}$.

The copolymers prepared from MMMP* and CPBA-6 were found to exhibit nematic phases at low MMMP* composition values only. The possibility that these phases were in fact chiral nematic phases with very long pitch lengths could not be ruled out however. Further investigation of this phase is needed. These copolymerisations were also seen to suffer from branching reactions which resulted in crosslinked products if the conversions were allowed to run too high. It is thought that the branching occurs via the labile hydrogen which is attached to the chiral carbon of MMMP*. One of these copolymerisations was allowed to run to high conversion, forming a liquid crystalline elastomeric product. The

side chains of this material were found to undergo macroscopic re-orientation on the application of stress in both the elastomeric-nematic and isotropic states, causing large changes in the optical properties of both.

CHAPTER FIVE

A STUDY OF ITACONATE-BASED CHOLESTERYL COPOLYMERS

5. A STUDY OF ITACONATE-BASED CHOLESTERYL COPOLYMERS

The most widely used types of chiral comonomer in the study of comb-branch chiral nematic polymers are those containing the cholesteryl moiety.[34] The various long-term practical applications of these materials are somewhat limited, however, due to the inherent susceptibility of the cholesteryl structure to oxidative degradation. Nevertheless, such materials must still be investigated from the point of view of fostering a more comprehensive understanding of the relationships between the copolymer constitution, helical structure and the resultant optical properties. To this end an attempt was made to prepare and characterise novel cholesteryl-containing copolymers which were substantially different from those already reported.

The following two sections of this chapter deal with two novel itaconate monomers bearing pendant cholesteryl groupings. The copolymers prepared from one of these with the previously reported monomer CPBA-6 (see section 4.4 for structure)[105] will also be reported and discussed. The structures of these monomers are shown below:

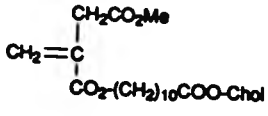

ChMI-10

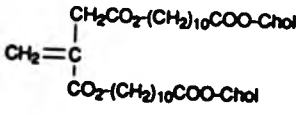

DChI-10

5.1 Copolymers of ChMI-10 and CPBA-6

5.1.1 Mesomorphic properties of ChMI-10 and PChMI-10

The cholesteryl containing mixed ester monomer ChMI-10 was prepared by known routes (see section 3.1.3 for the preparative procedure and reaction scheme)[106] and the corresponding homopolymer PChMI-10 was prepared by polymerisation of ChMI-10 in bulk at 70°C using 0.5 mole % AIBN (see table 3.4, chapter 3). From dsc and microscopy studies it was observed that both the monomer and the homopolymer showed the same smectic A and cholesteric (chiral nematic) mesophases; the phase transition temperatures of both the monomer and polymer are shown below and the dsc heating trace of PChMI-10 is displayed in figure 5.1.

$$k \xrightarrow{16^{o}C} S_A \xrightarrow{42^{o}C} N^* \xrightarrow{54^{o}C} I \qquad \text{(ChMI-10)}$$

$$g \xrightarrow{-35^{o}C} k \xrightarrow{41^{o}C} S_A \xrightarrow{52^{o}C} N^* \xrightarrow{64^{o}C} I \qquad \text{(PChMI-10)}$$

The increased phase transition temperatures, $T_{S_A\text{-}N^*}$ and $T_{N^*\text{-}I}$, of the polymer relative to the monomer is a well known feature of PLCs[56,58] and is due to the mesogens being linked together by the polymer backbone. This then reduces translational and rotational motions and leads to a more thermally stable mesophase.[33,126] The fact that the phase transition temperatures of the polymer are only 10°C higher than those of the monomer suggests that the molecular weight of the polymer is fairly low, since differences in T_{Cl} of up to 50°C are known.[126] The measured

molecular weight of the polymer was indeed found to be rather low: Mn = 9700 g mol^{-1}, DP_n = 14. As is the case with previously studied itaconate polymers, low molecular weight values such as this may be attributed to degradative chain transfer and steric effects.[123]

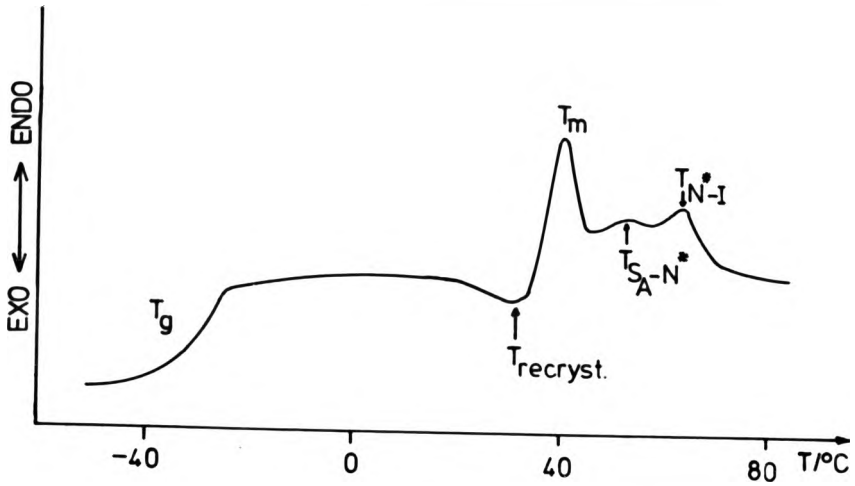

FIGURE 5.1 Dsc heating trace of PChMI-10 recorded during the second heating scan at 20°C/minute.

Unfortunately, the low value of DP_n measured for PChMI-10 means that a meaningful comparison of its phase transition temperatures with those of the structurally similar acrylate and methacrylate polymers reported by Freidzon et al.[151] is not possible. This molecular weight effect is highlighted when one attempts to compare the value of Tg of PChMI-10 (Tg = -35°C) with that of the analogous acrylate polymer.[151] Intuitively, one would expect the Tg of the acrylate polymer to be lower than that of the itaconate

polymer due to the ability of its backbone to undergo less hindered rotation.[124] However, the Tg value measured by Freidzon was found to be 35°C. Since PChMI-10 was analysed as pure and solvent free (tlc and dsc analysis), the only remaining factor which could explain its low Tg is its low molecular weight.

On the other hand, the phase transition temperatures of Freidzon's monomers with ChMI-10 can be compared. These are displayed in table 5.1 and are discussed below.

TABLE 5.1 Phase transition temperatures of some cholesteryl-containing monomers having the following general structure:

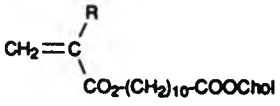

Monomer	R	Type of mesophase and transition temperatures (°C)
ChA-10[a]	H	$k_I \xrightarrow{28} k_{II} \xrightarrow{42} S \xrightarrow{67} N^* \xrightarrow{78} I$
ChM-10[a]	CH_3	$k \xrightarrow{55} S \xrightarrow{58} N^* \xrightarrow{62} I$
ChMI-10	$CH_2CO_2CH_3$	$k \xrightarrow{16} S_A \xrightarrow{42} N^* \xrightarrow{54} I$

a - These monomers were prepared and characterised by Freidzon, et al. (reference 151).

From the results displayed above it can be clearly seen that the mesophase thermal stability (T_{N*-I}) decreases as the size of R increases. This is due to the increasing size of R broadening the molecule and therefore decreasing both the anisotropy of molecular polarisability ($\Delta\alpha$) and the ability of the molecules to align themselves in a favourable manner.[28] The effect of the increasing size of R also decreases the thermal stability of the smectic phase for the same reasons, however it does not destroy the ability of the monomer to form the smectic phase altogether.

Polarising hot-stage microscopy investigations showed that on cooling both ChMI-10 and PChMI-10, a grey coloured, homogeneous planar texture with white oily streaks formed spontaneously. This texture is also known as the Grandjean texture and is typical of such cholesteryl esters.[96] It should be noted here that the planar texture of the monomer formed more quickly than the polymer: This is due to the monomer having a reduced viscosity relative to the polymer.[33] On cooling ChMI-10 further towards the cholesteric-smectic A transition, the selective reflection of blue light was seen to occur. This effect is shown by the photomicrograph displayed in figure 5.2. On nearing T_{N*-S} the reflection colour was seen to change through the colours of the spectrum towards red. Figure 5.3 shows a photomicrograph of the homogeneous planar texture during this change. These colour effects were also observed for PChMI-10 under the same circumstances. Finally, the red reflectance colour changed to white, shortly after which the planar texture quickly transformed into the focal-conic fanned texture of the smectic A phase.[18] Again the same effects were observed in the case of PChMI-10, except the colour changes were seen to occur more slowly.

FIGURE 5.2 Photomicrograph of ChMI-10 showing the planar texture with oily streaks and the selective reflection of blue light (Magnification x 100).

FIGURE 5.3 Photomicrograph of ChMI-10 showing the planar texture with oily streaks and the changing selective reflection of light from green to red (Magnification x100).

Figures 5.4 and 5.5 show similar photomicrographs of the smectic A phase exhibited by ChMI-10 and PChMI-10 respectively. These are typical textures of the smectic A phase.[18,96]

The change in reflectance colour near the cholesteric to smectic transition is caused by a rapid lengthening of the helical pitch length (see equation 1.4 in chapter 1 for the relationship between the pitch length and the wavelength of reflected light λ_R) and is usually attributed to a pre-transitional effect.[15,33] This is a common phenomenon in cholesteric or chiral nematic systems when there is a smectic phase present at lower temperatures and is due to the formation of smectic clusters at a temperature slightly above T_{N^*-S}. These smectic clusters tend to enlarge the pitch[15] and, in the case of polymeric species, alter the conformation of the backbone and its symmetry.[33,76] The temperature dependence of the pitch in polymeric systems will be discussed in more detail in section 5.1.2.

5.1.2 Mesomorphic properties of ChMI-10/CPBA-6 copolymers.

The compositions of the copolymers prepared from ChMI-10 and CPBA-6 could not be measured since only small amounts of the copolymers could be obtained at low conversion values. The results presented here are therefore discussed in terms of the monomer feed only. Similarly, the availability of only small amounts of sample meant that molecular weight measurement was impossible if the osmometric techniques employed in this study were to be used. However, enough monomer starting material was available for the preparation of one representative copolymer sample for molecular weight measurement purposes. The molecular weight of this

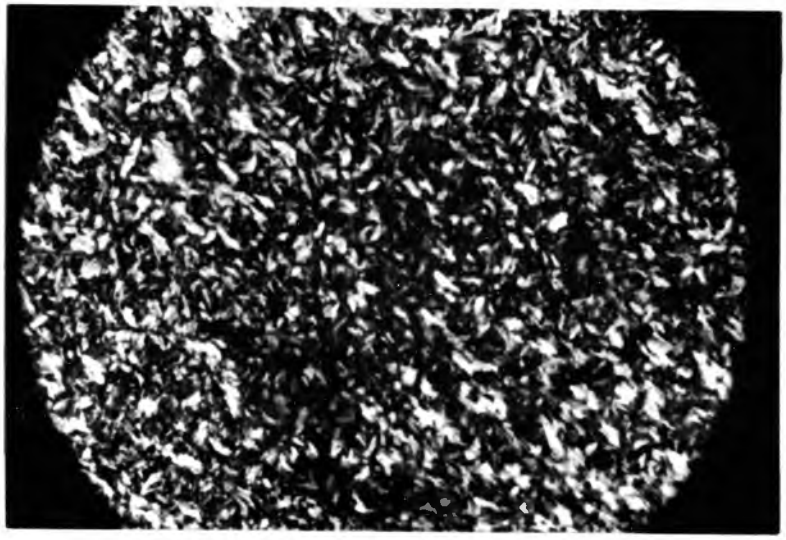

FIGURE 5.4 Photomicrograph showing the focal-conic fanned texture of the smectic A phase formed by cooling the cholesteric phase of ChMI-10 (Magnification x 200).

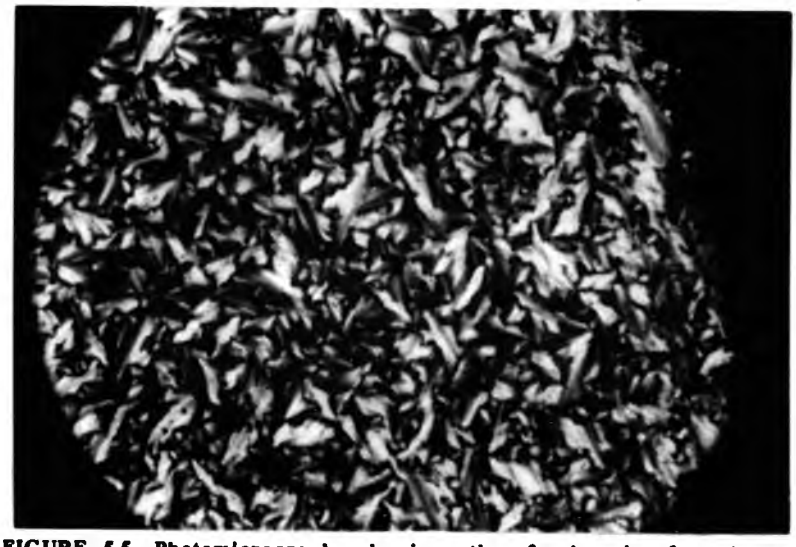

FIGURE 5.5 Photomicrograph showing the focal-conic fanned texture of the smectic A phase formed by cooling the cholesteric phase of PChMI-10 (Magnification x 200).

copolymer (copolymer 4b, $f_{ChMI-10}$ = 0.25, table 5.2) was found to be 30,000 g mol^{-1}. From this value and those of PCPBA-6 (65,000 g mol^{-1}) and PChMI-10 (9700 g mol^{-1}) it may be reasonable to assume that the molecular weights of the other copolymers are in the region of 10,000 to 60,000 g mol^{-1}. This would mean that their phase transition temperatures should not be too molecular weight dependent, especially in the CPBA-6-rich copolymers.

The phase transition temperatures of the ChMI-10 and CPBA-6 copolymers are tabulated in table 5.2 and displayed graphically in figure 5.13 as a function of the monomer feed mole fraction. Their thermal and textural behaviour is discussed below. The mesomorphic properties of CPBA-6 are discussed in chapter 4 and in reference 105.

5.1.2.1 Thermal and textural behaviour of copolymers 4a and 4b

As with ChMI-10 and PChMI-10, the mesomorphic behaviour of copolymers 4a and 4b was analysed by both dsc and polarising microscopy. Figure 5.6 shows typical dsc heating traces of copolymers 4a and 4b recorded above the glass transition.

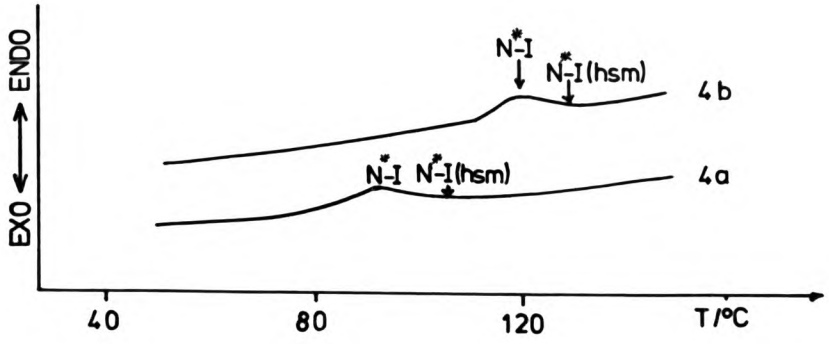

FIGURE 5.6 **Dsc heating trace of copolymers 4a and 4b recorded at 20°C/minute during the second heating scan.**

TABLE 5.2 The phase transition temperatures of ChMI-10/CPBA-6 copolymers.[a,b]

Copolymer Number	$f_{ChMI-10}$	Tg/°C[a]	Tm/°C	T_{S-N*}/°C	T_{N*-I}(dsc)/°C	T_{N*-I}(hsm)/°C[c]	Remarks
3a	0.00	37			126	130	Marbled nematic texture
4a	0.10	26			94	107	Temperature dependent pitch
4b	0.25	28			120	129	Temperature dependent pitch
4c	0.50	19			115	120	Temperature dependent pitch
4d	0.75	7		69	80	97	(Temperature dependent pitch
4e	1.00	-35	41	52	64	72	(observable near N*-S transition only

a - All phase transition temperatures were measured using the Perkin Elmer dsc2 except the Tg values which were measured using the Du Pont thermal analyser (dsc).

b - All temperatures were recorded during the second heating scan at 20°C/minute.

c - T_{N-I*}(hsm) refers to the temperature at which birefringence disappears totally during the microscopy experiment.

Both copolymers 4a and 4b were found to exhibit only one mesophase, namely the cholesteric mesophase, between their glass transitions and the endotherms shown by the dsc traces in figure 5.6. These broad endotherms are again due to a biphasic phenomenon which is caused by the polydispersity of the samples.[132] The transition temperatures in table 5.2 are therefore quoted as T_{N^*-I}(dsc) which corresponds to both the maximum of the dsc endotherm and the first appearance of the isotropic liquid, whilst T_{N^*-I}(hsm) corresponds to the disappearance of the last traces of birefringence. The biphasic region of these copolymers is also displayed in figure 5.13.

From the microscopy investigations, both polymers were found to exhibit a pale-blue, homogeneous, planar texture with white oily streaks on cooling the isotropic melt. With further cooling the reflection colour was seen to change slowly through the visible spectrum to a red/orange colour.

The different temperature dependent colours observed on cooling the planar texture of polymer 4a are displayed by the photomicrographs in figure 5.7(a), (b) and (c). These correspond to temperatures of 95°C, 64°C and 40°C respectively. By comparing these photomicrographs with those of the planar texture of ChMI-10 (figures 5.2 and 5.3) one can see that the reflected colours are not as clear and that the textures are not as well defined as those of ChMI-10. This may be due to the following two effects which are a direct consequence of the more viscous, macromolecular nature of polymer 4a.[33] Firstly, chain entanglements will be present in the polymer sample which give rise to defects in the helical structure and therefore the planar texture. These will make the texture seem

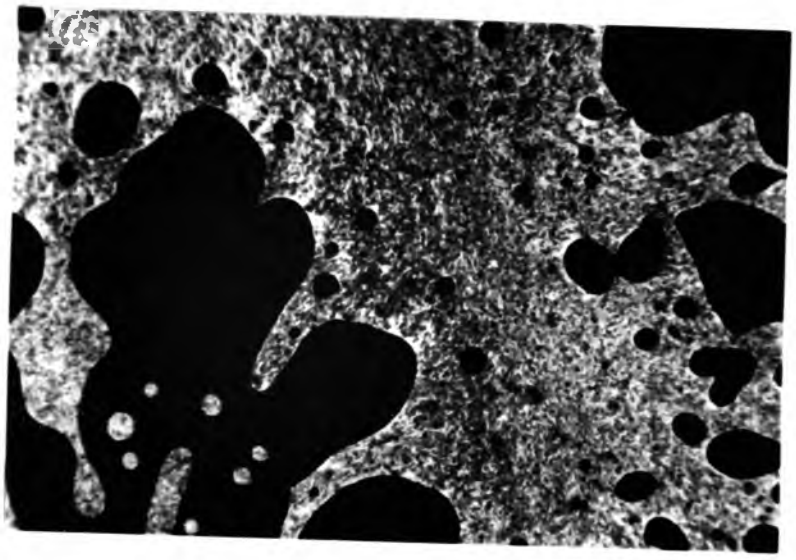

FIGURE 5.7 (a) Photomicrograph of the planar cholesteric texture of polymer 4a at 95°C, showing the reflection of pale-blue light (Magnification x 100).

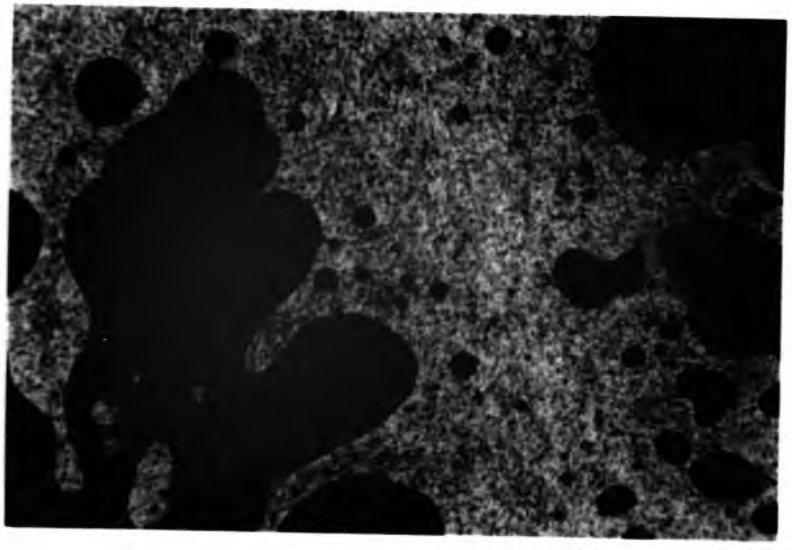

FIGURE 5.7 (b) Photomicrograph of the planar cholesteric texture of polymer 4a at 64°C, showing the reflection of predominantly yellow light (Magnification x 100).

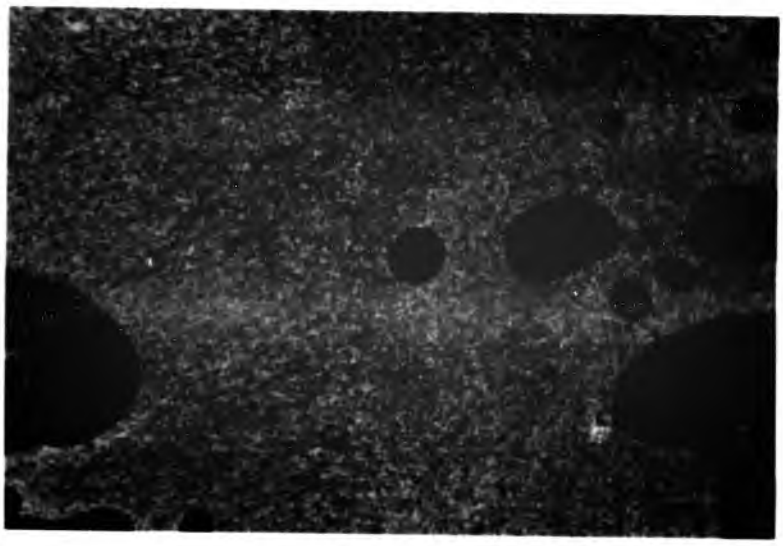

FIGURE 5.7 (c) **Photomicrograph of the planar cholesteric texture of polymer 4a at 40°C, showing the reflection of red light in the centre and yellow light at the sides, indicating a difference in temperature of the two areas (Magnification x 100).**

more imperfect than in the case of the low molecular weight species. Such defects can be removed or reduced in number if long annealing times are employed however. In the case of the photomicrographs of copolymer 4a displayed in figure 5.7, the texture formed spontaneously; no annealing process was carried out, therefore only the more defective texture was observed. Secondly, chain entanglements and the increased viscosity in the cholesteric phase of polymer 4a will cause some of the helices and helix aggregates to deviate and tilt away from the planar situation. This is depicted in figure 5.8.

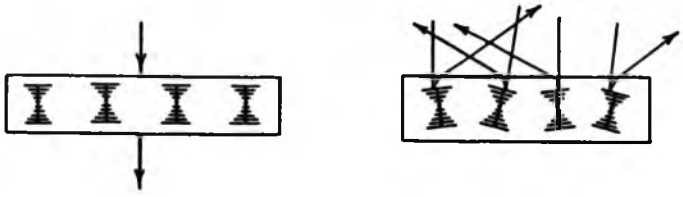

ChMI-10 Polymer 4a

FIGURE 5.8 Schematic diagram of the planar texture of a low molecular weight compound (ChMI-10) and of the "disrupted" planar texture of a polymeric species (polymer 4a).

A deviation of the helical aggregates such as is shown above will cause a scattering of light as well as a possible shift in wavelength from some of the less-well ordered domains.[15] The overall reflected colour will therefore be a diffuse mixture of some

slightly different wavelengths. It should also be borne in mind at this point that the intensity of light reflected also depends on the sample thickness and the angle of viewing.

As with copolymer 4a, copolymer 4b was seen to have a temperature dependent pitch. Photomicrographs displaying the different reflection colours from the planar texture of polymer 4b are shown in figure 5.9(a)-(d).

In both polymer samples the reflection colours were seen to change in reverse order on heating.

As previously mentioned in both section 1.2.2, chapter 1, and in section 5.1.1 in this chapter, the change in colour of both polymer samples with temperature is due to a change in the pitch length of the helical structure. From the results reported here and from relationship 1.4 in section 1.2.2[17] it is obvious that the pitch length increases as the samples are cooled. Such a temperature dependence has previously been reported for low molecular weight species[15] and both main chain[51] and comb-branch[39] cholesteric or chiral nematic polymers. Other examples of the opposite effect of temperature dependence (i.e. increasing pitch and therefore λ_R with temperature) in comb-branch systems are also known, e.g. copolymers 6.1-6.4 in table 1, chapter 1.[77] In addition to both of the above cases, several examples exist where there is a negligible temperature dependence.[80]

The temperature dependence of the helical pitch in the absence of any pre-transitional effects[15] (i.e. in systems where only the cholesteric phase exists or at temperatures far above any transition to the smectic phase) can be rationalised in terms of the mechanism discussed below.

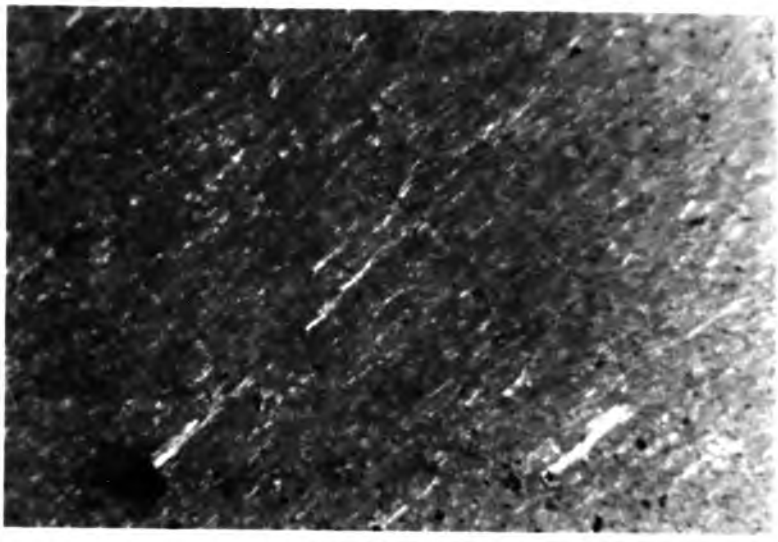

FIGURE 5.9 (a) Photomicrograph of the planar texture of copolymer 4b at 82°C, showing the reflection of blue light and some white "oily streaks" (Magnification x 100).

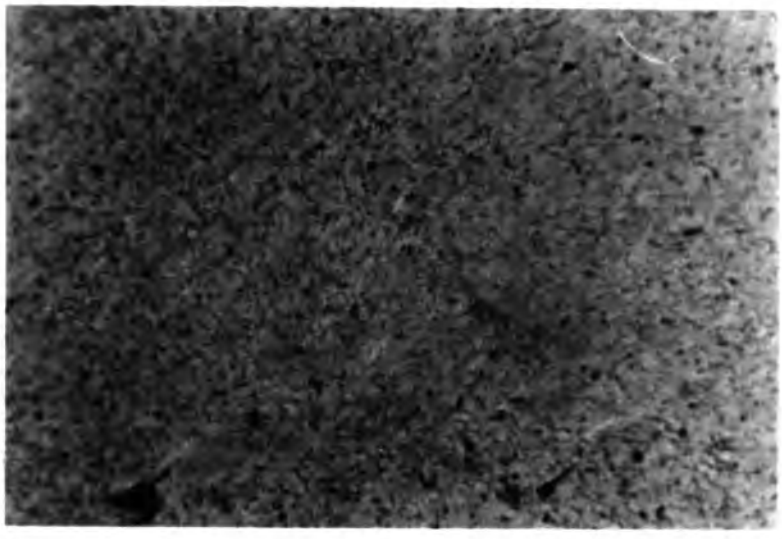

FIGURE 5.9 (b) Photomicrograph of the planar texture of copolymer 4b at 68°C, showing the colour of reflected light changing from blue to green/yellow (Magnification x 100).

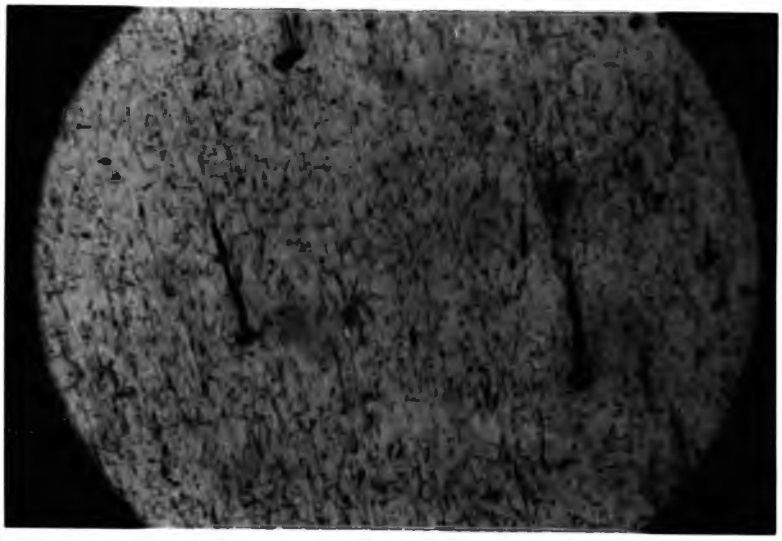

FIGURE 5.9 (c) Photomicrograph of the planar texture of copolymer 4b at about 50°C, showing the reflection of yellow light (Magnification x 100).

FIGURE 5.9 (d) Photomicrograph of the planar texture of copolymer 4b at 25°C showing the reflection of red/orange light (Magnification x 100).

As the temperature of the helical structure is raised there is more thermal motion in the molecules which comprise the mesophase and as a result, the molar volume increases. Each molecule then has a larger volume requirement which can affect the helical pitch in two opposing ways:

1. The intermolecular distance along the helical axis increases, tending to increase the pitch; and
2. the displacement angle θ between the adjacent molecules in the helical stack increases, thus causing a decrease in the pitch.

These two opposing mechanisms are shown schematically in figure 5.10.

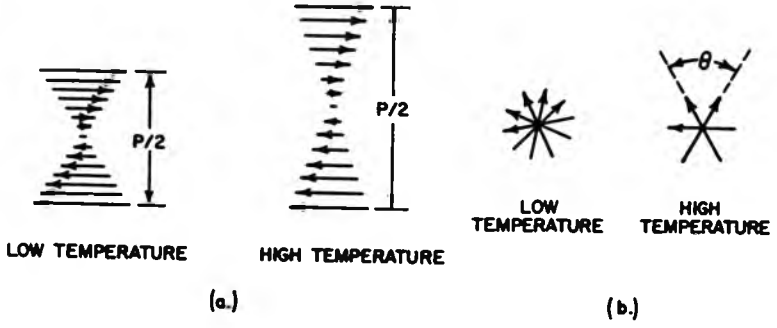

FIGURE 5.10 **Possible effects of temperature on pitch: (a) alteration of intermolecular spacing resulting in an increase of pitch with temperature and (b) alteration of displacement angle θ resulting in a decrease of pitch with temperature.**

The second of these mechanisms has been treated theoretically by Keating[78] and is based upon anharmonic intermolecular forces. Obviously the true mechanism must be a balance between these two opposing ones and in the case of polymers 4a and 4b, the second effect (figure 5.10(b)) is the more dominant of the two.

From the results presented here and those in the literature, it appears that there is no simple relationship between the mode of temperature dependence and the chemical consitution or composition of cholesteric and chiral nematic copolymers. Even copolymers with very similar structures give rise to different modes of temperature dependence.

In systems where smectic phases are also present, an additional pre-transitional effect will occur. This will be a much stronger effect than either of the two effects mentioned above, however, as the helical structure is untwisted by the formation of smectic clusters.[15,33] The colour change is also known to be slower in polymers than in monomers. This is because the formation of smectic clusters in polymers also requires rearrangement of the polymer backbone.[76]

With copolymers 4a and 4b it was shown that it is possible to "freeze" any of the selective reflection colours into the glassy polymer matrix without any appreciable effect on the helical structure.[34] This was achieved by simply quenching the polymer sample to below Tg from the temperature at which the sample reflected the required wavelength of light. This is shown schematically in figure 5.11.

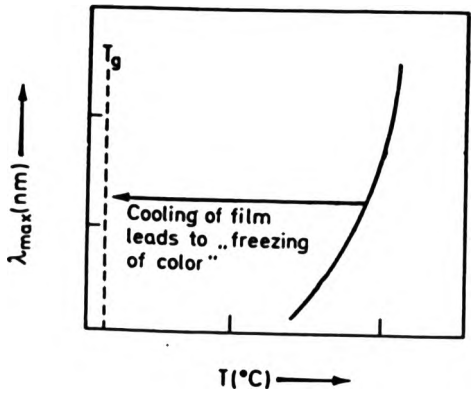

FIGURE 5.11 Relationship between the wavelength of maximum reflection and the temperature of a cholesteric or chiral nematic copolymer.

It should be remembered that this quenching process can only be carried out if there are no smectic or crystalline phases present at lower temperatures, since these would tend to cause an untwisting of the helix at rates comparable to the quenching rate.

5.1.2.2 Thermal and textural behaviour of copolymers 4c and 4d.

The dsc heating trace of copolymer 4c ($f_{ChMI\text{-}10}$ = 0.50) was found to be similar to those of copolymers 4a and 4b, with there being only one endotherm present. Microscopy investigations proved this to be the transition from the cholesteric phase to the isotropic liquid. As with copolymers 4a and 4b a biphasic region was again found to exist. This covered a range of 5°C.

The dsc trace of copolymer 4d ($f_{ChMI\text{-}10}$ = 0.75) on the other hand showed two endotherms at 69°C and 80°C, with the second of these being rather broad. Microscopic analysis of the polymer revealed that these endotherms corresponded to transitions from the smectic A to cholesteric and from the cholesteric to isotropic phases respectively. Microscopy also revealed the presence of a much wider cholesteric/isotropic biphasic region in this case. This was found to cover a range of 17°C, with the width of this range being associated with the broad endotherm at 80°C. (The dsc heating traces of polymers 4c and 4d are not shown.)

More detailed microscopy investigations were carried out on polymers 4c and 4d, and both were seen to exhibit various optical effects. These are discussed below in more detail.

On cooling the isotropic melt of polymer 4c a grey/blue coloured planar texture was seen to form spontaneously. This is shown by the photomicrograph in figure 5.12(a). In contrast to the newly formed textures of polymers 4a and 4b (displayed in figures 5.7(a) and 5.9(a) respectively), this texture appears more imperfect, with there being some large white areas as well as grey/blue areas. As mentioned before, these imperfections are due to chain entanglements and defects[33] which are easily removed by annealing the sample. Figure 5.12(b) shows the more "perfect" planar texture of polymer 4c, obtained after annealing the sample for 12 hours. The reflected colour of the texture of polymer 4c also seems much more indistinct than the vivid "blue" colours reflected by the planar textures of polymers 4a and 4b. This may be due to the possibility that the wavelength of reflected light has been shifted into the uv region of the spectrum.

This possibility may arise because the helical pitch and hence

λ_R, are known to decrease with increasing mole fraction of chiral monomer in the polymer (equation 1.5, chapter 1) at constant reduced temperatures (e.g. T_{N^*-I} - 10°C).[33,34] Attempted measurement of the reflection of this wavelength of light would prove fruitless, since the cyanophenylbenzoate moieties in the copolymer absorb in this region of the spectrum.

On cooling the annealed planar texture (figure 5.12(b)) the colour of reflection was seen to change very slowly to a pale blue colour. This was the final colour of the texture at room temperature and is shown by the photomicrograph displayed in figure 5.12(c). This is further evidence for the reflection wavelength at higher temperatures being in the uv region, assuming that the temperature dependence of the pitch is still the same, i.e. the pitch length increases with decreasing temperature.

On cooling the isotropic melt of copolymer 4d a grey coloured planar texture similar to that described for copolymer 4c was seen to form spontaneously. However, in this case the biphasic regions of the texture were much more prevalent. As mentioned earlier the biphasic phenomenon was seen to exist over a range of 17°C. Further cooling produced very little change in texture, i.e. the texture was similar to that in figure 5.12(a), until a few degrees above the cholesteric to smectic A transition. At this point the reflection of blue light became visible, followed sequentially by the other colours of the spectrum through to red. After this pre-transitional phenomenon[15,33] the planar texture was transformed totally into the typical focal-conic fanned texture of the smectic A phase.[18] This texture was very similar to that shown for polymer 4e (PChMI-10) in figure 5.5. The reflection colours from the planar texture of

FIGURE 5.12 (a) Photomicrograph of the planar texture of the cholesteric phase of copolymer 4c before annealing (Magnification x 100).

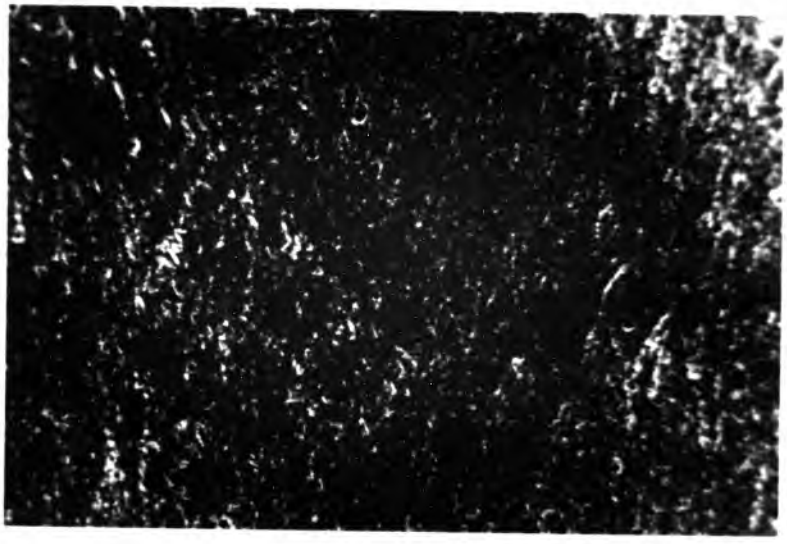

FIGURE 5.12 (b) Photomicrograph of the planar texture of the cholesteric phase of copolymer 4c after annealing for 12 hours (Magnification x 100).

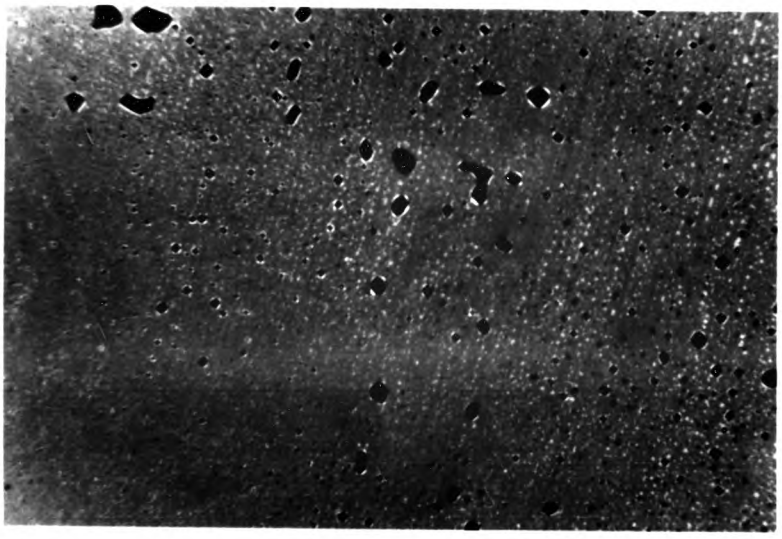

FIGURE 5.12 (c) Photomicrograph of the planar texture of the cholesteric phase of copolymer 4c after cooling to room temperature. This shows the selective reflection of pale blue light (Magnification x 100).

polymer 4d were not as bright as those shown by either PChMI-10 or ChMI-10 however. Possible reasons for the appearance of diffuse reflection colours are presented in section 5.1.2.1.

5.1.3 General properties and trends associated with the ChMI-10/CPBA-6 copolymer system.

The phase transition temperatures of each of the polymers 3a and 4a-4e are plotted as a function of the mole fraction of ChMI-10 in the monomer feed and are displayed in figure 5.13. Since only the monomer feed values are known it should be borne in mind that the actual copolymer compositions may vary quite substantially from these. The points drawn on the phase diagram in figure 5.13 are drawn only to give an idea of the general trends shown by these copolymers.

As one would expect, the Tg values of the copolymers were found to lie between the Tg values of the respective homopolymers. The copolymer Tg values were also seen to deviate in a slightly positive fashion from ideal Tg versus monomer feed mole fraction behaviour. Such deviations are expected when copolymers are prepared from monomers as different as CPBA-6 and ChMI-10[136] and reasons for this type of behaviour are discussed in chapter 4. The slight drop in Tg (and much larger drop in T_{N*-I}) on going to copolymer 4a is difficult to explain. The only explanation for this could be a drop in the molecular weight of copolymer 4a relative to polymer 3a and copolymer 4b.

The liquid crystalline order of the copolymers 4a to 4d was seen to increase as the mole fraction of ChMI-10 in the monomer feed increased. This was manifest in the appearance of the smectic

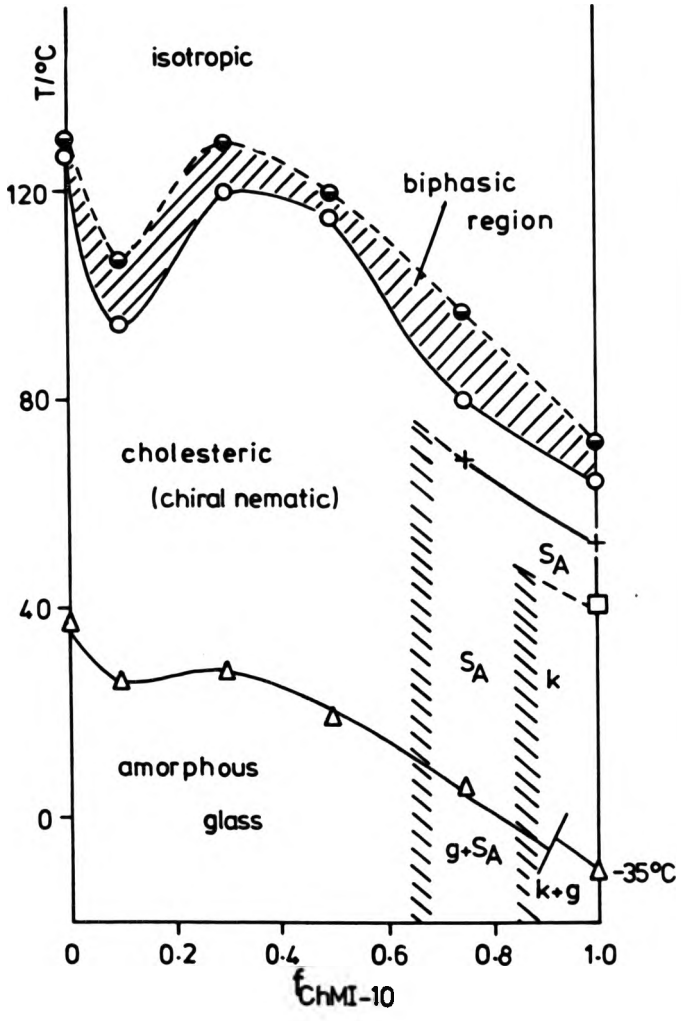

FIGURE 5.13 Plot of phase transition temperatures (°C) of ChMI-10/CPBA-6 copolymers versus the mole fraction of ChMI-10 in the monomer feed ($f_{ChMI-10}$) (Δ): Tg; (□): Tm; (+): $T_{S_A-N^*}$; (O) T_{N^*-I}(dsc); (⊖) T_{N^*-I}(hsm).

A phase in copolymer 4d which drastically reduced the cholesteric mesophase range to only 11°C. Further incorporation of ChMI-10 leads to even more ordered structures as demonstrated by PChMI-10 (polymer 4e), which exhibits the crystalline phase in addition to both the smectic A and cholesteric phases. The trend in the smectic A to cholesteric phase transitions is seen to follow the trend in both Tg and T_{N^*-I}.

The trend in T_{N^*-I} (or clearing temperature, T_{CI}) can be seen to follow the same general trend of Tg values, with the clearing temperatures lying between those of the corresponding homopolymers, with the exception of copolymer 4a. The clearing temperature of copolymer 4a is seen to be 33°C below that of polymer 3a (PCPBA-6) and 26°C below that of copolymer 4b ($f_{ChMI-10}$ = 0.25). As mentioned earlier, the only possible reason for this large drop could be that copolymer 4a has a much lower molecular weight than either 3a or 4b. The trend in the clearing temperature observed by microscopy (T_{N^*-I}(hsm)) was also found to follow the same general trend as the clearing temperature measured by dsc (T_{N^*-I}(dsc)). This suggests that the copolymers prepared may all have similar polydispersities, that is the biphasic region does not change too much between polymers.[132]

The optical properties of the cholesteric phase of each of the copolymers are also seen to follow certain trends. Firstly, the helical pitch length and hence the wavelength of reflected light of all copolymers has been seen to increase with decreasing temperature. Secondly, the wavelength of reflection has been seen to move to shorter wavelengths (i.e. to the uv region of the spectrum) as greater amounts of ChMI-10 have been incorporated into the polymer. For

example, polymers 4a and 4b show the reflection of pale blue light at about T_{N^*-I} -10°C, whereas polymers 4c, 4d and 4e show very little reflected light at this temperature. These samples must be cooled in order to increase their helix pitch length, before they will reflect visible (blue) light. Similarly, by comparing the room temperature reflection colours of the polymers that have no smectic phases (polymers 4a, 4b and 4c), one can see that polymers 4a and 4b reflect red/orange light whereas polymer 4c reflects blue light (all observations were made whilst keeping the cooling rate the same in all cases). The comparison of room temperature reflection colours may be less meaningful than comparing the reflection colours at T_{Cl} -10°C, however, since the degree of temperature dependence may be different for each copolymer. Further work would need to be carried out in order to analyse the effect of copolymer composition on the temperature dependence of the helical pitch. Nevertheless, there is some evidence to suggest that the degree of temperature dependence does not change with copolymer composition.[80]

The observed shift of the wavelength of reflected light to shorter wavelengths as greater amounts of ChMI-10 are incorporated into the copolymer is a well known feature of cholesteric (or chiral nematic) copolymer systems.[33,34,80] This infers that the mechanism of mesophase formation in cholesteric copolymers is the same as in low molar mass nematic/cholesteric liquid crystal mixtures.[80]

5.2 The Di-substituted, Cholesteryl-containing Itaconate Monomer . DChI-10

An extension of the above approach to novel cholesteric copolymers is the use of a di-substituted, cholesteryl-containing monomer in place of the mono-substituted species. By using a di-substituted monomer, it should be possible to obtain cholesteric copolymers similar to those described above, but which contain much less of the cholesteryl monomer component. The monomer DChI-10 was therefore prepared.

5.2.1 Mesophasic properties of DChI-10

As with the monosubstituted monomer ChMI-10, the analogous di-substituted monomer DChI-10 was found to exhibit both the smectic A and cholesteric phases. The phase transition temperatures of DChI-10 are as follows:

$$k \xrightarrow{39^{o}C} S_A \xrightarrow{65^{o}C} N^* \xrightarrow{72^{o}C} I$$

By comparing these temperatures with those of ChMI-10, ChM-10[151] and ChA-10[151] in table 5.1, it is obvious that both the smectic and cholesteric mesophase thermal stabilities of DChI-10 are much higher than those of ChM-10 and ChMI-10. This is most likely due to the di-substituted monomer having a much higher axial ratio than these monomers. That is, its molecular length is greatly increased relative to its molecular width, therefore its anisotropy of molecular polarisability is also increased.[28] The mesophase thermal stabilities of ChA-10 are still higher than those of DChI-10 however.

From the limited work carried out in this study no explanation for this can be given at the moment. It is possible that X-ray analysis of the mesophase structures of either monomer might explain this observation.

DChI-10 produced the same liquid crystalline textures as ChMI-10, with the cholesteric phase exhibiting the Grandjean planar tecture with oily streaks[96] and the smectic A phase exhibiting the focal-conic fanned texture.[18] Again, a typical pre-transitional effect[15,33] was observed just before the transformation of the cholesteric phase into the smectic A phase.

5.2.2 Attempted synthesis of PDChI-10 by polymerisation and by polymer-analogous reaction.

Unlike ChMI-10 and the other di-substituted itaconate monomers examined in this study, the cholesteryl-containing di-substituted monomer DChI-10 would not polymerise to any extent. Bulk, solution and a combination of these two methods proved fruitless (the attempted polymerisation details are described in chapter 3). This is surprising, since the monomer DMBI-6, which has the same steric crowding in the vicinity of the double bond and similar side chain polarity, could be polymerised to at least a molecular weight of 8000. (The structure of DMBI-6 is shown in section 4.2). The reason as to why the reactivity of DChI-10 is drastically reduced relative to DMBI-6 is unclear. It may be that the itaconate vinyl bond in DChI-10 is much more "diluted" with respect to the size of the molecule, or that the larger bulk of the cholesteryl side chains may impede the successful approach of a monomer radical to another monomer.

From the results presented in section 3.2.3 it was shown that PDCh-10 could not be prepared by the polymer-analogous route of Keller,[64] whether the same or different molar quantities were used. Equally, substitution of poly(disodium itaconate) for poly(dicesium itaconate) did not yield the required mesomorphic polymer. In fact, in all of the above attempts, the bromo-cholesteryl starting material was left essentially unaffected (from tlc and melting point analysis).

It is difficult ot think of a reason for this behaviour; although the cholesteryl starting material is large and bulky, the reactive site is quite a distance from the cholesteryl core structure, therefore only the reaction time should be affected. However, experiments showed that the anticipated polymer was not present, even after 96 hours reaction time.

Chen and Maa[65] recently disputed some of Keller's findings. These workers showed that poly(sodium acrylate) dissociated to such an extent in the aqueous phase that the pH of the system became fairly high. The sodium hydroxide formed was found to hydrolyse the ester functionalities of the mesogenic starting materials and the hydrolysed products were subsequently seen to couple together, forming a di-mesogenic compound instead of the supposed mesogenic polymer. However, this type of reaction can be discounted in the attempted synthesis of PDCh-I-10, since the starting material was recovered unaffected.

Lastly, it is surprising that not even some partially substituted polymer was found. Obviously these polymer-analogous condensation reactions require a much closer examination.

5.3 Conclusions

The work in this chapter has demonstrated that cholesteric LC copolymers can be prepared using the itaconate-based monomer ChMI-10 as the chiral comonomer and CPBA-6 as the nematogenic comonomer. The properties of the range of copolymers prepared were found to be of a similar nature of most of the previously described cholesteric systems.[34,39] Firstly, the copolymers rich in ChMI-10 were found to exhibit smectic phases due to the tendency of the cholesteryl mesogens to form layered structures. Secondly, the planar texture of the cholesteric phase of each copolymer was found to reflect visible light selectively, the colour of which depending on both the copolymer composition and the sample temperature. The wavelength of reflected light was seen to decrease with increasing mole fraction of ChMI-10 in the monomer feed and conversely to increase with decreasing temperature. Lastly, for the copolymers which formed the cholesteric phase only, it was possible to retain the helical structure and hence the reflection colour associated with it in the glassy matrix by rapid quenching of the sample from the appropriate annealing temperature.

The use of a cholesteryl monomer based on itaconic acid in the preparation of cholesteric copolymers therefore provides a reasonable alternative to the more commonly used acrylate and methacrylate cholesteric monomers for the preparation of coloured films. Additionally, it is also possible, due to the difunctionality of the itaconate species, that further derivatives which may have suitably modified properties can be prepared. It should be noted however, that there is a limit to the size of difunctional monomers that can be prepared since, if they are too large, as in the case of DChI-10, they may not be easily polymerised.

CHAPTER SIX

NOVEL CHIRAL NEMATIC COPOLYMERS HAVING THE CHIRAL CENTRE IN THE FLEXIBLE SPACER

6. NOVEL CHIRAL NEMATIC COPOLYMERS HAVING THE CHIRAL CENTRE IN THE FLEXIBLE SPACER

As mentioned in the previous chapter, the possible use of cholesteryl esters as coatings materials in an external environment is limited due to their chemical and photochemical instability. Similarly, in the case of low molecular weight LC applications, the use of these types of materials is also restricted and the focus of attention has shifted towards the investigation of the properties of non-steroidal chiral nematic materials.[14] Consequently, this has stimulated an interest in polymeric analogues of these stable, chiral nematic compounds.

Most of the conventional chiral nematic LCs reported to date have had the chiral centre situated near to the aromatic mesogenic core, in one (or sometimes both) of the terminal alkyl chains. By following a similar principle, various workers have synthesised chiral comb-branch polymers where the mesogen is connected to the polymer backbone via the terminal, non-chiral alkyl chain, which acts as a decoupling spacer. The chiral alkyl chain then functions as the mesogenic tail unit, which is essential in such polymeric systems.[34] Typical examples of both low molecular weight and polymeric chiral nematic materials are shown below:

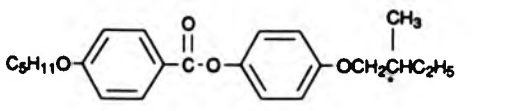

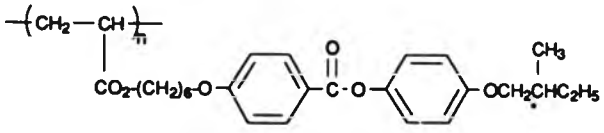

This approach has met with limited success, however, with respect to the preparation of polymers which exhibit the chiral nematic phase only. In most cases smectic phases have resulted.[82-86] On the other hand, one major advantage these do possess is their ability to form chiral smectic C phases, which of course exhibit excellent ferroelectric properties.[87]

An alternative route to chiral nematic polymers is by the attachment of the mesogen to the polymer backbone via the chiral alkyl chain which will then act as a flexible chiral spacer. With this type of structure one would expect the chiral centre to have a greater perturbing effect on the mesogen which will enhance the helical twisting of the mesophase structure. Furthermore, by attachment of the mesogen in this manner it is possible to alter the nature of the non-chiral alkyl chain, so as to promote nematic (and therefore chiral nematic) phase formation. This can be achieved by using short, polar substituents.[33,34] Similarly, copolymers formed from this type of monomer with other nematogenic monomers, or monomers with different spacer lengths should also promote chiral nematic phase formation.[33] This chapter details the preparation of three such monomers with chiral spacer units, namely MBM*, CBM* and XMBM* and the properties of the copolymers prepared from them. The structures of these monomers are shown below:

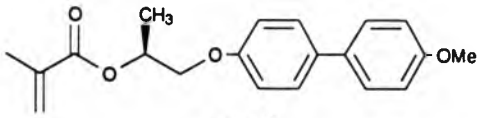

MBM*

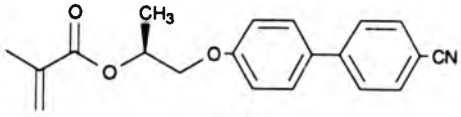

CBM*

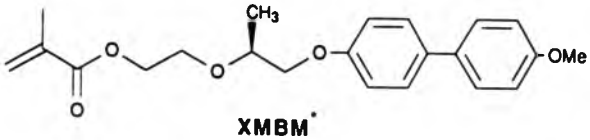

XMBM*

To date, no publications have appeared in either the patent or the open literature which describe these (or similar) types of chiral, mesogenic monomer, where the chiral centre is incorporated in the flexible spacer portion of the molecule. The results presented in this chapter concerning the preparation and use of these monomers in copolymeric systems have therefore been the subject of a European patent application (No 88308271, filed 7/9/88, under the trade name Stamicarbon B.V.) in conjunction with the company who have funded this work, namely Dutch State Mines. A copy of this patent is included in appendix B.

6.1 Synthetic Approach to the Chiral-Spacer Monomers MBM*, CBM* and XMBM*

The synthetic strategy employed in the synthesis of the

methacrylate-based monomers MBM*, CBM* and XMBM* follows a route by which these monomers can be efficiently synthesised with retention of configuration and without appreciable reduction in the optical purity of the starting material. The route used was based on a procedure first reported by Ghirardelli,[110] who prepared (S)-2-methyloxirane from the starting material (S)-ethyl lactate, which is readily available in high enantiomeric purity. The synthetic route to the monomers MBM*, CBM* and XMBM* is outlined in scheme 12. Recently, Walba et al.[154] and Otterholm et al.[111] reported the use of this route in the synthesis of low molecular weight LC compounds which exhibited the chiral smectic C phase with its inherent ferroelectric properties.

The hydroxyl group of the starting alcohol, (S)-ethyl lactate was protected by reaction with dihydropyran according to the method of Ghirardelli.[110] The molecule was then subsequently reduced by lithium aluminium hydride in diethylether, affording the alcohol 2-(tetrahydro-2-pyranoxy)-1-propanol. The primary alcohol functionality of this compound was converted into its tosylate, TTP(25) which was then used as a precursor in the preparation of both MBM* and CBM*. The tosyloxy group of TTP was displaced by the sodium phenoxide of either 4-methoxy-4'-hydroxybiphenyl or 4-cyano-4'-hydroxybiphenyl in DMF to yield the protected alcohols (26) and (29) respectively. These were subsequently deprotected using acidic ethanol to furnish the alcohols (27) and (30) in good yields. The monomer MBM* was prepared by refluxing the alcohol (27) with methacrylic acid and a suitable polymerisation inhibitor in toluene, whilst the monomer CBM* was prepared by esterifying the alcohol (30) with methacryloyl chloride in benzene, in the presence

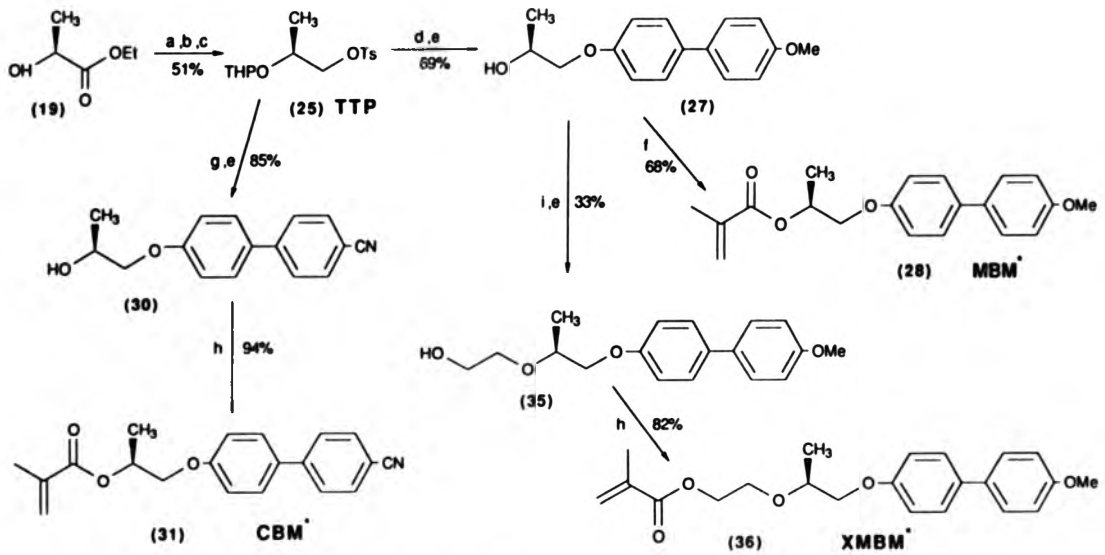

SCHEME 12 a. DHP, conc. HCl (5 drops); b. $LiAlH_4$, Et_2O; c. TsCl, Pyridine; d. 4-methoxy- 4'-hydroxy biphenyl, NaH, DMF; e. H^+, EtOH; f. methacrylic acid, PTSA, toluene, 2,6-di-t-butyl-4-methyl phenol; g. 4-cyano-4'-hydroxy biphenyl, NaH, DMF; h. methacryloyl chloride, NEt_3, benzene, 2,6-di-t-butyl-4-methyl phenol; i. 1-bromo-2-(tetrahydro-2-pyranoxy)ethane, NaH, DMF.

of triethylamine and a polymerisation inhibitor. Finally, the extended spacer version of MBM*, namely XMBM*, was prepared in the following way: The length of the methylene spacer was increased by reacting the sodium alkoxide of (27) with 1-bromo-2-(tetrahydro-2-pyranoxy)ethane which was previously prepared by the method of Newkome and Marston.[112] This produced the protected alcohol (34) in somewhat poorer yield which was then efficiently deprotected to give the alcohol (35). Esterification with methacryloyl chloride in benzene, in the presence of triethylamine and a polymerisation inhibitor afforded the monomer XMBM* (36).

The next sections of this chapter describe the copolymerisation properties of these monomers and the mesomorphic properties of the resultant copolymers.

6.2 Copolymers of MBM* and DMBI-6

6.2.1 Copolymerisation characteristics of MBM* with DMBI-6

The copolymerisation behaviour of MBM* with DMBI-6 shows a marked deviation from "ideal" behaviour. As discussed in section 4.3, this is because of the increased reactivity of the methacrylate radical relative to the itaconate radical and the greater steric crowding associated with the itaconate monomer.[123] These effects are relatively common in the copolymerisation of itaconate esters with methacrylate esters[123] and may lead to copolymers containing fairly long sequences of methacrylate monomer. Figure 6.1 shows the copolymerisation curve of MBM* and DMBI-6 along with their respective reactivity ratios (r_{MBM*} = 8.94, r_{DMBI-6} = 0.68).

Molecular weights could only be measured for PDMBI-6, PMBM* and copolymer 5b (F_{MBM*} = 0.63) from this system due to the limited availability of large samples of each copolymer. The DP_n values of these polymers were found to be approximately 12, 1300 and 100, respectively (table 3.5, chapter 3). From the results presented in section 4.3 and the knowledge that MBM* is much more reactive than DMBI-6, it is reasonable to assume that, with the possible exception of copolymer 5a (F_{MBM*} = 0.32), the DP_n values of the remaining copolymers will have $DP_n > 100$. In fact, the molecular weights of these copolymers should be of the order of the values measured for the structurally similar CBM*/DMBI-6 copolymers (table 3.6, chapter 3), with those rich in DMBI-6 being much lower than those rich in MBM*. PDMBI-6 and copolymer 5a are the only polymers whose transition temperatures might possibly be in a temperature dependent region due to their low DP_n values,[39] i.e. their properties could vary with chain length when this is low.

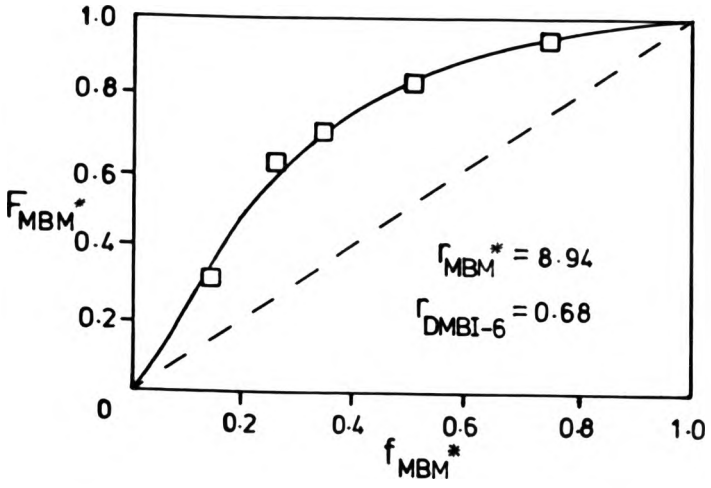

FIGURE 6.1 Plot of the mole fraction of MBM* in the copolymer (F_{MBM*}) versus the mole fraction of MBM* in the monomer feed (f_{MBM*}).
(□): Experimental point.
(—): Calculated best fit to experimental data.

6.2.2 Mesomorphic properties of MBM*/DMBI-6 Copolymers

The mesomorphic behaviour of the range of copolymers prepared from MBM* and DMBI-6 was studied by both dsc and hot-stage polarising microscopy. All of the copolymers were found to exhibit enantiotropic behaviour, with those rich in DMBI-6 forming

smectic, crystalline and chiral nematic phases, whilst the copolymers rich in MBM* were found to form only the chiral nematic phase. The results are presented in table 6.1 and are discussed below.

6.2.2.1 Thermal and textural behaviour of copolymer 5a

In addition to the crystalline and smectic A phases, copolymer 5a (F_{MBM*} = 0.32) was found to exhibit the chiral nematic phase over a narrow temperature interval of only 5°C. Figure 6.2 shows the dsc heating and cooling traces of copolymer 5a. By correlation with hot-stage polarising microscopy investigations, the thermal events shown on the dsc heating trace were found to correspond to the following transitions:

$$g \xrightarrow{78^{\circ}C} k \xrightarrow{118^{\circ}C} S_A \xrightarrow{132^{\circ}C} N^* \xrightarrow{137^{\circ}C} I$$

The dsc cooling trace also displays the same transitions in the reverse order, with each transition being supercooled by the following amounts:

$$I \xrightarrow{7^{\circ}C} N^* \xrightarrow{7^{\circ}C} S_A \xrightarrow{15^{\circ}C} k$$

These are of a similar magnitude to previously reported values.[91]

Hot-stage polarising microscopy observations of copolymer 5a revealed the presence of the smectic A phase which formed as a slightly imperfect focal-conic fanned texture on cooling the chiral nematic phase below about 125°C. This texture was seen to be quite

TABLE 6.1 The phase transition temperatures of MBM*/DMBI-6 copolymers [a]

Copolymer Number	F_{MBM*}	Tg/°C	T_m/°C	T_{S-N*}/°C (T_{S_A-I})/°C [b]	T_{N*-I}(dsc)/°C	T_{N*-I}(hsm)/°C	Colour of reflected light against a dark background
1a	0	64	125	(150)[b]	c	c	-
5a[d]	0.32	78	118	132	137	150	-
5b	0.63	67	-	108	117	122	-
5c	0.70	68	-	-	91	-	blue
5d	0.83	79	-	-	103	-	violet/blue
5e	0.95	97	-	-	114	-	-
5f	1.00	105	-	-	120	-	-

a - All temperatures are recorded during the second heating scan at a rate of 20°C/minute.
b - This temperature corresponds to the maximum of the smectic A-isotropic transition endotherm (noted as $T_{S_A-S_A/I}$ in tables 4.1 and 4.2).
c - No chiral nematic phases are exhibited by this polymer.
d - Chiral nematic phase in this copolymer is possibly biaxial in nature.

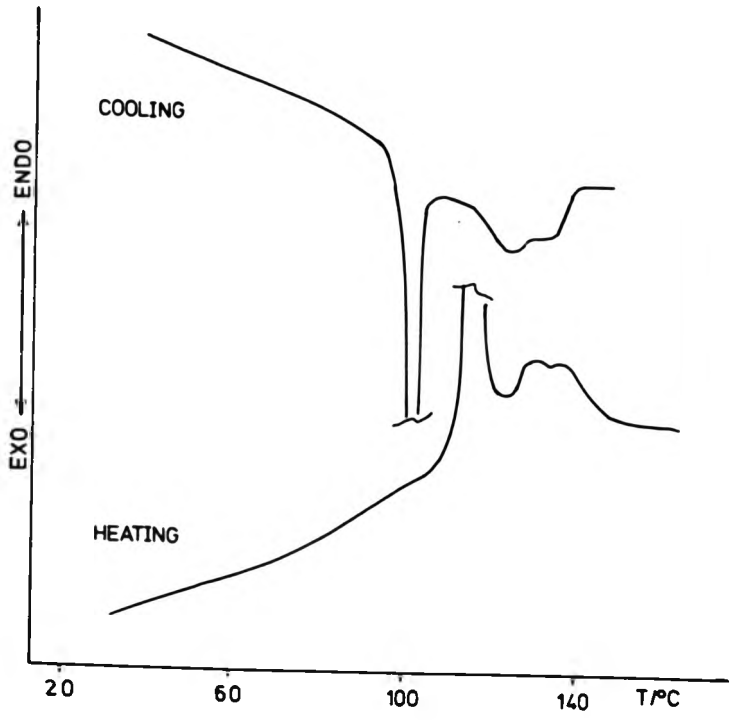

FIGURE 6.2 Dsc heating and cooling traces of copolymer 5a recorded at 20°C/minute. The heating trace was recorded during the second heating scan.

similar to those reported previously in sections 4.2 and 4.3. Further cooling resulted in crystallisation at about 110°C which was characterised by a reduction in the sample birefringence and concomitant destruction of the focal-conic fanned texture.

On cooling the isotropic melt, the chiral nematic phase surprisingly did not separate in the normal way and droplet areas were seen to form. Furthermore, the eventual texture formed was not the usual planar texture, but was in fact a fingerprint texture.[89,152] Both of these features are shown by the photomicrograph in figure 6.3. The aptly named fingerprint texture of the cholesteric or chiral nematic phase occurs much more rarely than the usual planar or focal-conic textures. As with the focal-conic texture, the fingerprint texture is characterised by the helicoidal axes lying parallel to the glass-slides. This texture has been known to exist for certain low molecular weight chiral nematic materials of long pitch length, at temperatures near T_{Cl}[152] and for some long pitch, chiral nematic lyotropic materials.[153] With normal, uniaxial chiral nematic materials, the fingerprint lines always appear as dark lines. These dark lines correspond to the arrangement where the director of the molecular long axes in a certain quasi-nematic plane is normal to the glass-slides. The distance between the lines is P/2 where P is the helical pitch length. Normally, textures such as these only exhibit dark and light lines, with the colour of these light lines being uniform throughout the texture. Although the study of the fingerprint texture in figure 6.3 is unavoidably limited by low magnification, close inspection of the texture revealed the presence of many interference colours, with there being very little colour contrast between the light and dark lines in some areas. In fact,

FIGURE 6.3 **Photomicrograph displaying the highly coloured fingerprint texture of the chiral nematic phase of copolymer 5a.**

some of these contrasting lines had different colours rather than being merely dark and light. Finkelmann and co-workers[89] also observed such coloured "fingerprints" for a chiral nematic comb-branch polymer where the mesogens were laterally rather than terminally attached to the polymer backbone. This polymer has previously been discussed and its structure is depicted in section 1.7. The coloured texture in the case of Finkelmann's copolymer was described as being due to the formation of a stable, biaxial chiral nematic phase rather than the usual uniaxial one. The presence of such a phase was also confirmed by other experiments.[89]

In a biaxial phase, whether it is nematic or chiral nematic, the rotation of the molecules about their long molecular axis is hindered and the mesogens align as lath-like particles, as depicted in figure 6.4 below:

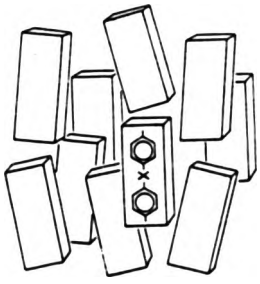

FIGURE 6.4 Biaxial arrangement of lath-like particles.

In this state, orientational correlations amongst the molecules exist not only between their long axes but also between their short axes. This changes the optical properties of these species, with the optical

axis of the phase no longer coinciding with the molecular long axis (and the quasi-nematic layer director, in the chiral nematic case). This means that the dark lines in the fingerprint texture are replaced by coloured lines, since birefringence is now possible when the quasi-nematic layer director is perpendicular to the glass-slides.[89]

Although the formation of a thermotropic, biaxial chiral nematic phase was first theoretically predicted by Goosens[155] and later by Pleiner and Brand[156] amongst others, it was not until much later that Finkelmann and co-workers reported the first series of well-defined, biaxial nematic and chiral nematic, thermotropic polymers.[89] The reasons as to why these materials exhibit biaxial phases is obvious - rotation around the mesogenic long axis is prevented by the lateral attachment of the mesogen to the polymer chain.

In the case of conventional comb-branch polymers with terminally attached mesogens, only uniaxial, chiral nematic or smectic phases have been reported in the past. This is because rotation of the mesogenic groups around their long molecular axis is less restricted, with the only restriction to rotation arising from the flexible spacer.[76] If one now considers copolymer 5a, it may be possible that the rotational motions of the mesogens are sufficiently restricted so as to cause the formation of a biaxial, chiral nematic phase and therefore the formation of a texture similar to that exhibited by Finkelmann's polymer. Conceivably, this restricted rotation must arise from the short, sterically crowded chiral spacer. The restrictive effect of this short chiral spacer on mesogenic rotation is discussed in greater detail in section 6.2.2.4 with relation to the helical twisting power of the MBM* monomeric units in other copolymers of different composition.

Although copolymer 5a contains only 20% of the MBM* chiral side chains, it is not known whether the restricted rotation of these side chains will in fact restrict the rotations of the remaining 80% itaconate side chains. These non-chiral side chains will themselves be able to undergo less restricted rotation, as they have a longer spacer length of 6 carbon atoms.

This may lead to limited biaxial domains or possibly no biaxiality at all. Clearly, one can only speculate as to the formation of the biaxial, chiral nematic phase in this instance and further work must be carried out in order to ascertain the true nature of the phase exhibited by copolymer 5a.

6.2.2.2 Thermal and textural behaviour of copolymer 5b.

Copolymer 5b (F_{MBM*} = 0.63) was found to exhibit only smectic and chiral nematic phases. No crystallinity was detected in the sample by either dsc or microscopy. Figure 6.5 shows the dsc heating and cooling traces of copolymer 5b.

As with copolymer 5a, both liquid crystalline transitions were seen to supercool by about 5°C.[91]

Hot-stage microscopy revealed the presence of a grey-blue planar texture typical of the chiral nematic phase, which formed almost spontaneously upon cooling the isotropic liquid below about 112°C. In contrast to the previously discussed copolymer (5a), the planar texture appeared in the normal manner;[96] no droplets were seen to separate from the isotropic liquid in this instance. Figure 6.6(a) shows a photomicrograph of this grey-blue chiral nematic texture. Upon cooling this texture the colour (reflection colour) was seen to change firstly to pale yellow (figure 6.6(b)) then to an

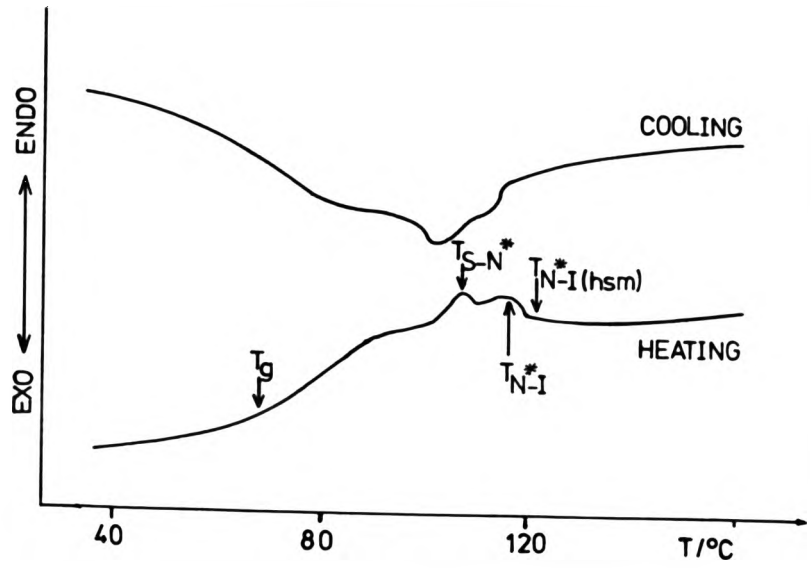

FIGURE 6.5 Dsc heating and cooling traces of copolymer 5b recorded at 20°C/minute. The heating trace was recorded during the second heating scan.

orange-brown colour (figure 6.6(c)) just before the chiral nematic to smectic transition. On further cooling, no textural changes were seen to occur except that the colour of the orange/brown texture darkened and a reduction in birefringence was observed. Annealing the sample at a temperature of 85-90°C resulted in little textural change, even after prolonged annealing times were employed (~24 hours). The viscosity of this phase was also seen to have increased relative to the chiral nematic phase.

FIGURE 6.6 (a) Photomicrograph of the grey-blue planar texture of the chiral nematic phase of copolymer 5b, taken at 105°C (Magnification x 200).

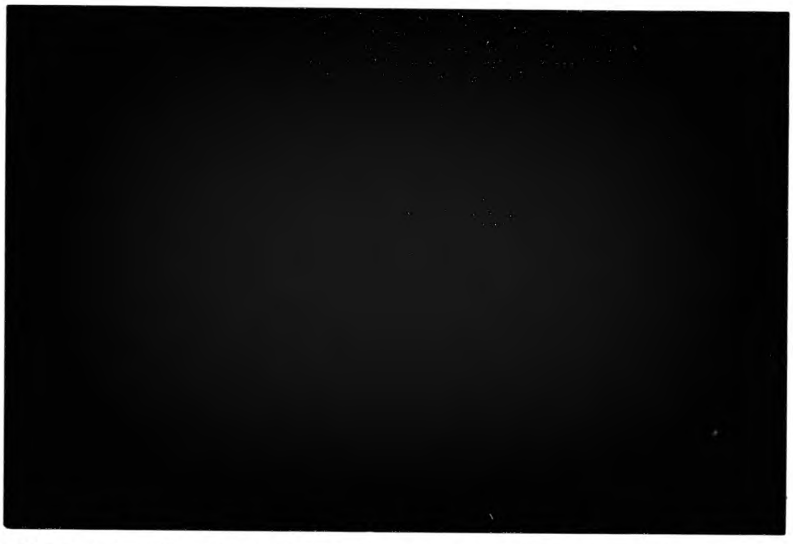

FIGURE 6.6 (b) Photomicrograph of the yellow planar texture of the chiral nematic phase of copolymer 5b, taken at about 103°C (Magnification x 200).

FIGURE 6.6 (c) Photomicrograph of the orange/brown planar texture of the chiral nematic phase of copolymer 5b, taken at 90°C (Magnification x 200).

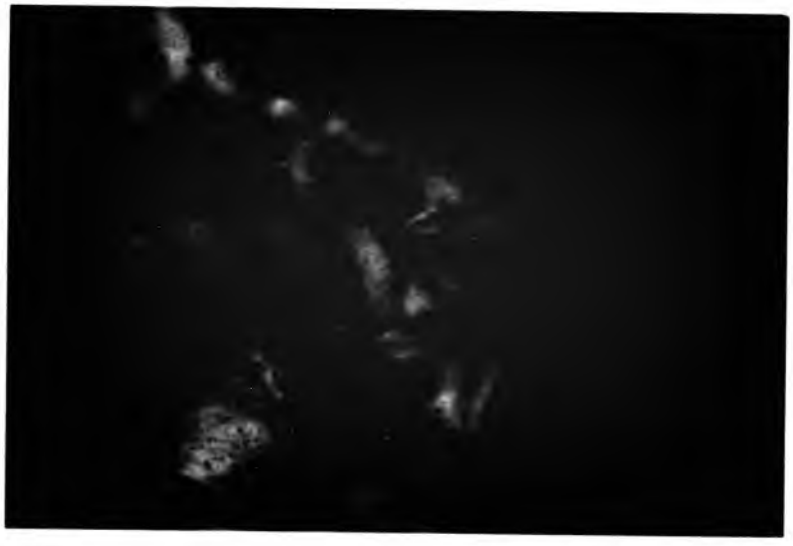

FIGURE 6.6 (d) Photomicrograph of the deep-blue planar texture of the chiral nematic phase of copolymer 5b, taken after annealing the texture shown in figure 6.6(a) for 1 hour at 105°C (Magnification x 200).

These results indicate that the pitch of the chiral nematic helix is temperature dependent, especially in the region of the chiral nematic to smectic transition, where the pre-transitional effect manifests itself.[15,33] This effect, which always occurs near chiral nematic (cholesteric) to smectic transitions has previously been discussed in chapter 5 (section 5.1.1). Unfortunately, the colours of the chiral nematic textures did not seem very bright. However, after annealing the sample at 105°C for some time, the blue/grey texture was seen to develop further into a deep-blue coloured texture. Obviously during the annealing process the mesogens in this viscous, polymeric phase had time to untangle and arrange themselves into more perfect helical structures and larger planar domains.[33] Figure 6.6(d) illustrates the deep-blue colour of the chiral nematic phase after the sample was annealed at 105°C for about one hour. A photomicrograph of the edge of the sample was taken and the bright interference colours close to the edge (at the left hand side of the photomicrograph) are caused by the imperfect alignment of the mesogens and the helices in this boundary region. None of the above results indicate the possible formation of a biaxial chiral nematic phase. Without a specialised investigation into the possibility of biaxial phase formation by this polymer, no further comment can be made with regard to the existence of this structure at present.

The lack of a well-defined texture corresponding to the smectic phase is puzzling, since normally one would expect the formation of focal-conic domains or some other textural feature common to smectic phases, especially after annealing the sample for any length of time. From the results presented here it is impossible

to determine the exact nature of the phase except that it may be smectic in nature. Without further work or other evidence from X-ray diffraction studies for example, unambiguous identification of this phase is impossible.

6.2.2.3 Thermal and textural behaviour of copolymers 5c-5e and homopolymer 5f.

The chiral nematic mesophase was the only mesophase observed for polymers 5c-5f. In each case the mesophase interval was found to be rather narrow, with T_{N^*-I} generally occurring about 10-20°C above Tg; in other words, just above the upper temperature limit of the glass transition region. Figure 6.7 shows representative dsc heating traces and a cooling trace for polymer 5d (F_{MBM^*} = 0.83). The thermal behaviour of this polymer (as with the others) seems rather odd on first sight, however a possible explanation for this behaviour will be given below.

The first dsc heating scan (trace 1) was carried out using a freshly precipitated polymer. The only thermal treatment prior to the first heating scan entailed drying the polymer under vacuum at 60°C for 24 hours. From this trace one can see an exothermic event centred at 74°C and an endothermic event centred at 107°C.

From hot-stage microscopy investigations, the endothermic event was seen to correspond to the chiral nematic-isotropic transition. No textural changes corresponding to the lower, exothermic event were detected. After recording trace 1 the sample was quenched quickly from 137°C to room temperature and the second dsc heating scan recorded immediately afterwards (trace 2). This trace no longer showed the lower, exothermic event and, in addition, the endothermic event was seen to be much reduced in

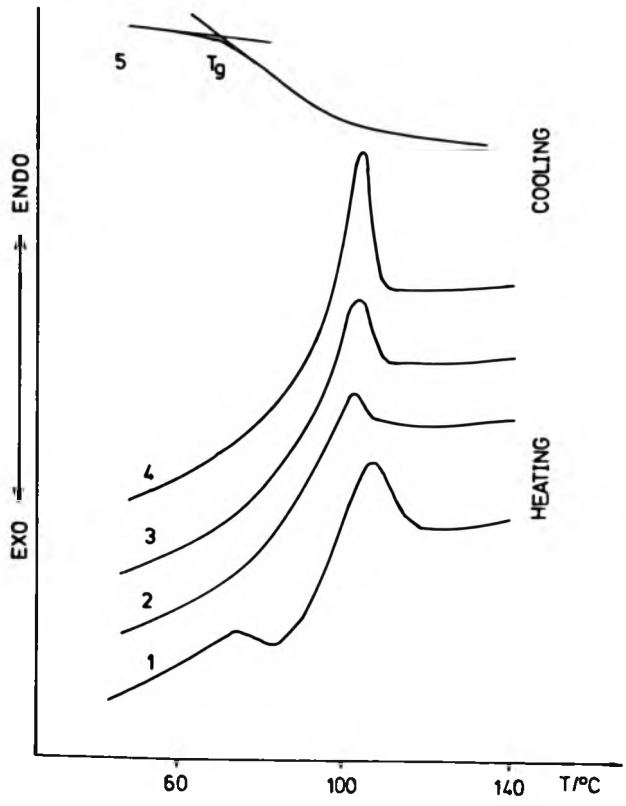

FIGURE 6.7 **Dsc heating traces and a cooling trace of copolymer 5d (F_{MBM*} = 0.83) recorded at 20°C/min after the following thermal treatments:**

1: 1st dsc heating trace of virgin sample
2: 2nd dsc heating trace, recorded immediately after the first heating trace, after quenching from 137°C.
3: 3rd dsc heating trace, recorded after cooling the sample from 137°C to 97°C at 5°C/minute, annealing the sample at 97°C for 40 minutes then cooling at 20°C/minute to 27°C.
4: 4th dsc heating trace, recorded after cooling the sample from 137 to 92°C at 5°C/minute, annealing the sample at 92°C for 40 minutes then cooling at 20°C/minute to 27°C.
5: Dsc cooling trace, recorded at 20°C/minute from 137°C.

size. This dsc trace shows a possible glass transition at about 80°C and a chiral nematic to isotropic transition at about 103°C. The presence of the former was confirmed by the dsc cooling trace (trace 5) and the occurrence of a softening point (~85°C) which was detected by microscopy. The isotropic to chiral nematic transition is not observed on the cooling trace since at the cooling rate used it is supercooled into the glass transition region. Dsc traces 3 and 4 display an enhancement of the endotherm corresponding to the chiral nematic to isotropic transition when prior thermal treatment of the sample included slow cooling and annealing treatments. Although an increase in the magnitude of this endotherm is expected since these prior thermal treatments encourage ordering and mesogen alignment, the increase shown by both traces 3 and 4 seems rather large. This may, in part, be due to an additional enthalpic relaxation effect which manifests itself in the same region as the mesophase transition. Unfortunately, very little explanation can be given for the occurrence of the exothermic event shown by trace 1 at the moment without further investigation. It may be possible that this event is associated with a "~~freezing~~ release" of the frozen molecular motions and the motions of the mesogens in particular, as the glass is heated. This may allow the mesogens to align and form ordered domains which are then subsequently destroyed upon heating past T_{N^*-I}.

Hot-stage microscopy investigations of polymers 5c and 5d revealed the presence of planar textures which exhibited the reflection of blue light. These textures were not formed spontaneously however. This is because of the highly viscous nature of the mesophase of each polymer which is due to the proximity of T_{Cl} to Tg and the fact that a large proportion of each polymer

consists of MBM* monomer units (F_{MBM*} = 0.7 and 0.83 for polymers 5c and 5d respectively) which have short spacers. Because of these short spacer lengths the anisotropic interactions of the MBM* mesogens will be ineffectively decoupled from the polymer backbone, which will always attempt to take on a statistical conformation. This means that the polymer backbone motions will dominate the mesophase formation. These features necessitate the employment of long annealing times so as to allow for mesogen alignment and the eventual formation of the helical structures of the chiral nematic phase,

The blue planar texture of polymer 5c is displayed in figure 6.8, with the texture being obtained after annealing the sample for about 24 hours. Unfortunately in this case, the actual blue colour observed could not be reproduced in the photomicrograph due to unavoidable background illumination of the sample. This occurred because of the employment of a Linkam PR 600 microprocessor controlled heating stage rather than the usual Reichert stage, for this sample only. The Linkam heating stage unfortunately allowed more background light into the sample area. The blue colour observed when using the Reichert stage is in fact very similar to that displayed by polymer 5b in figure 6.6(d). Polymer 5d was found to form a very similar planar texture after annealing overnight, however the textural colour was found to be a violet rather than deep-blue colour. This is an expected feature and is due to polymer 5d containing a greater amount of MBM*.[33,34,80] This phenomenon is also discussed in section 5.1.3 and in section 6.2.2.4 of this chapter.

As discussed in chapter 5, section 5.1.2.1, a common feature of polymers which exhibit the chiral nematic (or cholesteric) phase

FIGURE 6.8 Photomicrograph of the blue planar texture of the chiral nematic phase of polymer 5c after annealing overnight at 101-103^{o}C.

and no other LC phases is the possibility of one retaining the planar texture which exhibits the reflection of visible light by cooling the sample quickly below Tg.[34] This process was employed with samples of polymers 5c and 5d which were coated onto glass-slides. After annealing these samples in the region just below T_{Cl} but above Tg, in order to develop the chiral nematic planar textures of each polymer, the samples were quickly cooled below Tg. This resulted in the formation of blue and violet coloured, semi-transparent, glassy films for polymers 5c and 5d respectively. The reflection colour of these films were seen to be brightest when viewed against a dark background and were seen to have a yellow appearance when transmitted white light was viewed through them. As was mentioned previously, these coloured films are free of any chromophores or dye molecules, with the colours being imparted solely by the chiral nematic helical structure. These films were found to be fairly robust and the potential uses of such coloured films in coatings applications where the coating temperature does not exceed the Tg of the polymers are obvious.

Copolymer 5e and homopolymer 5f (PMBM*) also form chiral nematic phases. However, the planar textures were much harder to produce and again very long annealing times had to be employed, for the reasons mentioned earlier. In contrast to the other MBM*/DMBI-6 copolymers, no reflection colours were apparent for these polymers. This is obviously a result of their very short helical pitch lengths which is caused by both polymers being very rich in MBM*. These short pitch lengths will cause the reflected light to be in the uv region of the electromagnetic spectrum, which will in turn be absorbed by the biphenyl mesogenic groups.

In polymers 5c to 5f there were no textural features which would infer the possibility of biaxial phase formation. This possibility cannot be discounted however, without further, more detailed investigations.

6.2.2.4 General properties and trends associated with the MBM*/DMBI-6 copolymer system.

The phase transition temperatures of the MBM*/DMBI-6 copolymers 5a-5f are displayed as a function of the mole fraction of MBM* in the copolymer in figure 6.9.

The general increase in Tg with incorporation of the methacrylate MBM* monomer is caused by a restriction in the conformational mobility of the backbone, which arises from the steric bulk of the MBM* side chain and the vinyl α-methyl group. Additionally, internal plasticisation arising from the hexamethylene spacers of DMBI-6 is also reduced and consequently the Tg increases as the polymers become richer in MBM*. The drop in Tg on going from copolymer 5a (F_{MBM*} = 0.32) to copolymer 5b (F_{MBM*} = 0.63) can most likely be associated with the disappearance of crystallinity in the latter sample.

The presence of smectic phases and crystallinity in the copolymers rich in DMBI-6 is of course due to the tendency of DMBI-6 to form ordered smectic and crystalline layers, as was reported and discussed in chapter 4. Layered phase formation is also encouraged as the proportion of mesogenic units with long spacer moieties increases, since long spacer lengths are known to favour smectic phase formation.[34] The incorporation of the MBM* monomer with its short spacer length into the copolymer leads to defective packing in the smectic layers at fairly low compositions, as is evidenced by the presence of the chiral nematic phase at F_{MBM*} = 0.32 (copolymer 5a). This disruption, which is caused by the displacement of the centres of gravity of adjacent mesogens results in nematic ordering on a local scale. This in turn allows for the development of the

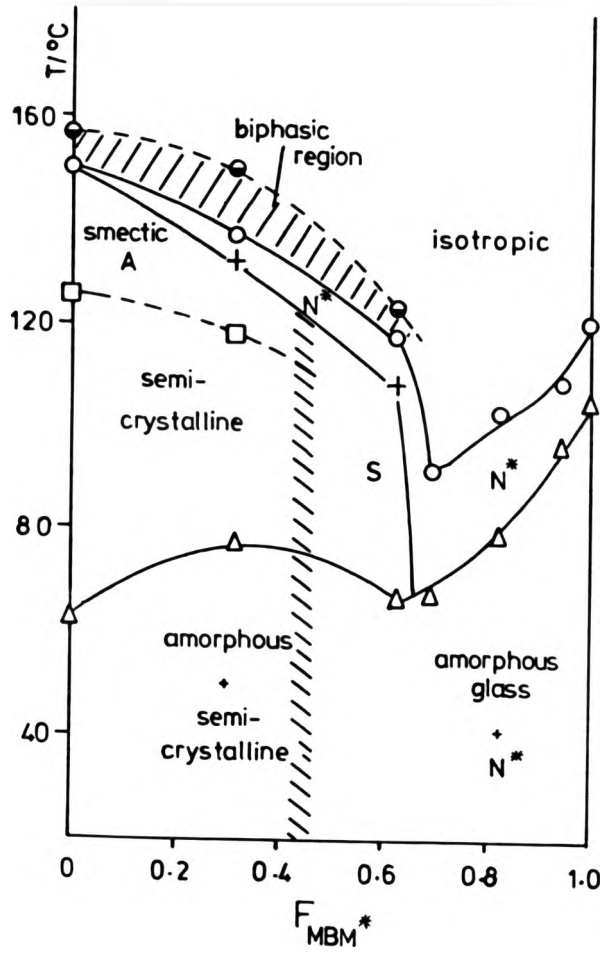

FIGURE 6.9 Plot of the phase transition temperatures (°C) of MBM*/DMBI-6 copolymers versus the mole fraction of MBM* in the copolymer (F_{MBM*}). (Δ): Tg; (□): Tm; (+): T_{S-N*}; (O): $T_{S_A-S_A/I}$ for PDMBI-6 and T_{N*-I}(dsc) for the other polymers; (⊖) $T_{S_A/I-I}$ for PDMBI-6 and T_{N*-I}(hsm) for other polymers.

chiral nematic helical structure. Figure 6.10 shows this disruption schematically:

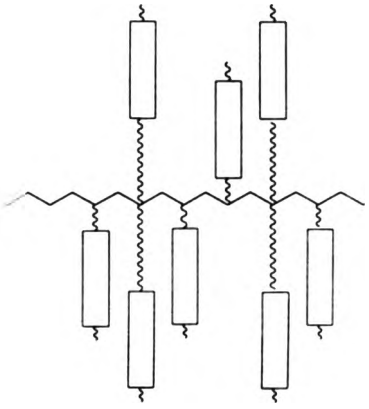

FIGURE 6.10 Schematic of the disruption caused by the introduction of MBM* monomers into the layered PDMBI-6 homopolymer.

The drop in T_{Cl} (T_{N^*-I}) can also be attributed to this increasing level of disruption, as the anisotropic interactions between the mesogens will be lessened and the packing more defective due to the difference in spacer lengths. An additional factor which may influence T_{Cl} to a lesser extent in this system is the presence of the branching CH_3 at the chiral carbon of MBM*. As one would expect, this group will cause a significant change in the axial ratio of the MBM* side chain which, in turn, will lead to a decrease in T_{Cl}.[28] The following crude comparison shows the effect of introducing this chiral CH_3 branch into the short spacer of one of these polymers: Finkelmann and co-workers[94] reported the phase transition temperatures of a methacrylate polymer similar to PMBM* (polymer

5f), in which the branching CH_3 group was replaced by a hydrogen atom. In other words, Finkelmann's polymer had a methylene spacer length of two carbons with no branches. These workers found T_{Cl} to be higher than that of MBM* by about 32°C, which infers that the branched spacer of MBM* does affect the axial ratio of MBM* and hence the side chain interactions quite strongly. This comparison must not be treated too rigorously however, since Finkelmann does not report the DP_n of the polymer, the type of dsc or the heating rates employed.

In figure 6.9, the sharp drop in T_{N*-I} on going from polymer 5b (F_{MBM*} = 0.63) to polymer 5c (F_{MBM*} = 0.70) is difficult to rationalise. It seems, however, that it must be associated with the disappearance of the smectic phase in the polymer system. A tentative explanation for both of these observations may be that the fraction of DMBI-6 monomer units in the copolymer has reached a critical limit, whereby their mesogens cannot interact effectively due to their being spaced apart by long sequences of MBM* monomers. The possibility of the occurrence of long sequences of MBM* in the polymer is discussed in section 6.2.1. On progressing to greater values of F_{MBM*}, T_{N*-I} rises again as the numbers of DMBI-6 monomer units which disrupt the MBM* rich copolymers decreases.

The biphasic region in this copolymer system could only be detected easily for the first three copolymers 5a, 5b and 5c as well as for homopolymer 1a. This region is shown in figure 6.9. Biphasic regions could not be detected for any of the other polymers, although they will most likely exist. Biphasic regions have been discussed earlier in both chapter 4 and chapter 5 and the reasons for their appearance in this system are not likely to be different from those given previously.

The optical properties of the chiral nematic textures of the MBM*/DMBI-6 copolymers appear to differ markedly from those described in chapter 5, for example. In the ChMI-10/CPBA-6 copolymer system of chapter 5, the temperature dependent reflection of visible light is observed for all copolymer compositions except for copolymer 4d, which only exhibits visible light reflection in the pre-transitional region. In the MBM*/DMBI-6 copolymers on the other hand, copolymer 5b exhibits the reflection of blue light which changes to an orange/brown colour on cooling, due to the pre-transitional effect; copolymer 5c exhibits only the reflection of a deep-blue colour; copolymer 5d exhibits only the reflection of a blue/violet colour and copolymer 5e and homopolymer 5f probably exhibit the reflection of uv light. These results indicate that the helical structure of the copolymers in the MBM*/DMBI-6 system must be of a much shorter pitch length in each case compared to that of the ChMI-10/CPBA-6 copolymers, if calculated from relationship 1.4 given in chapter 1. This implies that the chiral monomer MBM* induces a greater helical twist in the copolymer system, so causing the reflected light to arise predominantly in the blue and uv regions of the spectrum. These results can be readily explained in terms of the theories advanced by Goosens,[11,155] Vertogen[12] and Finkelmann and Stegemeyer,[13] for the basis of the induced helical structure. The results presented in this chapter give further experimental evidence in support of these theories.

Following the theories cited above, the formation of the helical structure has been proposed as being due to hindered rotation of the chiral molecules about their long molecular axis and assymmetrical dipole-quadrupole interactions which exist between

the chiral and achiral molecules which comprise the system. Results obtained from studies of mixtures of low molecular weight nematic and chiral molecules such as MBBA (4-butyl-N-[4-methoxybenzylidene] aniline) and DDCO (4,5-diphenyl dinaptho[2,1-e:1',2'-g] [1,4]diazocine) were found to endorse these theories,[13] with the inherently assymmetric planar molecule DDCO causing the system to have a very tight helical twist. This is reflected in its extremely high optical rotation ($[\alpha]_D = 2000^o$) and the presence of hindered rotation about its long molecular axis. The structures of DDCO and MBBA are shown below:

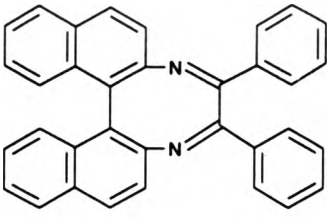

DDCO

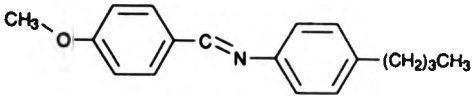

MBBA

In chiral nematic (cholesteric) comb-branch polymer systems, Finkelmann and Rehage[76] also showed that the helical twisting power of a polysiloxane-based cholesteric copolymer was strongly affected by the length of the flexible spacer connecting the nematogenic mesogen to the polymer backbone:

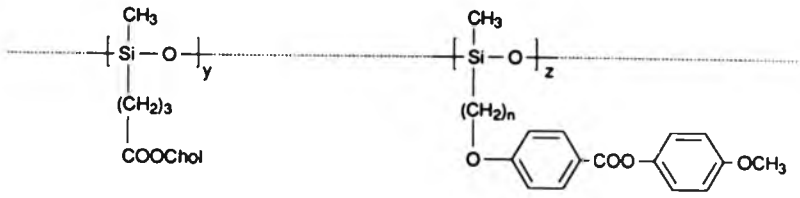

n = 3 - 6.

These workers found that shorter spacer lengths (n=3, for example) gave the tightest helical twists. This was rationalised on the basis of the aforementioned theories as being due primarily to the shorter spacer lengths restricting rotation around the long molecular axes to greater extents that the longer spacer lengths. These short spacer lengths restrict long axis rotation in the following way: Free rotation around the molecular long axis requires cooperative movements of the spacer carbon skeleton via the conformational states which are lowest in energy. Therefore, as the spacer length decreases to n = 3, the numbers of low energy conformational states are limited and rotation becomes restricted. It should be noted here that in the case of the polymers with n = 3, the mesogenic motions will also be strongly influenced by the polymer backbone motions, which may additionally affect the twisting of the helix. Although the theories only consider hindered rotation of the chiral molecule, it is highly likely that hindered rotation of the nematogenic as well as the chiral moieties will favour highly twisted phases to an even greater extent.

On the basis of the proposed theories and the above

discussion, it would appear that, apart from the molecular shape and optical rotation of the chiral molecule (whether it is mesogenic or non-mesogenic), the length of the flexible spacer also plays a dominant role in determining the chiral nematic pitch length. One can therefore see why most of the copolymers prepared from the monomers ChMI-10 and CPBA-6, which have long spacer lengths of 10 and 6 respectively, exhibit a wide range of visible reflection colours. Conversely, from these arguments one would expect the copolymers of the MBM*/DMBI-6 system to form helical structures with extremely small pitch lengths, since the spacer length of the chiral monomer MBM* is very short (2 carbons). The tendency of this short spacer to restrict mesogenic long-axis rotation will be increased further due to the presence of the methyl group which is attached to the spacer at the chiral centre. This causes further steric crowding and forces the mesogen to adopt a slightly bent shape. As expected, these structural features result in the MBM*/DMBI-6 copolymers exhibiting chiral nematic phases with very short pitch lengths indeed. The shortening of the helical pitch length as the polymers become richer in MBM* is also expected, on the basis of hindered rotation, since the rotation of the mesogens will inevitably become more restricted as the numbers of MBM* monomers increases.

Lastly, since the presence of biaxiality in relation to the chiral "dopant" molecules is implicit in the aforementioned theories and the results in this section appear to support them, it is possible that the polymers reported here may in fact be of a biaxial nature as was suggested earlier.

6.3 Copolymers of CBM* and DMBI-6

6.3.1 Copolymerisation characteristics of CBM* with DMBI-6

As with the very similar MBM*/DMBI-6 system, the copolymerisation behaviour of CBM* with DMBI-6 shows a marked deviation from "ideal" behaviour. The reasons for this are of course due to the differing reactivities of the methacrylate and itaconate radicals as discussed in section 6.2.1 and section 4.3 in chapter 4.

If one examines the respective copolymerisation curves of each pair of monomers, MBM*/DMBI-6 and CBM*/DMBI-6, which are displayed in figure 6.11, each system can be seen to vary from ideal copolymerisation behaviour to differing extents. Although this is surprising, since both methacrylate monomers are identical except for the nature of the terminal group (-OMe in MBM* and -CN in CBM*), it should be borne in mind that the polymerisations were carried out under different conditions. The copolymerisation of MBM* with DMBI-6 was carried out in benzene at 70°C, whilst the copolymerisation of CBM* with DMBI-6 was carried out in THF at 55°C.

As can be seen from the molecular weights measured for these copolymers, (table 3.6 in chapter 3), most have molecular weights in the region where their mesomorphic properties will not be appreciably affected by chain length variations. Those with compositions rich in DMBI-6 may be a little more doubtful, however, and they may exhibit lower transition temperatures.[39]

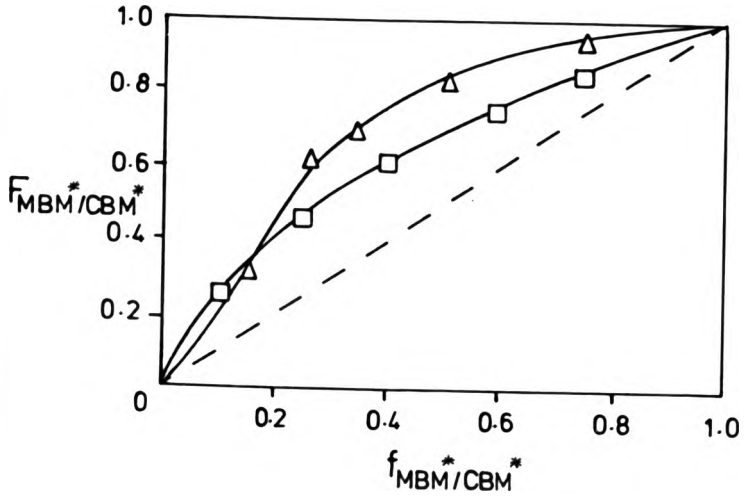

(Δ): MBM*/DMBI-6 $r_{MBM^*} = 8.94$, $r_{DMBI\text{-}6} = 0.68$; $r_{MBM^*}.r_{DMBI\text{-}6} = 6.06$;

(□): CBM*/DMBI-6 $r_{CBM^*} = 1.82$; $r_{DMBI\text{-}6} = 0.27$; $r_{CBM^*}.r_{DMBI\text{-}6} = 0.49$.

FIGURE 6.11 Plots of the mole fractions of MBM* and CBM* in the copolymer (F_{MBM^*} and F_{CBM^*} respectively) versus the mole fractions of MBM* and CBM* in the monomer feed (f_{MBM^*} and f_{CBM^*} respectively).
(–): Calculated best fit to experimental data.

6.3.2 Mesomorphic properties of CBM*/DMBI-6 copolymers.

The range of copolymers prepared from CBM* and DMBI-6 were found to exhibit enantiotropic mesomorphic behaviour and were studied by both dsc and hot-stage polarising microscopy. As with the previous MBM* system, the copolymers rich in DMBI-6 were found to exhibit crystalline and smectic phases whilst those rich in CBM* were found to exhibit either chiral nematic mesophases or no mesophase at all. In contrast to the previous system, none of the copolymers were found to exhibit both smectic and chiral nematic phases. These results are presented in table 6.2 and are discussed below.

6.3.2.1 Thermal and textural behaviour of copolymers 6a and 6b.

Both copolymers 6a and 6b were found to exhibit both crystalline and smectic A phases in the range F_{CBM*} = 0.00-0.50, but there was no evidence of chiral nematic phases in this composition range, in contrast to the previously described MBM*/DMBI-6 system. Figure 6.12 shows the dsc heating and cooling traces of polymer 6b (F_{CBM*} = 0.47) which are representative of these polymers.

The Tg of polymer 6b was located at about 93°C and above this, two endotherms were observed as 121°C and 136°C. By correlation with microscopy observations, the larger endotherm at 121°C and the smaller one at 136°C were found to correspond to transitions from the crystalline to the smectic A phase and the smectic A to the isotropic phase respectively. On cooling, the same transitions and the corresponding exotherms were seen to occur in reverse order, as figure 6.12 shows. The main feature of these two

TABLE 6.2 The phase transition temperatures of CBM*/DMBI-6 copolymers [a]

Copolymer Number	F_{CBM*}	Tg/°C	T_m/°C	$(T_{S_A}\text{-}S_A/I)$/°C [b]	$T_{S_A/I\text{-}I}$ °C	$T_{N*\text{-}I}$(dsc)/°C[b]	Colour of reflected light against a dark background
1a	0.00	64	125	150	157		
6a	0.26	81	131	148	155		
6b	0.47	93	121	136	147		
6c	0.62	82				116	Pale-blue
6d	0.76	94				112	
6e	0.85	96					
6f	1.00	105					

a - All temperatures are recorded during the second heating scan at a rate of 20°C/minute.

b - $T_{N*\text{-}I}$(hsm) is not included in this table since the point at which the complete disappearance of birefringence occurred was difficult to identify optically.

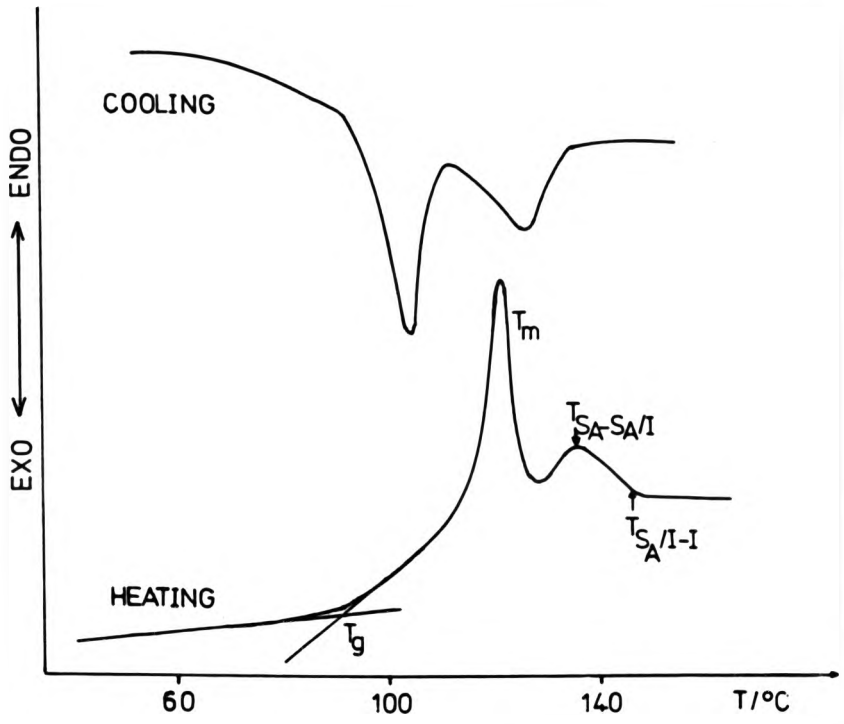

FIGURE 6.12 **Dsc heating and cooling traces of copolymer 6b recorded at 20°C/minute. The heating trace was recorded during the second heating scan.**

dsc traces is the magnitude of supercooling observed, which was 9°C and 16°C for the upper and lower temperature transitions respectively. The supercooling of the smectic A - isotropic transition in particular appears to be much larger than any previously reported transitions of this type, for this heating rate. It is therefore worthy

of note.[91] PDMBI-6 (polymer 1a) only shows a supercooling of 5°C under these same conditions (section 4.2.2.1). Polymer 6a shows similar dsc traces and similar supercooling effects.

Microscopy investigations of these polymers showed the formation of the usual focal-conic fanned texture typical of the smectic A phase, upon cooling the isotropic melt.[18] Figure 6.13 shows an example of the focal-conic fanned texture of the smectic A phase of polymer 6a. As with all of the other copolymers examined in this work, a biphasic region was apparent and the smectic A phase was seen to co-exist with the isotropic liquid phase over a finite temperature inteval. This interval was seen to increase slightly as the copolymers became richer in CBM*, inferring that the polydispersity of the samples may be increasing slightly with increasing CBM* content.[132] As with the smectic polymers described in chapter 4, the biphasic region exists between $T_{S_A\text{-}S_A/I}$ (which corresponds to the endotherm maximum) and $T_{S_A/I\text{-}I}$ which was observed by polarising microscopy. These temperatures are recorded in table 6.2.

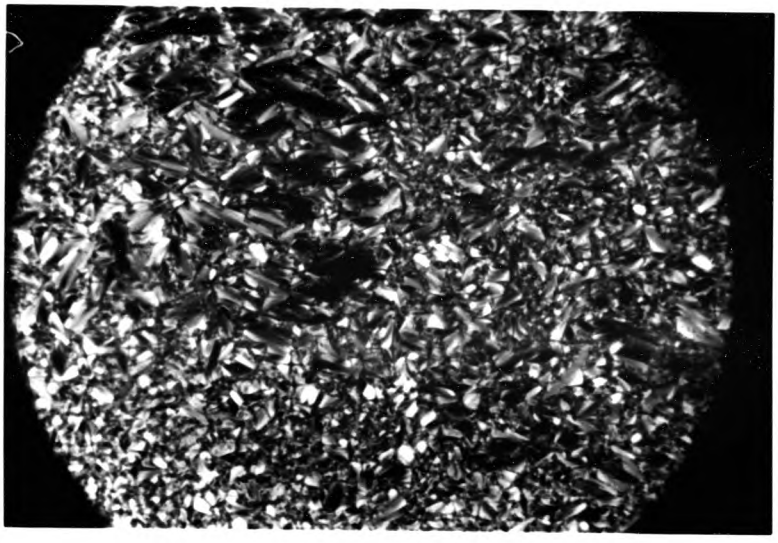

FIGURE 6.13 **Photomicrograph of the smectic A phase of copolymer 6a showing the fanned focal-conic domains (Magnification x 200).**

6.3.2.2 Thermal and textural behaviour of copolymers 6c-6e and homopolymer 6f.

In total contrast to the previously discussed polymers 6a and 6b, copolymers 6c and 6d exhibit only the chiral nematic phase. No ordered phases such as smectic or crystalline phases were detectable by either dsc or microscopy. Figure 6.14 shows the dsc heating traces of these copolymers, which show only the glass transition and an endotherm corresponding to the nematic to isotropic transition.

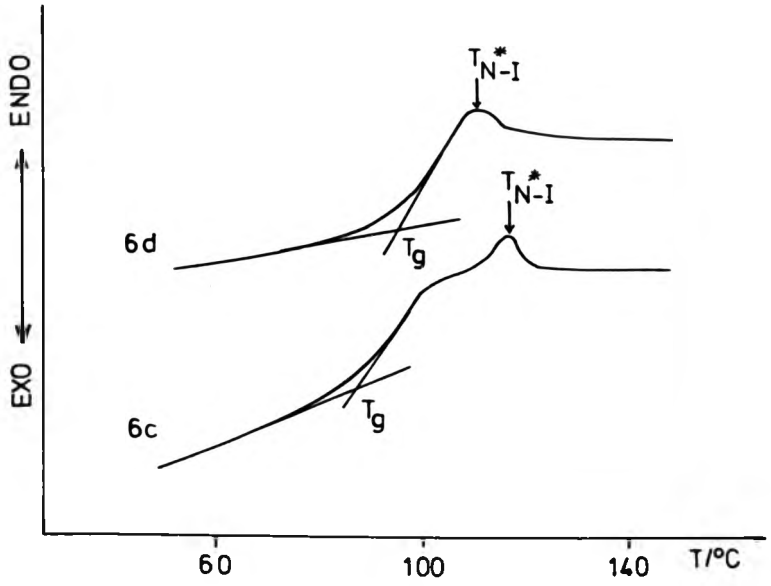

FIGURE 6.14 **Dsc heating traces of copolymers 6c and 6d recorded at 20°C/minute during the second heating scan.**

From the dsc heating trace of copolymer 6d, one can see that the endotherm associated with the chiral nematic to isotropic

transition is rather broad. This again may be due to polydispersity of the sample.[132] Unfortunately, any biphasic phenomena which could be associated with this broad transition were not easily detected by microscopy. In contrast to the similar dsc traces for polymers 5c-5f of the MBM* system, the magnitude of this endotherm could not be increased to any great extent either by slowly cooling or by annealing the samples. In other words, no enthalpic relaxation process was observable by dsc over the time-scale or temperature regions used for these thermal treatments. This contrast may be due to differing sample molecular weights, molecular weight distributions or differing interactions caused by the presence of the cyano rather than methoxy terminal groups on the chiral biphenyl.

The endothermic events shown by the dsc traces in figure 6.14 were easily correlated with hot-stage microscopy. These invetigations showed that both polymers formed the planar texture of the chiral nematic phase, although not spontaneously. Fairly long annealing times (~12 hours) were needed to produce the typical textures and the samples often needed to be sheared by sliding the cover-slips, in order to induce texture formation. The long annealing times are a consequence of the highly viscous nature of those polymers and the high probability of chain entanglements which impede mesogenic alignment.[33] Alignment is also impeded by the short, bulky spacer of the CBM* comonomers, which does not allow for the effective decoupling of the backbone from the pendant mesogenic units. Long annealing times therefore also allow the backbone enough time to attain a conformation suitable for the interaction of large numbers of these mesogenic side chains.[33,34]

The planar texture of copolymer 6c was found to reflect pale-blue light. No colour change was observed upon cooling the sample further, indicating that there was little change in the helical pitch length before the structure had frozen into the glass. As with the MBM*/DMBI-6 copolymers whose planar textures exhibited bright reflection colours, it was possible to prepare films of copolymer 6c which reflected pale-blue light against a dark background. This film was seen to be coloured yellow upon viewing white light through it. Films such as these were prepared by casting the polymer on a glass surface from its solution in chloroform, heating the film above T_{N^*-I} and allowing it to cool slowly, then annealing it at a temperature just below T_{N^*-I} for several hours before cooling. This film was seen to be tough and semi-transparent.

In contrast to copolymer 6c, copolymer 6d exhibited no bright reflection colours. This is due to the helical pitch length being so short that only u v light is reflected, which in turn is absorbed by the biphenyl groups in the film. A tighter helical pitch is expected for this copolymer since it contains a greater amount of the chiral monomer CBM*.[33,34,80] Again, this can be rationalised on the basis of the theories mentioned earlier where incorporation of greater amounts of the short spacer CBM* increases the hindered rotation of the mesogens in the polymer and therefore induces a greater helical twist.[11,12,13,155]

Copolymer 6e and homopolymer 6f (PCBM*) were both found to be non-mesomorphic. This is merely an effect of the chemical constitution of the CBM* monomer: the anisotropic interactions between the mesogens are not great enough to sustain liquid crystallinity.

6.3.2.3 General properties and trends associated with the CBM*/DMBI-6 copolymer system.

The phase transition temperatures of the CBM*/DMBI-6 copolymers (numbers 6a-6f) are displayed in figure 6.15 as a function of the mole fraction of CBM* in the copolymer. The general mesomorphic properties of these copolymers and the trends associated with them are discussed and compared with those of the MBM*/DMBI-6 system. The phase diagram corresponding to this system is displayed in figure 6.9.

As expected, the Tg values of the CBM* copolymers are seen to lie between those of the corresponding homopolymers and these values generally increase as the copolymers become richer in CBM*. This is of course due to the conformational mobility of the backbone becoming increasingly restricted as the more sterically hindered vinyl group of CBM* is incorporated. A "drop" in Tg of 11°C on going from polymer 6b ($F_{CBM*} = 0.47$) to polymer 6c ($F_{CBM*} = 0.62$) was seen to occur and is clearly associated with the disappearance of crystalline and smectic layered ordering in the system. The polymer backbone in these phases is known to lie between the ordered layers and is constrained to a conformation where the layered mesogens are arranged perpendicular to it.[34] This raises the Tg relative to the more disordered chiral nematic phase, where the backbone can more easily assume a disordered, statistical conformation. A similar drop in Tg was seen with the disappearance of the crystalline order in the MBM*/DMBI-6 system.

Again, the crystalline and smectic A phases were seen to disappear between $F_{CBM*} = 0.47$ (polymer 6b) and $F_{CBM*} = 0.62$ (polymer 6c). Obviously a critical point is reached between these

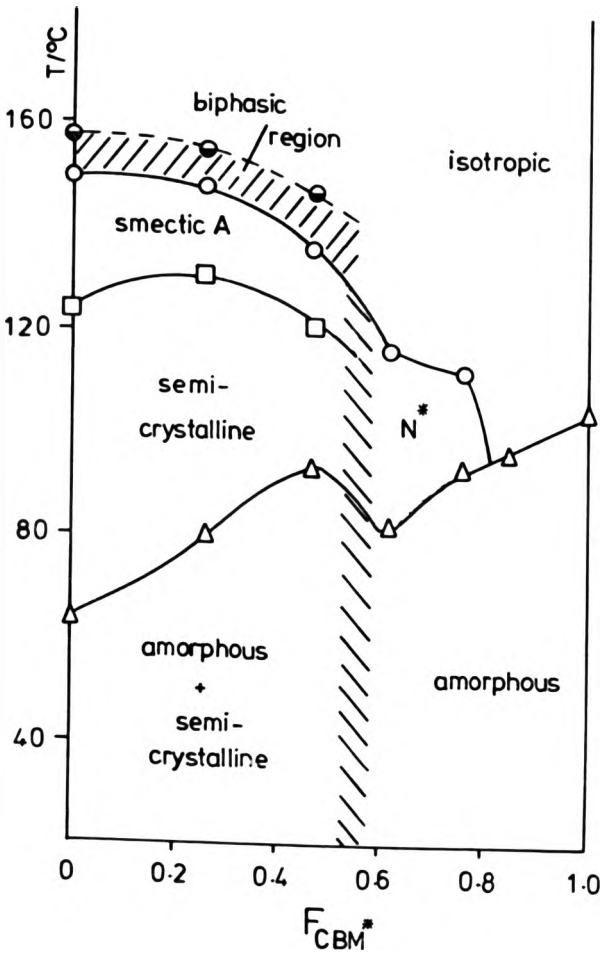

FIGURE 6.15 Plot of the phase transition temperatures (^{0}C) of CBM*/DMBI-6 copolymers versus the mole fraction of CBM* in the copolymer (F_{CBM*}). (Δ): Tg; (□): Tm; (O) T_{S_A}-S_A/I and T_{N*}-I(dsc); (●) T_{S_A}/I-I.

two composition values where the system becomes more disordered due to the proportion of CBM* monomers (which have short spacer lengths) in the copolymer. The effect of this disordering is also manifest in the thermal stability of the crystalline state and the thermal stability of the smectic A mesophase, which both decrease as the copolymers become richer in CBM*. This trend was also apparent in the MBM*/DMBI-6 system. It should be pointed out here whilst discussing the $T_{S_A\text{-}I}$ and $T_{k\text{-}S_A}$ transitions of these more ordered copolymers that their molecular weights are a little on the low side (copolymer 6a: $DP_n \sim 14$ and copolymer 6b: $DP_n \sim 27$). These molecular weights are in a region where the transition temperatures may still be temperature dependent.[33,34] It may be possible that the transition temperatures of the same copolymers (and homopolymer PDMBI-6) having increased molecular weights could in fact be higher. Unfortunately, time did not allow for the preparation of higher molecular weight polymers of similar composition.

In contrast to the MBM*/DMBI-6 system, no chiral nematic phases were observed for $F_{CBM*} < 0.6$. This infers that there may be a greater propensity for order in this system in the compositional region $F_{CBM*} < 0.6$. Although there is very little difference between the MBM* and CBM* copolymers except for the nature of the mesogen terminal grouping, it is conceivable that the cyano-terminated biphenyl of CBM* may interact with the methoxy-terminated biphenyl of DMBI-6 in an acceptor-donor fashion, within the smectic layers. These specific interactions may then lead to enhanced mesophase stability and ordering in the liquid crystalline state. In fact, Ringsdorf and Zentel have reported that on the

copolymerisation of methoxy-terminated and cyano-terminated monomers, they also found increased mesophase stability and the presence of a more ordered LC state.[34,158]

In general, it can be concluded that the two copolymer systems, namely MBM*/DMBI-6 and CBM*/DMBI-6, are fairly similar with the exception of those points mentioned above. Both systems show ordered smectic and crystalline phases at the DMBI-6-rich end of the phase diagram and chiral nematic phases at higher chiral monomer compositions. The helical structure of the chiral nematic phases of either system is seen to be rather short and the reflection of blue or ultraviolet light predominates.

By examining both the phase diagram of the CBM*/DMBI-6 copolymer series in figure 6.15 and the phase diagram of the MBM*/DMBI-6 copolymer series in figure 6.9, it is clear that wholly chiral nematic copolymers having no other phases cannot be prepared at compositions of less than $F_{CBM*} = 0.6$ or $F_{MBM*} = 0.65$. This is because of the tendency of the di-substituted DMBI-6 monomer to pack into layered structures.

In order that one could obtain chiral nematic copolymers at either $F_{CBM*} < 0.6$ or $F_{MBM*} < 0.65$ which would exhibit longer pitch lengths and therefore display longer wavelength reflection colours, another non-chiral nematogenic comonomer was sought. From the results reported in chapter 4, the ideal monomer for this purpose seemed to be CPBA-6. The use of this monomer as the non-chiral comonomer for copolymerisation with CBM* is discussed in the next section of this chapter.

6.4 Copolymers of CBM* and CPBA-6

As mentioned at the end of the previous section, there was a need to prepare and characterise chiral nematic LC copolymers whose compositions were relatively low in CBM* (i.e. F_{CBM*} <0.6), so that longer pitch chiral nematic materials exhibiting longer wavelength reflection colours could be produced. In an attempt to obtain such materials copolymers of CBM* and CPBA-6 were prepared and analysed. It was envisaged that the use of a nematogenic monomer such as CPBA-6 would, in principle, alleviate the problem of the appearance of layered LC phases which were prevalent at low chiral compositions in both the MBM*/DMBI-6 and CBM*/DMBI-6 copolymer systems.

6.4.1 Mesomorphic properties of CBM*/CPBA-6 copolymers.

The composition of the copolymers prepared from CBM* and CPBA-6 could not be measured since only small amounts of these copolymers were obtained at the low conversion values required. The results presented in this section are therefore discussed in terms of the monomer feed only. The availability of only small amounts of sample meant that molecular weight measurement was difficult, however, a large enough sample of one of the copolymers (7d, f_{CBM*} = 0.50) was prepared which allowed measurement of its molecular weight and this was taken to be representative of the series. The molecular weight of this polymer was found to be 72,000 $gmol^{-1}$ and the molecular weights of the homopolymers PCPBA-6 and PCBM* were found to be 65,000 $gmol^{-1}$ (DP_n ~165) and 200,000 $gmol^{-1}$ (DP_n ~620) respectively.

It would thus seem reasonable to assume that the molecular

weights of the remaining copolymers are also fairly high and that they are probably in excess of 10,000 $gmol^{-1}$. This means that their mesomorphic properties should not be too dependent on their chain lengths[39,126] and so valid comparisons between the properties of each copolymer can be made.

The phase transition temperatures of the CBM*/CPBA-6 copolymers are tabulated in table 6.3 and displayed graphically in figure 6.17 as a function of the monomer feed. From both dsc and hot-stage polarising microscopy analysis, each of the copolymers was found to exhibit the chiral nematic phase only. Their thermal and textural characteristics are discussed below.

6.4.1.1 Thermal behaviour of CBM*/ CPBA-6 copolymers.

As has just been mentioned, the mesomorphic behaviour of all of the copolymers prepared was found to be the same. This resulted in the dsc traces of these polymers being very similar, with each trace exhibiting only a glass transition and an endothermic event. From microscopy studies this endotherm was found to be associated with the chiral nematic to isotropic transition as expected. Figure 6.16 shows the dsc heating and cooling traces of copolymer 7a. These are typical of the traces obtained for the other copolymers. From these dsc traces a supercooling of the isotropic to chiral nematic phase transition by 7°C was found to occur. This is similar to the results obtained for the MBM*/DMBI-6 and CBM*/DMBI-6 systems, and from other sources.[91]

As with all of the other copolymers studied in this work, a stable mesophase/isotropic liquid biphasic region was found to exist over a finite temperature range. From microscopy, the onset of this

TABLE 6.3 The phase transition temperatures of CBM*/CPBA-6 copolymers[a]

Copolymer Number	f_{CBM*}	Tg/^oC	T_{N*-I}(dsc)/^oC[b]	T_{N*-I}(hsm)/^oC[b,c]	Colour of reflected light against a dark background
3a	0.00	37	(126)[b]	(130)[b]	
7a	0.10	44	111	120	pink/red
7b	0.15	52	112	120	turquoise/blue
7c	0.25	44	105	108	pale-blue
7d	0.50	100	112	115	
7e	0.75	97	119	125	
6f	1.00	105	-	-	

a - All phase transition temperatures were measured by dsc during the second heating scan, at a rate of 20^{o}C/minute.

b - This temperature corresponds to the nematic to isotropic transition in the case of PCPBA-6.

c - T_{N*-I}(hsm) refers to the temperature at which birefringence disappears totally, during the microscopy experiment.

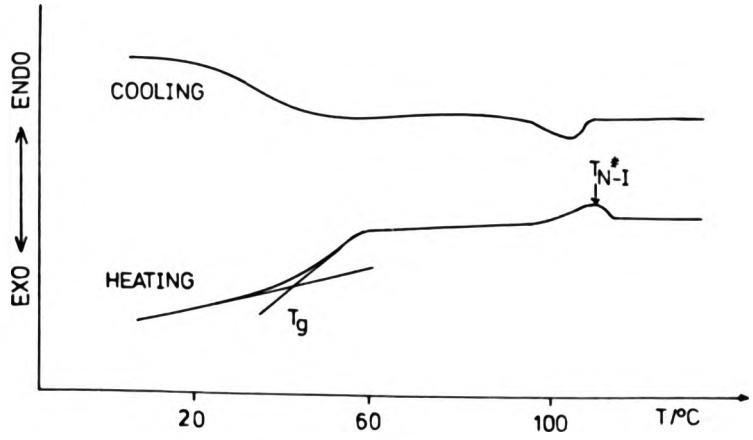

FIGURE 6.16 **Dsc heating and cooling traces of copolymer 7a (f_{CBM*} = 0.10) recorded at 20°C/minute. The heating trace was recorded during the second heating scan.**

phenomenon was seen to correspond with the maximum of the chiral nematic to isotropic endotherm on each dsc trace. The width of the biphasic region for each of the copolymers 7a-7e (see table 6.3 and figure 6.17) can be seen to exist over a fairly narrow range which varies between 3°C and 9°C. These widths appear to be much narrower than those of some of the other copolymers examined in this work (compare polymer 4d, chapter 5, which has a biphasic temperature interval of 17°C) and they may indicate narrower molecular weight distributions for these copolymer samples.[132]

6.4.1.2 Textural and optical behaviour of CBM*/CPBA-6 copolymers.

Polarising microscopy studies carried out on copolymers 7a,

7b and 7c revealed the presence of typical, brightly coloured, planar chiral nematic textures. Similarly, solvent-cast films of each of these polymers were also seen to exhibit these fairly bright reflection colours (see tables 6.3 and 6.4) after appropriate thermal treatment. This treatment generally consisted of heating the solvent-cast film (the casting solvent for these polymers was dichloromethane) up to T_{N^*-I} + 20°C, cooling it slowly to T_{I-N^*} - 10°C and then annealing it at this temperature for several hours (2-4 hours). Bright colours were observed to form almost immediately, then change slowly over 10-15 minutes to the colour eventually preserved after the annealing process. This colour change is consistent with the helical pitch length adjusting itself to an equilibrium value for the annealing temperature used and it occurs slowly since it involves changes in both backbone and side chain conformation.[33,76] The final colours obtained were easily retained by cooling the films quickly below Tg. It is interesting to note that even when cooling these films slowly from the annealing temperature, the reflection colour did not change. This infers that the helical pitch in this system is not temperature dependent to any great extent, unlike the cholesteric polymers described in chapter 5. Similar observations were also made from the microscopic textural behaviour of each copolymer sample. The reflection colours from these samples were best observed when they were viewed against a dark background at oblique angles, and when viewing white light through these samples bright transmission colours were also seen. These are noted along with the observed reflection colours in table 6.4, below:

TABLE 6.4 Reflection and transmission colours observed from polymers 7a, 7b and 7c.

Copolymer number	f_{CBM*}	Reflection colour[a]	"Transmission colour"[b]
7a	0.10	pink/red	pale-blue
7b	0.15	turquoise/blue	pink
7c	0.25	pale-blue	yellow

a - Reflection colour was observed by placing the sample against a dark background.

b - "Transmission" colour was observed when viewing white light through the sample.

The planar chiral neamtic textures of polymers 7d and 7e were not seen to exhibit any bright reflection colours. This is most likely due to the reflected light being in the u v region of the spectrum. The textures observed were, however, typical of the chiral nematic phase.[96]

6.4.2 General properties and trends associated with the CBM*/CPBA-6 copolymer system.

The phase transition temperatures of the CBM*/CPBA-6 copolymers are displayed in figure 6.17 as a function of the monomer feed. It must be remembered at this point that the copolymer composition is not known and that the composition may be quite different from the initial monomer feed ratios. This means that the phase transition temperatures may be displaced to either

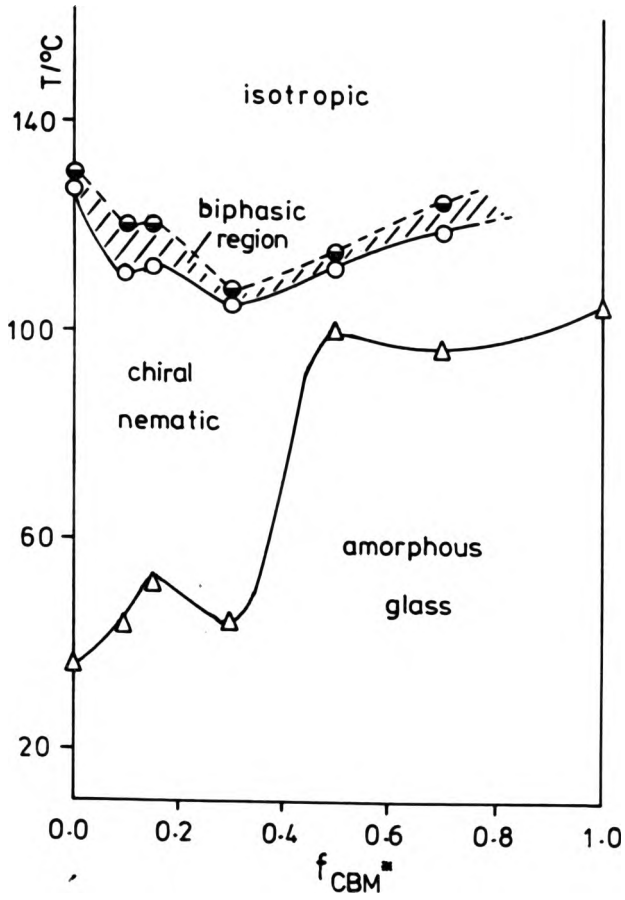

FIGURE 6.17 **Plot of the phase transition temperatures (^oC) of the CBM*/CPBA-6 copolymers versus the mole fraction of CBM* in the monomer feed (f_{CBM*}).**
(Δ): Tg; (O): T_{N*-I} (dsc) (or T_{N-I} in the case of PCPBA-6); (⊖): T_{N*-I} (hsm).

the right or the left if the feed axis referred instead to copolymer composition.

As expected, the Tg values of the copolymers were seen to lie between the Tg values of the respective homopolymers. An unexpected drop in the Tg value on going from copolymer 7b (f_{CBM*} = 0.15 to copolymer 7c (f_{CBM*} = 0.25) was observed, however. This behaviour is rather odd, since a drop in the Tg of this magnitude usually indicates a change in phase.[33] From microscopy and dsc studies no phases other than the chiral nematic phase were seen to be present. Several other reasons may also explain this "drop" in Tg. For example, polymer 7c may have a much lower molecular weight than polymer 7b, or it may have a much broader molecular weight distribution incorporating various low molecular weight oligomeric species. The latter reason is unlikely however, since the repeated precipitation process would have sufficiently fractionated the sample into a narrower distribution of molecular weights. As stated earlier, the narrow width of the biphasic region actually implies a narrower molecular weight distribution in this case. A drop in the Tg such as this may also be caused by the presence of some impurities that were not removed during the precipitation process. The nature of these impurities, if there are any present, is not known since both tlc and ^1H nmr analyses indicated the presence of the polymer only. The reasons cited above may also explain the observation that the drop in Tg is acompanied by a drop in T_{N*-I} of about the same magnitude. It is important to stress that without knowing either the molecular weights or the molecular weight distribution of these polymers one can only speculate on the reasons for unexpected trend deviations. Also, these comments on the observed trends are

equally limited by the fact that one is always referring to feed compositions and not to the actual copolymer compositions.

The clearing temperature of the copolymers was seen to fall as the copolymers became richer in CBM* then increase again above $f_{CBM*} = 0.3$. The fall in the clearing temperature is of course due to the disruption caused by the introduction of CBM* with its shorter spacer length, as discussed in sections 6.2 and 6.3. The fall on going to copolymer 7c may also be, in part, due to a difference in the molecular weight of the copolymers, as discussed earlier. The increase in T_{N*-I} after further incorporation of CBM* may again be due to lengthening sequences of CBM* monomer units stabilising the mesophase. This behaviour has also been discussed in sections 6.2 and 6.3 with respect to the DMBI-6-containing systems.

In comparison with the two previously discussed systems, MBM*/DMBI-6 and CBM*/DMBI-6, bright reflection colours were observed at low chiral monomer compositions since CPBA-6 tends to promote nematic (and hence chiral nematic) instead of smectic or crystalline behaviour. Thus, reflection colours other than blue were observed, with copolymers 7a and 7b reflecting pink/red and turquoise/blue light respectively. As one would expect, the wavelength of reflected light (and hence the pitch length) was seen to decrease as the amount of CBM* in the copolymer was increased. Again this may be attributed to the increasingly hindered rotations of the chiral CBM* mesogens. Unfortunately, as with the previously discussed systems, copolymers rich in CBM* were not seen to reflect light in the visible region of the spectrum. This is primarily due to the use of very short chiral spacers which must severely hinder the rotation of the chiral mesogens about their long axes, especially at such high concentrations of chiral monomer. In an attempt to obtain

a series of chiral nematic copolymers which would exhibit a complete range of reflection colours over a whole range of compositions, the series of copolymers described in the next section of this chapter were prepared. These are based on a monomer having a longer chiral spacer, namely XMBM*.

6.5 Copolymers of XMBM* and CPBA-6

With the copolymers prepared in this section, an attempt was made to ascertain the effect of increasing the length of the chiral spacer on the mesomorphic properties of the copolymers. XMBM*, a longer spacer analogue of MBM* was therefore chosen as a comonomer for the nematogenic monomer CPBA-6. The structure of XMBM* is shown at the beginning of this chapter.

By using the longer spacer length it was anticipated that the long-axis rotation of the chiral mesogens of XMBM* should be less hindered, on the basis of the theories and results discussed in section 6.2. Less hindered rotation should result in copolymers having longer pitch lengths which will cause them to exhibit a wider range of reflection colours. In this system CPBA-6 was again chosen as the nematogenic monomer since it fosters chiral nematic phase formation at low chiral component compositions, as was shown previously.

6.5.1 Copolymerisation characteristics of XMBM* and CPBA-6.

As with the other combination of acrylate- and methacrylate-based copolymers presented in this thesis (CPBA-6 with MMMP*), the copolymerisation behaviour was seen to deviate substantially from "ideality". This behaviour is shown by the copolymerisation curve in figure 6.18 which was drawn from the data tabulated in table 3.8, chapter 3.

The deviation from ideality is due to the greater reactivity of the methacrylate monomer XMBM* ($r_{XMBM*} = \overset{1.57}{\cancel{0.12}}$). 145 Again, this would tend to suggest that moderately long sequences of XMBM* are formed during the copolymerisation. The reasons for the increased

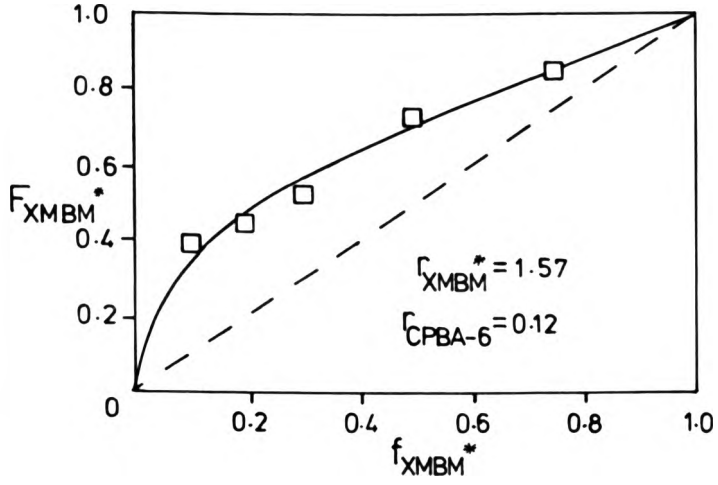

FIGURE 6.18 **A plot of the mole fraction of XMBM* in the copolymer (F_{XMBM*}) versus the mole fraction of XMBM* in the monomer feed (f_{XMBM*}) and the corresponding reactivity ratios for each monomer.**
(□): Experimental point.
(——): Calculated best fit to experimental data.

reactivity of XMBM* relative to CPBA-6 will be the same as those discussed in section 4.4.1 for the CPBA-6/MMMP* system, since the polymerisable vinyl groups are identical in each case. The nature of the side chain of XMBM* is also the same as that of MMMP* in the vicinity of the double bond, therefore the polarity and electronic nature of these groupings and their effects of the vinyl moiety and its polymerisation, should be similar.

6.5.2 Mesomorphic properties of XMBM*/CPBA-6 copolymers.

The molecular weights of each of the homopolymers and one of the copolymers (as a representative of the other copolymers in the system) were determined. These were found to be 65,000 (DP_n = 165) for PCPBA-6, ~153,000 (DP_n ~409) for copolymer 8d (F_{XMBM*} = 0.73) and 60,400 (DP_n = 163) for PXMBM*. These molecular weights are well above the region where the mesomorphic properties of the polymers are molecular weight dependent.[34,126] It is highly likely that the molecular weights of the remaining copolymers are also of this magnitude, therefore valid comparisons of their properties should be possible. The phase transition temperatures of these copolymers are tabulated in table 6.5 and are displayed graphically in figure 6.24 as a function of the copolymer composition. These results are discussed below.

6.5.2.1 Thermal and textural behaviour of copolymers 8a-8d.

Copolymers 8a - 8d were all seen to form the chiral nematic phase only, from dsc and microscopy experiments. Figure 6.19 shows the dsc heating and cooling traces of copolymer 8a which are typical of these copolymers.

As with the previously discussed copolymer systems, a biphasic chiral nematic/isotropic region is apparent. Again, the appearance of this region was seen to coincide with the chiral nematic to isotropic transition as measured by the dsc. Similarly, the upper limit of this biphasic region was determined by microscopy as the temperature at which birefringence disappeared.

TABLE 6.5 The phase transition temperatures of XMBM*/CPBA-6 copolymers[a]

Copolymer Number	F_{XMBM*}	Tg/°C	T_m/°C	T_{N*-I}(dsc)/°C[b]	T_{N*-I}(hsm)/°C[b]	Remarks
3a	0.00	37	-	(126)[b]	(130)[b]	marbled nematic texture
8a	0.39	35	-	107	115	Temperature dependent pitch
8b	0.45	35	-	98	110	Temperature dependent pitch
8c	0.53	40	-	86	100	Temperature dependent pitch
8d	0.73	51	-	106	112	Temperature dependent pitch
8e	0.85	-	122	-	-	Highly crystalline polymer
8f	1.00	-	130	-	-	Highly crystalline polymer

a. All phase transition temperatures were measured by dsc during the second heating scan, at a rate of 20°C/minute.

b. This temperature corresponds to the nematic to isotropic transition in the case of PCPBA-6.

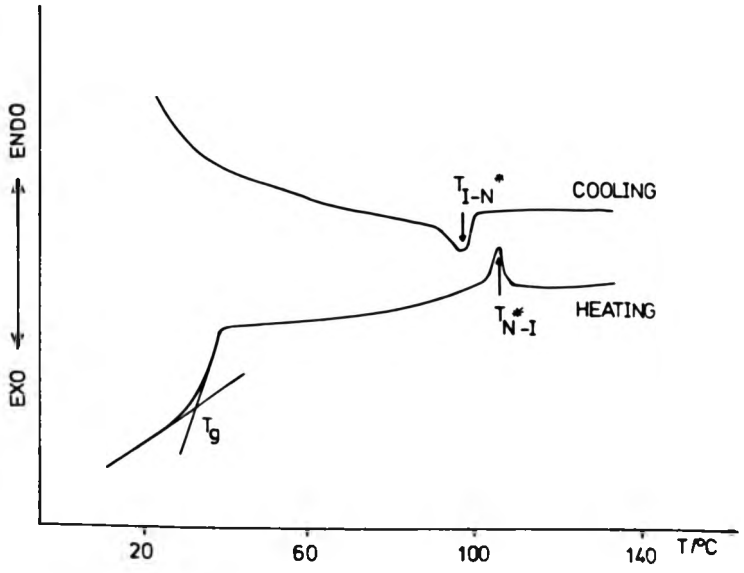

FIGURE 6.19 **Dsc heating and cooling traces of copolymer 8a recorded at 20°C/minute. The heating trace was recorded during the second heating scan.**

The existence of the biphasic phenomena merely indicates, as usual, that these copolymers are polydisperse in nature.[132]

Hot-stage polarising microscopy studies conducted on the chiral nematic phase of polymers 8a-8d indicated the presence of a temperature dependent helical pitch in each case, as the reflection colours exhibited by their homogeneous planar textures were seen to change from blue to orange or red upon cooling. Polymer 8a was observed to form a pale-blue planar texture on cooling the isotropic liquid to about 104°C. This texture is shown in the photomicrograph displayed in figure 6.20(a). After annealing this phase for forty

minutes at 104°C, in order to remove defects and improve the texture,[33] the reflection colour was observed to have changed into a deeper blue colour, as figure 6.20(b) shows. The temperature was then reduced slowly, and the reflection colours were seen to change firstly to yellow at about 96°C (as shown by figure 6.20(c)), then to an orange colour at 74°C (figure 6.20(d)) and finally to a pink/red colour at about 50°C (figure 6.20(e)). This colour remained, even when the sample was cooled below Tg. On reheating the sample, the same colour changes were seen to take place except in reverse order. A temperature dependent pitch such as this, where the pitch length increases on cooling the sample has already been presented and discussed in section 5.1.2.1, chapter 5, for the ChMI-10/CPBA-6 system. As was stated in chapter 5 this is the most commonly observed type of temperature dependence in the case of comb-branch chiral nematic polymers[39] and it can be rationalised in terms of there being a decrease in the molar volume associated with the molecules as the temperature falls, which causes the displacement angle between adjacent molecules to decrease and hence the pitch to lengthen. This is discussed in more detail in section 5.1.2.1.

Copolymers 8b and 8c show similar textural colour changes to those described above, with the blue reflection colour always appearing at about $T_{I\text{-}N^*}$ -5°C. This indicates that the helical pitch length does not seem to be too drastically affected by the copolymer composition in contrast to the previously discussed copolymer systems. The possible reason for such behaviour will be discussed later in section 6.5.3. The textural reflection colours observed for copolymers 8b and 8c at various temperatures are displayed by the photomicrographs in figures 6.21(a) and (b) and 6.22(a), (b) and (c) respectively.

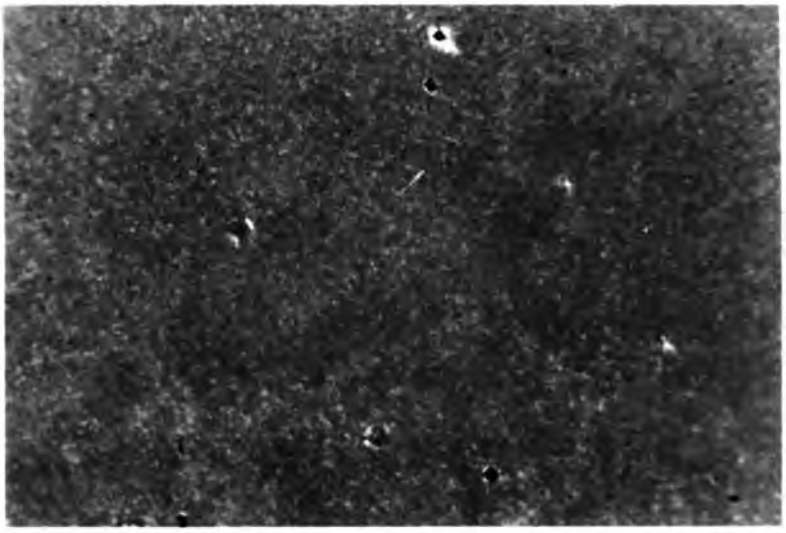

FIGURE 6.20 (a) Photomicrograph of the planar texture of copolymer 8a at 104°C exhibiting the reflection of pale-blue light (Magnification x 200).

FIGURE 6.20 (b) Photomicrograph of the planar texture of copolymer 8a at 104°C exhibiting the reflection of deep-blue light (Magnification x 200). (Photomicrograph taken after annealing the texture in figure 6.20(a) for 40 minutes.)

FIGURE 6.20 (c) Photomicrograph of the planar texture of copolymer 8a at 96°C exhibiting the reflection of yellow light (Magnification x 200).

FIGURE 6.20 (d) Photomicrograph of the planar texture of copolymer 8a at 74°C exhibiting the reflection of yellow/orange light (Magnification x 200).

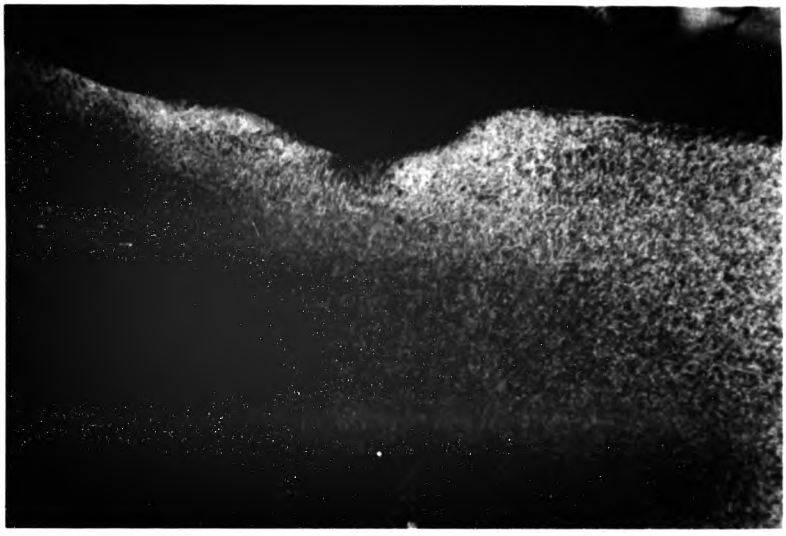

FIGURE 6.20 **(e) Photomicrograph of the planar texture of copolymer 8a at about 50°C exhibiting the reflection of pink/red light (Magnification x 200).**

FIGURE 6.21 (a) Photomicrograph of the planar texture of copolymer 8b at 90°C exhibiting the reflection of blue light (Magnification x 100).

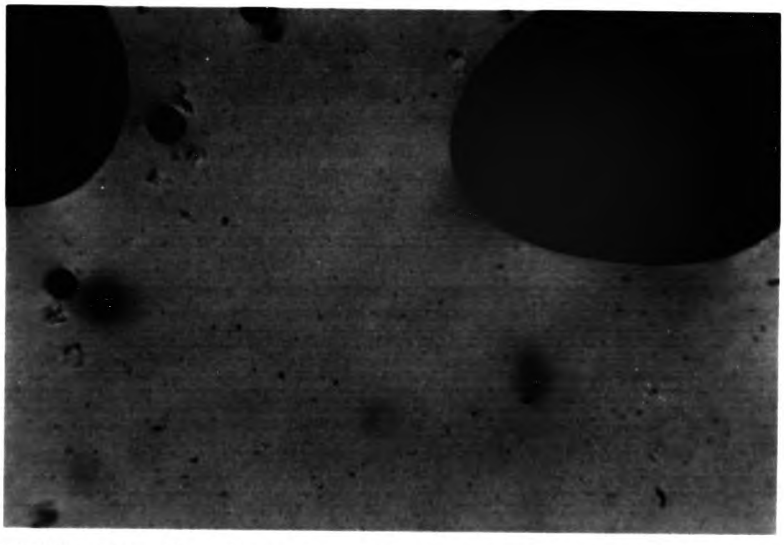

FIGURE 6.21 (b) Photomicrograph of the planar texture of copolymer 8b at 30°C exhibiting the reflection of yellow light (Magnification x 100).

FIGURE 6.22 (a) Photomicrograph of the planar texture of copolymer 8c at 83°C exhibiting the reflection of blue light (Magnification x 100).

FIGURE 6.22 (b) Photomicrograph of the planar texture of copolymer 8c at 76°C exhibiting a change in reflection colour between blue and yellow light (Magnification x 100).

FIGURE 6.22 **(c) Photomicrograph of the planar texture of copolymer 8c at about 57^{o}C exhibiting the reflection of yellow/orange light (Magnification x 200).**

Similar to the previously described copolymers, copolymer 8d also shows a temperature dependent pitch. However, in the case of this polymer, the pitch seems to change at a much higher temperature: On cooling the isotropic melt the chiral nematic texture which separates starts to reflect pale-blue light at about 102°C; further cooling results in an orange-like reflection colour at 88°C and an orange/red colour at 78°C. Unfortunately, no explanation can be given at present as to why the pitch changes at higher temperatures than in the other copolymers, especially in the absence of any smectic phases (as shown by dsc) which would cause pre-transitional effects. Clearly a much more detailed investigation of the chiral nematic phase exhibited by this copolymer must be conducted before any conclusions can be drawn as to the reasons for this seemingly premature unwinding of the helix.

6.5.2.2 Thermal and textural behaviour of copolymer 8e and homopolymer 8f (P_{XMBM*}).

Dsc and microscopy investigations of polymers 8e and 8f revealed the presence of highly ordered, crystalline phases and no liquid crystalline phases. In addition, the glass transitions of both polymers could not be detected by dsc, suggesting that their crystalline regions must be very extensive indeed. Although the Tg of these polymers cannot be detected by dsc, a technique such as dilatometry might help to identify this transition which has only a small change in heat capacity associated with it. The crystallinity in these polymers arises from the interactions of the side chains only, as has been shown by various workers in the past who studied similar systems.[94] The dsc heating and cooling traces of these polymers are shown in figure 6.23 below.

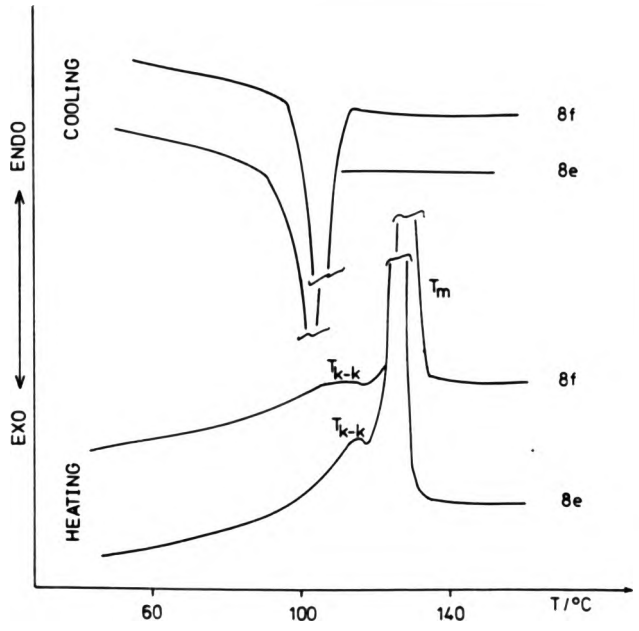

FIGURE 6.23 **Dsc heating and cooling traces of copolymer 8e and homopolymer 8f (PXMBM*) recorded at a rate of 20°C/minute. The heating traces were recorded during the second scan.**

From the dsc heating traces shown in figure 6.23 it can be seen that there are endothermic events below Tm. These most likely correspond to crystal-crystal transitions which arise from there being more than one structural modification of the crystalline phase. Obviously X-ray diffraction studies would be required in order to confirm this observation. Extensive supercooling of the crystal-isotropic transition is also noticeable from the dsc heating and cooling traces and this is expected for such crystalline transitions.[91]

6.5.3 General properties and trends associated with the XMBM*/CPBA-6 system.

The general trends of the phase transition temperatures of the XMBM*/CPBA-6 copolymer system are displayed graphically in figure 6.24 as a function of copolymer composition.

The Tg values of the copolymers in the XMBM*/CPBA-6 phase diagram are seen to increase smoothly on the incorporation of XMBM*, as one would expect. At about $F_{XMBM*} > 0.8$ however, the Tg of the copolymers is seen to disappear, with the Tg being replaced by crystalline melting transitions in copolymer 8e and homopolymer 8f. This drastic change is also accompanied by a total disappearance of mesomorphism. These results are surprising since there is no obvious hint of the system becoming more ordered prior to this. One would usually expect the smectic and crystalline phases to become apparent as F_{XMBM*} increases and tends towards $F_{XMBM*} \sim 0.8$, as was exhibited by the DMBI-6-containing copolymer systems in previous sections.

T_{N*-I}, the chiral nematic mesophase thermal stability, is seen to decrease at first and then increase again after about $F_{XMBM*} = 0.55$. This initial decrease can only be attributed to the incorporation of increasing amounts of XMBM* which has a relatively lower inherent mesophase thermal stability than CPBA-6. This becomes obvious when one compares their respective homopolymers - PCPBA-6 is liquid crystalline whilst PXMBM* does not show any mesomorphic properties, even although it contains elements of mesogenic structure. The presence of the branching chiral-methyl group of XMBM* will also tend to reduce anisotropic interactions between the copolymer mesogens. The increase in T_{N*-I} after $F_{XMBM*} = 0.55$ is much harder to explain however. It may be partly explained by the polymer backbone becoming much stiffer due to the larger numbers of methacrylate units

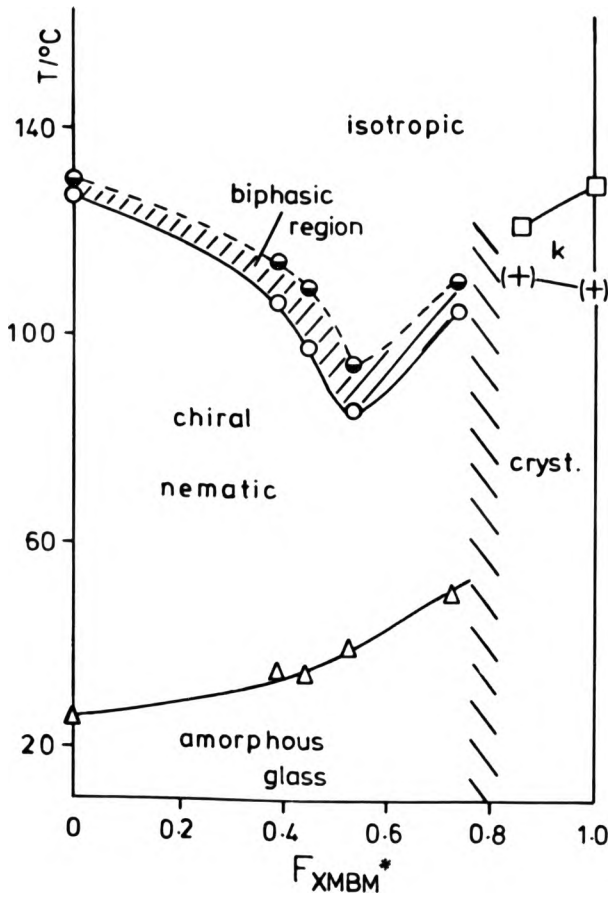

FIGURE 6.24 **Plot of the phase transition temperatures (^{o}C) of the XMBM*/CPBA-6 copolymers versus the mole fraction of XMBM* in the copolymer (F_{XMBM*}).**

(Δ): Tg; (O): T_{N*-I}(dsc); (●): T_{N*-I}(hsm); (□): Tm; ((+)): T_{k-k}.

present. This will tend to encourage mesogenic packing to some degree which is then reflected in the higher T_{N^*-I} values. Results such as these are well known in comb-branched PLC systems as has been demonstrated by Finkelmann and Rehage.[33] These workers examined the effect of changing the nature of the polymer backbone of a comb-branch mesogenic material and they showed that the mesophase thermal stability as well as the Tg of the polymer decreased as the backbone became more flexible. They also observed no change in the mesophase type.

As mentioned in section 6.5.2.1, the textural behaviour of the chiral nematic polymers 8a-8d is different to that exhibited by the copolymer systems having shorter chiral spacer lengths. In the case of polymers 8a-8d there appears to be very little change in the reflection colour at T_{I-N^*} -5°C with increasing XMBM* composition, with each of these copolymers reflecting blue light at this temperature. This indicates that the helical pitch length does not depend too strongly on the copolymer composition in this system, in contrast to the shorter spacer MBM* and CBM* systems. This reduction in the composition dependence of the pitch can be rationalised in terms of the hindered rotation model discussed earlier. The longer spacer length of XMBM* causes the long-axis rotation of its mesogenic group to be less hindered than in the case of MBM*, since the effect of the mesogen being covalently linked to the polymer backbone is alleviated to a greater extent with XMBM*. This will cause the XMBM* monomer to have a decreased helical twisting power (relative to MBM*), which will tend towards the un-bound, conventional low molecular weight nematic/chiral nematic mixture situation. Such conventional mixtures

(with some exceptions) are known to have low helical twisting powers in comparison to some previously reported chiral nematic copolymer systems, such as those prepared by Finkelmann and co-workers.[76] Because of the reduced helical twisting power of XMBM*, it will have a much smaller effect on the helical pitch length when it is incorporated in a copolymer structure, even when large amounts of it are present. Considerations such as these should result in a less composition-dependent pitch as was actually observed. Similar results were also obtained by Finkelmann and Rehage[76] who arrived at similar conclusions. These workers studied the system described earlier in section 6.2.2.4 and they found that as the length of the non-chiral mesogenic spacer was increased from 3 to 6 carbons, the helical twisting power of the cholesteryl derivative was decreased and consequently the helical pitch was seen to become less composition dependent.

6.6 Conclusions.

The results presented in this chapter demonstrate that chiral mesogenic monomers having the chiral centre in the flexible spacer part of the molecule can be prepared from (S)-ethyl lactate in reasonable yields, and that when these novel monomers are copolymerised with non-chiral mesogenic monomers, chiral nematic phases result. The general findings from these copolymersiation results are summarised below.

It was noted that the copolymers prepared from both MBM* and CBM* and DMBI-6 exhibited chiral nematic phases with short helical pitch lengths. This was manifest in the appearance of only blue, violet or possibly ultra violet reflection colours from these phases. The tight helical pitch induced by these chiral monomers can be explained by the hindered rotation model proposed by Goosens,[11,155] Vertogen[12] and Finkelmann and Stegemeyer.[13] This model implies that the short spacer length of MBM* and CBM* should cause the long-axis rotation of their mesogenic groups to be severely hindered, thus giving rise to the observed short helical pitch lengths. Limited evidence has also been presented which suggests that one of the MBM*/DMBI-6 copolymers may in fact exhibit a biaxial chiral nematic phase. This suggestion would seem reasonable since, on the basis of the aforementioned model, an element of molecular biaxiality must be assumed if one is to consider hindered rotation.

Both copolymers of MBM* with DMBI-6 and CBM* with DMBI-6 having compositions of less than 60% chiral monomer were found to exhibit layered smectic and crystalline phases. This was found to be due to the smectogenic nature of DMBI-6.

Copolymers of CBM* with CPBA-6 on the other hand were found

to exhibit only chiral nematic phases, with those having low CBM* feed values exhibiting the reflection of pink/red, turquoise/blue and pale blue light. Similar to the previously mentioned DMBI-6 chiral nematic copolymers, no reflection colours were observed at higher CBM* feed values, with the wavelength of reflection being in the ultraviolet region of the spectrum. This again indicates the expected short helical pitch lengths. Furthermore, the helical pitch in this system was seen to be virtually temperature independent.

Copolymers prepared from the longer chiral spacer monomer XMBM* with CPBA-6 were also found to form chiral nematic phases. In contrast to the previous systems however, the pitch lengths of each of these copolymers were found to be temperature dependent, with a range of reflection colours being exhibited in each case. By comparing the reflection colour of each copolymer at a reduced temperature very little change was detected. This again can be explained by the hindered rotation model which implies that chiral monomers with longer spacer lengths should have a weaker helical twisting power.

Finally, it has been demonstrated in this chapter that brightly-coloured plastic films could be produced from each of the copolymer systems and that in some cases the reflection colour could be varied by either changing the copolymer composition or the annealing temperature used, prior to quenching (or cooling).

CHAPTER SEVEN
GENERAL CONCLUSIONS AND SUGGESTIONS FOR FURTHER WORK

7. GENERAL CONCLUSIONS AND SUGGESTIONS FOR FURTHER WORK

From the results presented in this thesis, several main features were identified with respect to the preparation of comb-branch chiral nematic (cholesteric) LC copolymers. These are summarised below.

It was found that induced chiral nematic phases that reflect visible light could not be produced (at least with the systems studied here) by the simple copolymerisation of chiral non-mesogenic monomers with achiral mesogenic monomers. Smectic and crystalline phases were found to result when the mesogenic monomer employed was smectogenic in nature and phases which appeared to be of the nematic type were found to result when the mesogenic monomer employed was nematogenic in nature. The LC phases formed by the DMBI-6 copolymers were found to be of a more ordered nature than the LC phase formed by the homopolymer PDMBI-6. This was thought to be due to a relief of the steric crowding associated with the biphenyl side chains of the itaconate mesogenic monomer. With the latter type of copolymer, that is those containing the nematogenic and chiral monomers CPBA-6 and MMMP* respectively, the apparent absence of any induced helical twist has been attributed to the non-planar structure of MMMP* and its low rotational strength. This is in accordance with the theories advanced by Goosens,[11] Vertogen[12] and Finkelmann and Stegemeyer[13] which explain the induced helical twist in terms of the hindered rotation of the chiral molecules around their long molecular axes and their level of asymmetry. Without further work it was

difficult to interpret whether these apparent nematic phases were in fact chiral nematic phases of very long pitch length.

With the CPBA-6 and MMMP* copolymers, crosslinking was found to occur when the polymerisations were allowed to run to high conversion. One of these crosslinked copolymers was studied. The crosslinked copolymer (3x) was found to exhibit thermo-elastic and photo-elastic behaviour in both the nematic and isotropic states. The general properties of this LC elastomer were found to be similar to those of some previously reported LC elastomers. It is thought that crosslinking occurs via the side chain of MMMP*.

The use of the itaconate-based mono-cholesteryl monomer ChMI-10 as the chiral "dopant" monomer was found to offer a reasonable alternative to the use of the ubiquitous acrylate and methacrylate derivatives. Copolymers prepared from ChMI-10 and CPBA-6 formed cholesteric (chiral nematic) phases whose planar textures were found to reflect visible light. The wavelength of reflection was found to be dependent on both the sample temperature and the copolymer composition, with it being seen to decrease with both increasing temperature and mole fraction of ChMI-10.

The incorporation of a chiral centre into the flexible spacer of a mesogenic monomer and its subsequent polymerisation with either smectogenic or nematogenic comonomers resulted in copolymers whose chiral nematic phases exhibited bright reflection colours. These colours and other liquid crystalline properties were found to be dependent upon the length of the chiral spacer.

When the chiral spacer was short (e.g. with MBM* and CBM*) the reflection colour was seen to be independent of temperature but

dependent on the copolymer composition. The colours were observed to change to shorter wavelengths as the copolymers became richer in the chiral component and the predominant colour observed was blue. In addition, one of the copolymers of MBM* with DMBI-6 was found to display a chiral nematic texture which suggested that the phase may be biaxial in nature. These results may be explained by the hindered rotation model proposed by Goosens, Vertogen and Finkelmann and Stegemeyer.

When the spacer length was long, as in the case of the XMBM*/CPBA-6 copolymer system, the reflection colours were seen to be temperature dependent with the wavelength decreasing with increasing temperature. Furthermore, the wavelength was seen to be virtually independent of copolymer composition. These features were also explained in terms of the hindered rotation model.

Finally, it was found that the reflection colours exhibited by these materials could, in most cases, be retained in the glassy matrix by rapidly cooling the sample from the appropriate temperature to below Tg. This resulted in the production of tough, brightly coloured plastic films.

From the results presented in this thesis, there are a number of areas where suggestions can be made for further work and it is felt that one of the main areas where this work should be concentrated is on the chiral spacer approach to chiral nematic materials. From the results reported here it is clear that more work needs to be done in both optimising the structural characteristics of the monomers and characterising them more fully, so that a series of well-defined, easily tunable coloured materials can be realised. Some suggestions for further work are outlined below.

Since there appears to be a large difference in the properties of

the copolymers with different spacer lengths, it would seem pertinent to start by assessing the effect of spacer length on both the temperature and composition dependence, and on the helical pitch length. The distance of the chiral centre from the mesogen should also be studied, since it is known that this causes a variation in the pitch length in low molecular weight systems.[14,15]

It would also be advantageous to increase the temperature range of the chiral nematic phase in these materials, since it is anticipated that a wider range may allow one to control the quality of the texture to a greater extent. This can be achieved by either employing a more flexible backbone (e.g. acrylate, siloxane or phosphazene), or by selecting a different mesogenic unit (e.g. the phenyl benzoate moiety). The choice of backbone is also dictated by the nature of the application in which the material is to be used. Slight adaptations of the synthetic routes described in chapter 6 should result in the preparation of the materials above without too much difficulty.

Other potential uses of such materials in addition to their possible uses as coloured coatings or dichroic filters may include the following. By crosslinking these chiral nematic copolymers either chemically or photochemically, one should obtain brightly coloured chiral nematic elastomers which have a much enhanced dimensional integrity. Since it is known that LC elastomers exhibit both thermo- and photo-elastic behaviour,[33,148] it should be possible to alter the pitch length and hence the macroscopic optical properties of these materials by the application of a small uniform stress. It is therefore conceivable that these elastomers may act as coloured strain gauges.

The few suggestions outlined above are by no means exhaustive and many other approaches are possible.

REFERENCES

REFERENCES

1. Reinitzer F, Monatsch.Chem., 9, 421 (1888).
2. Lehmann O, Z.Phys.Chem., 4, 462 (1889).
3. Lehmann O, Z.Phys.Chem., 56, 750 (1906).
4. Lawrence A S C, Mol.Cryst.Liq.Cryst., 7, 1 (1969).
5. Windsor P A, Chem.Rev., 68, 1 (1968).
6. Windsor P A in "Liquid Crystals and Plastic Crystals", Eds G W Gray and P A Windsor, Vol 1, E Horwood Ltd., pp 199-287 (1974).
7. Samulski E T and Tobolski A V, in "Liquid Crystals and Plastic Crystals, Eds G W Gray and P A Windsor, Vol 1, E Horwood Ltd., pp 175-198 (1974).
8. Friedel G, Ann.de Physique, 18, 273 (1922).
9. Maier W, Saupe A, Z.Naturforsch, 139, 564 (1958).
10. Saeva F D, in "Liquid Crystals - The Fourth State of Matter", Ed F D Saeva, Marcel Dekker Inc. New York, Chpt 3, pp 73-97 (1979).
11. Goosens W J A, J.Phys.Colloq. (Orsay, France) 40, 158 (1979).
12. Van der Meer B W and Vertogen G, Phys.Lett., A59, 279 (1976).
13. Finkelmann H and Stegemeyer H, Ber.Bunsenges, Phys.Chem., 82, 1302-1308 (1978).
14. McDonnel D G in "Thermotropic Liquid Crystals" Ed G W Gray, Critical Reports on Applied Chemistry Series, Vol 22, Wiley and Sons, Chichester and New York, pp 120-144 (1987).
15. Gibson H W in "Liquid Crystals - The Fourth State of Matter" Ed F D Saeva, Marcel Dekker Inc. New York, pp 99-162 (1979).

16. Eliel E L, "Stereochemistry of Carbon Compounds", McGraw-Hill, New York, (1962).
17. De Vries, Acta Crystallogr., 4, 219 (1950).
18. Gray G W and Goodby J W G, "Smectic Liquid Crystals", Leonard Hill, Glasgow, (1984).
19. Leadbetter A J, Mazid M A, Kelly B A. Goodby J W G and Gray G W, Phys.Rev.Lett., 43, 630 (1979).
20. Sackman H and Demus D, Mol.Cryst.Liq.Cryst., 2, 81 (1961).
21. Leadbetter A J and Richardson R M in "The Molecular Physics of Liquid Crystals" Eds G R Luckhurst and G W Gray, Acad.Press, London and New York, (1979).
22. De Vries A, Ekachai A and Spielberg N, Mol.Cryst.Liq.Cryst., 49 143 (1979).
23. Leadbetter A J, Frost J C, Gaughan J P, Gray G W and Mosley A, J.Phys. (Paris), 40, 375 (1979).
24. Coates D, in "Thermotropic Liquid Crystals", Ed G W Gray, Critical Reports on Applied Chemistry Series Vol 22, Wiley and Sons, Chichester and New York, pp 99-119 (1979).
25. Castellano J A, in "Liquid Crystals - The Fourth State of Matter" Ed F D Saeva, Marcel Dekker Inc., New York. Chpt 12, pp 439-458 (1979).
26. Plate N A, Talroze V A and Shibaev V P, Makromol.Chem.Macromol.Symp., 12, 203-228 (1987).
27. Freidzon Ya S, Boiko N I, Shibaev V P, Tsukruk V V, Shilov V V and Lipatov Yu S, Polym.Comm., 27 (6), 190 (1986).
28. Toyne K J, in "Thermotropic Liquid Crystals", Ed G W Gray, Critical Reports on Applied Chemistry Vol 22, Wiley and Sons, Chichester and New York, pp 28-63 (1987).

29. Gray G W, Philos.Trans. R.Soc. London, A309, 77 (1983).

30. Sage I, in "Thermotropic Liquid Crystals, Ed G W Gray, Critical Reports on Applied Chemistry, Vol 22, Wiley and Sons, Chichester and New York, pp 64-98 (1987).

31. Weiss R G, Tetrahedron Report No 236, Tetrahedron, 44 (12), 3413 (1988).

32. Saeva F D and Sharpe P E, J.Amer.Chem.Soc., 97, 204 (1975).

33. Finkelmann H and Rehage G, Adv.Polym.Sci., 60/61, 99-172 (1984).

34. Shibaev V P and Plate N A, Adv.Polym.Sci. 60/61, 173-252 (1984).

35. McArdle C B, Clark M G, Haws C M, Wiltshire M C K, Parker A, Nestor G, Gray G W, Lacey D and Toyne K J, Liq.Cryst., 2 (5), 573-584 (1987).

36. Ringsdorf H, Schmidt H W, Baur G and Kiefer R in "Recent Advances in Liquid Crystal Polymers", Ed L L Chapoy, Elsevier Sci.Pub., Amsterdam, pp 253-260 (1985).

37. Eich M, Wendorff J H, Reck B and Ringsdorf H, Makromol.Chem., Rapid Commun., 8, 59-63 (1987).

38. Eich M and Wendorff J H, Makromol.Chem., Rapid Commun., 8, 467-471 (1987).

39. Plate N A and Shibaev V P in "Comb Shaped Polymers and Liquid Crystals", Speciality Polymer Series, Ed J M G Cowie, Plenum Press, New York and London, (1987).

40. Poddubnyi V I, Lavrentyev V K, Shevelev, V A, Mikhailova N K, Sidorovich A V and Baranov V G, Polym.Bull., 11, 41-45 (1984).

41. Beatty C L, Pochnan J M, Froix M F and Hinmann D D, Macromolecules, 8, 547 (1975).

42. Desper C and Schneider N, Macromolecules, 9, 424-432 (1976).

43. Desper C, Alexander M, Sagalyn P and Schneider N, Polym.Prepr., 18, 73-76 (1977).

44. Flory P J, Proc.Roy.Soc., A234, 60 (1956).

45. Flory P J, ibid., 73 (1956).

46. Wee E L and Miller W G, J.Phys.Chem., 75, 1446 (1971).

47. Hermans J J, Adv.Chem.Phys., B13, 707 (1967).

48. Du Pont (S L Kwolek), B P 1,283,064 (Priority 12th June 1968, USA).

49. Roviello A and Sirigu A, J.Polym.Sci., Polym.Lett.Ed., 13, 455 (1975).

50. Krigbaum W R, Cifferi A, Asrar J, Toriumi H and Preston J, Mol.Cryst.Liq.Cryst., 76, 79 (1981).

51. Wu H H, PhD Thesis, University of Stirling (1987).

52. Blumstein A and Hsu E C in "Liquid Crystalline Order in Polymers" Ed A Blumstein, Academic Press, New York, (1978).

53. Frosini V, Livita G, Lupinacci D and Magagnini P, Mol.Cryst.Liq.Cryst., 66, 341 (1981).

54. Strzelski L and Liebert L, Bull.Soc.Chim.Fr., Ser.C (2), 597-608 (1973).

55. Finkelmann H, Ringsdorf H, Siol W and Wendorff J, in "Mesomorphic Order in Polymers and Polymerisation in Liquid Crystalline Media" Ed A Blumstein, ACS Symposium Series No 74, ACS Washington DC, pp 22-32 (1978).

56. Finkelmann H, Ringsdorf H and Wendorff, J.Makromol.Chem., 179, 273-279 (1979).

57. Shibaev V P, Plate N A and Freidzon Ya S, in "Mesomorphic Order in Polymers and Polymerisation in Liquid Crystalline Media", Ed A Blumstein, ACS Symposium Series No 74, ACS Washington DC, pp 33-55 (1978).

58. Finkelmann H, n "Liquid Crystals of One and Two-dimensional Order", Eds W Helferich and G Heppke, Springer Series in Chemical Physics Vol 11, Springer-Verlag, Berlin and New York, 238-251 (1980).

59. Finkelmann H and Rehage G, Makromol.Chem.Rapid Commun., 1, 31-35 (1980).

60. Gemmel P A, Gray G W and Lacey D, Mol.Cryst.Liq.Cryst., 122 205-218 (1985).

61. (a) Gray G W, Lacey D, Nestor G and White M S, Makromol.Chem.Rapid Commun., 7, 71-76 (1986).
(b) Gray G W, Lacey D, Nestor G and White M S, Mol.Cryst. Liq.Cryst., 122

62. Hahn B and Percec V,Macromolecules, 20 (12), 2961-2968 (1987).

63. Paleous G, Margomenou-Leonidopoulous G, Eilippakis S and Malliaris A, J.Polym.Sci., Polym.Chem.Ed., 20, 2267-2271 (1982).

64. (a) Keller P, Macromolecules, 17, 2937 (1984).
(b) Keller P, Mol.Cryst.Liq.Cryst., 2, 101 (1985).
(c) Keller P, Macromolecules, 18, 2337 (1985).
(d) Keller P, Makromol.Chem. Rapid Commun., 6, 707 (1985).

65. Chen S H and Maa Y F, Macromolecules, 21 (4), 904 (1988).

66. Chiellini E and Galli G, in "Recent Advances in Liquid Crystalline Polymers" Ed L L Chapoy, Elsevier Applied Science Publications, Amsterdam, (1985).

67. Hsu E C, Clough R B and Blumstein A, J.Polym.Sci., Polym.Lett.Ed., 15, 545 (1977).

68. Blumstein A, Macromolecules, 10, 872 (1977).

69. Shibaev V P, Khartionov A V, Freidzon Ya S and Plate N A, Vysokomol.Soed., A21, 1849 (1979).

70. Finkelmann H and Rehage G, Makromol.Chem.,Rapid Commun., 3, 859 (1982).

71. Finkelmann H and Rehage G, ACS Polym.Prepr., 24 (2), 277 (1983).

72. Finkelmann H, Koldehoff J and Ringsdorf H, Angew.Chemie.Int.Ed. Eng., 17, 935-936 (1978).

73. Shibaev V P, Finkelmann H, Kharitonov A V, Portugall M, Plate N A and Ringsdorf H, Vysokomol.Soedin., A23, 919-924 (1981).

74. Mousa A M, Freidzon Ya S, Shibaev V P and Plate N A, Polym.Bull., 6, 485-488 (1982).

75. Finkelmann H, Ringsdorf H, Siol W and Wendorff J, Makromol.Chem., 179, 829-834 (1978).

76. Finkelmann H and Rehage G, Makromol.Chem., Rapid Commun., 1, 733-740 (1980).

77. Freidzon Ya S, Boiko N I and Plate N A, Abstracts of the 1st All-Union Symposium on Liquid Crystalline Polymers, Sudzal, pp 24-26 (1982).

78. Keating P N, Mol.Cryst.Liq.Cryst., 8, 315 (1969).

79. Freidzon Ya S, Tropsha Y G, Shibaev V P and Plate N A, Makromol.Chem., Rapid Commun., 6, 625-629 (1985).

80. Freidzon Ya S, Boiko N I, Shibaev V P and Plate N A, Eur.Polym.J., 22, 13-16 (1986).

81. Shannon P J, Mol.Cryst.Liq.Cryst., 110 (1-4), 135-144 (1984).

82. Shibaev V P, Kozlovsky M V, Beresnev L A, Blinov L M and Plate N A, Polym.Bull., 12, 299-301 (1984).

83. Decobert G, Soyer F and Dubois J C, Polym.Bull., 14, 179-186 (1986).

84. Decobert G, Dubois J C, Esselin S and Noel C, Liq.Cryst., 1 (4), 307-317 (1986).

85. Guglielminnetti J M, Decobert G and Dubois J C, Polym.Bull., 16 (5), 411-418 (1986).

86. Zentel R, Reckert G and Reck B, Liq.Cryst., 2 (1), 83-89 (1987).

87. Koide N, Uehara K and Iimura K, Mol.Cryst.Liq.Cryst., 157, 151-162 (1988).

88. Jones B A, Bradshaw J S, Nishioka M and Lee M L, J.Org.Chem., 49, 4947-51 (1984).

89. Hessel F, Herr R-P and Finkelmann H, Makromol.Chem., 188, 1597-1611 (1987).

90. Finkelmann H, in "Polymer Liquid Crystals", Eds A Cifferi, W R Krigbaum and R B Meyer, Academic Press, New York, (1982).

91. Noel C, in "Recent Advances in Liquid Crystal Polymers", Ed L L Chapoy, Elsevier Applied Science Publications, Amsterdam (1985).

92. Shibaev V P, Kostromin S G and Plate N A, Eur.Polym.J., 18, 651-659 (1982).

93. Uchida S, Mol.Cryst.Liq.Cryst., 155, 93-102 (1988).

94. Finkelmann H, Happ M, Portugall M and Ringsdorf H, Makromol.Chem., 179, 2541-2544 (1978).

95. Hahn B, Wendorff J H, Portugall M and Ringsdorf H, Colloid and Polym.Sci., 259 (9), 875-884 (1981).

96. Demus D and Richter L, "Textures of Liquid Crystals", Verlag Chemie, New York, (1978).

97. Meier G, Sackmann E and Grabmaier J G, "Applications of Liuqid Crystals", Springer-Verlag, Berlin, (1975).

98. Meurisse P, Noel C, Monnerie L and Fayolle B, British Polym.J., 13, 55 (1981).

99. Sackmann H and Demus D, Mol.Cryst.Liq.Cryst., 21, 239 (1973).

100. Lipatov Yu S, Tsukruk V V and Shilov V V, JMS-Rev.Macromol.Chem.Phys., C24 (2), 173-238 (1984).

101. De Vries A, in "Liquid Crystals - The Fourth State of Matter", Ed F D Saeva, Marcell-Dekker Inc., New York, pp 1-72 (1979).

102. Vogel A, "Textbook of Practical Organic Chemistry", 4th Edn, Longmann, London, (1979).

103. Still W C, Kahn M and Mitra A, J.Org.Chem., 43 (14), 2923-2925 (1978).

104. Van Alphen J, Recl.Trav.Chim.Pays-Bas, 50, 657-668 (1931).

105. Portugall M, Ringsdorf H and Zentel R, Makromol.Chem., 183. 2311-2321 (1982).

106. Freidzon Ya S, Kharitonov A V, Shibaev V P and Plate N A, Mol.Cryst.Liq.Cryst., 88, 87-97 (1982).

107. Ferguson R, PhD Thesis, University of Stirling (1983).

108. Baker B R, Schaub R E and Williams J H, J.Org.Chem., 17, 122 (1952).

109. Knuth C, M.Ch.E.Thesis, Polytechnic Institute of Brooklyn, New York (1947).

110. Ghirardelli R G, J.Amer.Chem.Soc., 95 (15), 4987-4990 (1973).

111. Otterholm B, Alstermark C, Flatischer K, Dahlgren A, Lagerwall S T and Skarp K, Mol.Cryst.Liq.Cryst., 146, 189-216 (1987).

112. Newkome G R and Marston C R, J.Org.Chem., 50, 4238-4245 (1985).

113. Hartshorne N H, "The Microscopy of Liquid Crystals", Microscope Publications Ltd., London, (1974).

114. Rabek J F, "Experimental Methods in Polymer Chemistry", Wiley-Interscience, New York, (1980).

115. Mayo F R and Lewis F M, J.Amer.Chem.Soc., 66, 1594-1601 (1944).

116. Dostal H, Monatsh, 69, 424-426 (1936).

117. Cowie J M G, in "Alternating Copolymers", Ed J M G Cowie, Plenum Press, New York, pp 1-17 and 19-238 (1985).

118. Gumbs R, Penczek S, Jagur-Grodzinski J and Szwarc M, Macromolecules, 2, 77-82 (1969).

119. Billmeyer F W Jr, "Textbook of Polymer Science", 2nd Ed., Wiley and Sons Inc., New York, (1971).

120. McEwen I J and Johnson A F, in "Alternating Copolymers", Ed J M G Cowie, Plenum Press, New York, pp 239-276 (1985).

121. Natta G, Dall'Asta G, Mazzanti G, Pasquon I, Valvassori A and Zambelli A, Makromol.Chem., 54, 95 (1962).

122. Bovey F A, "High Resolution NMR of Macromolecules", Academic Press, New York, (1972).

123. Tate B E, in "Vinyl and Diene Monomers Part 1", Ed E C Leonard, High Polymers Vol XXIV, Wiley-Intersceince, New York, pp 205-261 (1967).

124. Cowie J M G, "Polymers: Chemistry and Physics of Modern Materials", Intertext Ltd., (1973).

125. Dubois J C, Lavenu J C and Zann A, in "Mesomorphic Order in Polymers and Polymerisation in Liquid Crystalline Media", Ed A Blumstein, ACS Symp. Ser. Vol 74, ACS Washington, pp 22-32 (1978).

126. Stevens H, Rehage G and Finkelmann H, Macromolecules, 17, 851-856 (1984).

127. Antoun S, Lenz R W and Jin J-I, J.Polym.Sci., Polym.Chem.Ed., 19, 1901-1920 (1981).

128. Griffin A C and Havens S J, J.Polym.Sci., Polym.Phys.Ed., 19, 951 (1981).

129. Simon R and Coles H J, Polymer, 27 (6), 811-816 (1986).

130. Cowie J M G and Wu H H, Makromol.Chem., 189, 1511-1516 (1988).

131. Martin P G and Stupp S I, Macromolecules, 21, 1222-1227 (1988).

132. Finkelmann H, in "Thermotropic Liquid Crystals", Ed G W Gray, Critical Reports on Applied Chemistry, Vol 22, Wiley and Sons, New York, pp 145-170 (1987).

133. Shoji K, Nakajima Y, Veda E and Takeda M, Polymer Journal (Jpn), 17 (9), 997-1003 (1985).

134. Fox T G, Bull.Amer.Phys.Soc., 1, 123 (1956).

135. Pochan J M, Beatty C L and Pochan D F, Polymer, 20, 879 (1979).

136. Barton J M, J.Polym.Sci., Part C (30), 573 (1970).

137. Yamaguchi T, Okada M, Hayashi T and Nakamura N, Mol.Cryst.Liq.Cryst., 155, 501-510 (1988).

138. Iimura K, Uchida T and Takeda M, Reports on Progress in Polymer Physics in Japan Vol XXIII, 275-276 (1980).

139. Shibaev V P, Freidzon Ya S and Plate N A, Vysokomol.Soedin, A-20, 82 (1982).

140. Shibaev V P, Freidzon Ya S, Kharitonov A V and Plate N A, Preprints of Short Communications of the 26th International Symposium on Macromolecules, Mainz, FRG (1979).

141. Shibaev V P, Freidzon Ya S, Tal'roze R V and Plate N A, Preprints of the International Symposium on Macromolecules, Florence, Italy. Lutografia Felici, 3, 310 (1980).

142. Finkelmann H, Kock H and Rehage G, Makromol.Chem., 2, 317 (1981).

143. Gregg R A and Mayo F R, Discuss.Faraday Soc., 328 (1947).

145. (a) Voigt-Martin, I G and Durst H, Liq.Cryst., 2 (5), 585-600 (1987).

(b) Voigt-Martin I G and Durst H, ibid., 601-610.

145. Mayo F R and Walling C, Chem.Revs., 46, 191 (1950).

146. Flory, P J, "Principles of Polymer Chemistry", Cornell University Press, Ithaca, New York, (1953).

147. Finkelmann H and Kock H-J and Rehage G, Makromol.Chem., Rapid Commun., 2, 317-322 (1981).

148. Gleim W and Finkelmann H, Makromol.Chem., 188, 1489-1500 (1987).

149. Zentel R and Benalia M, Makromol.Chem., 188, 633-674 (1987).

150. Cano R, Bull.Soc.Fr.Mineral.Cristallogr., 91, 20 (1968).

151. Freidzon Ya S, Kharitonov A V, Shibaev V P and Plate N A, Eur.Polym.J., 21 (3), 211-216 (1985).

152. De Gennes P G, "The Physics of Liquid Crystals", Clarendon Press, Oxford, (1974).

153. De Pre D B and Samulski E T, in "Liquid Crystals - The Fourth State of Matter", Ed F D Saeva, Marcel Dekker Inc., pp 203-247 (1979).

154. Walba D M, Slater S C, Thurnes W N, Clark N A, Handschy M A, and Supon F, J.Amer.Chem.Soc., 108, 5210-5221 (1986).

155. Goosens W J A, J.Phys.(Paris), C3, 158 (1979).

156. Pleiner H and Brand H, Phys.Rev.Lett., 54, 1817 (1985).

157. Hardoin F, Moirez L, Keller P, Lambert M, Moussa F, and Pepy G, Mol.Cryst.Liq.Cryst., 155, 389-397 (1988).

158. Ringsdorf H and Zentel R, Abstracts of Communications of the 27th International Symposium on Macromolecules, Strasbourg, France, Vol 2, 969 (1981).

APPENDICES

APPENDIX A
^{1}H NMR SPECTRA

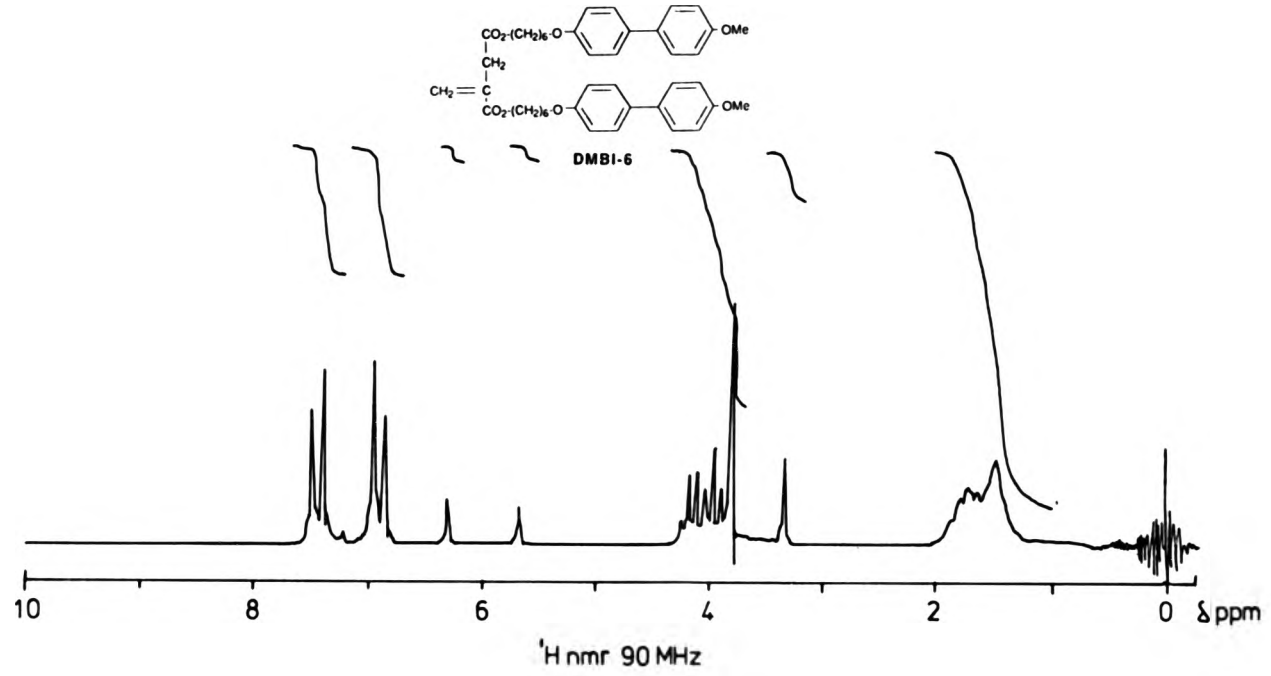
CO2-(CH2)6-O
OMe
CH2
CH2 = C
CO2-(CH2)6-O
OMe
DMBI-6
10
8
6
4
2
0
δ ppm
'H nmr 90 MHz

A1

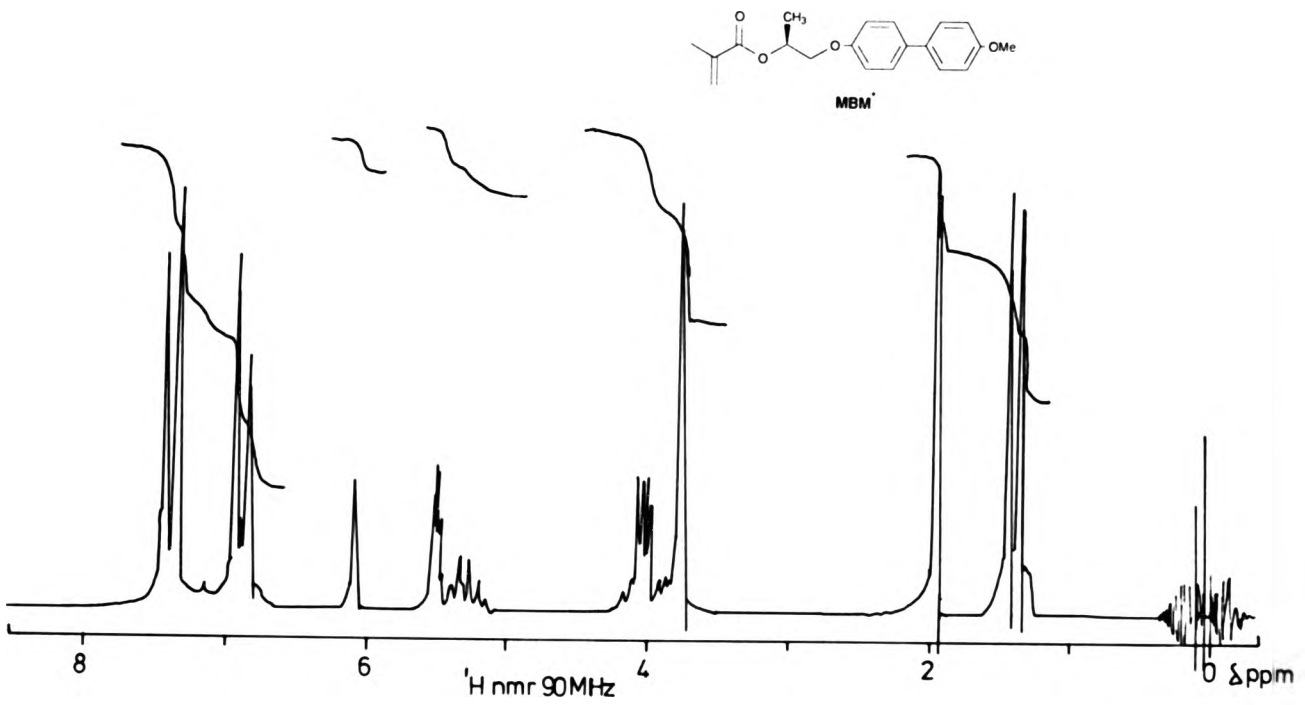

A 2

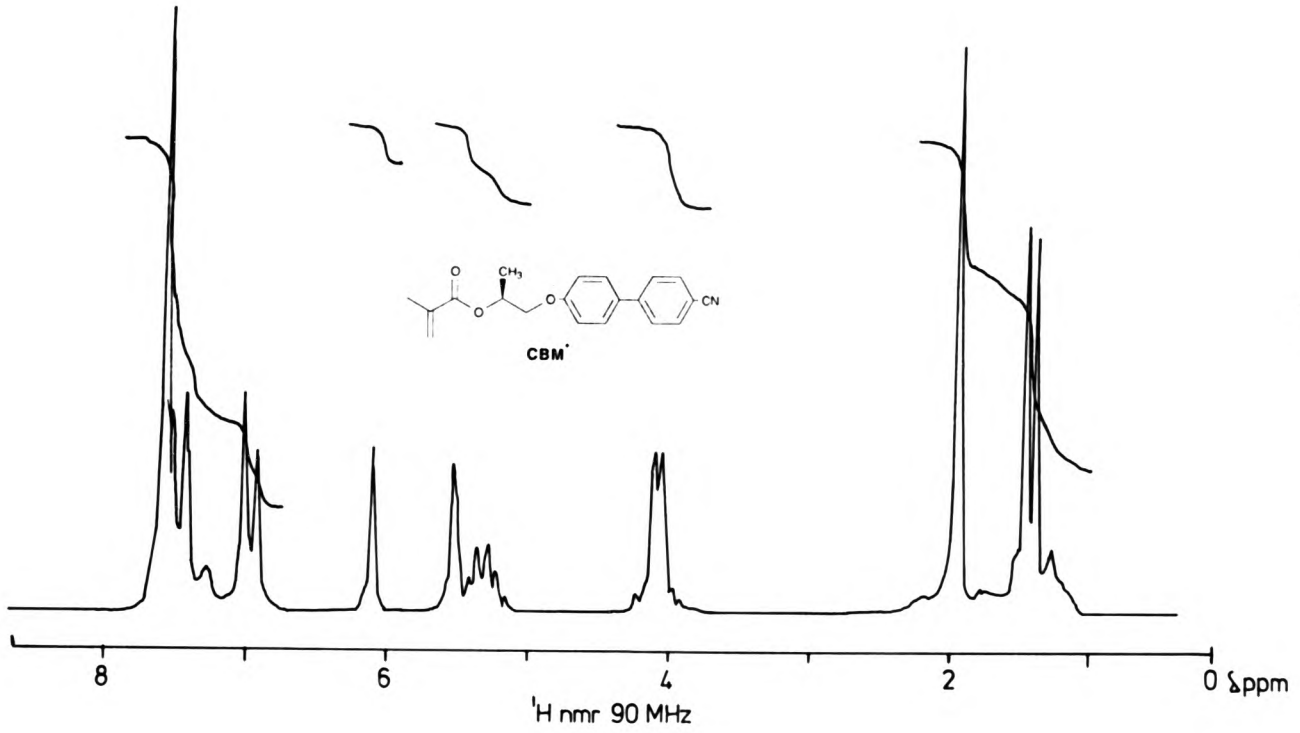

A3

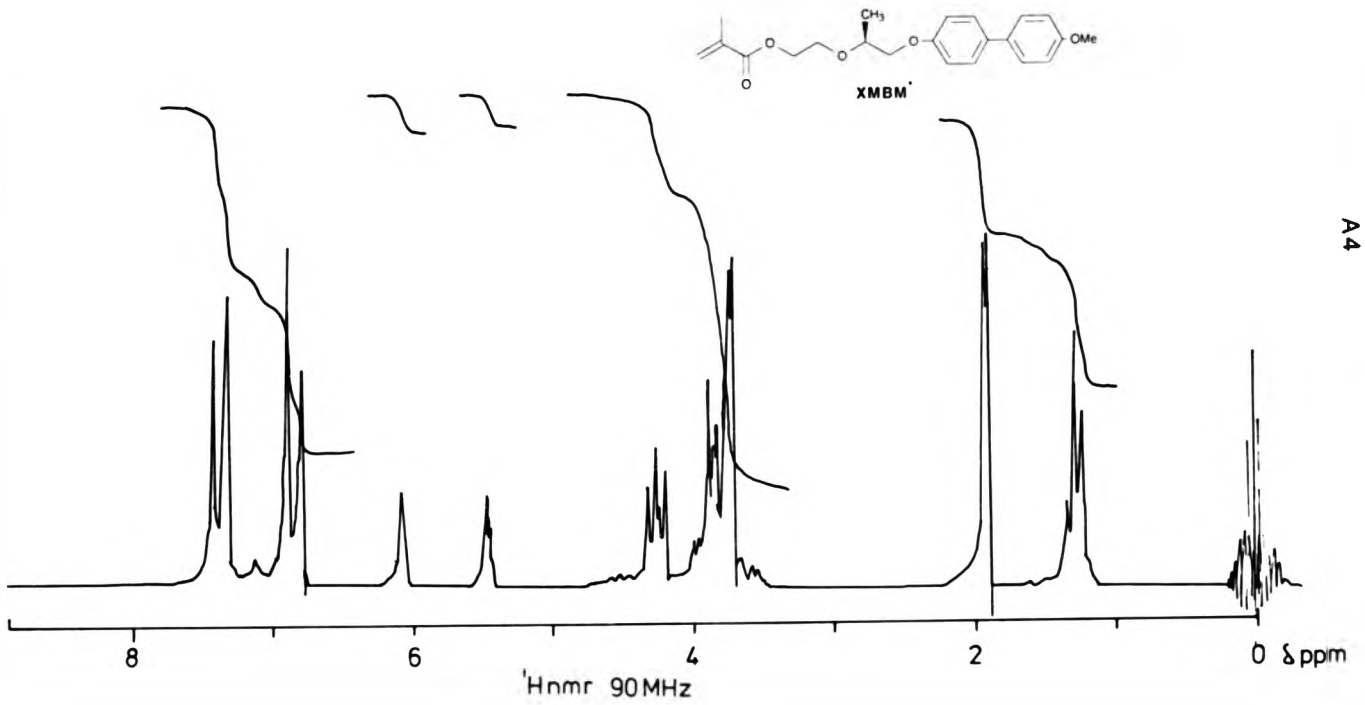

A4

APPENDIX B
PATENT

RPP/WP/ag

Vertrouwelijk	
Ingediend:	07.09.1988
Nummer:	88308271.1

EE 5842

POLYMER COMPOSITION, CAPABLE OF FORMING A CHIRAL NEMATIC MESOPHASE

The invention relates to polymer compositions comprising a polymer capable of forming a chiral nematic mesophase, the said polymer consisting of a main and side chain, the said side chain comprising at least a mesogenic unit and a chiral atom.

Such a composition is known from EP-A-0184482. This patent describes polymer compositions based on a monomer according to formula (I):

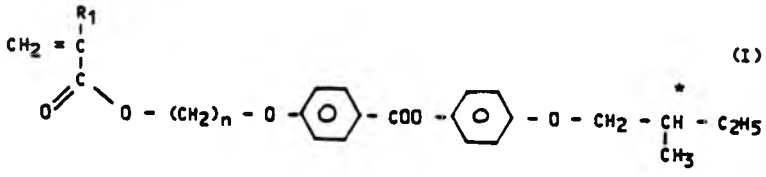

(I)

The C-atom which is marked is a chiral atom. This atom is present at the end of the side chain. The polymer obtained from the monomer of formula (I) may be used for non-linear optics, due to its liquid crystal properties. I.e. the polymer is highly orientated in the melt. The orientation is 'frozen' by cooling the polymer quickly beneath its glass transition temperature (Tg).

For some applications however, there may be a problem concerning the magnitude of the glass transition temperature, especially when the polymers have to be used at elevated temperatures.

Therefore there is a need for a polymer composition which exhibits a relatively high Tg.

It is the object of the invention to provide such polymer compositions.

The polymer composition according to the invention are characterized by the fact that the chiral C-atom is present in the 'spacer' part between the main and side chain, rather than on the

chain end.

By 'spacer' part is meant a flexible unit which links the main chain to the side chain mesogenic unit.

Surprisingly it has been found that the polymer compositions according to the invention not only exhibit an increased Tg, but also that these compositions are easy to process. These compositions are also useful as coloured coatings, information storage device materials and as selective light reflectors.

The compositions according to the invention comprise at least a monomer with formula (II)

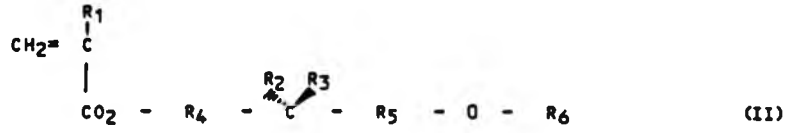

(II)

wherein

R_1 = hydrogen, alkyl with 1-3 C-atoms, or a halogen;

$R_2 \neq R_3$;

R_2, R_3 = hydrogen, alkylgroup with 1-3 C-atoms, halogen, aryl-, alkylaryl-, or phenylgroup;

R_4 = $(CH_2)_n$-group, or $(CH_2CH_2O)_n$, wherein n = 0-10;

R_5 = $(CH_2)_n$-group, wherein n = 0-10;

R_6 = 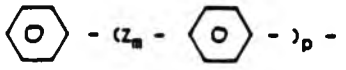

wherein

m = 0,1; p = 0, 1, 2, 3;

Z = -COO, -OCO-, $-SO_2-$, or $-C(CH_3)_2-$;

R_7 = $-O-(CH_2)_n H$;

$-(CH_2)_n H$;

$-COO-(CH_2)_n H$;

or a -CN group

where n = 0-4.

In the polymer composition according to the invention R_1, R_2 and R_3 are preferably a hydrogen or a methylgroup.

The polymer used in the composition according to the invention will be optically active, due to the chiral centre in the spacer part of the monomers.

The polymer used in the composition according to the invention is a chiral nematic liquid crystal polymer, capable of forming a chiral nematic mesophase. A chiral nematic liquid crystal polymer exhibits a twisted nematic phase in which the direction of the polymer side chain in a given region, is rotated through a fixed angle, thereby producing a supermolecular helical structure within the mesophase.

This configuration can account for exceptional biaxial modulus properties and allows the polymers to be used in forming sheets, films and coatings.

The invention is not limited to homopolymers made from the monomer of formula (II), but discloses also compositions wherein said monomers are used.

Compositions of polymers based on the monomers of formula (II) and a polymer based on monomers of formula (III) are especially preferred:

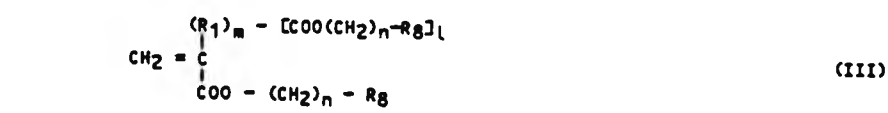

(III)

wherein

R_1 = hydrogen or an alkylgroup with 1-3 C-atoms or a halogen when $l = 0$; or a (CH_2)-group when $l = 1$;

n = 1-10;

m = 0,1 or 2;

l = 0,1

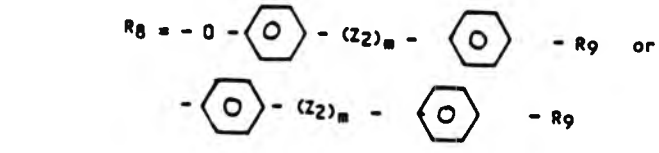

or

wherein

Z_2 = -COO-, -OCO-;

m = 0,1;

and R_9 = $-O-(CH_2)_q H$;

$-(CH_2)_q H$;

$-COO-(CH_2)_q H$;

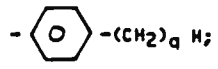

$-(CH_2)_q H$;

-CN;

$-O-CH_2-\underset{\underset{CH_3}{|}}{CH}-C_2H_5$;

wherein q = 1-12.

In this context it is noted that when properly chosen, some monomers according formula (III) are known from EP-A-0184482 and from DE-A-2722589.

The monomers to be used in the compositions according to the invention may be prepared in a manner which is known per se. For instance both EP-A-0184482 and DE-A-2722589 describes the preparation of the monomers. The preparation of the monomers is elucidated in the examples.

The copolymers described here are examples of thermotropic chiral copolymers which have the chiral centre in the 'spacer' part of the molecule. The copolymers exhibiting selective light reflection and, having only the chiral nematic structure, could conceivably be useful as selective light reflectors, information storage device materials and coloured coatings. In the copolymers where a terminal cyano group is present in either monomer, alignment in electric fields is possible, and this effect changes the wavelength of reflected light.

The invention will be elucidated on the basis of the following examples, without being restricted hereto.

Examples

The following monomers were prepared:

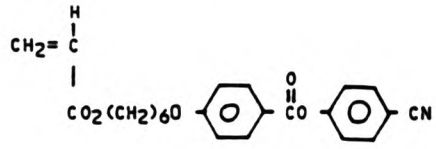

(I)

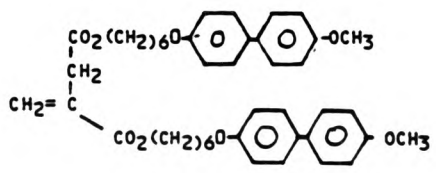

(II)

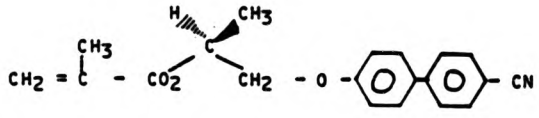

(III)

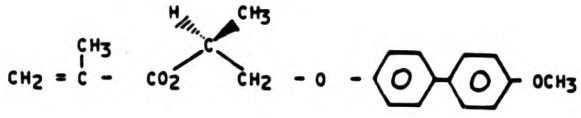

(IV)

The preparation of these monomers is set out below.

(I) Preparation of 4-cyanophenyl-4'-(6-acryloyloxyhexyloxy) benzoate (CPBA-6)

(A) 4-(6-Hydroxyhexyloxy)benzoic acid

4-Hydroxybenzoic acid (25.5g, 0.185 mol) was dissolved in a mixture of ethanol (65ml), water (28ml), potassium hydroxide (27.7g, 0.49 mol) and a pinch of potassium iodide. 1-Chloro-6-hydroxy hexane (23 g, 0.168 mol) was then added slowly dropwise and the mixture refluxed for 20 hours. After cooling the mixture, the ethanol was evaporated in vacuo and the residue dissolved in water (200ml). This aqueous solution was washed with diethylether (3x50ml) then adjusted to pH2 with 2N HCL and the resultant precipitate collected by filtration. After washing with water and drying, the crude product was recrystallised from ethanol. YIELD= 21.6g, 54%; melting point= 139-142°C.

(B) 4-(6-Acryloyloxy hexyloxy)benzoic acid

4-(6-Hydroxyhexyloxy)benzoic acid (21.6g, 0.09 mol) was esterified azeotropically with freshly distilled acrylic acid (26g, 0.36 mol) as the catalyst and hydroquinone (2g, 0.018 mol) as the polymerisation inhibitor. Reflux was continued for 20 hours. On cooling, the reaction mixture was diluted with diethylether (1000ml) and washed carafully with warm water until no more acrylic acid was detected. The organic layer was dried ($MgSO_4$), evaporated and the crude product recrystallised from isopropanol. YIELD= 17.6g, 67% Melting point= cryst. 86°C N, 90°C I (N=nematic phase; I = isotropic phase).

(C) 4-Cyanophenyl-4'-(6-acryloyloxyhexyloxy)benzoate

4-(6-Acryloyloxyhexyloxy)benzoic acid (17.3 g, 0.059 mol) was stirred with thionyl chloride (35.7 g, 0,3 mol) in the presence of DMF (2-drops) and 2,6-di-t-butyl-p-cresol (4.4g, 0.02 mol). After ca. 25 minutes, by which time solution was achieved, the excess thionyl chloride was removed by rotary evaporator. The acid chloride residue was dissolved in anhydrous chloroform (30ml) and added slowly dropwise into a stirred solution of 4-cyano phenol (7.03g, 0.059mol) and triethylamine (6.07g, 8.36ml, 0.06mol) in

chloroform (20ml) at 0°C. After the addition the mixture was stirred at room temperature for 24 hours then chloroform (200ml) was added.

This solution was washed with water (1x50ml) followed by 2N sodiumhydroxide solution (3x50ml) and water (2x50ml). The organic layer was dried ($MgSO_4$), evaporated, then subjected to flash chromatography using dichloromethane as the eluant. The ester was recrystallised from isopropanol and shown to be pure by t.l.c. YIELD = 16g, 69%; M.P.T.= 72-73°C.

Chemical analysis, ^1H NMR and I.R. analysis all correspond with expected data.

(II) Preparation of Di[6-(4-methoxy-4'-oxybiphenyl)hexyl]-2-methylene butane-1,4-dioate (MBI-6)

(A) 4-Methoxy-4'-hydroxybiphenyl

Biphenol (75g, 0.402 mol) was dissolved in 10% sodium hydroxide solution (0.804 mol equiv.) dimethyl sulphate (50g, 38ml, 0.402mol) was added and the mixture stirred mechanically for 30 minutes. The resultant precipitate was filtered, washed with 10% sodiumhydroxide solution and water. The precipitate was then dissolved in boiling water and filtered hot, the desired product finally being isolated by adding 2N H_2SO_4 carefully to the hot filtrate. The product was collected by filtration, washed with water, dried and recrystallised from ethanol. YIELD= 31.3g, 39%. M.P.T.: 183-185°C.

(B) 4-methoxy-4'-(6-hydroxyhexyloxy)biphenyl

4-Methoxy-4'-hydroxy biphenyl (30g, 0.15 mol) was dissolved in hot ethanol (200ml) and potassium hydroxide (9.26g, 0.165 mol) in water (45ml) added under stirring. 1-chloro-6-hydroxy hexane (22.5g, 0.165 mol) was added and the mixture refluxed for 24 hours. The solution was then diluted with an equal volume of water and the ethanol distilled off. The resultant precipitate was filtered and washed copiously with hot 10% potassium hydroxide solution, followed by water. The dried product was recrystallized from ethanol. YIELD= 30.6g, 68%; M.P.T. 130°C.

(C) Di[6-(4-methoxy-4'-oxybiphenyl)hexyl]-2-methylene butane-1,4-dioate

4-Methoxy-4'-(6-hydroxyhexyloxy) biphenyl (15.36g, 51 mmol) was esterified azeotropically with itaconic acid (2.21g, 17 mmol) in toluene (200ml) in the presence of p-toluene sulphonic acid (0.4g, 2mmol). Reflux was continued for 48 hours. Toluene (400ml) was added after this time, and the solution washed with 10% sodium bicarbonate solution (3x100ml) followed by water (100ml). The dried ($MgSO_4$) organic layer was evaporated and the crude product purified by column chromatography using silica gel (Fisons 60-120 mesh) and 5% ethyl acetate in chloroform as the eluant.
YIELD = 10g, 85%; M.P.T.: cryst. 68°C, S_B; 108°C I.

Chemical analysis, ^1H NMR and IR data correspond with expected values.

III Preparation of (S)-1-(4-Cyano-4'-oxibiphenyl)-2-Methacryloyloxy Propane

(A) Ethyl (S)-2-(tetrahydro-2-pyranoxy) propanoate.

Dihydro-2H-pyran (63g, 0.75 mol) followed by 12 N HCL (5 drops) were added to (S) ethyl lactate (53.1g, 0.45 mol) under stirring. Heat evolution was controlled by means of a water/ice bath. Stirring was continued for 20 hours after which time sodium bicarbonate (ca. 5g) was added. Stirring was continued for a further 2 hours then the solution was filtered and concentrated by rotary evaporation at 50°C. The pure products (since the THP ring introduces a second chiral centre) were isolated by distillation through a short Vigreaux column YIELD: 76.3g, 84%; BPT.: 64-68°C/0.03 mm Hg.

(B) (S)-2-(Tetrahydro-2-pyranoxy)-1-propanol.

Lithium aluminium hydride (8.0g, 0.214 mol) was slurried in cold (0°C) anhydrous diethylether (270ml) under nitrogen and a solution of ethyl-(S)-2-(tetrahydro-2-pyranoxy) propanoate (67g, 0.335 mol) in anhydrous diethyl ether (100ml), was added slowly over 2 hours.

The ice-bath was removed after the addition and the mixture was gently refluxed for 48 hours. On cooling water (8ml); 20% sodium hydroxide solution (6ml) and water (13ml) were added successively in a dropwise manner. After standing overnight the ether was evaporated and the remaining mixture subjected to extraction with diethylether in a Sohxlet apparatus for 4 hours. Distillation of the alcohol after evaporation of the ether gave a major fraction as a liquid. YIELD= 53.5g, 65%; BPT.: 42-44°C/0.1 mm Hg.

(C) (S)-1-(p-Toluene sulphonoxy)-2-(tetrahydro-2-pyranoxy)propane

To a cold (0°C) solution of (S)-2-(tetrahydro-2-pyranoxy)1-propanol (13.5g, 84 mmol) in dry pyridine (50ml) was added, in small portions over a period of 15 minutes, p-toluene sulphonylchloride (19.06g, 100mmol). Stirring was continued throughout the addition and overnight, whilst keeping the reaction mixture at 0°C. The precipitated pyridine hydrochloride was filtered off, washed with diethylether (2x100ml) and the combined filtrate and washings concentrated. Pyridine (15ml) was added, followed by water (20ml) and the mixture stirred for 2 hours in a ice-bath. Diethylether (200ml), and water (100ml) were then added to the mixture after t.l.c. analysis showed no starting materials were present and the layers were separated. The organic layer was then washed with aqueous coppersulphate solution followed by water (1x100ml). The organic layer was dried ($MgSO_4$) and evaporated to reveal an oil with a slight pink colour which was shown to be pure by t.l.c. analysis. YIELD= 24.8g, 94%.

(D) (S)-1-(4-Cyano-4'-oxybiphenyl)-2-(tetrahydro-2-pyranoxy) propane.

Sodium hydride (0.69g, 29 mmol) was slurried in DMF (15ml) under a flow of Nitrogen and a solution of 4-cyano-4'-hydroxy biphenyl (5.46g, 28mmol) in DMF (15ml) added slowly dropwise. The mixture was stirred for 45 minutes then a solution of (S)-1-(p-toluene sulphonoxy)-2-(tetrahydro-2-pyranoxy)propane (8g, 25 mmol) in DMF (10 ml) was added dropwise. After the addition the reaction temperature was raised to about 50°C and the mixture was left to stir overnight. After this time the DMF was removed from the reaction mixture by co-evaporation with xylene in vacuo. Chloroform and

water were then added and the separated organic layer washed with 20% potassium hydroxide solution (3x100ml) and water (100ml). The dried ($MgSO_4$) organic layer was concentrated and subjected to flash chromatography using chloroform as the eluant. YIELD= 7.58g, 90%. OIL, $[\alpha]_D^{20}$ = -17.5° ($CHCl_3$).

(E) (S)-1-(4-cyano-4'-oxybiphenyl)-2-hydroxypropane.
(S)-1-(4-cyano-4'1-oxybiphenyl)-2-tetrahydro-2-pyranoxy) propane (7g, 20.7 mmol) was dissolved in acidified ethanol (100ml). [prepared from ethanol (100ml) and 0.1 N HCL (1ml)] and refluxed for 15 minutes. T.l.c. analysis showed only product present, therefore the ethanol was evaporated off and chloroform (100ml), and water (100ml) added. The organic layer was washed further with water (2x100ml), dried ($MgSO_4$) and evaporated. YIELD= 4.97g, 95%, M.P.T.: 103-104°C. $[\alpha]_D^{20}$= +12.4° ($CHCl_3$).

(F) (S)-1-(4-cyano-4'-oxybiphenyl)-2-methacryloyloxy propane.
Methacryloyl chloride (1.16g, 11mmol) was added dropwise to an ice-cooled, stirred solution of (S)-1-(4-cyano-4'-oxybiphenyl)-2-hydroxy-propane (2.78g, 11mmol) and triethylamine (1.3g, 13mmol) in anhydrous benzene (75ml). After the addition 2,6-di-t-butyl-p-methylphenol (0.2g) was added, the ice bath was removed and the solution stirred vigorously for 4 hours. Benzene (100ml) was added, the mixture was washed with water (100ml), 10% sodium hydroxide solution (2x100ml), water (100ml), dried ($MgSO_4$) then evaporated. The crude product was purified by flash chromatography using a petroleum ether (40/60)/ethylacetate mixture (6:1). YIELD= 3.3g, 94%; M.P.T. 58-60°C; $[\alpha]_D^{20}$ = -19.2° ($CHCl_3$). Elemental analysis, ^1H NMR and IR data for the above series of compounds were consistent with expected values.

IV <u>(S)-1-(4-methoxy-4'-oxybiphenyl)-2-methacrylaloyloxy propane</u> was prepared in similar yields by similar methods as set out in (III).

<u>Copolymerisations</u>

Copolymerisations were carried out in benzene solution in

evacuated seal-off ampoules using α,α'-azobisisobutyronitrile (AIBN) as the initiator (0.5 mol%) and precipitations were carried out from either chloroform or dichloromethane solutions into cold diethyl ether, methanol or acetone depending on the system under study.

Copolymersations were generally stopped after ~ 10% conversion was reached.

The samples were examined between glass-slides on the hot-stage of a polarising microscope. A typical sample preparation is as follows:- The sample was heated above T_{n^*-I} then cooled slowly until the mesophase appeared (usually the characteristic texture appeared at about T_{n^*-I} -10°C). This was allowed to develop for up to 24 hours then rapidly cooled to below Tg.

Copolymers of I and III

Copolymers of I and III were found to produce chiral nematic structures over a wide range of feed values with the copolymers having feed ratios (I/III) 90/10, 85/15, 75/25 exhibiting selective light reflection in the visible region of the spectrum (See table 1). These colours can be retained by rapidly cooling the sample below Tg since the chiral nematic structure is unaffected.

TABLE 1

Ex	% chiral component III in copolymer feed	Tg (°C)	T_{n^*-I} (°C)	% conversion	colour of reflected light against dark background
A	0	33	133	60	—
I	10	44	111	8	Pink/red
II	15	52	112	8	turquoise/blue
III	25	44	105	4	blue/violet
IV	50	100	112	13	—
V	75	97	119	5	—
VI	100	105	—	62	—

Tg= glass transition temperature

T_{n^*-I} = temperature, at which the chiral nematic phase will be transformed into an isotropic phase.

Example A is a comparative example.

Copolymers of II and III

The same procedure was followed as carried out above. Copolymers of II and II were also found to produce chiral nematic structures. The results are summarized in table 2.

TABLE 2

Ex.	% chiral component (III) in copolymer (% in feed in brackets)	Tg (°C)	$T_{cryst-s}$ (°C)	T_{s-I} (°C)	T_{n^*-I} (°C)	% conversion	colour of reflected light against dark background
B	0	64	125	150	-	40	-
VII	26 (10)	81	131	148	-	10	-
VIII	47 (25)	93	121	136	-	12	-
IX	62 (40)	82	-	-	116	11	pale blue
X	76 (60)	94	-	-	112	8	-
XI	85 (75)	96	-	-	-	7	-
XII	100	105	-	-	-	62	-

$T_{cryst-s}$ = temperature at which the crystalline phase will be transformed into a smectic phase;

T_{s-I} = temperature at which the smectic phase will be transformed into an isotropic phase;

T_{n^*-I} = temperature at which the chiral nematic phase will be transformed into an isotropic phase.

Copolymers of I and IV

The same procedure was followed as carried out above. Copolymers of II and IV were also found to produce chiral nematic structures. The results are summarized in table 3.

TABLE 3

Ex	% chiral component IV in copolymer	Tg (°C)	Tcryst-s (°C)	Ts-n* (Ts-I)[a] (°C)	Tn*-I (°C)	% conversion	colour of reflected light against dark background
C	0	64	125	(150)[a]	—	40	—
III	32 (15)	78	118	132	137	6	—
XIV	63 (26)	69	—	108	117	10	—
XV	73 (34)	68	—	—	91	11	blue
XVI	83 (50)	79	—	—	103	8	voilet/blue
XVII	95 (75)	97	—	—	114	8	—
XVIII	100	105	—	—	120	69	—

a- The temperature in brackets refers to Ts-I rather than Ts-n*

Tcryst-s= temperature at which the crystalline phase will be transformed into a smectic phase.

Ts-n*= temperature at which the smectic phase will be transformed into a chiral nematic phase

Tn*-I= temperature at which the chiral nematic phase will be transformed into an isotropic phase.

Example C is a comparative example.

C L A I M S

1. Polymer composition comprising a polymer capable of forming a chiral nematic mesophase, the said polymer consisting of a main and a side chain, the said side chain comprising at least a mesogenic unit and a chiral atom, characterized in that the chiral atom is present in the 'spacer' part between the main chain and the mesogenic side group.

2. Polymer composition according to claim 1, characterized in that the polymer composition comprises at least a monomer as set out in formula (II)

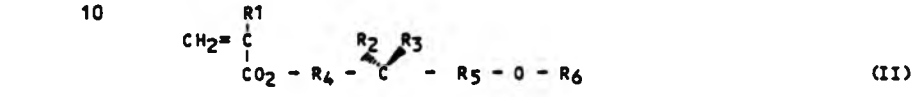

(II)

wherein

R_1= hydrogen, alkyl with 1-3 C-atoms, or a halogen;

$R_2 \neq R_3$;

R_2, R_3= hydrogen, alkylgroup with 1-3 C-atoms, halogen, aryl-, alkylaryl-, or phenylgroup;

R_4= $(CH_2)_n$ - group, or $(CH_2CH_2O)_n$, wherein n= 0-10;

R_5= $(CH_2)_n$-group, wherein n = 0-10;

R_6= 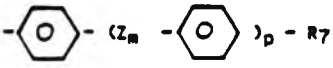

wherein m= 0,1; p= 0, 1, 2, 3;

Z= - COO - or - OCO - , - SO_2 -, or -$C(CH_3)_2$-;

R_7= - O-$(CH_2)_n$ H;

-$(CH_2)_n$ H;

- COO - $(CH_2)_n$ H;

or a - CN group;

where n = 0-4.

3. Polymer composition according to claim 2, characterized in that R_1, R_2 or R_3 is a hydrogen or a methylgroup.

4. Polymer composition according to any one of the claims 2-3, characterized in that the composition comprises

A) 1-100 wt.% of a monomer according formula II

B) 99-0 wt.% of a monomer according formula III

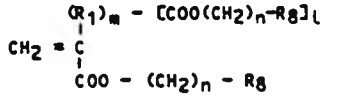

(III)

wherein

R_1 = hydrogen or an alkylgroup with 1-3 C-atoms or a halogen when $l = 0$; or a (CH_2)-group when $l = 1$;

n = 1-10;

m = 0,1 or 2;

l = 0,1;

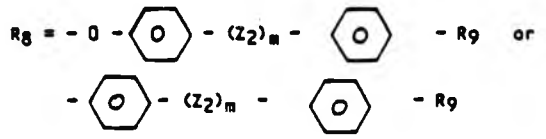

wherein Z_2 = - COO - , - OCO - ;

m = 0,1;

and

R_9 = - O - $(CH_2)_q$ H,

- $(CH_2)_q$ H;

- COO - $(CH_2)_q$ H;

- CN -;

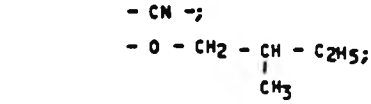

wherein q = 1 - 12.

5. Polymer composition as described in any of the claims 1-4 for the use in non-linear optics.
6. Coloured coatings prepared from a polymer composition according to any one of the claims 1-4.
7. Information storage device material comprising a polymer composition according to any one of the claims 1-4.
8. Polymer composition substantially as described and elucidated with reference to the examples.
9. Object made wholly or partly of a polymer composition according to any one of claims 1-4.

A B S T R A C T

The invention relates to novel polymer compositions based on thermotropic chiral polymers, capable of forming a chiral nematic mesophase, characterized by the fact that the compositions consist of monomers which have the chiral centre in the spacer part of the molecule, between the main chain and the mesogenic unit in the side chain. The compositions are conceivably useful as selective light reflectors, information storage device materials and coloured coatings. Furthermore they may be used in non-linear optics.